# MECHANISTIC DRIVERS OF MYCORRHIZAL TYPE EFFECTS ON SOIL CARBON AND NITROGEN CYCLING ACROSS SCALES

BY

GEORGIA S. SEYFRIED

DISSERTATION

Submitted in partial fulfillment of the requirements
for the degree of Doctor of Philosophy in Plant Biology
in the Graduate College of the
University of Illinois Urbana-Champaign, 2021

Urbana, Illinois

Doctoral Committee:

Associate Professor Wendy Yang, Chair and Director of Research
Professor Angela Kent
Professor James Dalling
Associate Professor Jennifer Fraterrigo

## ABSTRACT

A large portion of terrestrial carbon (C) and nitrogen (N) are stored in soil organic matter (SOM) yet the factors driving the balance between C and N storage versus loss from SOM remain unclear. Tree-mycorrhizal association has emerged as a promising predictor of SOM dynamics with ECM stands characterized by slow C and N cycling and AM stands characterized by rapid C and N cycling. This dissertation investigates the mechanisms driving formation of distinct mycorrhizal nutrient syndromes at the neighborhood, stand and watershed scales. First, I found that ECM effects on SOM dynamics and N cycling can differ in magnitude and direction between watersheds that differ in soil pH and fertility, demonstrating the potential for intrinsic soil properties to mediate the effects of ECM trees and associated fungi on SOM formation and persistence in the tropics. Second, I found that underlying soil acid-base chemistry can shape fungal communities that lead to variation in ECM effects on SOM accumulation and N cycling. Third, I found that litter chemical quality and environmental conditions mediate the manifestation of slower decomposition in ECM stands such that leaf litter decomposition rates cannot be predicted directly from litter mycorrhizal type or stand mycorrhizal type. Finally, I show that gross N mineralization rates can be greater in ECM relative to AM stands despite slow nitrification and minimal N losses, demonstrating that suppressed mineralization of low quality ECM leaf litter does not directly drive closed N cycling in ECM stands. This work revealed the central role of environmental and geologic context in determining the mechanisms driving ectomycorrhizal (ECM) effects at spatial scales from individual trees to forest stands to watersheds. I conclude that the mechanisms driving mycorrhizal effects can vary across ecosystems, informing efforts to predict mycorrhizal effects at the global scale.

## ACKNOWLEDGMENTS

I am incredibly thankful my time as a graduate student and have friends, family, and mentors to thank for making it so special. Most of all, I would like to thank my advisor, Wendy Yang, for being an endless well of positive energy and patience. Wendy's excitement about science was what drew me to Illinois and drove me to power through the many challenging experiences. Although I would like to think I will remember the numerous lessons Wendy passed on about conducting good science, I know I will remember what Wendy showed me through her mentorship. I would also like to thank the many graduate students and post-docs that have drifted in and out of the Yang lab through the years: Alex Krichels, Sada Egenriether, William Eddy, Joe Edwards, Chuck Hyde, Sean Khan Ooi, Mark Burnham, Adam von Haden, Kevin Ziliang Zhang and Di Liang. I feel lucky to call all of these people my colleagues and friends. Additionally, I am extremely grateful for to the crew of powerful lady technicians - Jess Mulcrone, Ingrid Holstrom, Ally Cook, Haley Ware, Avarna Jain, Taylor Bozman, and Sophie Fruchter – who have been wonderful friends inside and outside lab. I owe tremendous thanks to our lab manager, Rachel van Allen, who patiently guided me through instrument troubleshooting and met any and all questions with kindness, understanding, and a wealth of knowledge! Finally, I thank all my committee members, Jim Dalling, Angela Kent and Jennifer Fraterrigo for all of their guidance and Charlie Canham for the hours he spent with me on zoom.

I have three inspirational scientist - Margarita Prada, María Juliana Pardo and Jessica Lira – to thank for making my days in the Panamanian mountains extra special. I will always think fondly of our night time chats and infrequent, but lovely, days off together. Additionally, I thank Jim Dalling, and all the past members of the Dalling lab who have put tremendous amounts of hard work into creating and censusing the Fortuna plots, without which my dissertation would

not have been possible. I am honored to have been supported by Jim who shared his immense knowledge about tropical rainforests and patiently guided me through the logistics of tropical field work. Furthermore, I thank the Evidelio García, Carlos Espinosa and Alberto Gonzalez for constantly reminding me to bring a radio to the field, attempting to decipher my horrible Spanish and generally making sure I survived my time in Fortuna.

Outside the University, I am extremely thankful to have met an amazing crew of friends who were always ready to bust out of town and find rocks to climb on. I owe much of my sanity to these people and our trips together. Thanks for laughing at my jokes and pushing me to cultivate the impressive muscles that now allow me to complete THREE entire pullups!

Finally, I share this accomplishment with my amazing, ever-supportive family. I have been lucky to feel the unbelievable excitement and support of my parents as fellow soil-nerds. Thankyou for making your way to Panama multiple times. Thanks for digging holes in the rain and picking tiny roots from leaf litter and talking me through challenging decisions in the field. Most of all, thank you for sharing food and drinks and bringing love, laughter and companionship to my days in the mountains! An extra thanks to my mom for putting in many hours on the phone – we figured it all out! I thank my brother for bringing me perspective through laughter and for always being interested in me and my microbes! Perhaps most of all, I thank my partner Zane for bringing me unbelievable happiness and support in the last few years. Thank you for continually making the time for me and bringing creativity and joy into every day. It would not have been such a fun and interesting journey without you!!

Funding for this project was provided by the National Science Foundation Integrative Graduate Education and Research Traineeship Program, and the Illinois Distinguished Fellowship. I thank the University of Illinois School of Integrative Biology and Plant Biology

department for providing me with research funding. Additionally, I thank the Smithsonian Tropical Research Institute for providing logistical support at the Fortuna Forest Reserve.

*I dedicate this to my family for showing me the world, for teaching me to appreciate its beauty, and for always providing the art supplies that allowed me to create my own wild interpretations.*

*I dedicate this to my partner Zane and all the unknown excitement ahead of us!*

## TABLE OF CONTENTS

# CHAPTER 1

# INTRODUCTION

A large portion of terrestrial carbon (C) and nitrogen (N) are stored in soil organic matter (SOM) yet the factors driving the balance between C and N storage versus loss from SOM remain unclear. Importantly, C and N pools within SOM may feedback positively or negatively with global change factors and the strength and direction of these feedbacks may vary between systems. The potential role of SOM in mediating global change has prompted interest in characterizing the mechanistic drivers of storage versus loss from SOM pools. Tree-mycorrhizal association has recently emerged as a promising predictor of SOM dynamics. Most tree species associate with either ectomycorrhizae (ECM) or arbuscular mycorrhizae (AM). These major mycorrhizal groups interact with plant and soil properties to form distinct localized C and nutrient cycling syndromes: conservative nutrient use traits of ECM trees and associated mycorrhizal fungi promote formation of closed C and nutrient cycling while acquisitive nutrient use traits of AM trees and associated mycorrhizal fungi promote formation of open C and nutrient cycling (e.g. Averill, 2016; Cheeke et al., 2017; Lin et al., 2018; Phillips et al., 2013; Read and Perez-Moreno, 2003; Soudzilovskaia et al., 2015). However, mechanisms driving mycorrhizal nutrient syndromes remain unclear, making it difficult to generalize mycorrhizal effects on SOM dynamics across scales.

The current paradigm of mycorrhizal effects integrates above and belowground nutrient dynamics to define an organic N economy in ECM stands and an inorganic N economy in AM stands (Phillips et al., 2013). Differences in leaf litter decomposition dynamics between forest types are hypothesized to drive mycorrhizal nutrient cycling syndromes via two distinct mechanisms. First, lower N, higher lignin ECM leaf litter may suppress decomposition rates in

ECM stands while higher N, lower lignin AM leaf litter may stimulate decomposition rates in AM stands (McGuire et al., 2010; Midgley et al., 2015; Torti et al., 2001). Second, distinct decomposition dynamics between forest types may result from mycorrhizal differences in physiology related to nutrient acquisition. Ectomycorrhizal fungi can directly uptake organic N (Kohler et al., 2015; Lindahl and Tunlid, 2015; Read and Perez-Moreno, 2003) whereas AM fungi primarily scavenge inorganic N and can stimulate the free-living decomposer community to mineralize organic N for their uptake (Herman et al., 2012; Paterson et al., 2016; Talbot et al., 2008). Supported by host-supplied C, ECM may outcompete saprotrophs for low quality organic substrate and suppress decomposition rates by mining N from organic matter to leave behind C-rich, nutrient depleted compounds (Fernandez and Kennedy, 2016; Gadgil and Gadgil, 1971). Competition between fungal guilds is ultimately predicted to limit saprotrophic growth and result in C accumulation when N inputs are predominantly in forms that are energetically costly to take up (e.g. physically protected by lignin) and ECM are the superior competitors (Smith and Wan, 2019). Overall, nutrient use traits of ECM and AM trees may reinforce nutrient uptake strategies of associated mycorrhizal fungi, driving ECM and AM systems towards opposing C and N cycling syndromes (Averill et al., 2019). The goal of my dissertation work was to clarify the mechanisms hypothesized to underlie mycorrhizal nutrient economies and to investigate the context dependency of mechanistic drivers across environmental and geological conditions.

Ectomycorrhizal effects on soil C and N cycling are currently documented based on random sampling to determine average ECM effects at the stand scale leaving uncertainty in the generality of ECM effects across the different spatial scales at which soil properties are known to vary. In mixed forest, C and N cycling processes at the neighborhood scale are affected by ECM

and AM trees whose litterfall and rooting zones overlap (Bigelow and Canham, 2017) such that ECM effects may depend on the size and spatial distribution of ECM trees. Alternatively, ECM effects may average at the stand scale and vary with the percent basal area of ECM trees in a forest stand (Cheeke et al., 2017; Craig et al., 2018) rather than at the scale of an individual tree. Furthermore, ECM effects observed at neighborhood or stand scales may vary among ecosystems based on differences in soil pH and N availability which can mediate belowground C allocation patterns by host trees (Högberg et al., 2003; Kjoller et al., 2012) as well as functional variation within ECM communities (Corrales et al., 2016b; Lilleskov et al., 2002; Peay et al., 2010; Smith et al., 2011; Truong et al., 2019). In my second chapter, I use likelihood modelling techniques to investigate the effects of ECM-associated *Oreomunnea mexicana* on soil C and N pools at three spatial scales within a small geographic region: 1.) within tree neighborhoods where the size and spatial distribution of *O. mexicana* vary, 2.) within watersheds which exhibit gradients in ECM dominance at the stand scale and 3.) among watersheds that differ in soil properties due to variation in parent material and climate.

ECM effects can vary in magnitude and direction among watersheds that differ in soil pH and fertility (Seyfried et al., 2021a), yet it is currently unknown to what extent fungal communities beneath ECM trees drive these patterns. Local abiotic conditions can filter fungal communities and determine the functional capacity of the ECM community to affect soil C and N dynamics directly, through variation in morphological and physiological traits, or indirectly, through interactions with saprotrophic fungi (Pellitier et al., 2021). In particular, long distance exploration type ECM taxa may occur in higher relative abundance where N is predominantly available in recalcitrant forms (e.g. physically protected by N) and may perpetuate slow decomposition rates and accumulation of SOM where they establish by competing with

saprotrophic decomposers for organic N (Fernandez and Kennedy, 2016; Gadgil and Gadgil, 1971; Kyaschenko et al., 2017). In contrast, contact and short distance exploration type ECM taxa that produce less biomass and uptake inorganic N, may dominate in higher-N soils and have less capacity to drive an ecosystem towards conservative C and nutrient cycling. However, nutrient use traits of ECM and AM trees, such as leaf litter chemical quality, may also drive differences in ECM effects across systems (McGuire et al., 2010; Midgley et al., 2015; Torti et al., 2001). In chapter 3, I investigated fungal community composition as a potential driver of variation in ECM effects on SOM accumulation and N cycling in soils beneath ECM-associated *Oreomunnea mexicana*. I compared fungal community composition and function beneath ECM trees established in mixed ECM-AM versus ECM-dominated stands in four watersheds that differed in soil pH and fertility.

Differences in leaf litter decomposition between lower quality ECM leaf litter and higher quality AM leaf litter may initiate distinct nutrient cycling syndromes between forest types (McGuire et al., 2010; Midgley et al., 2015; Torti et al., 2001), but the relative importance of potential mechanisms in driving the contrasting decomposition patterns is uncertain. In temperate forests, the effect of leaf litter quality on decomposition is confounded with the effect of distinct decomposer communities that assemble in ECM versus AM-dominated stands. In N-limited temperate ecosystems, AM litter with lower C:N and lignin:N ratios decompose faster than ECM litter (Craig et al., 2018; Midgley et al., 2015; Sun et al., 2018). However, when considering greater species diversity at the global scale, ECM leaf litter does not necessarily have lower N or P content than AM leaf litter (Averill et al., 2019). As such, the role of leaf litter chemistry in driving distinct decomposition patterns in ECM and AM-dominated forests remains uncertain. At the stand scale, competition between ECM fungi and free-living saprotrophic fungi can suppress

leaf litter decomposition (Gadgil and Gadgil, 1971; Koide et al., 2014; McGuire et al., 2010; Schilling et al., 2016). However, while there is some evidence in support of this microbial competition hypothesis (Gadgil and Gadgil, 1971; Koide et al., 2014; McGuire et al., 2010; Schilling et al., 2016), ECM presence does not always suppress decomposition (Chuyong et al., 2002; Mayor and Henkel, 2006) and can even stimulate decomposition (Brzostek et al., 2015; Phillips and Fahey, 2006; Sulman et al., 2017). In Chapter four, I aimed to isolate the effects of litter quality and stand mycorrhizal type on decomposition using a high species diversity tropical rainforest within which ECM leaf litter is not necessarily lower quality than AM leaf litter. I decomposed two AM species higher and two AM species similar in leaf litter chemistry to two ECM species in ECM-and AM-dominated stands.

Tree association with ECM versus AM fungi clearly mediates distinct nutrient syndromes (e.g. Averill et al., 2014; Corrales et al., 2016; Lin et al., 2017; Phillips et al., 2013; Zhu et al., 2018), yet the mechanisms driving these mycorrhizal type patterns have remained unclear. Suppressed N mineralization due to slow decomposition of low quality ECM litter and organic N uptake by ECM fungi has been proposed to initiate cascading effects that result in an organic nutrient economy with closed N cycling in ECM stands (Brzostek et al., 2015; Phillips et al., 2013). However, net nitrification and downstream N losses are consistently suppressed in ECM relative to AM stands (e.g. Lin et al., 2017; Midgley and Phillips, 2016; Phillips et al., 2013) while patterns in net mineralization vary, with studies reporting lower (Lin et al., 2017; Midgley and Phillips, 2016), higher (Mushinski et al., 2021) and similar (Phillips et al., 2013) net mineralization rates in ECM compared to AM stands. Misalignment between net mineralization patterns and net nitrification patterns support mounting evidence in the literature that suppressed nitrification and downstream N losses in ECM stands are not necessarily driven by suppressed

mineralization (Midgley and Phillips, 2016; Mushinski et al., 2021). However, mycorrhizal mediation of N cycling is currently defined using inorganic N concentrations and net N cycling rates which conflate production and consumption pathways (e.g. Lin et al., 2017; Midgley and Phillips, 2016; Mushinski et al., 2021). As such, it is unclear what mechanisms underly greater net mineralization and nitrification rates in ECM compared to AM stands. In Chapter 5, I used the stable isotope pool dilution technique to quantify gross N cycling rates and investigate the role of N mineralization in driving mycorrhizal nutrient cycling syndromes in ECM versus AM-dominated temperate forest stands.

In Chapter 6, I summarize the results of this dissertation. Overall, my work emphasizes the importance of integrating environmental and geological context into our understanding of mycorrhizal mediated C and N cycling. I conclude that the mechanisms driving mycorrhizal effects can vary across ecosystems, informing efforts to predict mycorrhizal effects at the global scale.

## REFERENCES


Averill, C., 2016. Slowed decomposition in ectomycorrhizal ecosystems is independent of plant chemistry. Soil Biology and Biochemistry 102, 52–54. doi:http://dx.doi.org/10.1016/j.soilbio.2016.08.003

Averill, C., Bhatnagar, J.M., Dietze, M.C., Pearse, W.D., Kivlin, S.N., 2019. Global imprint of mycorrhizal fungi on whole-plant nutrient economics. Proceedings of the National Academy of Sciences of the United States of America 46, 23163–23168. doi:10.1073/pnas.1906655116

Averill, C., Turner, B.L., Finzi, A.C., 2014. Mycorrhiza-mediated competition between plants and decomposers drives soil carbon storage. Nature 505, 543–545. doi:10.1038/nature12901

Bigelow, S., Canham, C., 2017. Neighborhood-Scale Analyses of Non-additive Species Effects on Cation Concentrations in Forest Soils. Ecosystems 20, 1351–1363. doi:10.1007/s10021-017-0116-1

Brzostek, E.R., Dragoni, D., Brown, Z.A., Phillips, R.P., 2015. Mycorrhizal type determines the magnitude and direction of root-induced changes in decomposition in a temperate forest. New Phytologist 206, 1274–1282. doi:10.1111/nph.13303

Cheeke, T.E., Phillips, R.P., Brzostek, E.R., Rosling, A., Bever, J.D., Fransson, P., 2017. Dominant mycorrhizal association of trees alters carbon and nutrient cycling by selecting for microbial groups with distinct enzyme function. New Phytologist 214, 432–442. doi:10.1111/nph.14343

Chuyong, G.B., Newbery, D.M., Songwe, N.C., 2002. Litter breakdown and mineralization in a central African rain forest dominated by ectomycorrhizal trees. Biogeochemistry. doi:10.1023/A:1020276430119

Corrales, A., Mangan, S.A., Turner, B.L., Dalling, J.W., 2016. An ectomycorrhizal nitrogen economy facilitates monodominance in a neotropical forest. Ecology Letters 19, 383–392. doi:10.1111/ele.12570

Craig, M.E., Turner, B.L., Liang, C., Clay, K., Johnson, D.J., Phillips, R.P., 2018. Tree mycorrhizal type predicts within-site variability in the storage and distribution of soil organic matter. Global Change Biology 24, 3317–3330. doi:10.1111/gcb.14132

Fernandez, C.W., Kennedy, P.G., 2016. Revisiting the "Gadgil effect": do interguild fungal interactions control carbon cycling in forest soils? New Phytologist 209, 1382–1394. doi:10.1111/nph.13648

Gadgil, R.L., Gadgil, P.D., 1971. Mycorrhiza and litter decomposition. Nature 233, 133. doi:10.1038/233133a0

Herman, D.J., Firestone, M.K., Nuccio, E., Hodge, A., 2012. Interactions between an arbuscular mycorrhizal fungus and a soil microbial community mediating litter decomposition. Fems Microbiology Ecology 80, 236–247. doi:10.1111/j.1574-6941.2011.01292.x

Högberg, M.N., Bååth, E., Nordgren, A., Arnebrant, K., Högberg, P., 2003. Contrasting effects of nitrogen availability on plant carbon supply to mycorrhizal fungi and saprotrophs - A hypothesis based on field observations in boreal forest. New Phytologist 160, 225–238. doi:10.1046/j.1469-8137.2003.00867.x

Kjoller, R., Nilsson, L.O., Hansen, K., Schmidt, I.K., Vesterdal, L., Gundersen, P., 2012. Dramatic changes in ectomycorrhizal community composition, root tip abundance and mycelial production along a stand-scale nitrogen deposition gradient. New Phytologist 194, 278–286. doi:10.1111/j.1469-8137.2011.04041.x

Kohler, A., Kuo, A., Nagy, L.G., Morin, E., Barry, K.W., Buscot, F., Canbäck, B., Choi, C.,

Cichocki, N., Clum, A., Colpaert, J., Copeland, A., Costa, M.D., Doré, J., Floudas, D., Gay, G., Girlanda, M., Henrissat, B., Herrmann, S., Hess, J., Högberg, N., Johansson, T., Khouja, H.R., Labutti, K., Lahrmann, U., Levasseur, A., Lindquist, E.A., Lipzen, A., Marmeisse, R., Martino, E., Murat, C., Ngan, C.Y., Nehls, U., Plett, J.M., Pringle, A., Ohm, R.A., Perotto, S., Peter, M., Riley, R., Rineau, F., Ruytinx, J., Salamov, A., Shah, F., Sun, H., Tarkka, M., Tritt, A., Veneault-Fourrey, C., Zuccaro, A., Tunlid, A., Grigoriev, I. V., Hibbett, D.S., Martin, F., 2015. Convergent losses of decay mechanisms and rapid turnover of symbiosis genes in mycorrhizal mutualists. Nature Genetics 47, 410-U176. doi:10.1038/ng.3223

Koide, R.T., Fernandez, C., Malcolm, G., 2014. Determining place and process: functional traits of ectomycorrhizal fungi that affect both community structure and ecosystem function. New Phytologist 201, 433–439. doi:10.1111/nph.12538

Kyaschenko, J., Clemmensen, K.E., Karltun, E., Lindahl, B.D., 2017. Below-ground organic matter accumulation along a boreal forest fertility gradient relates to guild interaction within fungal communities. Ecology Letters 20, 1546–1555. doi:10.1111/ele.12862

Lilleskov, E.A., Fahey, T.J., Horton, T.R., Lovett, G.M., 2002. Belowground ectomycorrhizal fungal community change over a nitrogen deposition gradient in Alaska. Ecology 83, 104–115. doi:10.1890/0012-9658(2002)083[0104:befcco]2.0.co;2

Lin, G., Guo, D., Li, L., Ma, C., Zeng, D.H., 2018. Contrasting effects of ectomycorrhizal and arbuscular mycorrhizal tropical tree species on soil nitrogen cycling: the potential mechanisms and corresponding adaptive strategies. Oikos 127, 518–530. doi:10.1111/oik.04751

Lin, G., McCormack, M.L., Ma, C., Guo, D., 2017. Similar below-ground carbon cycling dynamics but contrasting modes of nitrogen cycling between arbuscular mycorrhizal and

ectomycorrhizal forests. New Phytologist 213, 1440–1451. doi:10.1111/nph.14206

Lindahl, B.D., Tunlid, A., 2015. Ectomycorrhizal fungi - potential organic matter decomposers, yet not saprotrophs. New Phytologist 205, 1443–1447. doi:10.1111/nph.13201

Mayor, J.R., Henkel, T.W., 2006. Do ectomycorrhizas alter leaf-litter decomposition in monodominant tropical forests of Guyana? New Phytologist 169, 579–588. doi:10.1111/j.1469-8137.2005.01607.x

McGuire, K.L., Zak, D.R., Edwards, I.P., Blackwood, C.B., Upchurch, R., 2010. Slowed decomposition is biotically mediated in an ectomycorrhizal, tropical rain forest. Oecologia 164, 785–795. doi:10.1007/s00442-010-1686-1

Midgley, M.G., Brzostek, E., Phillips, R.P., 2015. Decay rates of leaf litters from arbuscular mycorrhizal trees are more sensitive to soil effects than litters from ectomycorrhizal trees. Journal of Ecology 103, 1454–1463. doi:10.1111/1365-2745.12467

Midgley, M.G., Phillips, R.P., 2016. Resource stoichiometry and the biogeochemical consequences of nitrogen deposition in a mixed deciduous forest. Ecology 97, 3369–3378. doi:https://doi.org/10.1002/ecy.1595

Mushinski, R.M., Payne, Z.C., Raff, J.D., Craig, M.E., Pusede, S.E., Rusch, D.B., White, J.R., Phillips, R.P., 2021. Nitrogen cycling microbiomes are structured by plant mycorrhizal associations with consequences for nitrogen oxide fluxes in forests. Global Change Biology 27, 1068–1082. doi:10.1111/gcb.15439

Paterson, E., Sim, A., Davidson, J., Daniell, T.J., 2016. Arbuscular mycorrhizal hyphae promote priming of native soil organic matter mineralisation. Plant and Soil 408, 243–254. doi:10.1007/s11104-016-2928-8

Peay, K.G., Kennedy, P.G., Davies, S.J., Tan, S., Bruns, T.D., 2010. Potential link between plant

and fungal distributions in a dipterocarp rainforest: Community and phylogenetic structure of tropical ectomycorrhizal fungi across a plant and soil ecotone. New Phytologist 185, 529–542. doi:10.1111/j.1469-8137.2009.03075.x

Pellitier, P.T., Zak, D.R., Argiroff, W.A., Upchurch, R.A., 2021. Coupled Shifts in Ectomycorrhizal Communities and Plant Uptake of Organic Nitrogen Along a Soil Gradient: An Isotopic Perspective. Ecosystems. doi:10.1007/s10021-021-00628-6

Phillips, R.P., Brzostek, E., Midgley, M.G., 2013. The mycorrhizal-associated nutrient economy: A new framework for predicting carbon-nutrient couplings in temperate forests. New Phytologist 199, 41–51. doi:10.1111/nph.12221

Phillips, R.P., Fahey, T.J., 2006. Tree species and mycorrhizal associations influence the magnitude of rhizosphere effects. Ecology 87, 1302–1313. doi:10.1890/0012-9658(2006)87[1302:TSAMAI]2.0.CO;2

Read, D.J., Perez-Moreno, J., 2003. Mycorrhizas and nutrient cycling in ecosystems - a journey towards relevance? New Phytologist 157, 475–492. doi:10.1046/j.1469-8137.2003.00704.x

Schilling, E.M., Waring, B.G., Schilling, J.S., Powers, J.S., 2016. Forest composition modifies litter dynamics and decomposition in regenerating tropical dry forest. Oecologia. doi:10.1007/s00442-016-3662-x

Seyfried, G.S., Canham, C.D., Dalling, J.W., Yang, W.H., 2021. The effects of tree-mycorrhizal type on soil organic matter properties from neighborhood to watershed scales. Soil Biology and Biochemistry 108385. doi:https://doi.org/10.1016/j.soilbio.2021.108385

Smith, G.R., Wan, J., 2019. Resource-ratio theory predicts mycorrhizal control of litter decomposition. New Phytologist 223, 1595–1606. doi:10.1111/nph.15884

Smith, M.E., Henkel, T.W., Catherine Aime, M., Fremier, A.K., Vilgalys, R., 2011.

Ectomycorrhizal fungal diversity and community structure on three co-occurring leguminous canopy tree species in a Neotropical rainforest. New Phytologist 192, 699–712. doi:10.1111/j.1469-8137.2011.03844.x

Soudzilovskaia, N.A., van der Heijden, M.G.A., Cornelissen, J.H.C., Makarov, M.I., Onipchenko, V.G., Maslov, M.N., Akhmetzhanova, A.A., van Bodegom, P.M., 2015. Quantitative assessment of the differential impacts of arbuscular and ectomycorrhiza on soil carbon cycling. New Phytologist 208, 280–293. doi:10.1111/nph.13447

Sulman, B.N., Brzostek, E.R., Medici, C., Shevliakova, E., Menge, D.N.L., Phillips, R.P., 2017. Feedbacks between plant N demand and rhizosphere priming depend on type of mycorrhizal association. Ecology Letters 20, 1043–1053. doi:https://doi.org/10.1111/ele.12802

Sun, T., Hobbie, S.E., Berg, B., Zhang, H., Wang, Q., Wang, Z., Hättenschwiler, S., 2018. Contrasting dynamics and trait controls in first-order root compared with leaf litter decomposition. Proceedings of the National Academy of Sciences of the United States of America. doi:10.1073/pnas.1716595115

Talbot, J.M., Allison, S.D., Treseder, K.K., 2008. Decomposers in disguise: mycorrhizal fungi as regulators of soil C dynamics in ecosystems under global change. Functional Ecology 22, 955–963. doi:10.1111/j.1365-2435.2008.01402.x

Torti, S.D., Coley, P.D., Kursar, T.A., 2001. Causes and consequences of monodominance in tropical lowland forests. American Naturalist 157, 141–153. doi:10.1086/318629

Truong, C., Gabbarini, L.A., Corrales, A., Mujic, A.B., Escobar, J.M., Moretto, A., Smith, M.E., 2019. Ectomycorrhizal fungi and soil enzymes exhibit contrasting patterns along elevation gradients in southern Patagonia. New Phytologist 222, 1936–1950. doi:10.1111/nph.15714

Zhu, K., McCormack, M.L., Lankau, R.A., Egan, J.F., Wurzburger, N., 2018. Association of

ectomycorrhizal trees with high carbon-to-nitrogen ratio soils across temperate forests is driven by smaller nitrogen not larger carbon stocks. Journal of Ecology 106, 524–535. doi:10.1111/1365-2745.12918

# CHAPTER 2

# THE EFFECTS OF TREE-MYCORRHIZAL TYPE ON SOIL ORGANIC MATTER PROPERTIES FROM NEIGHBORHOOD TO WATERSHED SCALES[1]

## INTRODUCTION

A large portion of terrestrial carbon (C) is stored as soil organic matter (SOM). Consequently, the balance between C inputs to SOM and C loss through respiration has important implications for global climate change. Soil organic matter dynamics are controlled by biotic and abiotic factors that act at a range of spatial scales: broad climate patterns determine SOM formation and decomposition at the global scale while plant and microbial community composition and edaphic conditions act at the ecosystem scale. The identity of tree-mycorrhizal associations has emerged as a promising predictor of SOM dynamics in surface soils within temperate, boreal and tropical biomes (Averill et al., 2014; Craig et al., 2018; Lin et al., 2017; Zhu et al., 2018). Specifically, the delineation between tree species that associate with ectomycorrhizae (ECM) versus arbuscular mycorrhizae (AM) can integrate covarying plant and soil traits such that ecosystem C- and nitrogen (N)-cycling and SOM dynamics can be predicted by the relative proportion of ECM versus AM-associated trees in a forest stand (Cheeke et al., 2017; Craig et al., 2018; Zhu et al., 2018). However, functionally and taxonomically diverse ECM and host tree communities can establish based on underlying edaphic conditions (Corrales et al., 2016a; Peay et al., 2010; Smith et al., 2011), potentially causing variation in the

[1] This work was previously published through Elsevier in the journal *Soil Biology and Biochemistry.*
Full citation:
Seyfried, G.S., Canham, C.D., Dalling, J.W., Yang, W.H., 2021. The effects of tree-mycorrhizal type on soil organic matter properties from neighborhood to watershed scales. Soil Biology and Biochemistry 108385. doi:https://doi.org/10.1016/j.soilbio.2021.108385

mechanisms driving ECM effects on soil C and N cycling (Fernandez and Kennedy, 2016) as well as the capacity for ECM effects to determine ecosystem-scale patterns (Craig et al., 2019; Midgley and Sims, 2020). Therefore, uncertainty remains in the generality of ECM effects across the different spatial scales at which soil properties are known to vary.

The effects of ECM on SOM may vary at the neighborhood scale within forest stands because individual trees have a concentrated influence on soil properties in the area beneath their crown (Bigelow & Canham, 2017; Keller, Reed, Townsend, & Cleveland, 2013; Waring et al., 2015). Organic carbon accumulation in ECM surface soils likely originates from fine roots and associated ECM hyphae (Hölscher et al. 2009; Clemmensen et al. 2013), suggesting that ECM effects on SOM accumulation occur at the spatial scale of host tree fine root production. Alternatively, low quality leaf litter produced by ECM trees can suppress leaf litter decomposition rates (McGuire et al., 2010; Midgley et al., 2015; Torti et al., 2001), thereby contributing to greater SOM formation from leaf litter fragments incorporated into ECM surface soils (Averill, 2016; Averill et al., 2014; Craig et al., 2018). This mechanism may result in distinct spatial patterns of SOM accumulation if leaf litterfall patterns differ from those of fine root proliferation. Characterizing spatial patterns of ECM effects within forest stands could clarify which mechanisms underlie greater SOM accumulation in ECM relative to AM surface soils. However, past studies have typically documented these general patterns based on random sampling to determine average ECM effects at the stand scale (e.g., Cheeke et al., 2017; Craig et al., 2018). By instead using spatially explicit datasets and neighborhood models, we may be able to discern the spatial extent of ECM effects in mixed forests where C and nutrient cycling processes are affected by ECM- and AM-associated tree species whose litterfall and rooting zones overlap (Bigelow and Canham, 2017).

Along mycorrhizal gradients in temperate forests, ECM effects on SOM pools have been shown to scale linearly with ECM tree basal area (hereafter referred to as ECM dominance) in forest stands, with slow decomposition of low quality ECM leaf litter thought to result in a positive relationship between ECM dominance and mineral soil C:N (Cheeke et al., 2017; Craig et al., 2018). However, in boreal forests, some ECM fungal taxa can promote decomposition and decrease OM accumulation (Clemmensen et al., 2021; Kyaschenko et al., 2017; Lindahl et al., 2021), highlighting the importance of environmental context in determining ECM effects across biomes. Bulk soil patterns along mycorrhizal gradients may be best understood by conceptualizing SOM as two distinct fractions: particulate organic matter (POM) and mineral-associated organic matter (MAOM), which differ in formation, persistence and functioning (Lavallee et al., 2020). POM is formed through transport of relatively undecomposed organic matter fragments into the mineral soil from the litter, organic horizon or rhizosphere (Lavallee et al., 2020). Though it may be more physically accessible to the microbial community, POM tends to consist of large, insoluble molecules that are energetically expensive to assimilate (Kleber et al., 2015). Nutrient conservative traits of ECM-associated tree species, such as production of low N leaf and root litter, are hypothesized to complement the nutrient acquisition strategies of their ECM symbiont, suppressing decomposition and leading to accumulation of high C:N POM in an organic horizon or in the topsoil (Averill et al., 2019; Craig et al., 2018). In contrast, MAOM consists of mainly low-molecular weight compounds that adsorb to mineral surfaces (Lavallee et al., 2020). MAOM formation may occur via direct sorption of plant litter that has leached or been partially depolymerized, or via the microbial turnover pathway in which organic material is incorporated into microbial biomass before associating with mineral surfaces as microbial necromass (Liang et al., 2017; Sokol et al., 2019). Nutrient acquisitive traits of AM-associated

tree species, such as production of high N leaf and root litter, are hypothesized to complement the nutrient acquisition traits of their AM symbionts, resulting in in rapid decomposition, enhanced microbial growth efficiency and growth rate, and increased formation of low C:N MAOM (Averill et al., 2019; Cotrufo et al., 2013; Craig et al., 2018). This delineation between nutrient conservative ECM traits and nutrient acquisitive AM traits is less clear in tropical systems than in temperate systems because mixed AM litter and monodominant ECM litter can be chemically similar (Averill et al., 2019; McGuire et al., 2010; Torti et al., 2001). Additionally, high rainfall in the tropics may increase the importance of leaching as a mass loss pathway (Cleveland et al., 2006), decreasing the effect of distinct decomposer communities in ECM versus AM soils on leaf litter decomposition rates (Keller and Phillips, 2019; Seyfried et al., 2021b). Therefore, ECM effects on POM and MAOM formation remain uncertain in tropical ecosystems where tree-mycorrhizal association does not necessarily predict leaf litter decomposition dynamics.

ECM effects on SOM pools may also vary among forests based on differences in soil pH and N availability which can mediate belowground C allocation patterns by host trees (Högberg et al., 2003; Kjoller et al., 2012) as well as functional variation within ECM communities (Corrales et al., 2016a; Lilleskov et al., 2002; Peay et al., 2010; Smith et al., 2011; Truong et al., 2019). Studies conducted along natural fertility gradients, in which pH and N availability are often correlated, show that ECM abundance (Sterkenburg et al., 2015), mycelial production (Clemmensen et al., 2006; Kalliokoski et al., 2010) and ECM colonization levels of fine roots (Corrales, 2016) increase with pH and N availability. Additionally, natural variation in pH and N availability may shift ECM community composition and select for functional traits that directly or indirectly affect SOM accumulation: morphological traits of ECM taxa may determine the

amount and quality of ECM biomass entering the belowground C pool while the enzymatic capacity of ECM taxa to uptake organic N may affect decomposition dynamics (Karina E. Clemmensen et al., 2015; Clemmensen et al., 2021; Hagenbo et al., 2018; Kyaschenko et al., 2017). Supported by host-supplied C, ECM taxa with the enzymatic capacity to uptake organic nutrients may outcompete free-living saprotrophic fungi. As such, competition between fungal guilds is predicted to limit saprotrophic growth and result in C accumulation when N inputs are predominantly in organic forms that are energetically costly to take up (e.g. physically protected by lignin (Smith and Wan, 2019). Although the Gadgil effect has not been directly observed in tropical forests, past studies report smaller inorganic N pools and greater accumulation of SOM in ECM surface soils relative to AM surface soils, indicating that ECM trees and associated fungi may mediate decomposition dynamics in tropical forests (Corrales et al., 2016b; Hölscher et al., 2009; Lin et al., 2017). Furthermore, ectomycorrhizal external mycelium represent a significant source of belowground C (Clemmensen et al., 2013; Ekblad et al., 2013; Godbold et al., 2006) that likely contributes to observed SOM accumulation patterns along mycorrhizal gradients. However, mycorrhizal contribution to SOM may vary in space based on C allocation patterns and ECM community composition, manifesting in ECM effects on SOM pools that vary along mycorrhizal gradients and between forests that differ in their underlying fertility.

Variability in ECM effects among ecosystems can be investigated by comparing patterns in $\delta^{15}N$ of leaf litter and soil organic matter fractions across mycorrhizal gradients. First, foliar $\delta^{15}N$ can indicate host tree reliance on N transfer from ECM symbionts: ECM preferentially transfer $^{14}N$ to their hosts and retain $^{15}N$ in their biomass, such that trees which receive more N via their ECM symbionts produce foliar tissues more depleted in $^{15}N$ (Hobbie and Högberg, 2012; Högberg et al., 1999; Kohzu et al., 2000). Therefore, lower foliar $\delta^{15}N$ can reflect lower N

availability (Hobbie et al., 2000). The N isotopic composition of leaf litter samples collected from the forest floor is also affected by decomposition stage because microbes discriminate against $^{15}N$ when mineralizing organic matter such that the litter becomes increasingly $^{15}N$-enriched as decomposition progresses (Natelhoffer and Fry, 1988). As such, slower decomposition caused by ECM fungi would lead to lower $\delta^{15}N$ of forest floor leaf litter. With respect to both foliar and leaf litter $\delta^{15}N$, greater ECM effects would lead to lower $\delta^{15}N$. Second, the difference between the $\delta^{15}N$ of POM and MAOM fractions and the $\delta^{15}N$ of forest floor leaf litter ($\delta^{15}N_{POM\text{-}litter;\ MAOM\text{-}litter}$) can also reveal the relative magnitude of ECM effects. Greater differences in $\delta^{15}N$ between SOM fractions and forest floor leaf litter can result from greater ECM transfer of N to host trees leading to less $^{15}N$-enriched leaf litter and a larger proportion of SOM fractions derived from $^{15}N$-enriched ECM hyphal biomass leading to more $^{15}N$-enriched SOM (Wallander et al., 2009). The relative magnitude of ECM effects on N availability and SOM dynamics in watersheds that differ in underlying parent material can therefore be characterized by comparing the slope of the change in $\delta^{15}N$ of leaf litter and soil organic matter fractions from AM- to ECM-dominated stands within each watershed.

Here, we investigated the effects of ECM-associated *Oreomunnea mexicana*, a canopy tree found in mid-elevation forests from southern Mexico to western Panama (Stone, 1972), on soil C and N pools at three spatial scales within a small geographic region: 1.) within tree neighborhoods where the size and spatial distribution of *O. mexicana* vary, 2.) within watersheds which exhibit gradients in ECM dominance at the stand scale, and 3.) among watersheds that differ in soil properties due to variation in parent material and climate. By sampling in censused forest plots along mycorrhizal gradients in each watershed and using spatially explicit modeling techniques, we tested the hypothesis that ECM effects on SOM pools would vary in intensity

based on the size and spatial distribution of *O. mexicana* trees because larger trees closer to a sampling point should have a greater effect on SOM dynamics than small trees at a greater distance. Additionally, by sampling within four watersheds that differ in pH and soil fertility, as defined by effective cation exchange capacity and percent base saturation, we tested the hypothesis that the effect of ECM-associated trees on SOM accumulation would be greater in lower pH, lower fertility watersheds than in higher pH, higher fertility watersheds. We conducted our study in a tropical montane forest that harbors high species diversity of AM-associated trees as well as ECM monodominant stands defined as greater than 50% ECM-associated *O. mexicana* by basal area. Although tropical ECM taxa are often restricted to nutrient poor soils (Hall et al., 2020), *O. mexicana* monodominant stands in Fortuna have established in four watersheds that vary in underlying geology, leading to formation of soils that vary in pH, cation exchange capacity, base saturation, and phosphorus (P) and N availability (Prada et al., 2017, Turner and Dalling 2021). Variation among the watersheds in the abundance of *O. mexicana* host trees, the percent ECM infection of *O. mexicana* roots, and ECM community composition and function suggest that soil properties may partially determine ECM-host dynamics in Fortuna (Corrales et al., 2016a; Corrales et al., 2016b). However, how soil property mediated differences in ECM-host dynamics affects POM and MAOM pools has not previously been investigated.

## MATERIALS AND METHODS

### Site description

We conducted this study in the 13,000 ha Fortuna Forest Reserve (Fortuna), a lower montane tropical forest in western Panama (8°45’ N, 82°15’ W) with elevation ranging 1000-1400 masl. Tree communities in Fortuna are highly diverse, containing 61-153 species $ha^{-1}$ for

trees greater than 10 cm DBH (Prada et al., 2017). Most tree species in Fortuna associate with AM fungi, while some ECM-associated tree species occur at low abundance, including: *Quercus insignis*, *Quercus lancifolia* and *Coccoloba* spp. (Prada et al., 2017). One ECM-associated tree species, *Oreomunnea mexicana,* tends to dominate the forest where it grows, forming stands with >50% *O. mexicana* by basal area (Corrales et al., 2016b). In Fortuna, *O. mexicana* dominated stands form on a range of underlying parent materials in the four watersheds we used in this study: ultisols at Honda and Hornito are derived from rhyolite and dacite, respectively, ultisols and inceptisols at Zorro are derived from granodiorite, and inceptisols at Alto Frio are derived from undifferentiated mafic volcanics (Turner & Dalling, 2021). Differences in underlying parent material and climate among watersheds have resulted in soil development with a range of soil fertilities (Table 2.1, A.1, A.2). Soil properties and plant community composition at different sites in these watersheds are described in detail by (Turner & Dalling, 2021), with the specific sites of Alto Frio, Honda (A/B), HornitoB and ZorroA used in this study. Landslide activity at ZorroA has led to the formation of pedogenically younger inceptisols compared to more weathered ultisols found elsewhere in the watershed. Across the four watersheds, mean annual temperature in Fortuna ranges 19-22 °C (Cavelier et al., 1996) and mean annual precipitation ranges 5800-9000 mm (Andersen et al., 2012) (Table A.1). Seasonality of precipitation is evident in the Alto Frio, Zorro and Hornito watersheds, which experience a dry season from January through April (Prada et al., 2017).

**Soil sampling**

To characterize the effects of ECM dominance on soil C and N pools, we sampled from four 0.5-1 ha plots that each contained ECM-associated *O. mexicana* dominated stands, mixed species AM-associated stands, and ecotones between the two stand types ("mycorrhizal

gradient"). Mycorrhizal gradients sampled in the four watersheds encompassed different ranges of ECM dominance: in Alto Frio, Honda, Hornito and Zorro, ECM basal area within 20 m of a sampling location ranged 0-47%, 0-62%, 0-61% and 0.01-72%, respectively. In July 2017, we sampled 24, 16, 10 and 14 locations within Alto Frio, Honda, Hornito and Zorro watersheds, respectively. Within each watershed, we sampled in a grid such that all samples were surrounded by at least 20 m of censused forest and were separated by either 10 m or 20 m, depending on the size and shape of stands dominated by *O. mexicana*, to avoid autocorrelation between samples. At each of the 68 sampling locations, we collected forest floor and O horizon samples, including all roots with a diameter of approximately 1.5 cm or smaller, from a 0.25 m X 0.25 m area. The forest floor litter layer was sampled sampled by gently scraping the soil surface and therefore included a mixture of leaf litter and woody debris at varying stages of decomposition. For subsequent analyses, we separated the leaf litter from all other debris (hereafter referred to as "forest floor leaf litter"). The underlying organic horizon depth varied from 0-20.25 cm among sampling locations and included both Oe, organic matter under degradation, and in some locations, Oa, humified organic matter. Using a 10 cm diameter quantitative corer, we collected shallow mineral soils from 0-10 cm and 10-20 cm depth below the O horizon.

To characterize the effect of stand mycorrhizal association on soil C and N pools in deeper soils, we conducted a second sampling effort in July 2019. At each end of the mycorrhizal gradient (i.e., 50-70% and 0% ECM basal area) in each watershed, we chose three sampling locations separated by at least 20 m. We sampled the organic layer and mineral soils to 1 m depth in 20 cm increments using a non-quantitative, 2.54 cm diameter soil probe.

**Bulk soil analyses**

We calculated bulk density for organic and mineral soil layers to 20 cm depth by dividing dry soil mass by total sample volume and accounted for the contribution of roots <1.5 cm diameter to the measured bulk density (Section A.1). To determine dry soil mass, we recorded the total weight of our fresh soil samples then homogenized and oven dried a root free subsample at 105 °C for 24 hours to determine gravimetric soil moisture. Some O horizon samples contained roots which were too large to be removed; we subtracted the volume of these large roots from the total volume of the O horizon. Large root volume was approximated using the following equation in which L and d represent root length and diameter:

$$Large\ root\ volume = L * \pi * d$$

Air-dried and ground samples were analyzed for SOC and TN concentrations as well as $\delta^{13}C$ and $\delta^{15}N$ on a Vario Micro Cube elemental analyzer (Hanau, Germany) interfaced with an IsoPrime 100 isotope ratio mass spectrometer (Cheadle Hulme, UK). We measured soil pH in a 2:1 ratio of ml ultra-pure DI water to g dry soil for mineral soil and a 5:1 ratio for organic soil. Additionally, potassium (K), calcium (Ca), magnesium (Mg), manganese (Mn) , aluminum (Al), iron (Fe) and sodium (Na) concentrations were determined by barium chloride ($BaCl_2$) extraction of air-dried, sieved subsamples from 0-20 cm and 20-40 cm deep mineral soil samples from the deep soil sampling effort and detection by ICP-OES (Avio 200, Perkin Elmer, Waltham, Massachusetts, USA)(Hendershot et al., 1993) (Table A.2). Given that the location of the deep soil sampling for the AM stand in Hornito did not match up with the surface soil sampling across mycorrhizal gradients as they did in the other watersheds, we also analyzed base cation concentrations in the surface soil samples from the AM end of the mycorrhizal gradient in Hornito to better characterize the soil fertility underlying the Hornito mycorrhizal gradient

(Table 2.1, A.2). We averaged base saturation (BS), effective cation exchange capacity (ECEC; cmol (+) kg $soil^{-1}$) and base cation concentrations from 0-10 and 10-20 cm mineral soil depths to compare against the 0-20cm depth increment from our deep soil sampling effort. We calculated ECEC as the sum of all base cation concentrations (cmol (+) $kg^{-1}$) and percent base saturation as the sum of Ca, K, Mg and Na concentrations divided by ECEC and multiplied by 100.

**Soil fractionation**

To gain mechanistic insight into SOM formation, we separated our soil samples into particulate organic matter (POM) and mineral associated organic matter (MAOM) fractions following Bradford et al. (2008). Specifically, we dispersed 10 g of sieved soil in 40 mL of 5 g $L^{-1}$ sodium hexametaphosphate (NaHMP) and shook the soil solution on a reciprocal shaker for 16 hours. The soil solution was passed through a 53µm mesh sieve using ultra-pure deionized water. The POM fraction was defined as material that remained on top of the sieve while the MAOM fraction was defined as material that passed through the sieve. Oven-dried POM and MAOM fractions were ground and analyzed for SOC and TN elemental and isotopic compositions as described for the bulk soil samples.

To account for site variation in $\delta^{13}C$ or $\delta^{15}N$ of leaf litter, which is a source pool for SOM formation, we used the isotopic composition of POM ($\delta^{13}C_{POM\text{-}litter}$ and $\delta^{15}N_{POM\text{-}litter}$) and MAOM ($\delta^{13}C_{MAOM\text{-}litter}$ and $\delta^{15}N_{MAOM\text{-}litter}$) fractions relative to overlying leaf litter throughout our analyses. This was calculated by subtracting $\delta^{13}C$ or $\delta^{15}N$ of the leaf litter from the $\delta^{13}C$ or $\delta^{15}N$ of the POM or MAOM fractions.

**Equivalent soil mass corrections**

To compare elemental and isotopic stocks among watersheds varying in soil bulk density, we calculated SOC, TN, $^{13}C$ and $^{15}N$ stocks in the bulk mineral soil and POM and MAOM fractions based on equivalent soil mass rather than fixed depth intervals (von Haden et al., 2020). This approach was used for bulk soil as well as the POM and MAOM fractions. The equivalent soil mass method compares soil properties at consistent mass of mineral soil, rather than at a fixed depth, such that comparisons are not biased by changes in bulk density nor changes in SOM (von Haden et al., 2020). Reference masses for mineral soil samples taken in 10 cm increments to 20 cm depth were 3.60 and 10.17 g-soil $cm^{-2}$ and reference masses for mineral soil samples taken in 20 cm increments to 1 m depth were 15.68, 33.29, 57.46, 82.02 and 108.95 g-soil $cm^{-2}$. Reference masses were chosen to minimize the degree of extrapolation necessary in our corrections.

Due to high variability in O horizon depth and percent SOM among soil samples, we calculated O horizon SOC and TN stocks using the fixed depth method (Don et al., 2011), that is by multiplying the total sample dry mass (DW) by O horizon SOC or TN concentrations (C or N) and dividing by the area of soil surface sampled (A).

$$C \text{ or } N \text{ stocks } \left({}^{g}/_{cm^2}\right) = \frac{DW * C(or\ N)}{A}$$

**Likelihood statistical analyses**

To determine the spatial patterns of forest floor leaf litter and soil properties in mixed mycorrhizal forest stands, we utilized likelihood methods and model selection in place of traditional hypothesis testing (Canham and Uriarte, 2006). We developed a suite of alternative models to represent patterns that were based on our current understanding of mechanisms by

which ECM-associated trees alter C and N cycling within a forest stand (Table A.3). Using these alternative models, we estimated parameters that maximized the likelihood of observing the forest floor leaf litter or soil properties we measured. Specifically, we aimed to describe spatial variability in forest floor leaf litter or soil properties of mixed mycorrhizal stands by comparing $AIC_c$ values among three groups of alternative models.

For our simplest set of models, the mean models, we assumed that tree-mycorrhizal association had no effect on forest floor leaf litter or soil properties which were estimated by the following model

$$Y = a + \varepsilon$$

where $a$ is the mean of forest floor leaf litter or soil property $Y$ and $\varepsilon$ is the error term. We accounted for possible variation among watersheds using the watershed-means model in which $a$ was replaced with $a_s$, the mean of forest floor leaf litter or soil property $Y$ for each of our four watersheds.

In our non-spatial alternative models, we assumed the effect of ECM-associated trees on forest floor leaf litter or soil property $Y$ manifests at the stand scale such that the magnitude of ECM effects on forest floor leaf litter or soil properties scales with an ECM dominance term (Craig et al., 2018; Phillips et al., 2013):

$$ECM\ dominance = \frac{BA_{ECM}}{BA_{total}}$$

where $BA_{ECM}$ is the basal area of all trees within 20 m of a soil sampling location and $BA_{total}$ is the basal area of all ECM and AM-associated trees within 20 m of a sampling location.

In our spatially explicit alternative models, the effect of individual ECM-associated trees on forest floor leaf litter or soil property *Y* was expected to vary based on its DBH and as an inverse function of the distance to the neighbor. The total effect of $i = 1\ldots..n$ ECM-associated trees within a 20m radius of sampling points (neighborhood) was determined using the following equation:

$$neighborhood = \sum_{i=1}^{n} DBH_i^{\alpha} \exp(-\lambda * distance_i^{\beta})$$

where $DBH_i$ is the diameter at breast height of the $i^{th}$ ECM-associated tree and $distance_i$ is the distance to the $i^{th}$ ECM-associated tree. We set $\alpha = 2$ implying that the effect of an ECM-associated tree varies approximately linearly with plant biomass (Jenkins et al., 2003) and $\beta = 1$ such that the decrease in the ECM tree effect with distance follows a negative exponential decay. The parameter $\lambda$ determines the steepness of the decline of the ECM-associated tree effect with distance.

We ran the set of linear and non-linear models outlined in Table A.3 using the non-spatially explicit ECM-dominance term or the spatially explicit neighborhood term as the independent variables. We determined the parameter estimate that maximized the log likelihood given our observed data using simulated annealing, a global optimization procedure using the likelihood package (Murphey, 2015) in R (R Core Team, 2019). For each forest floor leaf litter and soil property, we used the $R^2$ of the observed vs. predicted regression as a metric of goodness of fit and used the slope as a measure of bias (Gómez-Aparicio and Canham, 2008). The $R^2$ values we report reflect models fit to a single forest floor leaf litter or soil property measured for all 68 sampling locations collected along mycorrhizal gradients across our four watersheds. We compared alternative models using the Akaike Information Criterion ($AIC_c$) corrected for small

sample sizes (Burnham and Anderson, 2002). For each parameter estimate, we used upper and lower support intervals to assess the strength of evidence for individual maximum-likelihood parameter estimates (Edwards, 1992). We considered there to be strong evidence for a model if all other alternative models had $AIC_c$ values that were 5 or more units higher, and weak evidence for a model if other alternative models were within 2 $AIC_c$ units.

**Statistical analysis for deep soil samples**

We fit linear models in R 3.6.2 (R Core Team 2019). Statistical significance was determined based on $P < 0.05$. To test for differences in C and N stocks and concentrations between soil samples taken in 20 cm increments to 1 m depth, we conducted two-way ANOVAs with watershed, stand mycorrhizal association (ECM or AM) and the interaction between watershed and stand mycorrhizal association as fixed effects and each soil property as the dependent variable. Post-hoc comparisons among watersheds and stand mycorrhizal association were performed using Tukey honestly significant difference (HSD) tests. To test for watershed differences in ECEC and percent BS between mineral soils at 0-20 cm depth from AM stands in four watersheds we conducted one-way ANOVAs with watershed as the fixed effect. Dependent variables were ln-transformed when necessary to achieve normally distributed residuals as determined using the Shapiro-Wilk test.

## RESULTS

**ECM effects on soil properties at the neighborhood to stand scales**

Variation in O horizon depth and C concentration were the only forest floor leaf litter or soil properties best described by spatially explicit models ($R^2$ = 0.65 and 0.69 for O horizon

depth and C concentration, respectively; Figure 2.1a, A.1a). For these models, the neighborhood parameter was used as the independent variable, taking into account the mycorrhizal association, DBH and spatial distribution of all trees within 20 m of a sampling point ($R^2$ = 0.65 and 0.69 for O horizon depth and C concentration, respectively; Figure 2.1a, A.1a). For both O horizon depth and C concentration, the neighborhood value of a tree decreased gradually as the distance between the tree and the sampling point increased ($\lambda$ = 0.13 and 0.15, respectively; Figure A.2ab).

In general, properties measured for forest floor leaf litter, O horizon, bulk mineral soils, and POM and MAOM fractions (other than O horizon depth and C concentration) were better explained by the percent basal area of ECM-associated trees within a 20m radius of a sampling point (non-spatial models) than by basic mean models in which the effect of ECM-associated trees was ignored or by spatially explicit models which considered the effect of an ECM-associated tree to be proportional to its DBH and distance from the sampling point (Table A.4). In only seven cases, the watershed-means model, which estimates dependent variables as the mean of that variable in each watershed, had the lowest $AIC_c$ values (Table A.4).

**ECM effects on soil properties across watersheds**

For 25 of the forest floor leaf litter and soil chemical properties we measured, models including at least one watershed specific parameter (that was not the intercept) were the best fit (Table A.4). This signifies variation among watersheds in the rate or direction of change in forest floor leaf litter or soil chemical properties along gradients of ECM dominance. We found strong evidence for a watershed-dependent relationship between pH and ECM dominance ($R^2$=0.85, 0.80, and 0.74 for the O horizon, 0-10 cm depth mineral soil, and 10-20 cm depth mineral soil,

respectively). Soils in Alto Frio and Hornito were consistently less acidic than Zorro and Honda in AM-dominated stands, with a greater rate of change in pH with ECM dominance in Alto Frio and Hornito such that pH converged around 3.5-4.5 in ECM dominant stands across all watersheds (Figure 2.2, A.3ab). In contrast, $\delta^{15}N_{litter}$ and O horizon depth were similar among watersheds in AM-dominated stands but diverged among watersheds at high levels of ECM dominance and high neighborhood values respectively ($R^2$=074, 0.65 respectively; Figure 2.1ab), with a stronger effect of tree mycorrhizal type apparent in the lower pH, lower fertility watersheds, Zorro and Honda. Watershed-dependent variation in O horizon depth likely drove patterns in O horizon SOC and TN stocks which increased with ECM dominance following non-linear curves that describe initially slow rates of change in SOC and TN stocks at low levels of ECM dominance followed by a rapid increase as ECM dominance increases ($R^2$ = 0.56 and 0.41, for SOC and TN stocks, respectively; Figure A.1cd).

Across all watersheds, bulk mineral soil and MAOM C:N ratios increased along mycorrhizal gradients (Figure 2.3ab; $R^2$ = 0.52, 0.65, respectively) driven by bulk mineral soil and MAOM SOC stocks which decreased with ECM dominance more slowly than bulk mineral soil and MAOM TN stocks (Figure A.4a-d). However, C:N ratios increased at different rates among watersheds. Particulate organic matter C:N ratios followed a similar watershed-dependent pattern as bulk mineral soil and MAOM C:N ratios ($R^2$=61): C:N ratios increased at the fastest rate along a mycorrhizal gradient in Alto Frio relative to the other three watersheds (Figure 2.3a-c). However, unlike bulk mineral soil and MAOM C:N ratios, there was no apparent effect of ECM dominance on POM C:N ratios in Hornito, Honda or Zorro (Figure 2.3c). Similarly, the effect of ECM dominance on the ratio of SOC and TN stored in MAOM relative to POM mineral soil fractions was greater in Alto Frio relative to the other three watersheds ($R^2$ = 0.72 and 0.65

for SOC and TN, respectively; Figure 2.4ab). In Alto Frio the proportion of SOC and TN stored in MAOM relative to POM decreased with ECM dominance while this proportion remained relatively constant across mycorrhizal gradients in Hornito, Honda and Zorro (Figure 2.4ab).

Across all watersheds, we found that ECM dominance was consistently a strong predictor of mineral soil $\delta^{15}N$ patterns. However, the effect of ECM dominance on $\delta^{15}N_{MAOM\text{-}litter}$ and $\delta^{15}N_{POM\text{-}litter}$ was non-linear and varied among watersheds with distinct responses in higher pH, higher fertility watersheds, Alto Frio and Hornito, relative to lower pH, lower fertility watersheds, Honda and Zorro ($R^2$ = 0.75, 0.75, for $\delta^{15}N_{MAOM\text{-}litter}$ and $\delta^{15}N_{POM\text{-}litter}$ at the 0-10 cm mineral soil depth, respectively) (Figure 2.5ab). In the lower pH, lower fertility watersheds, Honda and Zorro, $\delta^{15}N_{MAOM\text{-}litter}$ and $\delta^{15}N_{POM\text{-}litter}$ began increasing exponentially at an ECM dominance level of approximately 0.2 before leveling off at an ECM dominance level of approximately 0.4 (Figure 2.5ab). In the higher pH, higher fertility watersheds, Alto Frio and Hornito, $\delta^{15}N_{MAOM\text{-}litter}$ and $\delta^{15}N_{POM\text{-}litter}$ decreased slightly between ECM dominance values of 0.2 to 0.4, or did not change along a mycorrhizal gradient (Figure 2.5ab).

Although the effect of ECM dominance on some forest floor leaf litter and soil properties varied in strength and direction among watersheds, for other soil properties, the effect of ECM dominance was consistent across all four watersheds. Forest floor leaf litter C:N ratios increased linearly ($R^2$ = 0.26) from species rich AM stands to *O. mexicana* dominated stands (Figure 2.6a) with slope and intercept parameter estimates constant across watersheds. The observed positive relationship between forest floor leaf litter C:N and ECM dominance was driven by leaf litter C concentrations which also increased linearly with ECM dominance ($R^2$ = 0.40; Figure A.5a). In contrast, ECM dominance did not predict variation in leaf litter TN concentrations (Figure A.5b). Furthermore, we found that O horizon SOC and TN concentrations increased with ECM

dominance and MAOM SOC and TN stocks decreased with ECM dominance at the same rate across all watersheds (Figure A.1ab, A.4cd). For O horizon C:N ratios, the model with the lowest $AIC_c$ values suggested a watershed-dependent effect of ECM dominance ($R^2$ = 0.17; Figure 2.6b). However, the mean model, which estimated O horizon C:N ratios as a single mean across all watersheds had an $AIC_c$ value that was only 0.33 units higher than the linear model described above. Therefore, the models provide weak evidence for an effect of ECM dominance on O horizon C:N ratios.

Although we found a strong watershed dependent relationship between ECM dominance and N isotopes in the leaf litter and mineral soil fractions, ECM dominance explained relatively little variation in $\delta^{13}C_{litter}$, $\delta^{13}C_{MAOM\text{-}litter}$ or $\delta^{13}C_{POM\text{-}litter}$ ($R^2$ = 0.20, 0.19 and 018 for $\delta^{13}C_{litter}$, and $\delta^{13}C_{MAOM\text{-}litter}$ and $\delta^{13}C_{POM\text{-}litter}$ at 0-10 cm depth, respectively). There was no change in $\delta^{13}C_{litter}$, $\delta^{13}C_{MAOM\text{-}litter}$ or $\delta^{13}C_{POM\text{-}litter}$ in any of the four watersheds (Figure 2.5cd).

**Effect of stand mycorrhizal type on soil chemical properties of deep mineral soil profiles**

Mineral soil total N stocks were significantly greater in *O. mexicana* dominated relative to AM mixed forest stands measured cumulatively through the soil profile to 1 m depth or 108.95 g mineral soil equivalent ($F_{1, 15}$=4.99, $p$=0.04), but mineral SOC stocks were unaffected by stand mycorrhizal association. When we compared total N stocks and concentrations between stand mycorrhizal types for each 20 cm soil depth interval sampled, the effect of stand mycorrhizal association was only significant in surface mineral soils (0-15.68 g mineral soil mass equivalent or roughly 0-20 cm soil depth) ($F_{1, 16}$ = 6.79, $p$=0.02 and $F_{1,16}$=7.25, $p$=0.02, respectively) (Figure A.6a-c).

Base saturation (BS) and effective cation exchange capacity (ECEC; cmol (+) kg soil$^{-1}$), in AM stand soils at 0-20 cm depth differed significantly among watersheds ($F_{3,8}$= 64.4, $p$<0.0001; $F_{3,8}$= 10.2, $p$=0.004, respectively). Post-hoc pairwise comparisons show significantly higher percent BS and ECEC in Alto Frio and Hornito relative to Zorro and Honda with no differences between Alto Frio and Hornito or between Zorro and Honda (Table 2.1). Although ECEC trended lower in Honda compared to Alto Frio and Hornito, this difference was not statistically significant (Table 2.1).

## DISCUSSION

Soil C and N storage in POM and MAOM fractions have been shown to scale with percent ECM basal area in temperate forests (Craig et al., 2018), yet uncertainty remains in the generality of ECM effects across different spatial scales at which soil properties are known to vary. ECM effects in mixed mycorrhizal forest may be spatially variable, depending on the size and spatial distribution of ECM-associated trees and on abiotic conditions that alter the composition of ECM communities and their hosts. We utilized censused forest within four watersheds where ECM-associated *O. mexicana* dominated stands established within high-diversity AM forest, and tested the magnitude and direction of ECM effects at the scale of a tree neighborhood, along mycorrhizal gradients and between watersheds that differ in soil pH, fertility and climate. Consistent with studies conducted in temperate forests, we found that the C:N ratios of forest floor leaf litter and mineral soil layers increased with ECM dominance across mycorrhizal gradients in all watersheds. However, based on patterns in O horizon accumulation, POM:MAOM ratios and $\delta^{15}N$, we deduce that bulk soil patterns may be driven by distinct mechanisms in watersheds with higher soil pH and fertility, defined by higher effective

cation exchange capacity and base saturation (Table 2.2), compared to those with lower soil pH and fertility. Here we discuss evidence from our study suggesting that edaphic conditions may alter the mechanisms underlying ECM effects on soil C and N storage in POM and MAOM fractions as well as broader implications for generalizing ECM effects at the global scale.

**Spatial variation in ECM effects within tree neighborhoods**

An individual tree may impact ecosystem properties at the neighborhood scale (0-25 m) via processes such as litterfall, root turnover, or mycorrhizal symbioses, helping to explain spatial heterogeneity in forest floor leaf litter and soil properties (Bigelow and Canham, 2017; Binkley and Giardina, 1998; Gómez-Aparicio and Canham, 2008). However, we found that ECM effects varied between forest stands that differed in percent ECM basal area, but not necessarily at the scale of individual ECM-associated trees. Processes occurring at the spatial scale of a single tree may be less important in forest stands dominated by a single tree species where rooting and litterfall zones of neighboring conspecific individuals overlap, increasing uniformity in the soil environment (Friggens et al., 2020). In Fortuna, ECM-associated *O. mexicana* tend to dominate forest stands where they grow, limiting our sample size at intermediate levels of ECM dominance, and possibly constraining our capacity to detect spatial variability using neighborhood modelling techniques. While ECM effects average at the stand scale in Fortuna, more detailed spatial analysis may be warranted in forests with greater intermixing of ECM and AM species.

In contrast to most forest floor leaf litter and soil properties we measured, variation in O horizon depth and C concentration along mycorrhizal gradients were best explained by a spatially-explicit neighborhood term. Organic horizon formation in ECM stands may occur

through accumulation of fine roots and associated ECM biomass (Clemmensen et al., 2013; Hölscher et al., 2009), leading to predictable variation in O horizon properties at the spatial scale of *O. mexicana* fine root production. Individual tree effects may be more apparent for O horizon properties relative to forest floor leaf litter or mineral soil properties which may be shaped by more spatially dynamic processes: in Fortuna, windy conditions may disperse litterfall onto the forest floor, and high rainfall and bioturbation may cause vertical and lateral movement of organic matter into and through the mineral soil. Additionally, O horizon SOM accumulation may reflect the current distribution of trees while mineral soil SOM accumulation may reflect past distribution of trees because O horizon turnover occurs more rapidly than mineral soil SOM turnover (Gaudinski et al., 2000). Overall, this suggests that averaging soil properties at the stand scale may not accurately capture the effect of ECM-associated trees on O horizon SOM dynamics.

**Variation in O horizon properties across mycorrhizal gradients**

Although past studies show that POM accounts for a greater proportion of OM stocks in ECM relative to AM stands, variation in environmental context and soil properties may determine whether POM accumulation occurs in a surface organic horizon (Craig et al., 2018) or in the underlying mineral soil (Cotrufo et al., 2019). Consistent with this proposed mechanism, we found that the effect of ECM dominance on O horizon depth and mineral soil POM:MAOM ratios varied among mycorrhizal gradients established on soils that differ in pH and fertility. In the highest pH, highest fertility watershed where O horizon depth was minimal along a mycorrhizal gradient, we found patterns consistent with those reported in temperate forests (e.g., Cotrufo et al., 2019; Craig et al., 2018): the proportion of C and N stored in mineral soil POM

increased with ECM dominance, driving a concurrent increase in bulk mineral soil C:N ratios. In the other three watersheds where O horizon depth increased along mycorrhizal gradients, POM:MAOM ratios for C and N in the mineral soil were relatively unaffected by ECM dominance, corresponding to a less dramatic relationship between ECM dominance and bulk mineral soil C:N ratios. However, in one of these three watersheds, which was characterized by higher pH and fertility relative to the other two, O horizon formation was less significant and POM:MAOM ratios were lower at all levels of ECM dominance. Low soil fertility may promote O horizon formation by increasing root mortality and stimulating growth of replacement roots (Moser et al., 2011). Further, suppressed decomposition under acidic, low fertility conditions may result in accumulation of the resulting root necromass (Moser et al., 2011). Alternatively, the O horizon may form due to fine root proliferation at the soil surface which increases the efficiency of nutrient capture from leaf litter inputs when soil nutrient availability is low (Moser et al., 2011). Although ECM effects and underlying soil fertility are known to alter POM accumulation dynamics, the interaction between these two mechanisms remains uncertain. Does soil fertility mediated O horizon formation alter ECM effects on SOM formation and persistence in the mineral soil?

The presence of an O horizon may affect the composition and function of the underlying mineral soil MAOM fraction by filtering dissolved organic matter (DOM) (Fröberg et al., 2005; Sokol & Bradford, 2019), an important precursor of MAOM (Kaiser and Kalbitz, 2012; Kalbitz et al., 2005; Kalbitz and Kaiser, 2008). Intrinsically labile compounds derived from plants and microbes in the litter layer may be adsorbed or respired while passing through an organic horizon where microbial activity is high (Sokol and Bradford, 2019). Therefore, DOM leaching from the O horizon may be largely composed of organic compounds derived from roots and associated

mycorrhizal hyphae (Fröberg et al., 2007; Fröberg et al., 2005) which underlie O horizon formation in ECM systems (Clemmensen et al., 2013; Hölscher et al., 2009). In lower pH, lower fertility watersheds where O horizon depth increased along mycorrhizal gradients, we found a concomitant increase in $\delta^{15}N_{MAOM\text{-}litter}$. This positive relationship between O horizon depth and $\delta^{15}N_{MAOM\text{-}litter}$ could reflect increasing contributions of O horizon derived compounds to DOM which can form MAOM by direct sorption or *in-vivo* microbial turnover (Sokol et al., 2019). Dissolved organic matter that is directly or indirectly derived from ECM roots and associated mycorrhizal hyphae is expected to be $^{15}N$-enriched relative to DOM derived from leaf litter because ECM transfer $^{15}N$-depleted N to their hosts and retain $^{15}N$-enriched N in their biomass (Hobbie and Högberg, 2012; Hogberg et al., 1996). Additionally, $^{15}N$ enrichment of the MAOM pool could result from greater microbial processing of DOM that passes through an O horizon (Sollins et al., 2009). In higher pH, higher fertility watersheds where O horizon depth increased less along mycorrhizal gradients, $\delta^{15}N_{MAOM\text{-}litter}$ did not shift with changes in ECM dominance, suggesting that $^{15}N$ enriched compounds derived from ECM hyphae make a smaller contribution to MAOM in ECM stands established on higher fertility soils. Importantly, compositional differences between DOM that leaches directly from leaf litter into the mineral soil (in the absence of an O horizon) versus DOM that leaches through leaf litter and an O horizon before passing into the mineral soil may have functional implications in terms of MAOM persistence (Haddix et al., 2020; Kaiser and Guggenberger, 2000) because DOM composition can determine its degradability even after being stabilized on a mineral surface (Kalbitz et al., 2005). Overall, changes in soil pH and fertility that mediate POM accumulation along mycorrhizal gradients may also affect MAOM formation and persistence within the mineral soil and alter the effect of ECM dominance on SOM (Figure 2.7).

**Variation in ECM effects among watersheds**

We observed watershed-scale variation in accumulation patterns of SOC and TN in POM and MAOM mineral soil fractions and in changes to organic horizon SOC and TN stocks along mycorrhizal gradients. These patterns align with decreasing $\delta^{15}N_{litter}$ and increasing $\delta^{15}N_{MAOM\text{-}litter,\ POM\text{-}litter}$ along mycorrhizal gradients in lower pH, lower fertility watersheds. Lower $\delta^{15}N_{litter}$ at high levels of ECM dominance suggests N-limitation is increased by establishment of *O. mexicana* and associated fungal communities in lower pH, lower fertility watersheds such that host tree productivity relies more on transfer of $^{15}N$-depleted N from ECM. Past studies report a positive feedback between ECM and N limitation, finding that greater belowground C allocation by host trees under N limited conditions increases N immobilization within ECM biomass, ultimately driving the system towards even greater N limitation (Franklin et al., 2014; Näsholm et al., 2013). However, given that we sampled mixed species forest floor leaf litter, as opposed to foliar litter, decomposition stage may have a confounding effect on $\delta^{15}N_{litter}$ patterns. Specifically, microbes preferentially mineralize the lighter nitrogen isotope during decomposition of organic nitrogen resulting in continual $^{15}N$-enrichment of leaf litter through the decomposition process. Therefore, in addition to indicating increased N limitation of host trees, lower $\delta^{15}N_{litter}$ at high levels of ECM dominance in lower pH, lower fertility watersheds could reflect accumulation of less decomposed forest floor leaf litter. High $\delta^{15}N_{MAOM\text{-}litter,\ POM\text{-}litter}$ in stands with lower $\delta^{15}N_{litter}$ suggests a greater contribution of $^{15}N$-enriched ECM biomass to SOM at high levels of ECM dominance in lower pH, lower fertility watersheds experiencing greater N-limitation. While greater ECM infection frequency in higher pH, higher fertility watersheds compared to lower pH, lower fertility watersheds in Fortuna suggests that ECM infection may be constrained by low pH and fertility (Corrales et al., 2016a), ECM infection frequency does not

necessarily dictate N transfer between ECM and their host trees or ECM biomass production. Instead, the establishment of functionally distinct ECM taxa in the lower versus higher fertility watersheds could play a role. Specifically, high biomass ECM fungi with medium or long exploration types which have been found to dominate in low pH, low N soils average 4-7‰ more enriched in $^{15}N$ than low biomass ECM fungi with short-distance exploration types that may dominate where nutrient availability is higher (Hobbie and Agerer, 2010; Lilleskov et al., 2002; Sterkenburg et al., 2015). Variation in $^{15}N$ enrichment among ECM taxa may be attributed to different underlying mechanisms related to ECM function: $^{15}N$-enriched ECM biomass may signal organic N uptake, formation of long-lived mycelial tissues with greater capacity for metabolic processing, and/or greater N transfer to host trees (Trudell et al., 2004). Ultimately, functional traits selected for by low pH, low fertility conditions may result in greater contribution of ECM biomass to belowground SOM and/or greater transfer of N to host trees, leading to the $\delta^{15}N$ patterns along mycorrhizal gradients observed in the lower pH, lower fertility watersheds that were not observed in the higher pH, higher fertility watersheds (Figure 2.7).

**Why might C isotopes tell a different story than N isotopes?**

Although patterns in $\delta^{15}N$ of the mineral soil fractions yielded insight into the mechanism contributing to SOM dynamics along mycorrhizal gradients in lower versus higher fertility watersheds, we found no effect of ECM dominance on $\delta^{13}C_{POM\text{-}litter}$ or $\delta^{13}C_{MAOM\text{-}litter}$ in any of the watersheds. Other studies have similarly reported that mycorrhizal mediation of C isotopes is weaker than mycorrhizal mediation of N isotopes (Corrales, 2016; Högberg et al., 2020; Wallander et al., 2009). Leaf and root litter, saprotrophic fungi and AM fungi are $^{15}N$-depleted relative to ECM fungi such that $^{15}N$ enrichment of the soil should increase as ECM fungi

contribute more to the SOM pool. However, average $\delta^{13}C$ enrichment of ECM fungi is intermediate between leaf litter, which is relatively $^{13}C$-depleted, and saprotrophic fungi, which are relatively $^{13}C$-enriched (Kohzu et al., 1999; Mayor et al., 2009). Therefore, we may expect ECM dominance to be a poor predictor of $\delta^{13}C_{POM\text{-}litter}$ and $\delta^{13}C_{MAOM\text{-}litter}$ if we assume that, in our relatively acidic forest soils, compounds derived from leaf litter, root litter, saprotrophic fungi and arbuscular mycorrhizal fungi underlie POM and MAOM formation in AM systems and compounds derived from ECM fungi and associated roots underlie POM and MAOM formation in ECM systems. Variation in $\delta^{13}C$ in SOM pools might also reflect decomposition dynamics because $\delta^{13}C$ increases as $^{12}C$ is preferentially respired during microbial decomposition (Werth and Kuzyakov, 2010). We may expect this to manifest along mycorrhizal gradients within our watersheds, leading to a positive relationship between ECM dominance and $\delta^{13}C_{POM\text{-}litter}$ or $\delta^{13}C_{MAOM\text{-}litter}$ because AM soils are often characterized by rapid C cycling relative to ECM stands (Phillips et al., 2013). However, differences in microbial respiration between ECM and AM stands suggested to drive $\delta^{13}C$ patterns along mycorrhizal gradients may be less apparent in our high rainfall study site where leaching may be an important decomposition loss pathway (Cleveland et al., 2006; Seyfried et al., 2021b). Overall, the factors affecting $^{13}C$-enrichment of SOM fractions are difficult to disentangle, such that, in our study system, there is no clear relationship between $\delta^{13}C$ of SOM pools and ECM dominance.

## CONCLUSION

We found that ECM effects on SOM pools occurred at the stand scale rather than the individual tree neighborhood scale in a tropical montane forest, with variation in ECM effects among watersheds and along mycorrhizal gradients. Although forest floor leaf litter and mineral

C:N ratios consistently increased with ECM dominance across watersheds, ECM effects on O horizon formation and the composition of SOM differed among watersheds. Based on patterns in O horizon accumulation, POM:MAOM ratios and $\delta^{15}N$, we deduce that bulk soil patterns may be driven by distinct mechanisms in watersheds with higher soil pH and fertility, compared to those with lower soil pH and fertility. We postulate two possible mechanisms by which edaphic conditions, such as soil pH and fertility, may alter ECM effects on SOM composition and persistence. First, although it is well-established that increasing ECM dominance leads to greater C storage in the POM fraction of SOM (Cotrufo et al., 2019; Craig et al., 2018), lower soil pH and fertility may promote greater POM accumulation in an O horizon while higher soil pH and fertility may promote POM accumulation in the mineral soil. The resulting variation in O horizon depth may have functional implications for MAOM formation and persistence. Second, soil pH and fertility may alter ECM community composition and function. In lower pH, lower fertility watersheds high biomass ECM taxa with medium or long-distance exploration types and the functional capacity to uptake organic nutrients may alter decomposition dynamics, and contribute more, slow-decomposing substrate to the belowground C pool. Overall, our results demonstrate that ECM effects on SOM pools cannot be assumed based solely on ECM dominance within a forest stand, but depend on edaphic factors such as soil pH and fertility. This elucidates observations that mycorrhizal effects on SOM pools are not consistent across sites (Craig et al., 2019; Midgley and Sims, 2020; Soudzilovskaia et al., 2019) and informs efforts to model mycorrhizal effects on soil carbon and nitrogen cycling at the global scale (e.g., Sulman et al., 2019).

## TABLE AND FIGURES

**Table 2.1.** Soil properties for ECM- and AM-dominated stands within four watersheds in Fortuna (Mean ± SE, n =3). Two lower fertility watersheds, Honda and Zorro, are characterized by lower effective cation exchange capacity (ECEC; cmol (+) $kg^{-1}$) and base saturation (BS) within AM-dominated forest relative to two higher fertility watersheds, Hornito and Alto Frio.

| | | Honda: lower fertility | | Zorro: lower fertility | | Hornito: higher fertility | | Alto Frio: higher fertility | |
|---|---|---|---|---|---|---|---|---|---|
| | Depth (cm) | ECM-dominated stand | AM-dominated stand | ECM-dominated stand | AM-dominated stand | ECM-dominated stand | AM-dominated stand | ECM-dominated stand | AM-dominated stand |
| ECEC (cmol (+) $kg^{-1}$) | 0-20 | 7.19 +/- 1.40 | 9.85 +/- 1.27 | 4.64 +/- 0.18 | 5.38 +/- 0.77 | 7.60 +/- 1.21 | 12.47 +/- 2.56 | 5.77 +/- 0.85 | 12.28 +/- 1.67 |
| | 20-40 | 3.75 +/- 0.43 | 5.19 +/- 0.57 | 2.75 +/- 0.29 | 2.87 +/- 0.34 | 5.68 +/- 0.24 | | 4.48 +/- 0.34 | 6.21 +/- 0.85 |
| Base saturation | 0-20 | 23.93 +/- 4.811 | 30.64 +/- 4.14 | 36.48 +/- 2.86 | 34.62 +/- 5.52 | 22.05 +/- 0.70 | 86.79 +/- 6.95 | 55.86 +/- 12.03 | 95.32 +/- 1.64 |
| | 20-40 | 54.01 +/- 4.08 | 27.26 +/- 0.94 | 64.49 +/- 11.48 | 45.75 +/- 6.59 | 19.46 +/- 1.89 | | 39.95 +/- 10.92 | 93.82 +/- 1.05 |
| C:N | 0-20 | 14.54 +/- 0.71 | 14.70 +/- 0.09 | 14.60 +/- 0.92 | 13.64 +/- 0.39 | 15.07 +/- 0.59 | 10.76 +/- 0.26 | 15.08 +/- 0.76 | 11.16 +/- 0.46 |
| | 20-40 | 14.34 +/- 0.62 | 14.09 +/- 0.57 | 14.90 +/- 0.66 | 14.42 +/- 0.98 | 13.19 +/- 1.30 | 12.75 +/- 1.93 | 13.57 +/- 0.76 | 10.71 +/- 0.14 |

**Figure 2.1.** The relationship between ectomycorrhizal-associated *Oreomunnea mexicana* dominance and organic horizon properties as described by a spatially explicit neighborhood models for (a) organic horizon depth (N=63, $R^2$ = 0.65) and by non-spatial likelihood models for (b) forest floor leaf litter $\delta^{15}N$ (N=63, $R^2$ = 0.74). Colored lines indicate relationships for each of the following four watersheds when watershed-specific slope and/or intercept parameter estimates were significant in the model: Alto Frio (green), Honda (orange), Hornito (purple) and Zorro (pink). Shaded regions indicate 2-unit support intervals.

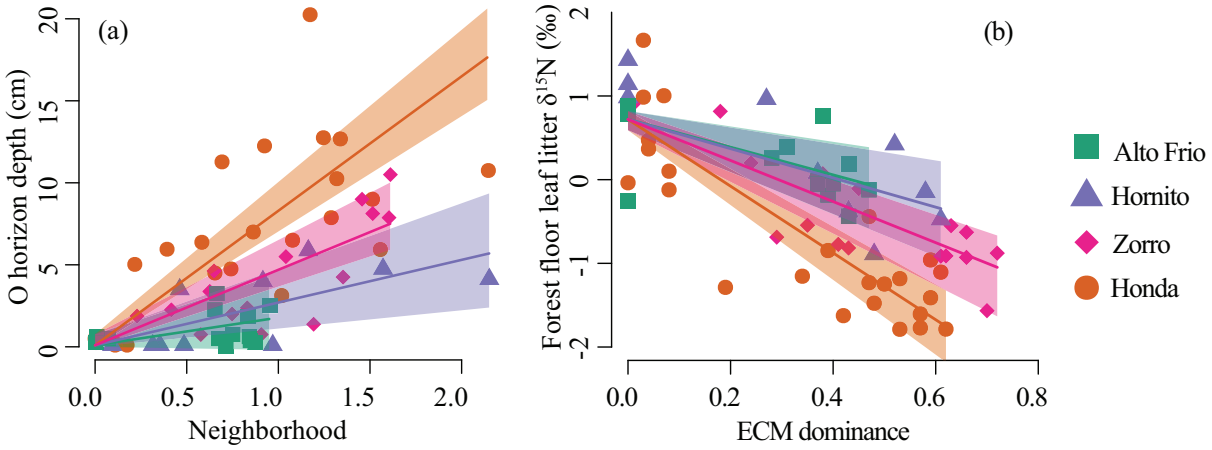

**Figure 2.2.** The relationship between ectomycorrhizal-associated *Oreomunnea mexicana* dominance (percent basal area *O. mexicana*) and pH in the 0-10 cm depth mineral soil (N=64, $R^2$ = 0. 80) as described by non-spatial likelihood models. Colored lines indicate relationships for each of the following four watersheds when watershed-specific slope and/or intercept parameter estimates were significant in the model: Alto Frio (green), Honda (orange), Hornito (purple) and Zorro (pink). Shaded regions indicate 2-unit support intervals.

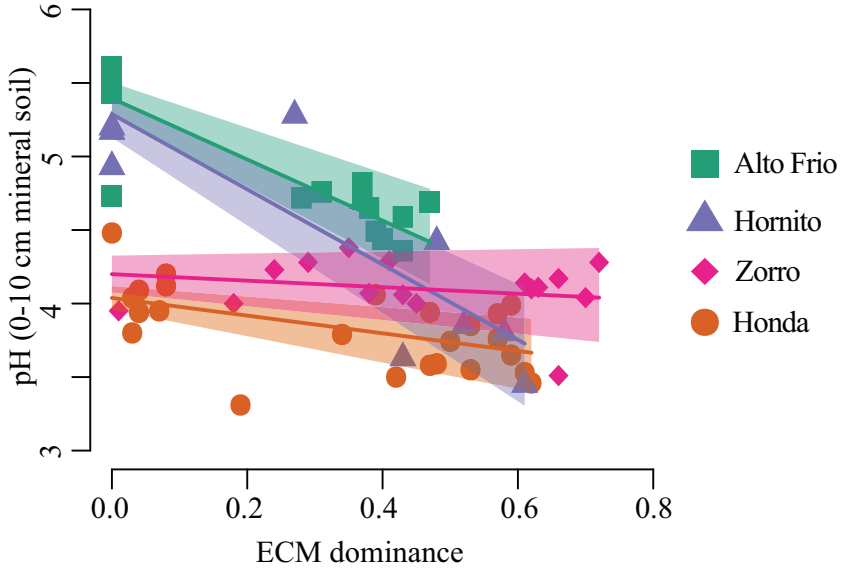

**Figure 2.3.** The relationship between ectomycorrhizal-associated *Oreomunnea mexicana* dominance and 0-20 cm depth mineral soil C:N ratios as described by non-spatial likelihood models: (a) bulk mineral soil (N=62, $R^2$ = 0.52), (b) MAOM fraction (N=63, $R^2$ = 0.65) and (c) POM fraction (N=63, $R^2$ = 0.61). Colored lines indicate relationships for each of the following four watersheds when watershed-specific slope and/or intercept parameter estimates were significant in the model: Alto Frio (green), Honda (orange), Hornito (purple) and Zorro (pink). Shaded regions indicate 2-unit support intervals.

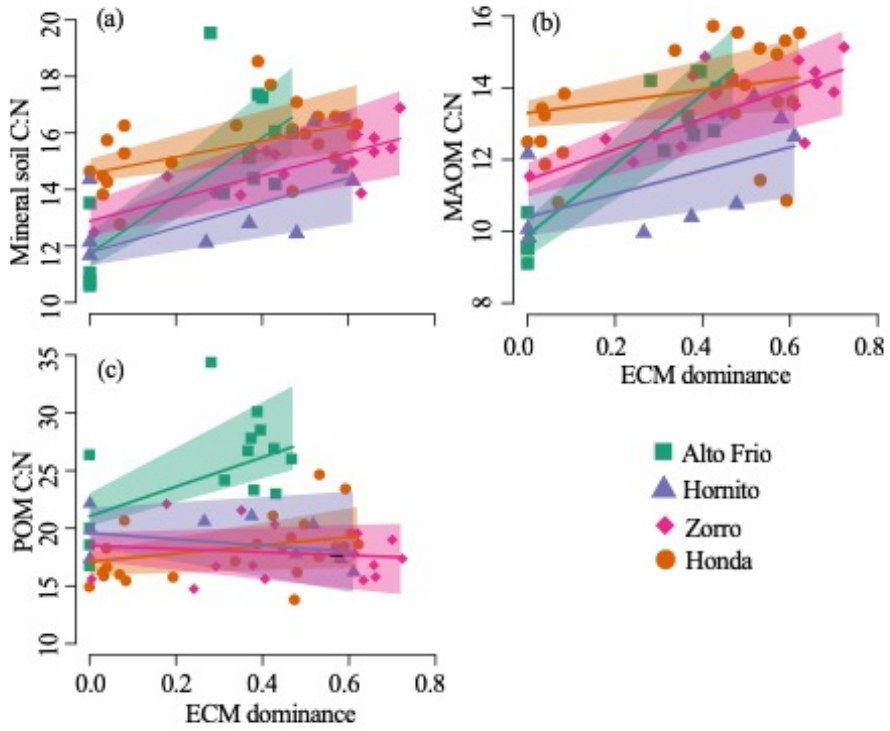

**Figure 2.4.** The relationship between ectomycorrhizal-associated *Oreomunnea mexicana* dominance and the MAOM:POM ratios for (a) soil organic carbon (N=63, $R^2$=0.72) and (b) total nitrogen (N=63, $R^2$=0.65) in the 0-10 cm depth mineral soil as described by non-spatial likelihood models. Colored lines indicate relationships for each of the following four watersheds when watershed-specific slope and/or intercept parameter estimates were significant in the model: Alto Frio (green), Honda (orange), Hornito (purple) and Zorro (pink). Shaded regions indicate 2-unit support intervals.

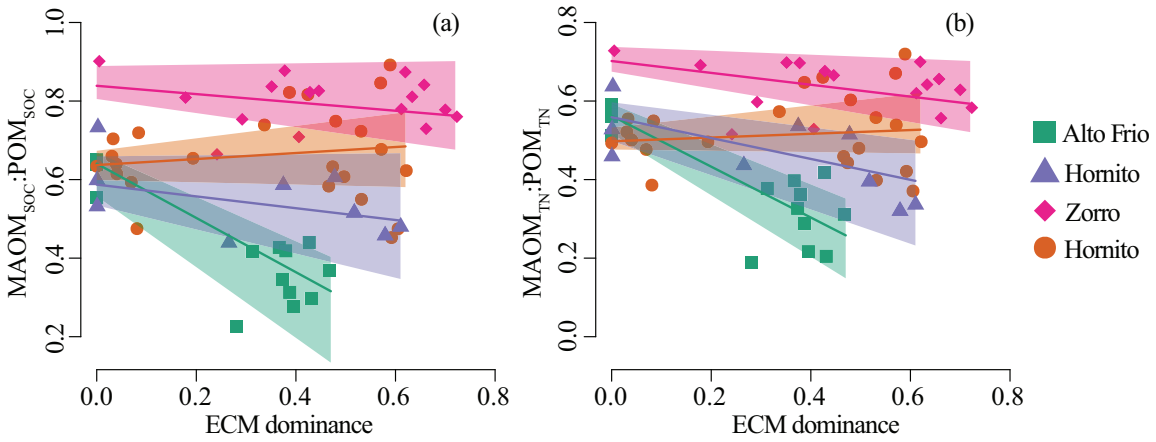

**Figure 2.5.** The relationship between ectomycorrhizal-associated *Oreomunnea mexicana* dominance and the following mineral soil properties at 0-10 cm depth, (a) $\delta^{15}N_{MAOM\text{-}litter}$ (N=64, $R^2$ = 0.75), (b) $\delta^{15}N_{POM\text{-}litter}$ (N=64, $R^2$ = 0.75), (c) $\delta^{13}C_{MAOM\text{-}litter}$ (N=64, $R^2$ = 0.19) and (d) $\delta^{13}C_{POM\text{-}litter}$ (N=64, $R^2$ = 0.38), as described by non-spatial likelihood models. Colored lines indicate relationships for each of the following four watersheds when watershed-specific slope and/or intercept parameter estimates were significant in the model: Alto Frio (green), Honda (orange), Hornito (purple) and Zorro (pink). Shaded regions indicate 2-unit support intervals.

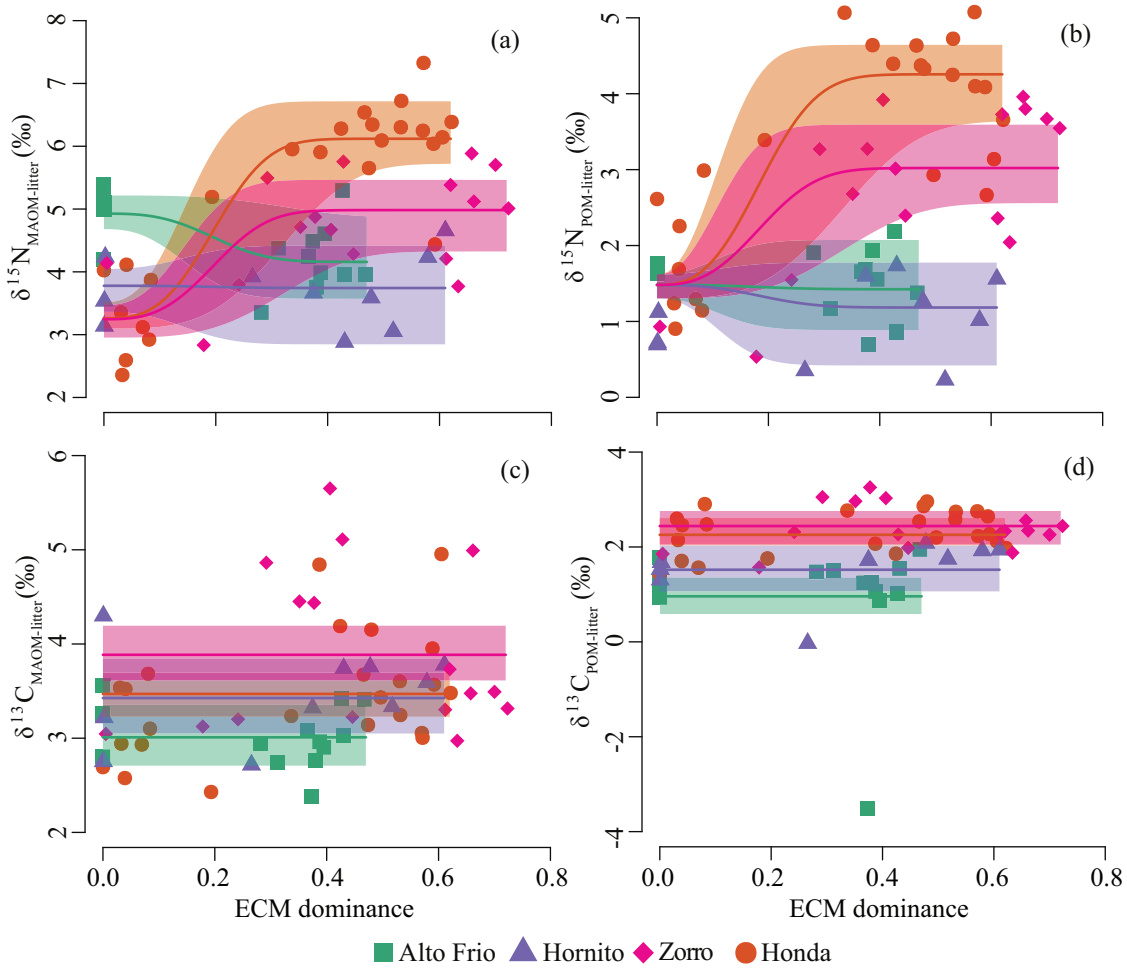

**Figure 2.6.** The relationship between ectomycorrhizal-associated *Oreomunnea mexicana* dominance and (a) forest floor leaf litter C:N ratios (N=63, $R^2$ = 0.26 and (b) O horizon C:N ratios (N=63, $R^2$ = 0.17), Colored lines indicate relationships for each of the following four watersheds when watershed-specific slope and/or intercept parameter estimates were significant in the model: Alto Frio (green), Honda (orange), Hornito (purple) and Zorro (pink). A single black line represents the relationship for all watersheds together when the relationship did not vary among the four watersheds. Shaded regions indicate 2-unit support intervals.

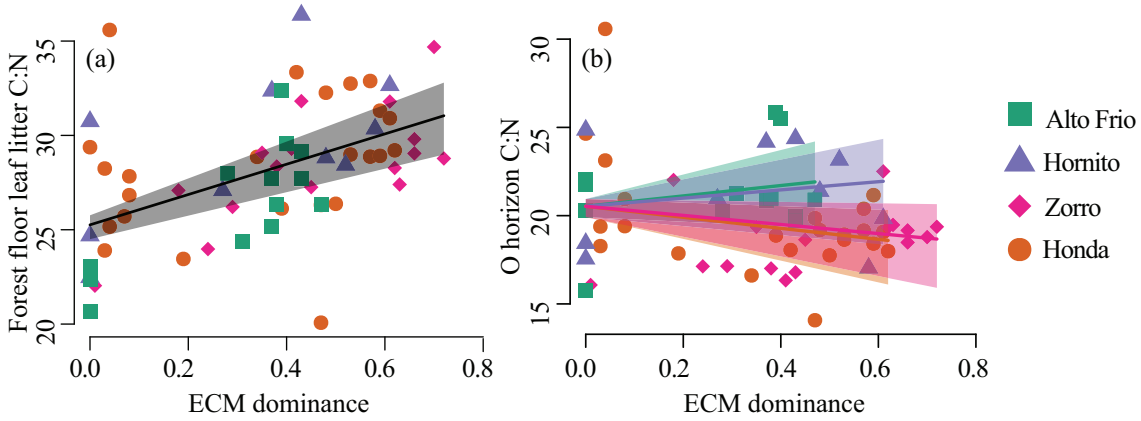

**Figure 2.7.** Conceptual model illustrating the potential effects of ectomycorrhizal (ECM)-associated trees along mycorrhizal gradients established in watersheds with higher pH and fertility relative to watersheds with lower pH and fertility as evidenced by $\delta^{15}N$ patterns. Relative to higher pH, higher fertility watersheds, ECM dominated stands in lower pH, lower fertility watersheds are characterized by lower leaf litter $\delta^{15}N$ suggesting that establishment of *O. mexicana* and associated ECM fungi induce greater N-limitation in these watersheds. Additionally, the difference between forest floor leaf litter and mineral soil fraction $\delta^{15}N$ increases along mycorrhizal gradients in lower pH, lower fertility watersheds, but does not change along mycorrhizal gradients in higher pH, higher fertility watersheds. The greater $\delta^{15}N_{soil\text{-}litter}$ at high levels of ECM dominance in lower pH, lower fertility watersheds may reflect greater contribution of $^{15}N$ enriched ectomycorrhizal biomass to particulate organic matter and mineral associated organic matter fractions. Further, significant O horizon formation in ECM dominated stands of lower pH, lower fertility watersheds may filter dissolved organic matter, such that dissolved organic matter entering the mineral soil in lower pH, lower fertility watersheds may originate from $^{15}N$-enriched hyphal biomass of long-distance exploration type ECM taxa that colonize low pH, SOM rich organic horizon soils (depicted in the inset). In contrast, dissolved organic matter entering the mineral soil in higher pH, higher fertility watersheds where organic horizon formation is minimal may originate leaf litter that is less enriched in $^{15}N$.

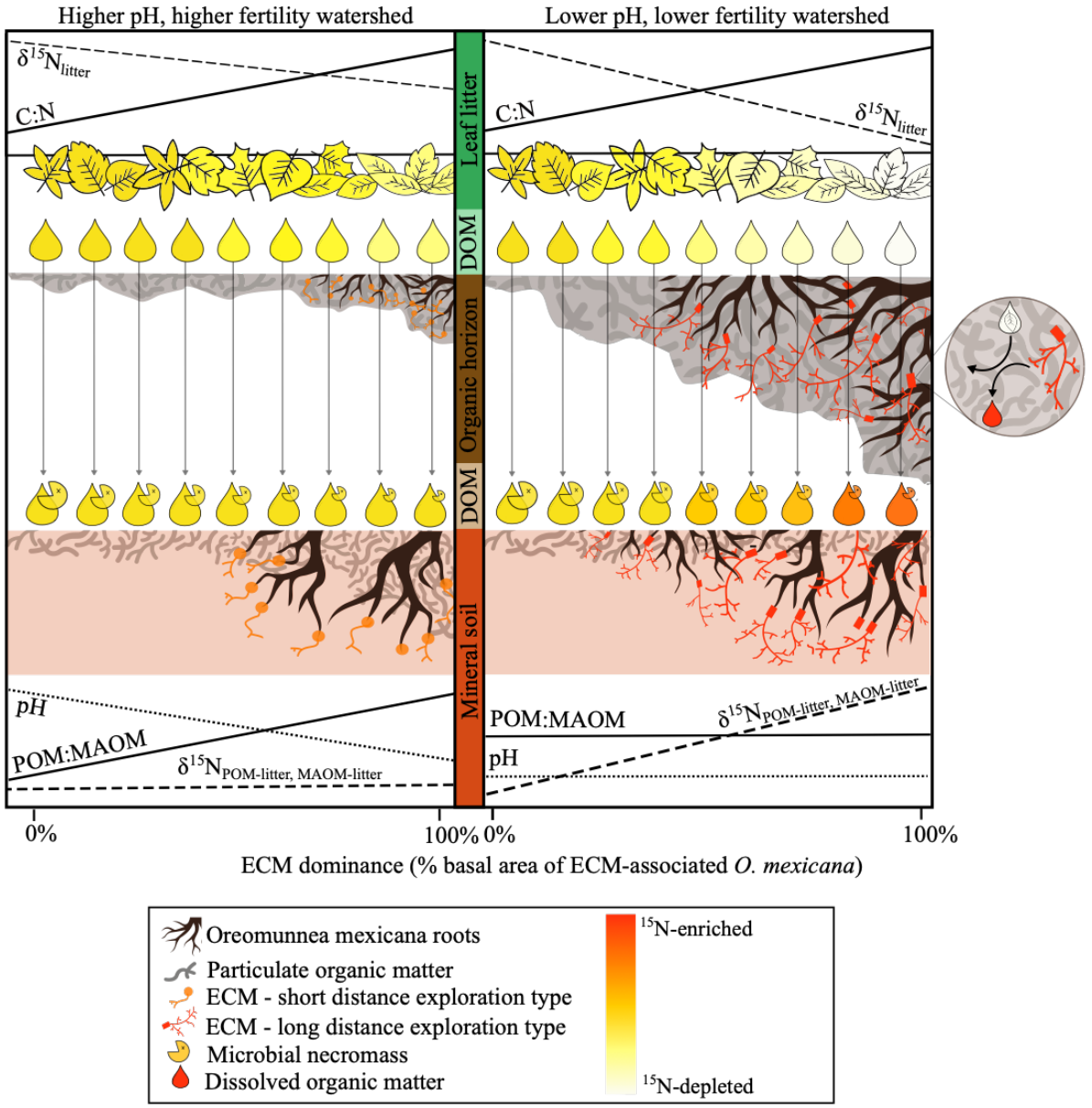

## REFERENCES


Andersen, K.M., Endara, M.J., Turner, B.L., Dalling, J.W., 2012. Trait-based community assembly of understory palms along a soil nutrient gradient in a lower montane tropical forest. Oecologia 168, 519–531. doi:10.1007/s00442-011-2112-z

Averill, C., 2016. Slowed decomposition in ectomycorrhizal ecosystems is independent of plant chemistry. Soil Biology and Biochemistry 102, 52–54. doi:http://dx.doi.org/10.1016/j.soilbio.2016.08.003

Averill, C., Bhatnagar, J.M., Dietze, M.C., Pearse, W.D., Kivlin, S.N., 2019. Global imprint of mycorrhizal fungi on whole-plant nutrient economics. Proceedings of the National Academy of Sciences of the United States of America 46, 23163–23168. doi:10.1073/pnas.1906655116

Averill, C., Turner, B.L., Finzi, A.C., 2014. Mycorrhiza-mediated competition between plants and decomposers drives soil carbon storage. Nature 505, 543–545. doi:10.1038/nature12901

Bigelow, S., Canham, C., 2017. Neighborhood-Scale Analyses of Non-additive Species Effects on Cation Concentrations in Forest Soils. Ecosystems 20, 1351–1363. doi:10.1007/s10021-017-0116-1

Binkley, D., Giardina, C., 1998. Why do tree species affect soils? The Warp and Woof of tree-soil interactions. Biogeochemistry 42, 89–106. doi:10.1007/978-94-017-2691-7_5

Bradford, M.A., Fierer, N., Reynolds, J.F., 2008. Soil carbon stocks in experimental mesocosms are dependent on the rate of labile carbon, nitrogen and phosphorus inputs to soils. Functional Ecology 22, 964–974. doi:10.1111/j.1365-2435.2008.01404.x

Burnham, K.P., Anderson, D.R., 2002. Model Selection and Multimodel Inference: A Practical Information-Theoretic Approach, 2nd ed. Springer-verlag, New York.

Canham, C.D., Uriarte, M., 2006. Analysis of neighborhood dynamics of forest ecosystems using likelihood methods and modeling. Ecological Applications 16, 62–73. doi:10.1890/04-0657

Cavelier, J., Solis, D., Jaramillo, M.A., 1996. Fog interception in montane forests across the Central Cordillera of Panama. Journal of Tropical Ecology 12, 357–369. doi:10.1017/S026646740000955X

Cheeke, T.E., Phillips, R.P., Brzostek, E.R., Rosling, A., Bever, J.D., Fransson, P., 2017. Dominant mycorrhizal association of trees alters carbon and nutrient cycling by selecting for microbial groups with distinct enzyme function. New Phytologist 214, 432–442. doi:10.1111/nph.14343

Clemmensen, K.E., Bahr, A., Ovaskainen, O., Dahlberg, A., Ekblad, A., Wallander, H., Stenlid, J., Finlay, R.D., Wardle, D.A., Lindahl, B.D., 2013. Roots and associated fungi drive long-term carbon sequestration in boreal forest. Science 339, 1615–1618. doi:10.1126/science.1231923

Clemmensen, K.E., Durling, M.B., Michelsen, A., Hallin, S., Finlay, R.D., Lindahl, B.D., 2021. A tipping point in carbon storage when forest expands into tundra is related to mycorrhizal recycling of nitrogen. Ecology Letters 24, 1193–1204. doi:https://doi.org/10.1111/ele.13735

Clemmensen, K.E., Finlay, R.D., Dahlberg, A., Stenlid, J., Wardle, D.A., Lindahl, B.D., 2015. Carbon sequestration is related to mycorrhizal fungal community shifts during long-term succession in boreal forests. New Phytologist 205, 1525–1536. doi:10.1111/nph.13208

Clemmensen, K.E., Michelsen, A., Jonasson, S., Shaver, G.R., 2006. Increased ectomycorrhizal fungal abundance after long-term fertilization and warming of two arctic tundra ecosystems. New Phytologist 171, 391–404. doi:10.1111/j.1469-8137.2006.01778.x

Cleveland, C.C., Reed, S.C., Townsend, A.R., 2006. Nutrient regulation of organic matter

decomposition in a tropical rain forest. Ecology 87, 492–503. doi:10.1890/05-0525

Corrales, A., 2016. Ectomycorrhizal associations in tropical montane forest: insights into their influence on nutrient cycling and functional responses to soil fertility. University of Illinois at Urbana-Champaign.

Corrales, A., Arnold, A.E., Ferrer, A., Turner, B.L., Dalling, J.W., 2016a. Variation in ectomycorrhizal fungal communities associated with Oreomunnea mexicana (Juglandaceae) in a Neotropical montane forest. Mycorrhiza 26, 1–17. doi:10.1007/s00572-015-0641-8

Corrales, A., Mangan, S.A., Turner, B.L., Dalling, J.W., 2016b. An ectomycorrhizal nitrogen economy facilitates monodominance in a neotropical forest. Ecology Letters 19, 383–392. doi:10.1111/ele.12570

Cotrufo, M.F., Ranalli, M.G., Haddix, M.L., Six, J., Lugato, E., 2019. Soil carbon storage informed by particulate and mineral-associated organic matter. Nature Geoscience 12, 989–994. doi:10.1038/s41561-019-0484-6

Cotrufo, M.F., Wallenstein, M.D., Boot, C.M., Denef, K., Paul, E., Cotrufo et al, F.M., 2013. The Microbial Efficiency-Matrix Stabilization (MEMS) framework integrates plant litter decomposition with soil organic matter stabilization: Do labile plant inputs form stable soil organic matter? Global Change Biology 19, 988–995. doi:10.1111/gcb.12113

Craig, M.E., Lovko, N., Flory, S.L., Wright, J.P., Phillips, R.P., 2019. Impacts of an invasive grass on soil organic matter pools vary across a tree-mycorrhizal gradient. Biogeochemistry 144, 149–164. doi:10.1007/s10533-019-00577-2

Craig, M.E., Turner, B.L., Liang, C., Clay, K., Johnson, D.J., Phillips, R.P., 2018. Tree mycorrhizal type predicts within-site variability in the storage and distribution of soil organic matter. Global Change Biology 24, 3317–3330. doi:10.1111/gcb.14132

Dalling, J.W., Turner, B.L., 2021. Soils of the Fortuna Forest Reserve. Smithsonian Contributions to Botany, Volume 112, in press.

Don, A., Schumacher, J., Freibauer, A., 2011. Impact of tropical land-use change on soil organic carbon stocks - a meta-analysis. Global Change Biology 17, 1658–1670. doi:10.1111/j.1365-2486.2010.02336.x

Edwards, A.W.F., 1992. Likelihood-expanded edition. Johns Hopkins University Press, Baltimore Maryland, USA.

Ekblad, A., Wallander, H., Godbold, D.L., Cruz, C., Johnson, D., Baldrian, P., Bjork, R.G., Epron, D., Kieliszewska-Rokicka, B., Kjoller, R., Kraigher, H., Matzner, E., Neumann, J., Plassard, C., 2013. The production and turnover of extramatrical mycelium of ectomycorrhizal fungi in forest soils: role in carbon cycling. Plant and Soil 366, 1–27. doi:10.1007/s11104-013-1630-3

Fernandez, C.W., Kennedy, P.G., 2016. Revisiting the "Gadgil effect": do interguild fungal interactions control carbon cycling in forest soils? New Phytologist 209, 1382–1394. doi:10.1111/nph.13648

Franklin, O., Näsholm, T., Högberg, P., Högberg, M., 2014. Forests trapped in nitrogen limitation—An ecological market perspective on ectomycorrhizal symbiosis. New Phytologist 203, 657–666. doi:10.1111/nph.12840

Friggens, N.L., Aspray, T.J., Parker, T.C., Subke, J.A., Wookey, P.A., 2020. Spatial patterns in soil organic matter dynamics are shaped by mycorrhizosphere interactions in a treeline forest. Plant and Soil 447, 521–535. doi:10.1007/s11104-019-04398-y

Fröberg, M., Jardine, P.M., Hanson, P.J., Swanston, C.W., Todd, D.E., Tarver, J.R., Garten, C.T., 2007. Low Dissolved Organic Carbon Input from Fresh Litter to Deep Mineral Soils.

Soil Science Society of America Journal 71, 347–354. doi:10.2136/sssaj2006.0188

Fröberg, M., Kleja, D.B., Bergkvist, B., Tipping, E., Mulder, J., 2005. Dissolved organic carbon leaching from a coniferous forest floor - A field manipulation experiment. Biogeochemistry 75, 271–287. doi:10.1007/s10533-004-7585-y

Gaudinski, J.B., Trumbore, S.E., Davidson, E.A., Zheng, S., 2000. Soil carbon cycling in a temperate forest: Radiocarbon-based estimates of residence times, sequestration rates and partitioning of fluxes. Biogeochemistry 51, 33–69. doi:10.1023/A:1006301010014

Godbold, D.L., Hoosbeek, M.R., Lukac, M., Cotrufo, M.F., Janssens, I.A., Ceulemans, R., Polle, A., Velthorst, E.J., Scarascia-Mugnozza, G., De Angelis, P., Miglietta, F., Peressotti, A., 2006. Mycorrhizal hyphal turnover as a dominant process for carbon input into soil organic matter. Plant and Soil 281, 15–24. doi:10.1007/s11104-005-3701-6

Gómez-Aparicio, L., Canham, C.D., 2008. Neighborhood models of the effects of invasive tree species on ecosystem processes. Ecological Monographs 78, 69–86. doi:10.1890/06-2036.1

Haddix, M.L., Gregorich, E.G., Helgason, B.L., Janzen, H., Ellert, B.H., Francesca Cotrufo, M., 2020. Climate, carbon content, and soil texture control the independent formation and persistence of particulate and mineral-associated organic matter in soil. Geoderma 363, 114160. doi:10.1016/j.geoderma.2019.114160

Hagenbo, A., Kyaschenko, J., Clemmensen, K.E., Lindahl, B.D., Fransson, P., 2018. Fungal community shifts underpin declining mycelial production and turnover across a Pinus sylvestris chronosequence. Journal of Ecology 106, 490–501. doi:10.1111/1365-2745.12917

Hall, J.S., Harris, D.J., Saltonstall, K., Medjibe, V. de P., Ashton, M.S., Turner, B.L., 2020. Resource acquisition strategies facilitate Gilbertiodendron dewevrei monodominance in African lowland forests. Journal of Ecology 108, 433–448. doi:10.1111/1365-2745.13278

Hendershot, W.H., Lalande, H., Duquette, M., 1993. Ion exchange and exchangeable cations. Soil Sampling and Methods of Analysis 19, 167–176.

Hobbie, E.A., Agerer, R., 2010. Nitrogen isotopes in ectomycorrhizal sporocarps correspond to belowground exploration types. Plant and Soil 327, 71–83. doi:10.1007/s11104-009-0032-z

Hobbie, E.A., Högberg, P., 2012. Nitrogen isotopes link mycorrhizal fungi and plants to nitrogen dynamics. New Phytologist 196, 367–382. doi:10.1111/j.1469-8137.2012.04300.x

Hobbie, E.A., Macko, S.A., Williams, M., 2000. Correlations between foliar δ15N and nitrogen concentrations may indicate plant-mycorrhizal interactions. Oecologia 122, 273–283. doi:10.1007/PL00008856

Högberg, M.N., Bååth, E., Nordgren, A., Arnebrant, K., Högberg, P., 2003. Contrasting effects of nitrogen availability on plant carbon supply to mycorrhizal fungi and saprotrophs - A hypothesis based on field observations in boreal forest. New Phytologist 160, 225–238. doi:10.1046/j.1469-8137.2003.00867.x

Högberg, M.N., Skyllberg, U., Högberg, P., Knicker, H., 2020. Does ectomycorrhiza have a universal key role in the formation of soil organic matter in boreal forests? Soil Biology and Biochemistry 140, 107635. doi:10.1016/j.soilbio.2019.107635

Högberg, P., Högberg, M.N., Quist, M.E., Ekblad, A., Näsholm, T., 1999. Nitrogen isotope fractionation during nitrogen uptake by ectomycorrhizal and non-mycorrhizal Pinus sylvestris. New Phytologist 142, 569–576. doi:https://doi.org/10.1046/j.1469-8137.1999.00404.x

Hogberg, P., Hogbom, L., Schinkel, H., Hogberg, M., Johannisson, C., Wallmark, H., 1996. 15N abundance of surface soils, roots and mycorrhizas in profiles of European forest soils. Oecologia 108, 207–214. doi:10.1007/BF00334643

Hölscher, D., Dunker, B., Harbusch, M., Corre, M., 2009. Fine root distribution in a lower montane rain forest of Panama. Biotropica 41, 312–318. doi:10.1111/j.1744-7429.2009.00492.x

Jenkins, J.C., Chojnacky, D.C., Heath, L.S., Birdsey, R.A., 2003. National-scale biomass estimators for United States tree species. Forest Science 49, 12–35. doi:10.1093/forestscience/49.1.12

Kaiser, K., Guggenberger, G., 2000. The role of DOM sorption to mineral surfaces in the preservation of organic matter in soils. Organic Geochemistry 31, 711–725. doi:10.1016/S0146-6380(00)00046-2

Kaiser, K., Kalbitz, K., 2012. Cycling downwards - dissolved organic matter in soils. Soil Biology and Biochemistry 52, 29–32. doi:10.1016/j.soilbio.2012.04.002

Kalbitz, K., Kaiser, K., 2008. Contribution of dissolved organic matter to carbon storage in forest mineral soils. Journal of Plant Nutrition and Soil Science 171, 52–60. doi:10.1002/jpln.200700043

Kalbitz, K., Schwesig, D., Rethemeyer, J., Matzner, E., 2005. Stabilization of dissolved organic matter by sorption to the mineral soil. Soil Biology and Biochemistry 37, 1319–1331. doi:10.1016/j.soilbio.2004.11.028

Kalliokoski, T., Pennanen, T., Nygren, P., Sievänen, R., Helmisaari, H.S., 2010. Belowground interspecific competition in mixed boreal forests: Fine root and ectomycorrhiza characteristics along stand developmental stage and soil fertility gradients. Plant and Soil 330, 73–89. doi:10.1007/s11104-009-0177-9

Keller, A.B., Phillips, R.P., 2019. Leaf litter decay rates differ between mycorrhizal groups in temperate, but not tropical, forests. New Phytologist 222, 556–564. doi:10.1111/nph.15524

Keller, A.B., Reed, S.C., Townsend, A.R., Cleveland, C.C., 2013. Effects of canopy tree species on belowground biogeochemistry in a lowland wet tropical forest. Soil Biology & Biochemistry 58, 61–69. doi:10.1016/j.soilbio.2012.10.041

Kjoller, R., Nilsson, L.O., Hansen, K., Schmidt, I.K., Vesterdal, L., Gundersen, P., 2012. Dramatic changes in ectomycorrhizal community composition, root tip abundance and mycelial production along a stand-scale nitrogen deposition gradient. New Phytologist 194, 278–286. doi:10.1111/j.1469-8137.2011.04041.x

Kleber, M., Eusterhues, K., Keiluweit, M., Mikutta, C., Mikutta, R., Nico, P.S., 2015. Mineral-Organic Associations: Formation, Properties, and Relevance in Soil Environments. Advances in Agronomy 130, 1–140. doi:10.1016/bs.agron.2014.10.005

Kohzu, A., Tateishi, T., Yamada, A., Koba, K., Wada, E., 2000. Nitrogen isotope fractionation during nitrogen transport from ectomycorrhizal fungi, Suillus granulatus, to the host plant, Pinus densiflora. Soil Science and Plant Nutrition 46, 733–739. doi:10.1080/00380768.2000.10409138

Kohzu, A., Yoshioka, T., Ando, T., Takahashi, M., Koba, K., Wada, E., 1999. Natural 13C and 15N abundance of field-collected fungi and their ecological implications. New Phytologist 144, 323–330. doi:10.1046/j.1469-8137.1999.00508.x

Kyaschenko, J., Clemmensen, K.E., Karltun, E., Lindahl, B.D., 2017. Below-ground organic matter accumulation along a boreal forest fertility gradient relates to guild interaction within fungal communities. Ecology Letters 20, 1546–1555. doi:10.1111/ele.12862

Lavallee, J.M., Conant, R.T., Paul, E.A., Cotrufo, M.F., 2018. Incorporation of shoot versus root-derived 13C and 15N into mineral-associated organic matter fractions: results of a soil slurry incubation with dual-labelled plant material. Biogeochemistry 137, 379–393.

doi:10.1007/s10533-018-0428-z

Lavallee, J.M., Soong, J.L., Cotrufo, M.F., 2020. Conceptualizing soil organic matter into particulate and mineral-associated forms to address global change in the 21st century. Global Change Biology 26, 261–273. doi:10.1111/gcb.14859

Liang, C., Schimel, J.P., Jastrow, J.D., 2017. The importance of anabolism in microbial control over soil carbon storage. Nature Microbiology 2, 17105. doi:10.1038/nmicrobiol.2017.105

Lilleskov, E.A., Fahey, T.J., Horton, T.R., Lovett, G.M., 2002. Belowground ectomycorrhizal fungal community change over a nitrogen deposition gradient in Alaska. Ecology 83, 104–115. doi:10.1890/0012-9658(2002)083[0104:befcco]2.0.co;2

Lin, G., McCormack, M.L., Ma, C., Guo, D., 2017. Similar below-ground carbon cycling dynamics but contrasting modes of nitrogen cycling between arbuscular mycorrhizal and ectomycorrhizal forests. New Phytologist 213, 1440–1451. doi:10.1111/nph.14206

Lindahl, B.D., Kyaschenko, J., Varenius, K., Clemmensen, K.E., Dahlberg, A., Karltun, E., Stendahl, J., 2021. A group of ectomycorrhizal fungi restricts organic matter accumulation in boreal forest. Ecology Letters 24, 1341–1351. doi:https://doi.org/10.1111/ele.13746

Mayor, J.R., Schuur, E.A.G., Henkel, T.W., 2009. Elucidating the nutritional dynamics of fungi using stable isotopes. Ecology Letters 12, 171–183. doi:10.1111/j.1461-0248.2008.01265.x

McGuire, K.L., Zak, D.R., Edwards, I.P., Blackwood, C.B., Upchurch, R., 2010. Slowed decomposition is biotically mediated in an ectomycorrhizal, tropical rain forest. Oecologia 164, 785–795. doi:10.1007/s00442-010-1686-1

Midgley, M.G., Brzostek, E., Phillips, R.P., 2015. Decay rates of leaf litters from arbuscular mycorrhizal trees are more sensitive to soil effects than litters from ectomycorrhizal trees. Journal of Ecology 103, 1454–1463. doi:10.1111/1365-2745.12467

Midgley, M.G., Sims, R.S., 2020. Mycorrhizal Association Better Predicts Tree Effects on Soil Than Leaf Habit. Frontiers in Forests and Global Change 3, 74. doi:10.3389/ffgc.2020.00074

Moser, G., Leuschner, C., Hertel, D., Graefe, S., Soethe, N., Iost, S., 2011. Elevation effects on the carbon budget of tropical mountain forests (S Ecuador): The role of the belowground compartment. Global Change Biology 17, 2211–2226. doi:10.1111/j.1365-2486.2010.02367.x

Murphey, L., 2015. likelihood: Methods for Maximum Likelihood Estimateion., in: R Package Version 1.7.

Näsholm, T., Högberg, P., Franklin, O., Metcalfe, D., Keel, S.G., Campbell, C., Hurry, V., Linder, S., Högberg, M.N., 2013. Are ectomycorrhizal fungi alleviating or aggravating nitrogen limitation of tree growth in boreal forests? New Phytologist 198, 214–221. doi:https://doi.org/10.1111/nph.12139

Natelhoffer, K.J., Fry, B., 1988. Controls on Natural Nitrogen-15 and Carbon-13 Abundances in Forest Soil Organic Matter. Soil Science Society of America Journal 52, 1633–1640. doi:https://doi.org/10.2136/sssaj1988.03615995005200060024x

Peay, K.G., Kennedy, P.G., Davies, S.J., Tan, S., Bruns, T.D., 2010. Potential link between plant and fungal distributions in a dipterocarp rainforest: Community and phylogenetic structure of tropical ectomycorrhizal fungi across a plant and soil ecotone. New Phytologist 185, 529–542. doi:10.1111/j.1469-8137.2009.03075.x

Phillips, R.P., Brzostek, E., Midgley, M.G., 2013. The mycorrhizal-associated nutrient economy: A new framework for predicting carbon-nutrient couplings in temperate forests. New Phytologist 199, 41–51. doi:10.1111/nph.12221

Prada, C.M., Morris, A., Andersen, K.M., Turner, B.L., Caballero, P., Dalling, J.W., 2017. Soils and rainfall drive landscape-scale changes in the diversity and functional composition of tree communities in premontane tropical forest. Journal of Vegetation Science 28, 859–870. doi:10.1111/jvs.12540

Seyfried, G.S., Dalling, J.W., Yang, W.H., 2021. Effects of mycorrhizal type on leaf litter decomposition depend on litter quality and environmental context. Biogeochemistry 155, 21–38. doi:10.1007/s10533-021-00810-x

Smith, G.R., Wan, J., 2019. Resource-ratio theory predicts mycorrhizal control of litter decomposition. New Phytologist 223, 1595–1606. doi:10.1111/nph.15884

Smith, M.E., Henkel, T.W., Catherine Aime, M., Fremier, A.K., Vilgalys, R., 2011. Ectomycorrhizal fungal diversity and community structure on three co-occurring leguminous canopy tree species in a Neotropical rainforest. New Phytologist 192, 699–712. doi:10.1111/j.1469-8137.2011.03844.x

Sokol, N.W., Bradford, M.A., 2019. Microbial formation of stable soil carbon is more efficient from belowground than aboveground input. Nature Geoscience 12, 46–53. doi:10.1038/s41561-018-0258-6

Sokol, N.W., Sanderman, J., Bradford, M.A., 2019. Pathways of mineral-associated soil organic matter formation: Integrating the role of plant carbon source, chemistry, and point of entry. Global Change Biology 25, 12–24. doi:10.1111/gcb.14482

Sollins, P., Kramer, M.G., Swanston, C., Lajtha, K., Filley, T., Aufdenkampe, A.K., Wagai, R., Bowden, R.D., 2009. Sequential density fractionation across soils of contrasting mineralogy: Evidence for both microbial- and mineral-controlled soil organic matter stabilization. Biogeochemistry 96, 209–231. doi:10.1007/s10533-009-9359-z

Soudzilovskaia, N.A., van Bodegom, P.M., Terrer, C., Zelfde, M. van't, McCallum, I., Luke McCormack, M., Fisher, J.B., Brundrett, M.C., de Sá, N.C., Tedersoo, L., 2019. Global mycorrhizal plant distribution linked to terrestrial carbon stocks. Nature Communications 10, 5077. doi:10.1038/s41467-019-13019-2

Sterkenburg, E., Bahr, A., Brandström Durling, M., Clemmensen, K.E., Lindahl, B.D., 2015. Changes in fungal communities along a boreal forest soil fertility gradient. New Phytologist 207, 1145–1158. doi:10.1111/nph.13426

Stone, D.E., 1972. New World Juglandaceae, III. A New Perspective of the Tropical Members with Winged Fruits. Annals of the Missouri Botanical Garden 59, 297. doi:10.2307/2394761

Sulman, B.N., Shevliakova, E., Brzostek, E.R., Kivlin, S.N., Malyshev, S., Menge, D.N.L., Zhang, X., 2019. Diverse Mycorrhizal Associations Enhance Terrestrial C Storage in a Global Model. Global Biogeochemical Cycles 33, 501–523. doi:https://doi.org/10.1029/2018GB005973

Team, R.C., 2019. R: A language and environment for statistical computing. R Fouondataion for Statistical Computing, Vienna, Austria.

Torti, S.D., Coley, P.D., Kursar, T.A., 2001. Causes and consequences of monodominance in tropical lowland forests. American Naturalist 157, 141–153. doi:10.1086/318629

Trudell, S.A., Rygiewicz, P.T., Edmonds, R.L., 2004. Patterns of nitrogen and carbon stable isotope ratios in macrofungi, plants and soils in two old-growth conifer forests. New Phytologist 164, 317–335. doi:10.1111/j.1469-8137.2004.01162.x

Truong, C., Gabbarini, L.A., Corrales, A., Mujic, A.B., Escobar, J.M., Moretto, A., Smith, M.E., 2019. Ectomycorrhizal fungi and soil enzymes exhibit contrasting patterns along elevation

gradients in southern Patagonia. New Phytologist 222, 1936–1950. doi:10.1111/nph.15714

von Haden, A.C., Yang, W.H., DeLucia, E.H., 2020. Soils' dirty little secret: Depth-based comparisons can be inadequate for quantifying changes in soil organic carbon and other mineral soil properties. Global Change Biology 26, 3759–3770. doi:10.1111/gcb.15124

Wallander, H., Mörth, C.M., Giesler, R., 2009. Increasing abundance of soil fungi is a driver for 15N enrichment in soil profiles along a chronosequence undergoing isostatic rebound in northern Sweden. Oecologia 160, 87–96. doi:10.1007/s00442-008-1270-0

Waring, B.G., Álvarez-Cansino, L., Barry, K.E., Becklund, K.K., Dale, S., Gei, M.G., Keller, A.B., Lopez, O.R., Markesteijn, L., Mangan, S., Riggs, C.E., Rodríguez-Ronderos, M.E., Max Segnitz, R., Schnitzer, S.A., Powers, J.S., 2015. Pervasive and strong effects of plants on soil chemistry: A meta-analysis of individual plant 'zinke' effects. Proceedings of the Royal Society B: Biological Sciences 282, 1812. doi:10.1098/rspb.2015.1001

Werth, M., Kuzyakov, Y., 2010. 13C fractionation at the root-microorganisms-soil interface: A review and outlook for partitioning studies. Soil Biology and Biochemistry 42, 1372–1384. doi:10.1016/j.soilbio.2010.04.009

Zhu, K., McCormack, M.L., Lankau, R.A., Egan, J.F., Wurzburger, N., 2018. Association of ectomycorrhizal trees with high carbon-to-nitrogen ratio soils across temperate forests is driven by smaller nitrogen not larger carbon stocks. Journal of Ecology 106, 524–535. doi:10.1111/1365-2745.12918

# CHAPTER 3

# UNDERLYING SOIL ACID-BASE CHEMISTRY MEDIATES FUNGAL COMMUNITY CONTRIBUTIONS TO ECTOMYCORRHIZAL BIOGEOCHEMICAL SYNDROMES

## INTRODUCTION

Tree-mycorrhizal association has emerged as a promising predictor of soil organic matter (SOM) dynamics, with the effect of trees and their associated ectomycorrhizal (ECM) fungi on soil carbon (C) and nutrient cycling scaling with the percent basal area of ECM-associated trees in a forest stand (Cheeke et al., 2017; Craig et al., 2018; Phillips et al., 2013). As the dominance of ECM-associated trees increases, nutrient conservative traits of ECM trees and their associated mycorrhizae (Averill et al., 2019) are predicted to suppress decomposition rates, resulting in accumulation of high C:N particulate organic matter (POM) in an organic horizon or in the topsoil (Averill et al., 2019; Craig et al., 2018). However, watershed-scale variation in underlying soil fertility due to differences in soil parent material has been shown to correspond with distinct effects of ECM-associated trees on N cycling and SOM dynamics (Seyfried et al., 2021a). Soil fertility influences plants and microbiota, possibly altering mycorrhizal mediation of plant-soil feedbacks (Weemstra et al., 2020). Specifically, local abiotic conditions can filter fungal communities and determine the functional capacity of the ECM community to affect soil C and N dynamics directly, through variation in morphological and physiological traits, or indirectly, through interactions with saprotrophic fungi (Pellitier et al., 2021). Yet it is currently unknown to what extent fungal communities beneath ECM trees, as opposed to other aspects of the host tree-ECM symbiosis, contribute to variation in ECM effects among ecosystems that differ in soil fertility.

Free-living saprotrophic (SAP) fungi and root-associated ECM fungi are largely responsible for organic matter degradation within forest soils, but these two fungal guilds play contrasting roles in ecosystem C cycling (Högberg et al., 2010; Lindahl & Tunlid, 2015; Nguyen et al., 2016). While SAP fungi obtain C through decomposition of organic matter, ECM fungi receive labile C from their host such that organic matter decay by ECM fungi is instead targeted towards nutrient acquisition (Lindahl and Tunlid, 2015). Uptake of N from organic matter by ECM fungi (Kuyper, 2017), which may be an important nutrient acquisition strategy when N availability is low, can increase SOM C:N ratios and limit growth of increasingly N-limited saprotrophic fungi (Orwin et al., 2011). Therefore, competition between fungal guilds is hypothesized to suppress decomposition and result in SOM accumulation at the soil surface (Fernandez and Kennedy, 2016; Gadgil and Gadgil, 1971). However, there is increasing evidence that this relationship is context-dependent: suppressed decomposition in the presence of ECM fungi may depend on substrate quality and ECM community composition (Fernandez et al., 2019; Smith and Wan, 2019). The magnitude of ECM fungi effects on SOM accumulation may correlate with ECM:SAP ratios. Larger ratios may indicate more involvement of ECM fungi in decay, and result in greater SOM accumulation because ECM fungi contain a smaller suite of decomposing enzymes relative to SAP fungi (Lindahl and Tunlid, 2015).

Ectomycorrhizal fungi are characterized by a diverse suite of morphological and physiological traits that determine their interactions with SAP fungi and ultimately, their effects on forest C and N cycling (Tedersoo and Smith, 2013; Zak et al., 2019). For example, ECM fungi that obtain N from SOM through costly metabolic pathways may occur in higher relative abundance where N is predominantly available in recalcitrant forms (e.g. physically protected by lignin), but be outcompeted by taxa that exclusively uptake inorganic N at higher levels of N

availability (Smith and Wan, 2019; Van Der Linde et al., 2018). Organic N users may perpetuate slow decomposition rates and accumulation of SOM where they establish by competing with saprotrophic decomposers for limited N (Fernandez and Kennedy, 2016; Gadgil and Gadgil, 1971; Kyaschenko et al., 2017). These different N use strategies of ECM fungi may be associated with mycorrhizal exploration type (Agerer, 2001). Exploration types integrate morphological traits and nutrient acquisition strategies and can therefore be used as a proxy for ECM effects on ecosystem properties (Koide et al., 2014). Medium-distance fringe and long-distance exploration type ECM taxa may be efficient at scavenging from diffuse organic matter patches due to production of hydrophobic rhizomorphs that allow for long distance transport of nutrients. Additionally, these taxa may produce relatively large quantities of biomass that decay slowly, representing a significant source of SOM (Ekblad et al., 2013; Fernandez et al., 2016). In contrast, contact or short-distance exploration type ECM taxa optimize uptake of soluble inorganic N sources (Agerer, 2001; Hobbie and Agerer, 2010) and produce less biomass that also decomposes more quickly to contribute less to accumulation of particulate organic matter in ECM surface soils. Overall, ECM:SAP ratios in concert with functional information about ECM taxa present may indicate the functional potential of a fungal community to drive an ecosystem toward conservative biogeochemical cycling.

Fungal communities can be shaped by ecological filters such as edaphic factors (Moeller et al., 2014; Toljander et al., 2006; Weemstra et al., 2020). Saprotrophic fungi, which can produce a large suite of hydrolytic enzymes, acquire C by decomposing organic matter and tend to occur in higher relative abundance in the forest floor where labile C from freshly fallen leaf litter is readily available (Lindahl et al., 2007; McGuire et al., 2013). Saprotrophic fungal communities may therefore be most influenced by changes in leaf litter inputs related to shifts in

the tree communities within forests (Awad et al., 2019). In contrast, ECM fungi, which receive C from their hosts and use organic matter as a source of N (Lindahl and Tunlid, 2015), tend to occur in higher relative abundance in C-limited, N-rich substrate deeper in the soil profile and may therefore be most influenced by shifts in soil conditions such as moisture, temperature and pH (Awad et al., 2019). Furthermore, soil nutrient availability may alter belowground C allocation by host trees, affecting the degree of ECM colonization on roots as well as the morphological traits of the ECM taxa present (Högberg, Bååth, Nordgren, Arnebrant, & Högberg, 2003; Högberg et al., 2010; Kjoller et al., 2012). These patterns have been observed along pH and N availability gradients in boreal and tropical forests alike: medium or long-distance exploration type ECM fungi with the enzymatic capacity to uptake organic nutrients are abundant in lower N soils while contact or short-distance exploration type ECM fungi with which uptake inorganic forms of N are abundant in higher N soils (Corrales et al., 2017; Lilleskov et al., 2002; Pellitier et al., 2021; Sterkenburg et al., 2015). Therefore, filtering of fungal communities by local soil conditions may partially determine the role of fungal communities in driving ECM effects across ecosystems.

The role of fungal communities in driving different ECM effects on N cycling dynamics among ecosystems can be investigated by comparing patterns in fungal community composition with patterns in $\delta^{15}N$ of leaf litter and SOM. Foliar $\delta^{15}N$ can indicate host tree reliance on N transfer from ECM symbionts because ECM fungi preferentially transfer $^{14}N$ to their hosts and retain $^{15}N$ in their biomass. Therefore, trees growing in low N soils rely more heavily on their ECM symbionts for N and produce foliar tissues more depleted in $^{15}N$ (Hobbie and Högberg, 2012; Högberg et al., 1999; Kohzu et al., 2000). For leaf litter samples collected from the forest floor, the N isotopic composition will also be affected by decomposition stage because microbes

discriminate against $^{15}N$ when mineralizing organic matter. Therefore, forest floor leaf litter becomes increasingly $^{15}N$-enriched as decomposition progresses (Natelhoffer and Fry, 1988). As such, suppressed leaf litter decomposition rates in ECM stands may be expected to result in lower $\delta^{15}N$ of forest floor leaf litter. The difference between the $\delta^{15}N$ of mineral soil and the $\delta^{15}N$ of forest floor leaf litter ($\delta^{15}N_{\text{mineral soil-litter}}$) can also provide information about the relative magnitude of ECM effects. Greater $\delta^{15}N_{\text{mineral soil-litter}}$ can indicate greater transfer of N from ECM to host trees, resulting in less $^{15}N$-enriched leaf litter, and greater contribution of $^{15}N$-enriched hyphal biomass to SOM (Wallander et al., 2009). Therefore, it may be possible to characterize the relative magnitude of ECM effects on N availability and SOM dynamics across watersheds by comparing change in $\delta^{15}N$ of leaf litter and mineral soil beneath ECM associated trees in mixed ECM-AM versus ECM-dominated stands within watersheds. Furthermore, correlations between fungal community composition and $\delta^{15}N$ of leaf litter and mineral soil across stand mycorrhizal types may reveal the role of fungal communities beneath ECM trees in driving ECM effects on N cycling dynamics within a watershed.

Here we investigate fungal community composition as a potential driver of variation in ECM effects on SOM accumulation and N cycling in soils beneath *Oreomunnea mexicana*, an ECM-associated canopy tree found in mid-elevation tropical forests from Southern Mexico to Western Panama (Stone, 1972). First, we hypothesized that functional variation within the ECM community (i.e., relative abundances of different exploration types) and the overall fungal community (i.e., ECM versus SAP relative abundance) contributes to different ECM effects on SOM accumulation and N cycling in forests with lower underlying soil pH and fertility (defined by effective cation exchange capacity and percent base saturation) versus higher soil pH and fertility (Table 3.1). We tested this hypothesis by characterizing fungal communities and

chemical properties in forest floor leaf litter and soils beneath *O. mexicana* in mixed ECM-AM stands versus *O. mexicana*-dominated stands within four adjacent watersheds that varied in soil acid-base chemistry based on differences in soil parent material. Importantly, *O. mexicana* effects on organic horizon depth, the composition of SOM, and N limitation have previously been shown to differ between the lower soil pH and fertility watersheds and the higher soil pH and fertility watersheds (Seyfried et al., 2021a). In the lower pH and fertility watersheds, we expected to observe greater ECM:SAP ratios and greater relative abundance of higher biomass medium or long-distance exploration type ECM taxa (hereafter referred to as "high biomass ECM") in ECM-dominated relative to mixed ECM-AM stands. High biomass ECM taxa have a greater functional capacity to drive an ecosystem towards conservative C and nutrient cycling such that we expected to observe strong correlations between ECM effects on soil chemical properties and fungal community composition in lower pH and fertility watersheds. In contrast, in the higher pH and fertility watersheds, we expected to observe weaker correlations between ECM effects on soil chemical properties and fungal community composition because lower biomass contact or short-distance exploration type ECM taxa (hereafter referred to as "low biomass ECM") that establish in greater relative abundance in these watersheds have less functional capacity to initiate conservative C and nutrient cycling.

## MATERIALS AND METHODS

### Site description

We conducted this study in the 13,000 ha Fortuna Forest Reserve (Fortuna), a lower montane tropical forest in western Panama (8°45 N', 82°15' W) with elevation ranging 1000-1400 masl. Mean annual temperature ranges 19-22 °C (Cavelier et al., 1996) and mean annual

precipitation ranges 5800-9000 mm (Andersen et al., 2012). In Fortuna, tree communities are highly diverse, containing 61-153 species $ha^{-1}$ (Prada et al., 2017), and mostly associate with AM fungi. However, one ECM-associated tree species, *Oreomunnea mexicana* (Standl.) Leroy (Juglandaceae*),* tends to dominate the forest where it grows, forming stands >50% *O. mexicana* by basal area (Corrales et al., 2016b). Additionally, ECM-associated trees such as *Quercus insignis, Quercus lancifolia* and *Coccoloba* spp. occur in low abundance (Prada et al., 2017).

Our study was conducted within four watersheds in Fortuna where *O. mexicana*-dominated stands have formed on distinct soil parent materials: ultisols at Honda and Hornito are derived from rhyolite and dacite, respectively, ultisols and inceptisols at Zorro are derived from granodiorite, and inceptisols at Alto Frio are derived from undifferentiated mafic volcanics (Turner & Dalling, 2021). Among watersheds, differences in parent material and climate have resulted in development of soils that range in acid-base chemistry. Soil properties and plant community composition in Fortuna are described in detail by (Turner & Dalling, 2021), with the specific sites of Alto Frio, Honda (A/B), HornitoB and ZorroA used in this study. Across the four watersheds, seasonality of precipitation is evident in the Alto Frio, Zorro and Hornito watersheds, which experience a dry season from January through April (Prada et al., 2017).

**Soil sampling**

To investigate the effect of soil acid-base chemistry on the functional capacity of fungal communities to drive ECM effects, we sampled beneath ECM-associated *O. mexicana* focal trees established within four watersheds which varied in underlying soil pH and fertility, as defined by effective cation exchange capacity (ECEC; cmol (+) kg $soil^{-1}$) and base cation concentrations (Table 3.1). Additionally, to investigate the role of fungal community composition in driving

variable ECM effects across watersheds, within in each watershed we sampled beneath three *O. mexicana* focal trees established in mixed ECM-AM forest and three *O. mexicana* focal trees established in ECM-dominated forest. Focal trees sampled in mixed ECM-AM stands were the only *O. mexicana* individuals within a 20 m radius. Focal trees within ECM-dominated stands were surrounded by forest that was at least >50% *O. mexicana* by basal area within a 20 m radius.

We sampled one meter from the base of each *O. mexicana* focal tree in each of the four cardinal directions, collecting forest floor leaf litter, organic horizon, and mineral soil. For each focal tree, we composited the four samples collected from each layer. We collected litter and organic soils from a 5 cm x 5 cm square area of soil surface, and mineral soil from 0-5 cm and 15-20 cm depths using a 2.54 cm diameter soil probe. In the subsequent analyses, we report soil chemical property data for the forest floor leaf litter, O horizon and 0-5 cm mineral soil layers; for brevity and clarity, we do not present data from the 15-20 cm mineral soil layer because patterns were similar between 0-5 cm and 15-20 cm depths. Samples were stored in a -20ºC freezer and were transported on ice packs to the University of Illinois at Urbana-Champaign for molecular and chemical analysis.

**Edaphic variables**

We analyzed air-dried and ground forest floor leaf litter and soil samples for soil organic carbon (SOC) and total nitrogen (TN) concentrations as well as C and N stable isotopic composition on a Vario Micro Cube elemental analyzer (Hanau, Germany) interfaced with an IsoPrime 100 isotope ratio mass spectrometer (Cheadle Hulme, UK) at the University of Illinois

at Urbana-Champaign. Additionally, we measured soil pH in a 2:1 ratio of ml ultra-pure DI to g dry soil for mineral soil and 5:1 ratio for organic soil.

**Soil microbial community analyses**

To characterize the overall fungal and ECM community composition, we extracted genomic DNA from soil and forest floor leaf litter samples. Homogenized soils were subsampled and freeze-dried before being ground to a fine powder using a sterilized mortar and pestle. From all composited soil samples, DNA was extracted from 0.50 g subsamples of mineral soil and 0.30 g subsamples of O horizon using a FastPrep DNA Extraction Kit (MP Biomedicals). To minimize extraction of plant DNA and maximize reads from the fungal and bacterial community on the surface of the leaf litter, we followed a separate pre-DNA extraction protocol for composited leaf litter samples, based on methods adapted from Keymer and Kent (2014) and Li et al. (2016) for isolation of plant-associated microorganisms. We combined 1 g homogenized leaf litter, six glass beads, and 30 ml phosphate buffered saline + 0.15% Tween 80 in sterile 50 ml Falcon tubes. After shaking the Falcon tubes horizontally on ice for one hour, we passed the homogenate through ethanol-sterilized No. 25 USA standard test sieve (pore size 710 microns; Newark Wire Cloth Company, Clifton, NJ, USA) to remove larger litter particles. To settle smaller litter particles, we centrifuged the extracted liquid for 5 minutes at 1500 rpm and decanted the supernatant, which was then centrifuged for 10 minutes at 6500 rpm to pellet bacterial and fungal cells that had been dislodged from the plant litter. The resulting pellet was resuspended in 500 µl sterile DI water and DNA was extracted using the FastDNA Spin Kit (MP Biomedicals) following the manufacturer's protocol. DNA purity and concentration were analyzed using Nanodrop ND-1000 (Thermo Scientific, Wilmington, DE, USA). The DNA

extracts from leaf litter and soils were stored at −20 °C prior to Illumina sequencing (Illumina, San Diego, CA) of the fungal ITS2 gene.

DNA extracts were submitted to the Roy J. Carver Biotechnology Center at the University of Illinois at Urbana-Champaign for Fluidigm amplification and Illumina sequencing. DNA sequencing amplicons were prepared by PCR using a Fluidigm Access Array IFC chip, which allowed simultaneous amplification of each target gene (Fluidigm, San Francisco, CA). Initial reactions were carried out according to a two-step protocol using reagent concentrations following Fluidigm recommended parameters, and an annealing temperature of 55 °C. The first PCR was performed in a 100-μL reaction volume using 1 ng DNA template. This PCR amplified the target DNA region using the ITS2-specific primers (ITS 3 and 4) with Fluidigm-specific amplification primer pads CS1 (5′- GCATCGATGAAGAACGCAGC-3′) and CS2 (5′-TCCTCCGCTTATTGATATGC -3′), which produced amplicons including (1) CS1 Fluidigm primer pad, (2) 5‘-forward PCR primer, (3) amplicon containing the region of interest, (4) 3‘-reverse PCR primer, and (5) CS2 Fluidigm primer pad. A secondary 30-μL PCR used 1 μL of 1:100 diluted product from the first PCR as template, and PCR primers with CS1 and CS2 sequences and Illumina-specific sequencing linkers P5 (5′-AATGATACGGCGACCACCGAGATCT-3′) and P7 (5′-CAAGCAGAAGACGGCATACGAGAT-3′), along with a 10-bp sample-specific barcode sequence. The final construct consisted of (1) Illumina linker P5, (2) CS1, (3) 5‘-primer, (4) amplicon containing the region of interest, (5) 3‘-primer, (6) CS2, (7) sample-specific 10-bp barcode, and (8) the Illumina linker P7. Final amplicons were gel-purified, quantified (Qubit; Invitrogen, Carlsbad CA, USA), combined to the same concentration, and then sequenced from both directions on an Illumina MiSeq 2 × 250 bp V2 run.

Bioinformatics procedures for DNA sequences were carried out using a standard workflow. Barcodes were used to assign each sequence to its original sample. After de-multiplexing, paired-end sequences generated for fungal ITS regions were merged using software FLASH (Fast Length Adjustment of Short reads) (Magoč and Salzberg, 2011). Quality filtering of fastq files was performed using software in the FASTX-Toolkit (Gordon and Hannon, 2010), which removed sequences with more than 10% bases with quality score lower than 30 and sequences containing ambiguous bases "N" from downstream processing. Filtered sequences were clustered into operational taxonomic units (OTUs) using USEARCH (v. 8.1.1861) and a 99% similarity threshold (Edgar, 2010). USEARCH was used to (1) de-replicate sequences and remove singletons; (2) remove chimeras contained in the sequences using GOLD (Reddy et al., 2015) as a reference database; and (3) form OTU clusters from sequences that were 99% similar and represent each OTU by representative sequences. The cluster file was converted into an OTU table using functions available in MacQIIME (Kuczynski et al., 2011). Representative sequences for ITS OTUs were assigned taxonomic attribution in QIIME with the uclust algorithm (Edgar, 2010) using the Unite database as a reference (Nilsson et al., 2019). Based on the recommendations of Lindahl et al. (2013) and Oliver et al. (2015), we removed all OTUs with <10 reads per sample. Fungal guilds were identified at the genus level using FungalTraits (Põlme et al., 2020).

**Statistical analysis**

All statistical tests were performed in R v. 3.6.2 (R Developnent Core Team, 2019), and statistical significance was determined at $P < 0.05$. We assessed the main effects of watershed (Alto Frio, Hornito, Zorro, Honda) and stand type (mixed ECM-AM, ECM dominated) and the

interactive effect between watershed and stand type. These effects will hereafter be referred to as "treatment effects".

To assess variation in soil chemical properties among watersheds and between mixed ECM-AM and ECM-dominated stands (hereafter referred to as "stand types"), we measured the following forest floor leaf litter, O horizon and mineral soil chemical properties: pH, %C, %N, C:N ratios, $\delta^{13}C$ and $\delta^{15}N$ for all leaf litter and soil samples, and $\delta^{13}C_{\text{mineral soil-litter}}$ and $\delta^{15}N_{\text{mineral soil-litter}}$ for O horizon and mineral soil samples (Table B.1). We used a fixed-factor two-way analysis of variance (ANOVA) to assess treatment effects on forest floor leaf litter and soil chemical properties. Independent variables were ln-transformed to meet assumptions of normality assessed using the Shapiro-Wilk test (Shapiro and Wilk, 1965).

To investigate correlations between fungal community composition and soil chemical properties, we first used global non-metric multi-dimensional scaling (NMDS) ordinations to visualize overall and ECM fungal community composition using the "metaMDS" function in *vegan* (Oksanen et al., 2019). To assess the statistical significance of treatment effects on overall fungal and ECM community composition, we used Hellinger transformed raw sequence count data to run permutational analysis of variance (PERMANOVA) implemented in the *vegan* package ("adonis"; Oksanen et al., 2019). Environmental variables (Table B.1) were fit to NMDS ordinations using the "envfit" function (*vegan*; Oksanen et al., 2019). The ECM community, in addition to other fungal guilds, were classified based on the taxonomic identity of OTUs within the FungalTraits database (Põlme et al., 2020). We grouped specific fungal guilds into broader guild classifications for analyses (Table B.2).

To understand differences in the functional potential in fungal communities across treatments, we quantified two indicators of fungal community function. First, we divided the

relative abundance of OTUs classified as ECM and the relative abundance of OTUs classified as SAP to estimate ECM:SAP ratios. Second, within each sample we summed the relative sequence counts of medium-distance fringe, medium-distance mat and long-distance exploration type ECM taxa, which were defined at the genus level using Agerer (2001) and Põlme et al. (2020). This value was used to estimate the relative abundance of high biomass ECM taxa within our samples. To quantify treatment effects on ECM:SAP ratios and sequence counts of high biomass ECM taxa, we used a fixed-factor two-way analysis of variance (ANOVA). We performed multiple comparisons between each level of watershed and stand mycorrhizal type using the "emmeans" function in the emmeans package (Russell, 2021) with Tukey's adjustment for multiple comparisons. ECM:SAP ratios were ln-transformed to meet assumptions of normality assessed using the Shapiro-Wilk test (Shapiro and Wilk, 1965).

To test for treatment effects on the hundred most abundant fungal genera within the forest floor leaf litter, organic horizon and mineral soil, we used a negative binomial model and sequence count data to perform a multivariate GLM analysis as implemented in the *mvabund* package ("manyglm"; Wang et al., 2021). Significance was determined using a Wald statistic and P-values assigned following 999 iterations using the ANOVA function.

We performed partial correspondence analyses to investigate variation in the overall fungal and ECM community that could be explained by watershed, after the effect of stand type had been removed and by stand type after the effect of watershed had been removed. Environmental variables (Table B.1) were fitted to the ordination plots using the "envfit" function (*vegan*; Oksanen et al., 2019).

## RESULTS

### An overview of fungal diversity

We obtained 2186-74,859 ITS2 sequences per sample with saturation of accumulation curves at the sample level suggesting that we obtained an adequate sample of fungal diversity. A total of 4,386,559 sequences were clustered into 7,021 OTUs based on a 99% similarity threshold. After removing OTUs with less than 10 sequences across all samples and rarefying to a read depth of 2,186 sequences, 5,463 OTUs remained; these were the OTUs used in all subsequent analyses. Using the FungalTraits database, 413 OTUs (7.56%) and 112,644 sequences (32.00%) were classified as ECM, and 1,157 OTUs (28.50%) and 68,763 sequences (19.54%) were classified as SAP. This general classification as "saprotroph" is an aggregation of more specific classifications (Table B.2). Aspergillaceae (10.72%), Mycosphaerellaceae (8.38%), Hypocreaceae (6.11%) and Mortierellaceae (5.20%) were the only non-ECM families that made up greater than 5% of non-ECM sequences. The most abundant ECM family was Russulaceae, accounting for 55.29% of all ECM reads. Inocybaceae (6.91%), Cortinariaceae (6.42%) and Thelephoraceae (5.98%) were the next most abundant ECM families. We used the FungalTraits database to determine ECM genera classified as medium-distance fringe, medium-distance mat or long-distance exploration type, which together accounted for 14.77% of ECM OTUs and 4.14% of ECM sequences. These groups of ECM genera, which produce extramatrical hyphae, are hereafter referred to as "high biomass ECM" and occur in low relative abundance within the ECM community. *Cortinarius* and *Octaviania* were the most abundant high biomass ECM genera, accounting for 83.63% and 7.43% of all high biomass ECM sequences, respectively. Based on a limited ability to assign taxonomy at the genus level, 2,527 OTUs (46.26%) and 116,531 sequences (33.11%) had unresolved trophic modes.

Ectomycorrhizal fungi accounted for greater than 50% of fungal sequences in the organic horizon in mixed ECM-AM and ECM-dominated stands (Figure 3.1). Within the mineral soil, ECM constituted greater than 50% of the overall fungal community in ECM-dominated stands in Honda, Zorro and Hornito compared to only 25-50% in mixed ECM-AM stands in those watersheds as well as both stand mycorrhizal types in Alto Frio. Of the 50 most abundant OTUs in the forest floor leaf litter, none were ECM, 16 were non-ECM, and 34 were of unknown trophic mode. Of the 50 most abundant OTUs in the O horizon, 29 were ECM, 16 were non-ECM, and five were of unknown trophic mode. Of the 50 most abundant OTUs in the mineral soil, 25 were ECM, 16 were non-ECM and nine were of unknown trophic mode. Non-ECM OTUs were largely classified as saprotrophs (61.64% of non-ECM OTUs, 39.96% of non-ECM sequences) or plant pathogens (16.79% of non-ECM OTUs, 10.01% of non-ECM sequences).

**Fungal community composition and function among and within watersheds**

Watershed explained more variation in all subsets of the fungal community relative to stand mycorrhizal type and the interaction between watershed and stand type (Table B.3). This pattern was consistent across forest floor leaf litter, O horizon, and both mineral soil layers. In NMDS ordinations, overall fungal communities in mineral soils of Honda (the lowest soil pH and fertility watershed) and Alto Frio (the highest soil pH and fertility watershed) clustered into two distinct groups with Hornito and Zorro communities clustering between the two extremes (Figure 3.2a). ECM communities in the mineral soil exhibited similar clustering patterns as those for the overall fungal communities (Figure 3.2b). However, ECM communities in Alto Frio had distinct assemblages, while the overall fungal communities in Alto Frio were more similar (Figure 3.2ab).

We found watershed-scale variation in the effect of stand mycorrhizal type on overall fungal and ECM community composition in both mineral soil layers. PERMANOVA analyses indicated significant interactions between watershed and stand type on overall fungal and ECM communities within the mineral soil (Table B.3). In the lowest soil pH and fertility watershed, Honda, overall fungal communities in mixed ECM-AM stands were distinct from those in ECM-dominated stands, whereas in the highest soil pH and fertility watershed, Alto Frio, overall fungal communities were similar across forest types (Figure 3.2a). Ectomycorrhizal fungal communities differed between mixed ECM-AM and ECM-dominated stands in all watersheds (P=0.001, Table B.3), with the stand-specific differences being greatest in Hornito (Fig. 3.3b). There was no significant interaction between watershed and stand type on fungal communities in the O horizon (P=0.2, Table B.3), though this may reflect the fact that only Honda and Zorro had O horizons present in both mixed ECM-AM and ECM-dominated stands.

At 0-5 cm mineral soil depth, ECM:SAP ratios, a metric of fungal community function, differed among watersheds ($F_{3,15}$=3.175, P=0.05) (Figure 3.3). Honda, the lowest soil pH and fertility watershed, exhibited significantly higher ECM:SAP ratios compared to Alto Frio, the highest soil pH and fertility watershed (P=0.04). Within watersheds, ECM:SAP ratios were significantly greater in ECM-dominated stands relative to mixed ECM-AM stands in Honda (P=0.006), but not significantly different between forest types in Hornito, Zorro or Alto Frio (Figure 3.3). Therefore, ECM:SAP ratios followed a similar pattern to that observed for overall fungal community composition. For a second metric of fungal community function, the relative abundance of high biomass ECM taxa, there was no significant effect of watershed or stand mycorrhizal type. However, *Cortinarius*, which accounted for 83.63% of all high biomass ECM sequences, occurred in significantly higher relative abundance in ECM-dominated versus mixed

ECM-AM stands in the O horizon and in the surface mineral soil (F=4.49, P=0.04; F=6.77, P=0.03, respectively) (Figure 3.4ab; Table B.5), though *Cortinarius* was not present in Alto Frio and occurred in low relative abundance in Zorro.

Within the top 100 most abundant fungal genera in the mineral soil, 13 ECM genera differed significantly among watersheds, four of which were classified as high biomass (Table B.4). *Cortinarius*, *Tylopilus* and *Octaviana* occurred in higher relative abundance in Honda, Zorro, and/or Hornito compared to Alto Frio, the highest pH, highest fertility watershed (Table B.4). In contrast, *Austroboletus* was most abundant in Alto Frio. Within watersheds, *Cortinarius*, which was not present in Alto Frio, was the only high biomass ECM genus that differed in relative abundance between stand mycorrhizal types with significantly lower relative abundance in mixed ECM-AM compared to ECM-dominated stands in both the O horizon and 0-5 cm depth mineral soil (Table B.5). *Lactifluus*, *Leotia* and *Lactarius*, which were ECM taxa not classified as high biomass, also occurred in significantly higher relative abundance in ECM-dominated relative to mixed ECM-AM stands (Table B.5).

We found a significant interaction between watershed and stand mycorrhizal type on $\delta^{15}N_{litter}$ and $\delta^{15}N_{\text{mineral soil-litter}}$ that mirrored the interactive effect we observed for overall fungal community composition and for ECM:SAP ratios ($\delta^{15}N_{litter}$, $F_{3,15}=21.31$, $P<0.0001$; $\delta^{15}N_{\text{mineral soil-litter}}$, $F_{3,15}=73.3$, $P<0.0001$). In Alto Frio, there was no effect of stand type on $\delta^{15}N_{litter}$ or $\delta^{15}N_{\text{mineral soil-litter}}$ (Figure 3.5a-c). In contrast, in Honda, Hornito and Zorro, $\delta^{15}N_{litter}$ was significantly lower in ECM-dominated relative to mixed ECM-AM stands ($P<0.0001$, $P=0.0001$, $P=0.01$, respectively) (Figure 3.5a). Furthermore, in these three watersheds, $\delta^{15}N_{\text{mineral soil-litter}}$ was significantly higher in ECM-dominated relative to mixed ECM-AM stands at 0-5 cm mineral soil depth ($P<0.0001$, $P=0.0002$, and $P<0.0001$ for Honda, Hornito, and Zorro, respectively; Figure

3.5c). We used the "envfit" function (*vegan*; Oksanen et al., 2019) to fit soil chemical variables to NMDS ordinations and found that N isotopic composition of SOM was a strong predictor of overall fungal and ECM community composition in the leaf litter, O horizon, and both mineral soil layers. Specifically, $\delta^{15}N_{litter}$, a proxy for N availability, was the forest floor leaf litter property we measured that exhibited the strongest correlation with overall fungal community composition in the forest floor leaf litter ($R^2 = 0.64$, P=0.001). In the O horizon and in the 0-5 cm depth mineral soil, $\delta^{15}N_{\text{mineral soil-litter}}$, a proxy for the contribution of fungal biomass to SOM, exhibited the second strongest correlation with overall fungal community composition ($R^2 = 0.47$, P=0.03; $R^2 = 0.58$, P=0.001, respectively), with soil pH exhibiting the strongest correlation ($R^2 = 0.67$, P=0.003; $R^2 = 0.60$, P=0.001, respectively). Variation in ECM community composition in the surface mineral soil layer was most strongly correlated with $\delta^{15}N_{\text{mineral soil-litter}}$ ($R^2 = 0.75$, P=0.001).

We used partial correspondence analyses to isolate variation in overall fungal communities among watersheds and between mixed ECM-AM and ECM-dominated stands. By fitting soil chemical properties to the resulting ordination, we found that soil pH exhibited the strongest correlation with variation in overall fungal community composition among watersheds ($R^2 = 0.63$, P<0.0003, Figure 3.6a) while $\delta^{15}N_{\text{mineral soil-litter}}$ exhibited the strongest correlation with variation in overall fungal community composition between mixed ECM-AM and ECM-dominated stands ($R^2 = 0.53$, P<0.0001, Figure 3.6b).

## DISCUSSION

Underlying soil acid-base chemistry may determine the degree to which fungal communities drive ECM effects across systems. In Fortuna, establishment of ECM-associated

*O. mexicana* trees within mixed ECM-AM forests has distinct effects on soil chemical properties in higher soil pH and fertility watersheds relative to lower soil pH and fertility watersheds (Seyfried et al., 2021a). Strikingly, we observed that the effect of stand mycorrhizal type on overall fungal community composition also varied among watersheds in Fortuna and correlated with watershed-scale variation in soil acid-base chemistry. Fungal communities differed most between mixed ECM-AM and ECM-dominated stands in the lowest soil pH and fertility watershed, Honda, but were similar between stand types in the highest soil pH and fertility watershed, Alto Frio (Figure 3.2a). Corresponding divergence in fungal community composition and soil chemical properties between stand types in lower pH and fertility soils suggest that fungal communities could contribute to the greater ECM effects on soil chemical properties in the context of lower underlying soil pH and fertility (Figure 3.7). In contrast, in higher pH and fertility soils, assembly of compositionally similar fungal communities between stand mycorrhizal types that exhibit distinct soil chemical properties suggests that ECM effects are not mediated directly by fungal community functions but instead by different aspects of the tree-fungal symbiosis in the context of higher underlying soil pH and fertility (Figure 3.7). Here we discuss evidence that soil acid-base chemistry may shape fungal community composition and function, ultimately leading to variability among watersheds in the effect of ECM-associated trees and soil fungal communities on SOM accumulation and N cycling.

Interactions between ECM and SAP fungal guilds have long been hypothesized to play a role in suppressing SOM decomposition in ECM-dominated forests (Fernandez and Kennedy, 2016; Gadgil and Gadgil, 1971). However, it is increasingly recognized that interguild interactions as well as the implications of those interactions for biogeochemical cycling are context dependent (Fernandez et al., 2019; Smith and Wan, 2019). We found support for this,

with the greatest effect of stand mycorrhizal type on ECM:SAP ratios occurring within the lowest soil pH and fertility watershed and no effect of stand type on ECM:SAP ratios occurring within the highest soil pH and fertility watershed (Figure 3.3). Greater relative abundance of the high biomass ECM genus, *Cortinarius*, within organic and mineral soil horizons in the lowest soil pH and fertility watershed suggests that the underlying soil conditions may have selected for this ECM taxa which has a greater functional potential to outcompete SAP fungi for limiting nutrients. Competition between fungal guilds may ultimately decrease decomposition rates such that particulate organic matter accumulates at the soil surface because ECM fungi, relative to SAP fungi, have a reduced genetic potential to encode enzymes involved in degradation (Bödeker et al., 2016; Kohler et al., 2015). These patterns in ECM:SAP ratios and ECM community composition across watersheds suggest that underlying soil acid-base chemistry can mediate ECM-SAP competition such that ECM fungi become more abundant in the overall fungal community as soil pH and fertility decrease. Only in the lower pH and fertility watersheds do ECM-dominated stands exhibit lower soil pH and N availability than mixed ECM-AM stands (Seyfried et al., 2021a), creating a positive feedback loop that further favors ECM fungi in the ECM-dominated stands. In contrast, higher underlying soil pH and fertility may alleviate competition between fungal guilds and facilitate habitat sharing (Kyaschenko et al., 2017), leading to smaller differences in ECM:SAP ratios between stand types such that this positive feedback loop may be weaker. Overall, we found that soil fertility may mediate ECM community function and interguild interactions which may determine the capacity of a fungal community to drive a system towards conservative nutrient cycling.

Watershed-scale variation in fungal community composition and function aligned with patterns in N isotopic composition of forest floor leaf litter and mineral soil, revealing the role of

fungal communities in driving the interaction between soil conditions and ECM effects on soil properties. When underlying soil pH and fertility are low, establishment of ECM trees and associated fungi may increase N limitation and result in greater contribution of $^{15}N$-enriched ECM biomass to belowground SOM pools, as evidenced by lower $\delta^{15}N_{litter}$ and higher $\delta^{15}N_{mineral\ soil\text{-}leaf\ litter}$ in ECM stands, respectively. These patterns may result from greater belowground C allocation by host trees under N-limited conditions which can stimulate ECM to immobilize scavenged N, exacerbating N limitation experienced by host trees (Karst et al., 2021; Nasholm et al., 2013). This may be mediated by greater ECM colonization of tree roots and specifically by the selection of high biomass ECM taxa, such as *Cortinarius*, with the functional capacity to outcompete saprotrophic decomposers for organic substrate. These ECM taxa may also promote accumulation of organic nutrients through contribution of hydrophobic rhizomorphs to belowground SOM pools which are resistant to decay (Ekblad et al., 2013; Fernandez et al., 2016). When underlying soil pH and fertility are higher, ECM trees and associated fungi may not increase N limitation or significantly alter the contribution of ECM biomass to belowground SOM pools, as evidenced by similar $\delta^{15}N_{litter,}$ $\delta^{15}N_{mineral\ soil\text{-}leaf\ litter}$ and overall fungal community composition between mixed ECM-AM and ECM-dominated stands. However, although ECM effects within the highest fertility and pH watershed appeared minimal based on indices of fungal community composition and function used in this study, a past study observed substantial ECM effects on mineral soil POM:MAOM ratios, pH, ECEC and BS (Seyfried et al., 2021). Therefore, within higher soil pH and fertility watersheds, ECM effects may be driven by conservative resource traits that are characteristic of ECM-associated trees, such as production of low quality leaf litter (e.g., McGuire et al., 2010; Midgley et al., 2015; Torti et al., 2001), rather than by fungal communities. These findings highlight the fact that the mechanisms driving ECM effects

may vary between systems: although fungal community functional potential correlates strongly with ECM effects in lower pH and fertility watersheds, other aspects of the tree-mycorrhizal symbiosis may be more important in driving ECM effects in higher pH and fertility watersheds.

Positive feedback loops that form between soil chemical properties and fungal community composition can drive ecosystems towards contrasting nutrient syndromes (Kyaschenko et al., 2017; Mayer et al., 2021; Nasholm et al., 2013), but these feedback loops make it difficult to isolate mechanisms driving ECM effects on forests. By sampling among watersheds which differed in soil pH and fertility, and in mixed ECM-AM versus ECM-dominated stands within the watersheds, we could disentangle the effects of soil chemical properties on fungal communities (based on watershed scale variation) from the effects of fungal communities on soil chemical properties (based on stand mycorrhizal type differences within watersheds). We found that variation in overall fungal community composition among watersheds exhibited the strongest correlation with mineral soil pH (Figure 3.6a). In contrast, variation in overall fungal communities between mixed ECM-AM and ECM-dominated stands within watersheds exhibited the strongest correlation with $\delta^{15}N_{\text{mineral soil-litter}}$ (Figure 3.6b). Therefore, we infer that soil acid-base chemistry determines overall fungal community composition at the watershed scale, setting the potential for fungal communities to drive variation in soil chemical properties at the stand scale within watersheds and strengthen the positive feedback loop in ECM-dominated stands.

## CONCLUSIONS

We show that soil acid-base chemistry can filter fungal communities at the watershed scale to mediate the role of fungal communities in driving ECM effects on SOM accumulation

and N cycling at the stand scale. Within the lowest soil pH and fertility watershed, fungal communities in mixed ECM-AM stands were compositionally and functionally distinct from fungal communities in ECM-dominated stands. Using natural abundance N isotopes, we infer that differences in fungal community composition between stand mycorrhizal types were associated with increased N limitation and increased contribution of hyphal biomass to SOM pools in ECM-dominated stands compared to mixed ECM-AM stands. Therefore, in the watershed with the lowest soil pH and fertility, fungal communities may drive variation in ECM effects between mixed ECM-AM and ECM-dominated stands. In contrast, within the highest soil pH and fertility watershed, where fungal communities were compositionally similar between forest types, ECM effects may be driven more by conservative resource economies that are characteristic of ECM-associated trees than by morphological and physiological characteristics of the ECM symbionts. Overall, our results highlight the importance of understanding the geological context within which mycorrhizal mediated plant-soil feedbacks occur as underlying soil acid-base chemistry may play a key role in determining the mechanistic drivers of ECM effects on SOM accumulation and N cycling.

## TABLE AND FIGURES

**Table 3.1.** Mineral soil properties (effective cation exchange capacity, ECEC; base saturation; and carbon to nitrogen ratios, C:N) for mixed ECM-AM and ECM-dominated stands within four watersheds in Fortuna (Mean ± SE, n =3) (Seyfried et al., 2021a).

| | | Honda: lower fertility | | Zorro: lower fertility | | Hornito: higher fertility | | Alto Frio: higher fertility | |
|---|---|---|---|---|---|---|---|---|---|
| | Depth (cm) | ECM-dominated stand | AM-dominated stand | ECM-dominated stand | AM-dominated stand | ECM-dominated stand | AM-dominated stand | ECM-dominated stand | AM-dominated stand |
| ECEC (cmol (+) $kg^{-1}$) | 0-20 | 7.19 ± 1.40 | 9.85 ± 1.27 | 4.64 ± 0.18 | 5.38 ± 0.77 | 7.60 ± 1.21 | 12.47 ± 2.56 | 5.77 ± 0.85 | 12.28 ± 1.67 |
| | 20-40 | 3.75 ± 0.43 | 5.19 ± 0.57 | 2.75 ± 0.29 | 2.87 ± 0.34 | 5.68 ± 0.24 | | 4.48 ± 0.34 | 6.21 ± 0.85 |
| Base saturation | 0-20 | 23.93 ± 4.811 | 30.64 ± 4.14 | 36.48 ± 2.86 | 34.62 ± 5.52 | 22.05 ± 0.70 | 86.79 ± 6.95 | 55.86 ± 12.03 | 95.32 ± 1.64 |
| | 20-40 | 54.01 ± 4.08 | 27.26 ± 0.94 | 64.49 ± 11.48 | 45.75 ± 6.59 | 19.46 ± 1.89 | | 39.95 ± 10.92 | 93.82 ± 1.05 |
| C:N | 0-20 | 14.54 ± 0.71 | 14.70 ± 0.09 | 14.60 ± 0.92 | 13.64 ± 0.39 | 15.07 ± 0.59 | 10.76 ± 0.26 | 15.08 ± 0.76 | 11.16 ± 0.46 |
| | 20-40 | 14.34 ± 0.62 | 14.09 ± 0.57 | 14.90 ± 0.66 | 14.42 ± 0.98 | 13.19 ± 1.30 | 12.75 ± 1.93 | 13.57 ± 0.76 | 10.71 ± 0.14 |

**Figure 3.1.** Relative abundance of simplified fungal guilds in the forest floor leaf litter, organic horizon, mineral soil at 0-5 cm depth and mineral soil at 15-20 cm depth in (a) mixed ECM-AM stands and (b) ECM-dominated stands in Honda, the lowest pH and fertility watershed and (c) mixed ECM-AM stands and (d) ECM-dominated stands in Alto Frio, the highest pH and fertility watershed.

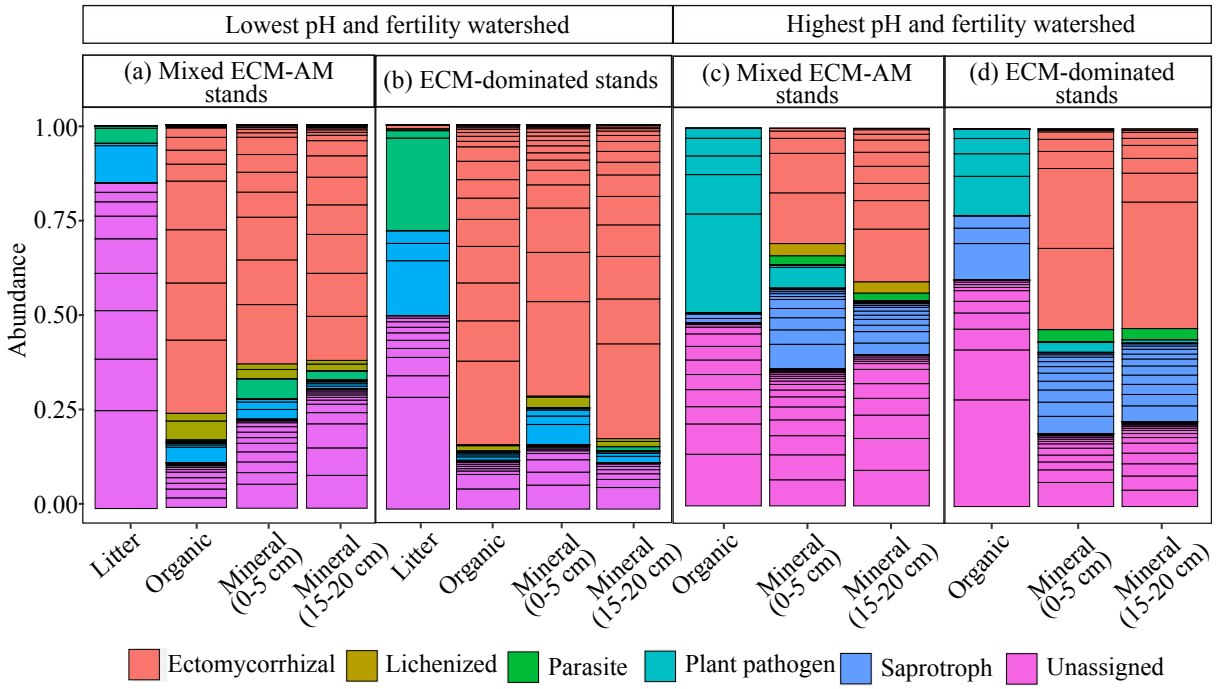

**Figure 3.2**. Non-metric multidimensional scaling (NMDS) plot of (a) the overall fungal community (stress value = 0.21) and (b) the ectomycorrhizal community (stress value = 0.15) in mineral soil (both 0-5 cm and 15-20 cm depths) beneath *Oreomunnea mexicana* focal trees. Colors indicate different watersheds: Alto Frio (green), Hornito (purple), Zorro (pink) and Honda (orange). Open circles denote samples from beneath *O. mexicana* in mixed ECM-AM stands, and closed circles denote samples from beneath *O. mexicana* in ECM-dominated stands.

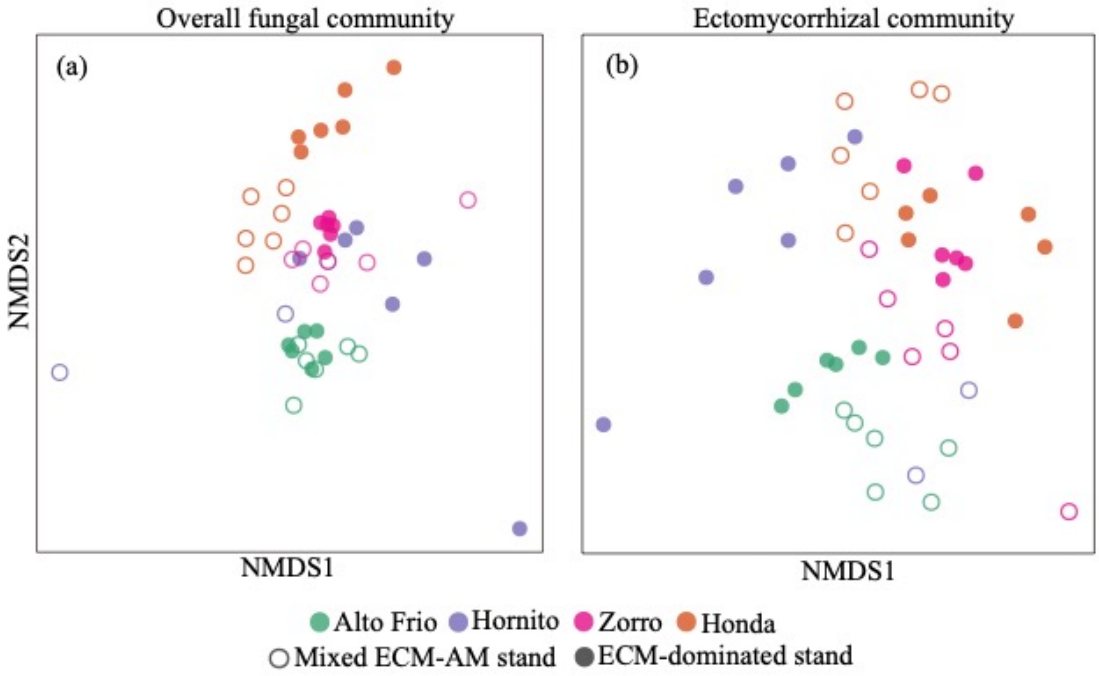

**Figure 3.3.** Boxplot illustrating variation in the ratio of ectomycorrhizal (ECM) relative abundance to saprotrophic (SAP) relative abundance (ECM:SAP) at 0-5 cm mineral soil depth beneath *Oreomunnea mexicana* focal trees in mixed stands of ECM- and arbuscular mycorrhizal (AM)-associated trees (denoted Mixed) and ECM-dominated stands (denoted ECM). Colors indicate different watersheds: Alto Frio (green), Hornito (purple), Zorro (pink) and Honda (orange). Letters denote statistically significant differences among watersheds based on Tukey post-hoc comparisons ($P<0.05$). Within watersheds, ECM:SAP ratios were significantly greater in ECM-dominated stands relative to mixed ECM-AM stands in Honda ($P=0.006$), but not significantly different between forest types in Hornito, Zorro or Alto Frio.

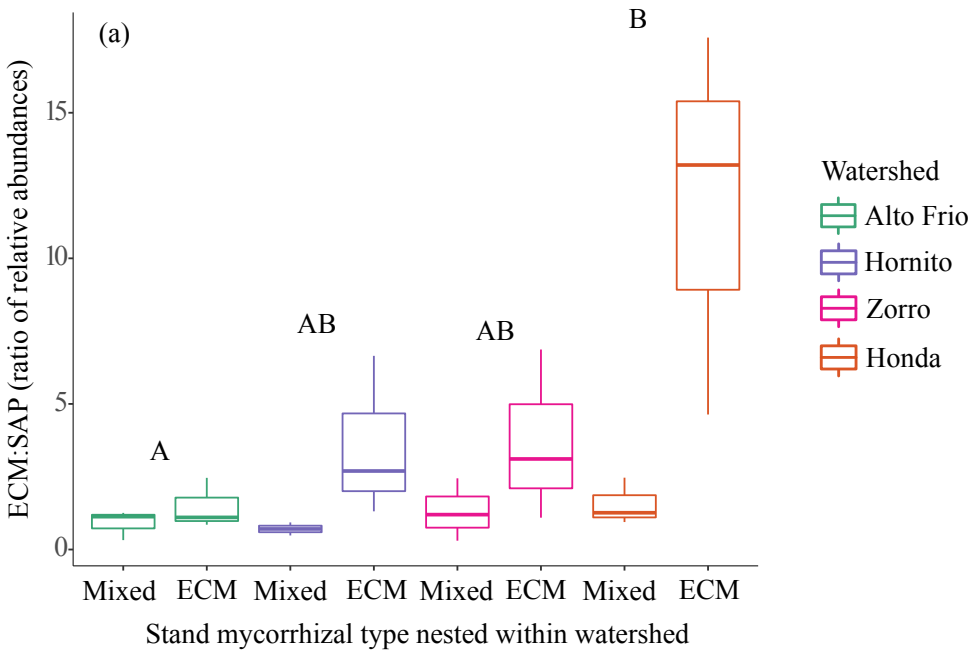

**Figure 3.4.** Boxplots illustrating variation in sequence counts of the "high biomass" ectomycorrhizal (ECM) genus *Cortinarius* in the (a) organic horizon and (b) 0-5 cm depth mineral soil beneath *Oreomunnea mexicana* focal trees in mixed stands of ECM- and arbuscular mycorrhizal (AM)-associated trees (denoted Mixed) and ECM-dominated stands (denoted ECM). Colors indicate different watersheds: Alto Frio (green), Hornito (purple), Zorro (pink) and Honda (orange). Organic horizon was not present in Alto Frio or in the mixed ECM-AM stands in Hornito.

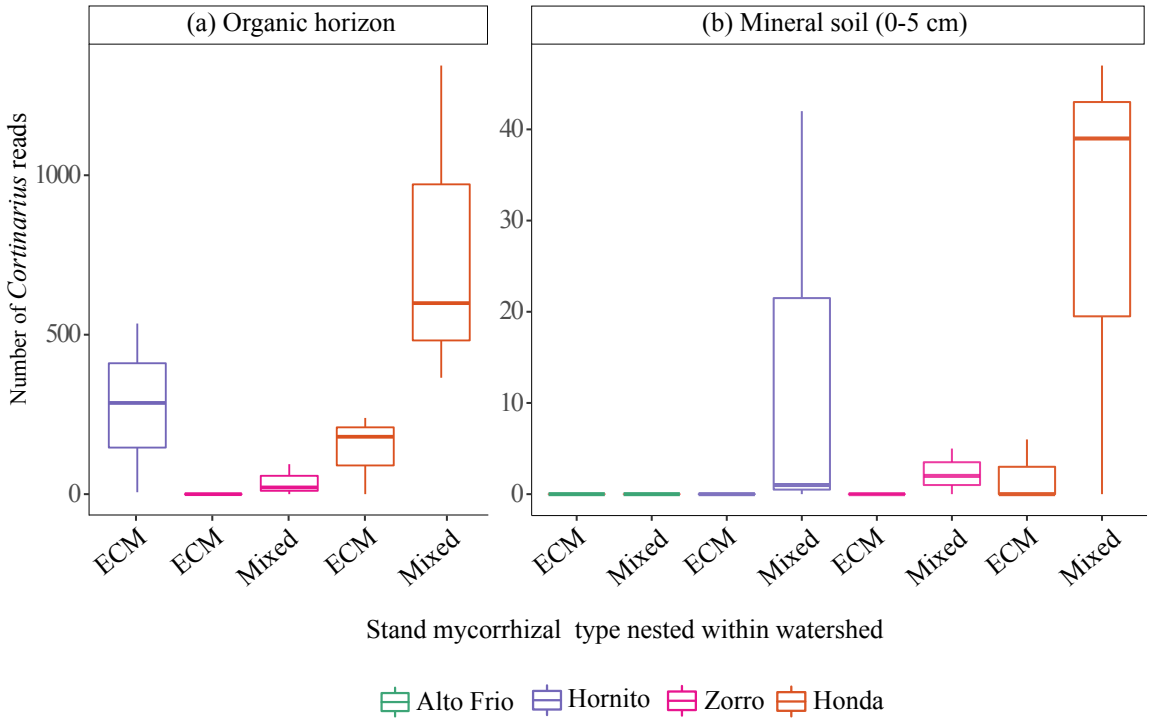

**Figure 3.5.** Comparison of (a) $\delta^{15}N_{litter}$ in the forest floor leaf litter, (b) $\delta^{15}N_{organic\ soil\text{-}litter}$ in the organic horizon, and (c) $\delta^{15}N_{mineral\ soil\text{-}litter}$ in the 0-5 cm depth mineral soil beneath *Oreomunnea mexicana* focal trees in mixed stands of ectomycorrhizal (ECM) and arbuscular mycorrhizal (AM)-associated trees (denoted Mixed) and ECM-dominated stands (denoted ECM). Colors indicate different watersheds: Alto Frio (green), Hornito (purple), Zorro (pink) and Honda (orange). Organic horizon was not present in Alto Frio or in the mixed ECM-AM stands in Hornito. Asterisks indicate statistically significant differences between stand mycorrhizal types.

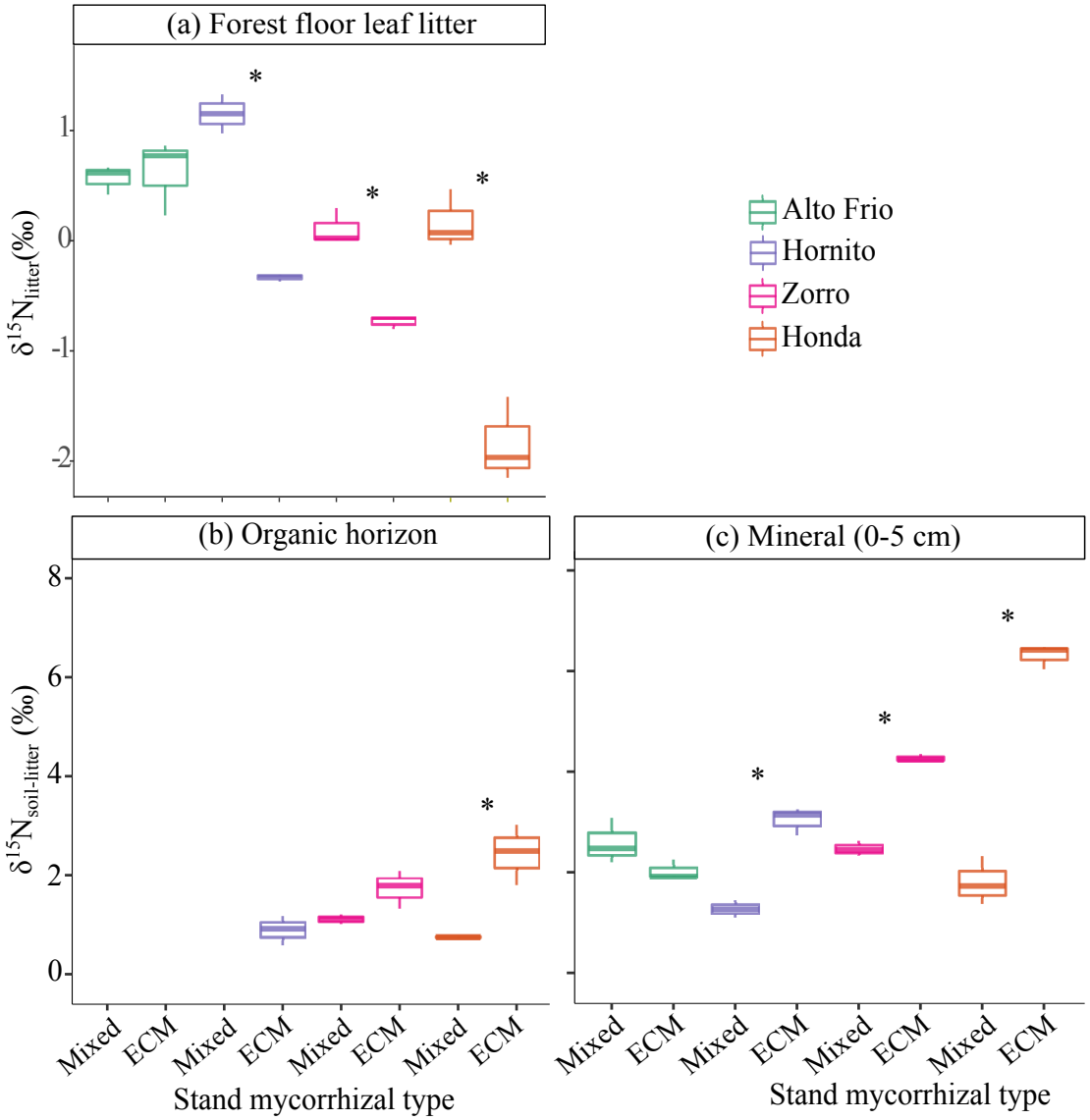

**Figure 3.6.** Partial correspondence analysis determining differences in the overall fungal community (a) between watersheds with variation due to stand mycorrhizal type removed, and (b) between mixed stands of ectomycorrhizal (ECM) and arbuscular mycorrhizal (AM)-associated trees and ECM-dominated stands with variation due to watersheds removed. pH ($R^2 = 0.44$) predicts the most variation in fungal communities among watersheds while $\delta^{15}N_{\text{mineral soil-litter}}$ ($R^2 = 0.55$) predicts the most variation in fungal communities among stand mycorrhizal types.

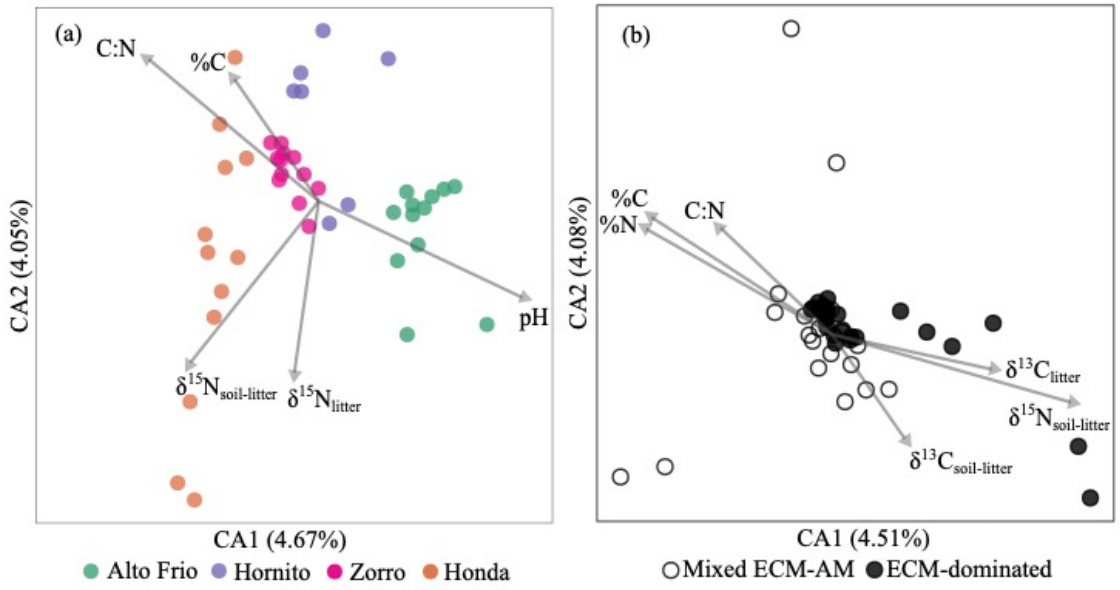

**Figure 3.7.** Conceptual diagram of the experimental design and the major conclusions drawn from the results at the watershed and stand scales. The location of the study site in the Fortuna Forest Reserve is indicated by the black square on the map of Panama (delineated by gray shading). The different colored rectangles represent the four watersheds studied in Fortuna, and the orange circles represent the sampling locations in each watershed with three locations in mixed stands of ectomycorrhizal (ECM) and arbuscular mycorrhizal (AM)-associated trees and three locations in ECM-dominated stands.

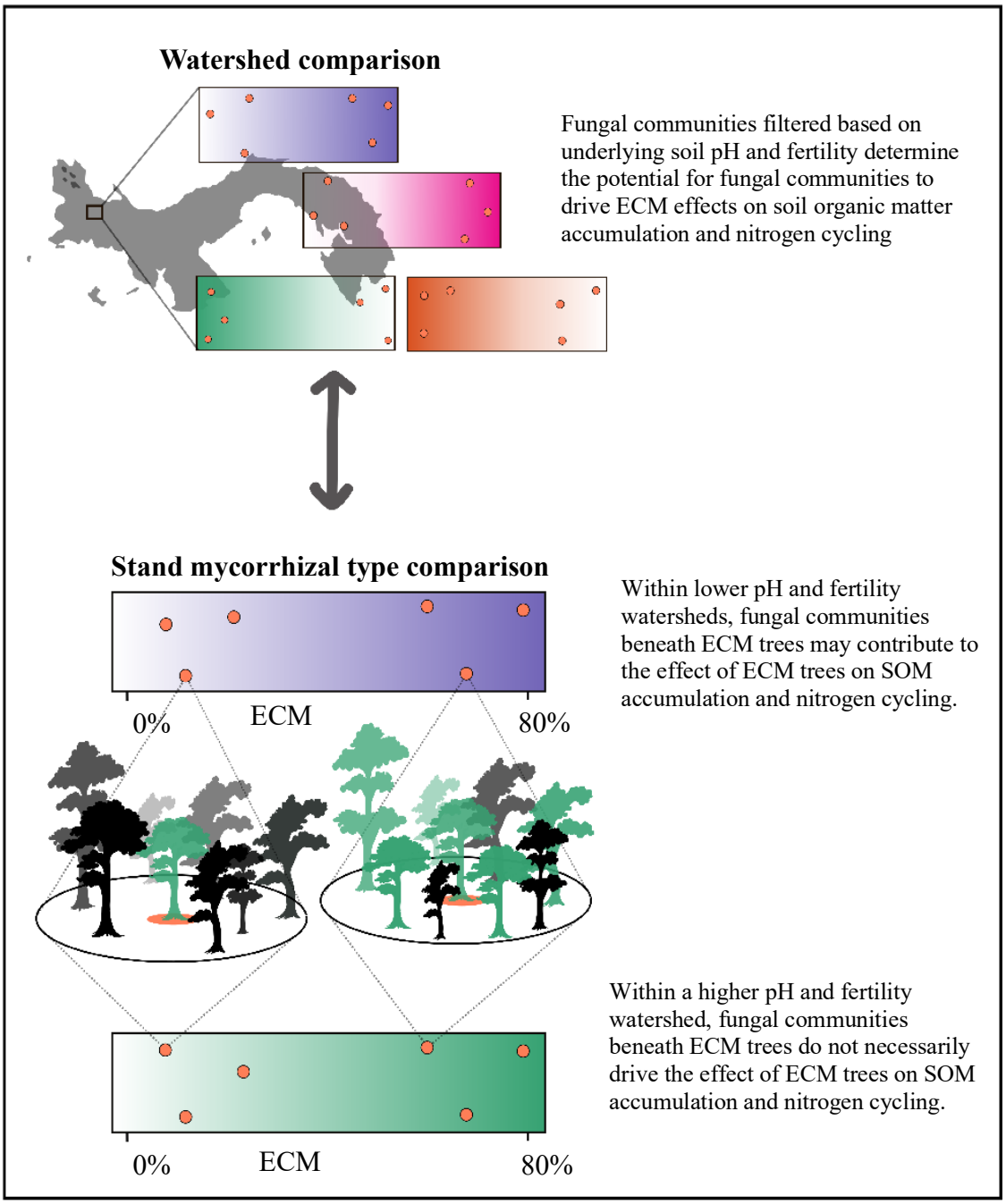

## REFERENCES


Agerer, R. (2001). Exploration types of ectomycorrhizae - A proposal to classify ectomycorrhizal mycelial systems according to their patterns of differentiation and putative ecological importance. *Mycorrhiza*, *11*(2), 107–114. doi: 10.1007/s005720100108

Andersen, K. M., Endara, M. J., Turner, B. L., & Dalling, J. W. (2012). Trait-based community assembly of understory palms along a soil nutrient gradient in a lower montane tropical forest. *Oecologia*, *168*(2), 519–531. doi: 10.1007/s00442-011-2112-z

Averill, C., Bhatnagar, J. M., Dietze, M. C., Pearse, W. D., & Kivlin, S. N. (2019). Global imprint of mycorrhizal fungi on whole-plant nutrient economics. *Proceedings of the National Academy of Sciences of the United States of America*, *46*, 23163–23168. doi: 10.1073/pnas.1906655116

Awad, A., Majcherczyk, A., Schall, P., Schröter, K., Schöning, I., Schrumpf, M., … Pena, R. (2019). Ectomycorrhizal and saprotrophic soil fungal biomass are driven by different factors and vary among broadleaf and coniferous temperate forests. *Soil Biology and Biochemistry*, *131*, 9–18. doi: 10.1016/j.soilbio.2018.12.014

Bödeker, I. T. M., Lindahl, B. D., Olson, Å., & Clemmensen, K. E. (2016). Mycorrhizal and saprotrophic fungal guilds compete for the same organic substrates but affect decomposition differently. *Functional Ecology*, *30*(12), 1967–1978. doi: https://doi.org/10.1111/1365-2435.12677

Cavelier, J., Solis, D., & Jaramillo, M. A. (1996). Fog interception in montane forests across the Central Cordillera of Panama. *Journal of Tropical Ecology*, *12*, 357–369. doi: 10.1017/S026646740000955X

Cheeke, T. E., Phillips, R. P., Brzostek, E. R., Rosling, A., Bever, J. D., & Fransson, P. (2017).

Dominant mycorrhizal association of trees alters carbon and nutrient cycling by selecting for microbial groups with distinct enzyme function. *New Phytologist*, *214*, 432–442. doi: 10.1111/nph.14343

Corrales, A., Mangan, S. A., Turner, B. L., & Dalling, J. W. (2016). An ectomycorrhizal nitrogen economy facilitates monodominance in a neotropical forest. *Ecology Letters*, *19*(4), 383–392. doi: 10.1111/ele.12570

Corrales, A., Turner, B. L., Tedersoo, L., Anslan, S., & Dalling, J. W. (2017). Nitrogen addition alters ectomycorrhizal fungal communities and soil enzyme activities in a tropical montane forest. *Fungal Ecology*, *27*, 14–23. doi: https://doi.org/10.1016/j.funeco.2017.02.004

Craig, M. E., Turner, B. L., Liang, C., Clay, K., Johnson, D. J., & Phillips, R. P. (2018). Tree mycorrhizal type predicts within-site variability in the storage and distribution of soil organic matter. *Global Change Biology*, *24*, 3317–3330. doi: 10.1111/gcb.14132

Dalling, J. W., & Turner, B. L. (2021). *Soils of the Fortuna Forest Reserve*. Retrieved from https://doi.org/10.5479/si.14315990

Edgar, R. C. (2010). Search and clustering orders of magnitude faster than BLAST. *Bioinformatics*, *26*(19), 2460–2461. doi: 10.1093/bioinformatics/btq461

Ekblad, A., Wallander, H., Godbold, D. L., Cruz, C., Johnson, D., Baldrian, P., … Plassard, C. (2013). The production and turnover of extramatrical mycelium of ectomycorrhizal fungi in forest soils: role in carbon cycling. *Plant and Soil*, *366*(1–2), 1–27. doi: 10.1007/s11104-013-1630-3

Fernandez, C. W., & Kennedy, P. G. (2016). Revisiting the “Gadgil effect”: do interguild fungal interactions control carbon cycling in forest soils? *New Phytologist*, *209*(4), 1382–1394. doi: 10.1111/nph.13648

Fernandez, C. W., Langley, J. A., Chapman, S., McCormack, M. L., & Koide, R. T. (2016). The decomposition of ectomycorrhizal fungal necromass. *Soil Biology and Biochemistry*, *93*, 38–49. doi: 10.1016/j.soilbio.2015.10.017

Fernandez, C. W., See, C. R., & Kennedy, P. G. (2019). Decelerated carbon cycling by ectomycorrhizal fungi is controlled by substrate quality and community composition. *New Phytologist*, *226*, 569–582. doi: 10.1111/nph.16269

Gadgil, R. L., & Gadgil, P. D. (1971). Mycorrhiza and litter decomposition. *Nature*, *233*, 133. doi: 10.1038/233133a0

Gordon, A., & Hannon, G. (2010). Fastx-toolkit. FASTQ/A Short-reads Pre-processing Tools.

Hobbie, E. A., & Agerer, R. (2010). Nitrogen isotopes in ectomycorrhizal sporocarps correspond to belowground exploration types. *Plant and Soil*, *327*, 71–83. doi: 10.1007/s11104-009-0032-z

Hobbie, E. A., & Högberg, P. (2012). Nitrogen isotopes link mycorrhizal fungi and plants to nitrogen dynamics. *New Phytologist*, *196*, 367–382. doi: 10.1111/j.1469-8137.2012.04300.x

Högberg, M. N., Bååth, E., Nordgren, A., Arnebrant, K., & Högberg, P. (2003). Contrasting effects of nitrogen availability on plant carbon supply to mycorrhizal fungi and saprotrophs - A hypothesis based on field observations in boreal forest. *New Phytologist*, *160*, 225–238. doi: 10.1046/j.1469-8137.2003.00867.x

Högberg, M. N., Briones, M. J. I., Keel, S. G., Metcalfe, D. B., Campbell, C., Midwood, A. J., … Högberg, P. (2010). Quantification of effects of season and nitrogen supply on tree below-ground carbon transfer to ectomycorrhizal fungi and other soil organisms in a boreal pine forest. *New Phytologist*, *187*(2), 485–493. doi: https://doi.org/10.1111/j.1469-8137.2010.03274.x

Högberg, P., Högberg, M. N., Quist, M. E., Ekblad, A., & Näsholm, T. (1999). Nitrogen isotope fractionation during nitrogen uptake by ectomycorrhizal and non-mycorrhizal Pinus sylvestris. *New Phytologist*, *142*(3), 569–576. doi: https://doi.org/10.1046/j.1469-8137.1999.00404.x

Karst, J., Wasyliw, J., Birch, J. D., Franklin, J., Chang, S. X., & Erbilgin, N. (2021). Long-term nitrogen addition does not sustain host tree stem radial growth but doubles the abundance of high-biomass ectomycorrhizal fungi. *Global Change Biology*, *00*, 1–14. doi: https://doi.org/10.1111/gcb.15713

Keymer, D. P., & Kent, A. D. (2014). Contribution of nitrogen fixation to first year Miscanthus × giganteus. *GCB Bioenergy*, *6*(5), 577–586. doi: https://doi.org/10.1111/gcbb.12095

Kjoller, R., Nilsson, L. O., Hansen, K., Schmidt, I. K., Vesterdal, L., & Gundersen, P. (2012). Dramatic changes in ectomycorrhizal community composition, root tip abundance and mycelial production along a stand-scale nitrogen deposition gradient. *New Phytologist*, *194*(1), 278–286. doi: 10.1111/j.1469-8137.2011.04041.x

Kohler, A., Kuo, A., Nagy, L. G., Morin, E., Barry, K. W., Buscot, F., … Martin, F. (2015). Convergent losses of decay mechanisms and rapid turnover of symbiosis genes in mycorrhizal mutualists. *Nature Genetics*, *47*, 410-U176. doi: 10.1038/ng.3223

Kohzu, A., Tateishi, T., Yamada, A., Koba, K., & Wada, E. (2000). Nitrogen isotope fractionation during nitrogen transport from ectomycorrhizal fungi, Suillus granulatus, to the host plant, Pinus densiflora. *Soil Science and Plant Nutrition*, *46*(3), 733–739. doi: 10.1080/00380768.2000.10409138

Koide, R. T., Fernandez, C., & Malcolm, G. (2014). Determining place and process: functional

traits of ectomycorrhizal fungi that affect both community structure and ecosystem function. *New Phytologist*, *201*(2), 433–439. doi: 10.1111/nph.12538

Kuczynski, J., Stombaugh, J., Walters, W. A., González, A., Caporaso, J. G., & Knight, R. (2011). Using QIIME to Analyze 16S rRNA Gene Sequences from Microbial Communities. *Current Protocols in Bioinformatics*, *36*(1), 10.7.1-10.7.20. doi: https://doi.org/10.1002/0471250953.bi1007s36

Kuyper, T. W. (2017). *Carbon and Energy Sources of Mycorrhizal Fungi: Obligate Symbionts or Latent Saprotrophs?* doi: https://doi.org/10.1016/B978-0-12-804312-7.00020-6

Kyaschenko, J., Clemmensen, K. E., Karltun, E., & Lindahl, B. D. (2017). Below-ground organic matter accumulation along a boreal forest fertility gradient relates to guild interaction within fungal communities. *Ecology Letters*, *20*, 1546–1555. doi: 10.1111/ele.12862

Li, D., Voigt, T. B., & Kent, A. D. (2016). Plant and soil effects on bacterial communities associated with Miscanthus × giganteus rhizosphere and rhizomes. *GCB Bioenergy*, *8*(1), 183–193. doi: https://doi.org/10.1111/gcbb.12252

Lilleskov, E. A., Fahey, T. J., Horton, T. R., & Lovett, G. M. (2002). Belowground ectomycorrhizal fungal community change over a nitrogen deposition gradient in Alaska. *Ecology*, *83*(1), 104–115. doi: 10.1890/0012-9658(2002)083[0104:befcco]2.0.co;2

Lindahl, B. D., Ihrmark, K., Boberg, J., Trumbore, S. E., Högberg, P., Stenlid, J., & Finlay, R. D. (2007). Spatial separation of litter decomposition and mycorrhizal nitrogen uptake in a boreal forest. *New Phytologist*, *173*, 611–620. doi: 10.1111/j.1469-8137.2006.01936.x

Lindahl, B. D., Nilsson, R. H., Tedersoo, L., Abarenkov, K., Carlsen, T., Kjøller, R., … Kauserud, H. (2013). Fungal community analysis by high-throughput sequencing of

amplified markers – a user's guide. *New Phytologist*, *199*(1), 288–299. doi: https://doi.org/10.1111/nph.12243

Lindahl, B. D., & Tunlid, A. (2015). Ectomycorrhizal fungi - potential organic matter decomposers, yet not saprotrophs. *New Phytologist*, *205*, 1443–1447. doi: 10.1111/nph.13201

Magoč, T., & Salzberg, S. L. (2011). FLASH: fast length adjustment of short reads to improve genome assemblies. *Bioinformatics*, *27*(21), 2957–2963. doi: 10.1093/bioinformatics/btr507

Mayer, M., Rewald, B., Matthews, B., Sandén, H., Rosinger, C., Katzensteiner, K., … Godbold, D. L. (2021). Soil fertility relates to fungal-mediated decomposition and organic matter turnover in a temperate mountain forest. *New Phytologist*. doi: https://doi.org/10.1111/nph.17421

McGuire, K. L., Allison, S. D., Fierer, N., & Treseder, K. K. (2013). Ectomycorrhizal-Dominated Boreal and Tropical Forests Have Distinct Fungal Communities, but Analogous Spatial Patterns across Soil Horizons. *Plos One*, *8*(7). doi: e6827810.1371/journal.pone.0068278

McGuire, K. L., Zak, D. R., Edwards, I. P., Blackwood, C. B., & Upchurch, R. (2010). Slowed decomposition is biotically mediated in an ectomycorrhizal, tropical rain forest. *Oecologia*, *164*(3), 785–795. doi: 10.1007/s00442-010-1686-1

Midgley, M. G., Brzostek, E., & Phillips, R. P. (2015). Decay rates of leaf litters from arbuscular mycorrhizal trees are more sensitive to soil effects than litters from ectomycorrhizal trees. *Journal of Ecology*, *103*, 1454–1463. doi: 10.1111/1365-2745.12467

Moeller, H. V, Peay, K. G., & Fukami, T. (2014). Ectomycorrhizal fungal traits reflect environmental conditions along a coastal California edaphic gradient. *FEMS Microbiology*

*Ecology*, *87*(3), 797–806. doi: 10.1111/1574-6941.12265

Nasholm, T., Hogberg, P., Franklin, O., Metcalfe, D., Keel, S. G., Campbell, C., … Hogberg, M. N. (2013). Are ectomycorrhizal fungi alleviating or aggravating nitrogen limitation of tree growth in boreal forests? *New Phytologist*, *198*(1), 214–221. doi: 10.1111/nph.12139

Natelhoffer, K. J., & Fry, B. (1988). Controls on Natural Nitrogen-15 and Carbon-13 Abundances in Forest Soil Organic Matter. *Soil Science Society of America Journal*, *52*(6), 1633–1640. doi: https://doi.org/10.2136/sssaj1988.03615995005200060024x

Nguyen, N. H., Williams, L. J., Vincent, J. B., Stefanski, A., Cavender-Bares, J., Messier, C., … Kennedy, P. G. (2016). Ectomycorrhizal fungal diversity and saprotrophic fungal diversity are linked to different tree community attributes in a field-based tree experiment. *Molecular Ecology*, *25*(16), 4032–4046. doi: https://doi.org/10.1111/mec.13719

Nilsson, R. H., Larsson, K.-H., Taylor, A. F. S., Bengtsson-Palme, J., Jeppesen, T. S., Schigel, D., … Abarenkov, K. (2019). The UNITE database for molecular identification of fungi: handling dark taxa and parallel taxonomic classifications. *Nucleic Acids Research*, *47*(D1), D259–D264. doi: 10.1093/nar/gky1022

Oksanen, J., Blanchet, F., Friendly, M., Kindt, R., Legendre, P., McGlinn, D., … Wagner, H. (2019). *vegan: Community Ecology Package*. Retrieved from https://cran.r-project.org/package=vegan

Oliver, A. K., Brown, S. P., Callaham, M. A., & Jumpponen, A. (2015). Polymerase matters: non-proofreading enzymes inflate fungal community richness estimates by up to 15 %. *Fungal Ecology*, *15*, 86–89. doi: https://doi.org/10.1016/j.funeco.2015.03.003

Orwin, K. H., Kirschbaum, M. U. F., St John, M. G., & Dickie, I. A. (2011). Organic nutrient uptake by mycorrhizal fungi enhances ecosystem carbon storage: a model-based

assessment. *Ecology Letters*, *14*(5), 493–502. doi: 10.1111/j.1461-0248.2011.01611.x

Pellitier, P. T., Zak, D. R., Argiroff, W. A., & Upchurch, R. A. (2021). Coupled Shifts in Ectomycorrhizal Communities and Plant Uptake of Organic Nitrogen Along a Soil Gradient: An Isotopic Perspective. *Ecosystems*. doi: 10.1007/s10021-021-00628-6

Phillips, R. P., Brzostek, E., & Midgley, M. G. (2013). The mycorrhizal-associated nutrient economy: A new framework for predicting carbon-nutrient couplings in temperate forests. *New Phytologist*, *199*(1), 41–51. doi: 10.1111/nph.12221

Põlme, S., Abarenkov, K., Henrik Nilsson, R., Lindahl, B. D., Clemmensen, K. E., Kauserud, H., … Tedersoo, L. (2020). FungalTraits: a user-friendly traits database of fungi and fungus-like stramenopiles. *Fungal Diversity*, *105*, 1–16. doi: 10.1007/s13225-020-00466-2

Prada, C. M., Morris, A., Andersen, K. M., Turner, B. L., Caballero, P., & Dalling, J. W. (2017). Soils and rainfall drive landscape-scale changes in the diversity and functional composition of tree communities in premontane tropical forest. *Journal of Vegetation Science*, *28*, 859–870. doi: 10.1111/jvs.12540

R Development Core Team. (2019). *R: A language and environment for statistical computing*. Vienna, Austria: R Fouondataion for Statistical Computing.

Reddy, T. B. K., Thomas, A. D., Stamatis, D., Bertsch, J., Isbandi, M., Jansson, J., … Kyrpides, N. C. (2015). The Genomes OnLine Database (GOLD) v.5: a metadata management system based on a four level (meta)genome project classification. *Nucleic Acids Research*, *43*(D1), D1099–D1106. doi: 10.1093/nar/gku950

Russell, V. L. (2021). *emmeans: Estimated Marginal Means, aka Least-Squares Means*. Retrieved from https://cran.r-project.org/package=emmeans

Seyfried, G. S., Canham, C. D., Dalling, J. W., & Yang, W. H. (2021). The effects of tree-

mycorrhizal type on soil organic matter properties from neighborhood to watershed scales. *Soil Biology and Biochemistry*, 108385. doi: https://doi.org/10.1016/j.soilbio.2021.108385

Shapiro, S. S., & Wilk, M. B. (1965). An Analysis of Variance Test for Normality (Complete Samples). *Biometrika*, *52*(3/4), 591–611. doi: 10.2307/2333709

Smith, G. R., & Wan, J. (2019). Resource-ratio theory predicts mycorrhizal control of litter decomposition. *New Phytologist*, *223*, 1595–1606. doi: 10.1111/nph.15884

Sterkenburg, E., Bahr, A., Brandström Durling, M., Clemmensen, K. E., & Lindahl, B. D. (2015). Changes in fungal communities along a boreal forest soil fertility gradient. *New Phytologist*, *207*, 1145–1158. doi: 10.1111/nph.13426

Stone, D. E. (1972). New World Juglandaceae, III. A New Perspective of the Tropical Members with Winged Fruits. *Annals of the Missouri Botanical Garden*, *59*, 297. doi: 10.2307/2394761

Tedersoo, L., & Smith, M. E. (2013). Lineages of ectomycorrhizal fungi revisited: Foraging strategies and novel lineages revealed by sequences from belowground. *Fungal Biology Reviews*, *27*(3), 83–99. doi: https://doi.org/10.1016/j.fbr.2013.09.001

Toljander, J. F., Eberhardt, U., Toljander, Y. K., Paul, L. R., & Taylor, A. F. S. (2006). Species composition of an ectomycorrhizal fungal community along a local nutrient gradient in a boreal forest. *New Phytologist*, *170*, 873–884. doi: 10.1111/j.1469-8137.2006.01718.x

Torti, S. D., Coley, P. D., & Kursar, T. A. (2001). Causes and consequences of monodominance in tropical lowland forests. *American Naturalist*, *157*, 141–153. doi: 10.1086/318629

Van Der Linde, S., Suz, L. M., Orme, C. D. L., Cox, F., Andreae, H., Asi, E., … Bidartondo, M. I. (2018). Environment and host as large-scale controls of ectomycorrhizal fungi. *Nature*, *558*. doi: 10.1038/s41586-018-0189-9

Wallander, H., Mörth, C. M., & Giesler, R. (2009). Increasing abundance of soil fungi is a driver for 15N enrichment in soil profiles along a chronosequence undergoing isostatic rebound in northern Sweden. *Oecologia*, *160*, 87–96. doi: 10.1007/s00442-008-1270-0

Wang, Y., Naumann, U., Eddelbuettel, D., Wilshire, J., & Warton, D. (2021). *mvabund: Statistical Methods for Analysing Multivariate Abundance Data*.

Weemstra, M., Peay, K. G., Davies, S. J., Mohamad, M., Itoh, A., Tan, S., & Russo, S. E. (2020). Lithological constraints on resource economies shape the mycorrhizal composition of a Bornean rain forest. *New Phytologist*, *228*(1), 253–268. doi: https://doi.org/10.1111/nph.16672

Zak, D. R., Pellitier, P. T., Argiroff, W. A., Castillo, B., James, T. Y., Nave, L. E., … Tunlid, A. (2019). Exploring the role of ectomycorrhizal fungi in soil carbon dynamics. *New Phytologist*, *223*, 33–39. doi: 10.1111/nph.15679

# CHAPTER 4

# EFFECTS OF MYCORRHIZAL TYPE ON LEAF LITTER DECOMPOSITION DEPEND ON LITTER QUALITY AND ENVIRONMENTAL CONTEXT [2]

## INTRODUCTION

Local scale factors known to exert control over litter decomposition such as litter quality, edaphic conditions and decomposer community co-vary through interactions between plants and soil microbial communities (Cornwell et al., 2008; Powers et al., 2009). Tree mycorrhizal association can integrate these covarying factors and create a framework for predicting litter decomposition rates (Keller and Phillips, 2019; Phillips et al., 2013). Most tree species associate with either ectomycorrhizal (ECM) or arbuscular mycorrhizal (AM) fungi. These major mycorrhizal groups interact with plants and soil properties to form distinct localized carbon (C) and nitrogen (N) cycling syndromes (Averill et al., 2019; Lin et al., 2018; Phillips et al., 2013; Soudzilovskaia et al., 2015). These distinct biogeochemical regimes appear to be initiated by slower leaf litter decomposition in ECM stands than in AM stands (McGuire et al., 2010; Midgley et al., 2015; Phillips et al., 2013; Torti et al., 2001), but organic versus inorganic nutrient uptake by ECM versus AM fungi, respectively, likely also contribute to establishment of these regimes (Averill et al., 2014; Orwin et al., 2011).The relative importance of potential mechanisms in driving the contrasting decomposition patterns in adjacent ECM and AM-dominated forest stands is uncertain because the effect of litter quality is confounded with the

[2] This work was previously published through Springer in the journal *Biogeochemistry*.
Full citation:
Seyfried, G.S., Dalling, J.W., Yang, W.H., 2021. Effects of mycorrhizal type on leaf litter decomposition depend on litter quality and environmental context. Biogeochemistry 155, 21–38. doi:10.1007/s10533-021-00810-x

effects of distinct decomposer communities that establish in ECM versus AM-dominated stands (hereafter referred to as "stand mycorrhizal type").

Differences in ECM and AM leaf litter chemical properties can initiate distinct decomposition rates between forest types, but it is unclear if the mycorrhizal association of the tree from which the litter was derived (hereafter referred to as "litter mycorrhizal type") can predict leaf litter decomposition rates across ecosystems. In temperate ecosystems, litter mycorrhizal type and litter chemical properties typically co-vary, with ECM-associated trees producing lower chemical quality leaf litter than AM-associated trees (Cornelissen et al., 2001; Craig et al., 2018; Keller and Phillips, 2019; Midgley et al., 2015). Low quality substrate is generally characterized by high concentrations of lignin and low concentrations of nutrients, which limit microbial C use and suppress decomposition due to nutrient limitation (Cleveland et al., 2006; Meentemeyer, 1978; Melillo et al., 1982). Indeed, in N-limited temperate ecosystems, AM litter with lower C:N and lignin:N ratios decompose faster than ECM litter (Craig et al., 2018; Midgley et al., 2015; Sun et al., 2018). However, a compilation of global leaf litter chemistry and decay data showed that ECM leaf litter had higher N and P concentrations than AM leaf litter in tropical latitudes, though this was not associated with differences in decay rates between mycorrhizal types (Keller and Phillips, 2019). When considering greater species diversity at a global scale and accounting for phylogenetic autocorrelation, senesced leaf litter N and P content correlated with mycorrhizal association in temperate and boreal latitudes, but not in tropical latitudes (Averill et al., 2019). These studies suggest that, in tropical ecosystems, distinct nutrient economies in ECM- versus AM-dominated stands may not necessarily be initiated by leaf litter chemistry differences (Averill, 2016). As such, the role of leaf litter

chemistry in driving distinct decomposition patterns in ECM and AM-dominated forests remains uncertain.

Slower litter decomposition rates in ECM-dominated compared with AM-dominated forest stands may also result from mycorrhizal differences in physiology related to nutrient acquisition. Some ECM lineages possess the enzymatic capacity to directly uptake organic nutrients, whereas AM lineages lack the ability to produce these enzymes and instead uptake inorganic nutrients mineralized by the free-living decomposer community (Kohler et al., 2015; Lindahl and Tunlid, 2015; Read and Perez-Moreno, 2003; Talbot et al., 2008). Supported by host-supplied C, ECM may outcompete saprotrophs for low quality organic substrate and suppress decomposition rates by mining N from organic matter to leave behind C-rich, nutrient depleted compounds (Fernandez and Kennedy, 2016; Gadgil and Gadgil, 1971). Competition between fungal guilds is ultimately predicted to limit saprotrophic growth and result in C accumulation when N inputs are predominantly in forms that are energetically costly to take up (e.g. physically protected by lignin) and ECM are the superior competitors (Smith and Wan, 2019). However, this proposed mechanism may have little effect on leaf litter decomposition rates based on evidence of vertical separation between fungal guilds in the soil profile with saprotrophs occupying leaf litter where labile C compounds are readily available and ECM occupying more decomposed, higher C:N substrate deeper in the soil profile (Baldrian et al., 2012; K. E. Clemmensen et al., 2015; Lindahl et al., 2007). Mechanistic uncertainty is reflected in the literature: while there is some evidence in support of this microbial competition hypothesis (Gadgil and Gadgil, 1971; Koide et al., 2014; McGuire et al., 2010; Schilling et al., 2016), ECM presence does not always suppress decomposition (Chuyong et al., 2002; Mayor and Henkel, 2006) and can even stimulate decomposition (Brzostek et al., 2015).

Stand mycorrhizal type may not always predict leaf litter decomposition rates because the effect of microbial competition for N in ECM-dominated stands may be mediated by leaf litter quality. Litter quality variables controlling decomposition rates can exhibit critical threshold values which determine if a single variable primarily regulates decomposition rates (Prescott, 2010). For example, litter lignin:N ratios above a threshold can lead to decomposition rates constrained by litter chemistry regardless of variation in stand characteristics, such as mycorrhizal association (Midgley et al., 2015). This litter quality threshold results in high quality litter decomposing faster in AM stands than ECM stands, and low quality litter exhibiting no effect of stand mycorrhizal type on decomposition rates (Midgley et al., 2015). However, this apparent litter quality dependent effect of stand mycorrhizal type could actually reflect the effects of decomposing high-quality litter in a low-quality litter matrix, and vice versa. Because past studies often confound litter quality and stand mycorrhizal type with lower quality ECM litter compared to higher quality AM litter, it has been difficult to characterize the interactive effect of litter quality and stand mycorrhizal type on decomposition.

Tropical ecosystems, where ECM-associated trees can dominate forest stands within diverse AM forests, provide an opportunity to separately test the effects of litter quality and stand mycorrhizal type on leaf litter decomposition rates while taking into account the possibly confounding influence of "home field advantage" (HFA). The HFA hypothesis predicts that leaf litter will decompose faster in its home environment where the local microbial community is optimized for decomposition of resident litter species (Gholz et al., 2000). Given the high species diversity and low abundance of AM-associated trees in the tropics, AM stands do not necessarily confer HFA to decomposition of individual AM litter species. Additionally, in ECM stands dominated by a single species, it is possible to account for HFA by comparing decomposition of

ECM and AM species with similar initial leaf litter chemistry. In tropical forests where the dominant ECM leaf litter can be biochemically similar to mixed AM leaf litter, both single species ECM leaf litter and mixed species AM leaf litter exhibit slower decomposition in ECM- relative to AM-dominated stands (McGuire et al., 2010; Torti et al., 2001). The distinct soil N and organic matter dynamics observed in ECM- and AM-dominated temperate forest stands have also been documented in these tropical forests (Corrales et al., 2016b; McGuire et al., 2010; Torti et al., 2001). While this suggests that microbial competition for N may be a more important mechanism than initial litter chemistry in slowing decomposition in ECM-dominated stands, comparisons of individual ECM species versus individual AM species of similar litter quality are needed to isolate the effect of stand mycorrhizal type. A recent meta-analysis reported similar leaf litter decomposition rates for individual ECM and AM species in tropical studies (Keller & Phillips, 2019), but the role of stand mycorrhizal type could not be assessed. Therefore, there remains an opportunity to utilize the high species diversity found in tropical forests to disentangle the effects of litter quality from the effects of stand mycorrhizal type.

Here, we ask if stand mycorrhizal type predicts leaf litter decomposition rates when leaf litter quality is not confounded with tree-mycorrhizal association. We conducted our study in a tropical montane forest that harbors high species diversity of AM-associated trees as well as ECM-dominated stands, defined as greater than 50% ECM-associated *Oreomunnea mexicana* by basal area. These ECM-dominated stands are characterized by lower soil inorganic N concentrations, higher soil organic C and total N concentrations and higher soil C:N ratios compared to neighboring AM-dominated stands (Corrales et al., 2016b), similar to patterns observed in temperate and boreal ecosystems (Averill et al., 2014; Clemmensen et al., 2013; Phillips et al., 2013). By decomposing the leaf litter in neighboring ECM- and AM-dominated

forest stands with similar climate and soil parent material but differing soil inorganic nitrogen pools (Corrales et al., 2016b), we tested the hypothesis that competition between free-living saprotrophs and ECM fungi for N suppresses decomposition in ECM-dominated stands. We decomposed litter from AM-associated tree species producing higher and similar chemical quality leaf litter compared to the ECM-associates species present in the same forest, allowing us to account for possible confounding effects of HFA on decomposition. We predicted that leaf litter decomposition of all species is slower in ECM-dominated stands compared to AM-dominated stands and that litter quality metrics including N are correlated with decomposition rates. By measuring a broad suite of leaf litter chemical properties, we were able to determine if litter quality metrics other than N control decomposition rates and how these properties interact with environmental conditions to mediate mycorrhizal effects on decomposition.

## MATERIALS AND METHODS

### Site description

This study was conducted in the 13,000 ha Fortuna Forest Reserve (Fortuna), a lower montane tropical forest in western Panama (8°45' N, 82°15' W) with elevation ranging 1000-1400 meters above sea level. Tree communities in Fortuna are highly diverse, containing 61-153 species $ha^{-1}$ for trees greater than 10 cm diameter at breast height (Prada et al., 2017), but mostly associated with AM fungi. One ECM-associated tree species, *Oreomunnea mexicana,* tends to dominate the forest where it grows, forming stands with >49% *O. mexicana* by basal area (Corrales et al., 2016b). In Fortuna, stands dominated by *O. mexicana* form on a range of underlying parent materials in the four watersheds we used in this study: ultisols at Honda and Hornito are derived from rhyolite and dacite, respectively, and inceptisols at Zorro and Alto Frio

are derived from granodiorite and undifferentiated mafic volcanics, respectively (Dalling and Turner, 2021). Across the four watersheds, mean annual temperature in Fortuna ranges 19-22 °C (Cavelier et al., 1996) and mean annual precipitation (MAP) ranges 5800-9000 mm (Andersen et al., 2012) (Table C.1). Seasonality of precipitation occurs in the Alto Frio, Zorro and Hornito watersheds, which experience a dry season from January through April (Prada et al., 2017).

**Experimental design**

To characterize the effects of litter chemistry and stand mycorrhizal type on leaf litter decomposition rates, we conducted a two-year long leaf litter decomposition experiment including two ECM species and four AM species decomposed in paired ECM- and AM-dominated stands. We estimated decomposition rates from mass loss of leaf litter in bags made from 2 mm mesh window screening that were placed on the soil surface. Ectomycorrhizal-dominated stands chosen for this study in Honda and Zorro watersheds were within censused 1 ha forest plots. ECM-dominated stands within the censused forest were 50-60% *O. mexicana* by basal area (Table C.1). The censused forest plots in the Alto Frio and Hornito watersheds did not include ECM-dominated stands, so we used stands visually consistent with ECM-dominated forest in Honda and Zorro watersheds (i.e., litter layer dominated by *O. mexicana* leaf litter and canopy dominated by *O. mexicana* trees) located adjacent (<50 m) to the censused plots. We selected AM stands within the censused plots in each watershed that were composed of 100% AM-associated tree species. Due to the high species diversity of AM-associated trees in Fortuna, abundant AM species varied between replicate AM stands in the four watersheds as well as between AM and ECM stands within sites (Table C.1).

To account for the possible role of HFA in determining decomposition dynamics, we decomposed four AM litter species with different life-history strategies which were expected to

produce leaf litter that ranged from similar to higher in chemical quality relative to two ECM species. Due to high species diversity at Fortuna, all selected species accounted for less than 1.5% basal area across mixed forest stands in all four watersheds. We collected freshly senesced leaf litter from two slow-growing, shade-tolerant ECM species, *O. mexicana* (ORE) and *Quercus insignis* (QUE), which are the only abundant ECM-associated species in Fortuna. The ECM-associated litter was collected at least twice a week from litter traps set up in ORE-dominated stands and beneath QUE individuals. We also selected four AM species expected to represent a range in leaf litter quality spanning from similar to higher in chemical quality compared to that of the ECM leaf litter based on life history traits: slow-growing, shade-tolerant *Micropholis melinoniana* (MIC), and fast-growing, light-demanding *Cecropia angustifolia* (CEC), *Citharexylum macradenium* (CIT), and *Sapium* sp. (SAP) (Dalling unpublished). The AM leaf litter was collected twice daily from a cleared patch of lawn surrounding the Fortuna field station, ensuring that they had been in contact with the ground for less than 12 hours. In our high species diversity study site where AM trees drop leaves throughout the year, this method enabled us to collect all leaf litter within one season and therefore minimize within species variation in litter quality that may occur as conditions change through the year.

To separate the effect of litter quality from stand mycorrhizal type, we decomposed leaf litter from all six species in neighboring ORE-dominated stands and AM-dominated mixed species stands (20-100 m between paired stands). The paired stands were located in or directly adjacent to a 1 ha census plot in each of the four watersheds (Prada et al., 2017) which were treated as experimental replicates. Two subreplicate sets of litter bags located at least 20 m apart were decomposed within adjacent ECM and AM stands. Subreplicate data were averaged to represent the ECM- and AM-dominated stands within each watershed (Figure 4.1).

**Leaf litter decomposition protocol**

We deployed leaf litter bags in the field in March 2016, at the end of dry season in the Alto Frio, Hornito and Zorro watersheds which experience seasonal rainfall. Each 2 mm mesh litter bag was filled with 5 g of freshly senesced leaf litter that had been oven-dried at 60 °C for five days. Leaves were kept intact whenever possible, but CEC and QUE leaves, which were often larger than the 20 cm x 20 cm dimensions of the litter bags, were cut to fit inside the bags. For all six litter species, two subreplicate sets of six litterbags were attached along nylon fishing line, with one bag for each collection time point on each string. Six strings of litter bags, one for each litter species, were placed in parallel at each location. The litter layer was cleared beneath the litter bags in order to allow direct contact with the soil, but the litter environment surrounding the litter bags was kept intact. In most stands, the soil contained an organic horizon which the litter bags contacted; but in the Alto Frio ECM- and AM-dominated stands as well as the Honda and Zorro AM-dominated stands where there was little or no organic soil horizon, the litter bags contacted mineral soil.

To determine litter mass loss rates, we collected the litter bags at six time points over two years: 1, 2, 4, 7, 12, and 25.5 months. For the two faster decomposing species, CIT and SAP, the last litter bags were collected at 15.5 months because the leaf litter was almost entirely decomposed at that point. To characterize decomposition curves, we determined the percent litter mass remaining (MR) of the initial leaf litter mass in each litter bag. We oven-dried collected litter bags at 60 °C for 5 days before weighing them. For the three later time points, ingrown roots were separated from litter bag contents before determining MR. Subsamples of homogenized litter bag contents were ashed at 450 °C for 4 hours to calculate percent ash-free dry mass and account for soil contamination of leaf litter (John M. Blair, 1988).

**Calculation of decomposition rate constants and time to 50% mass remaining**

To calculate decomposition rate constants, we fit single and dual exponential decay models to each combination of watershed, stand mycorrhizal type, and litter species. The single-phase model represents decomposition of a uniform C pool over time and is used in most short term studies (Harmon et al., 2009). However, this model poorly captures initial phases of rapid mass loss (Currie and Aber, 1997; Harmon et al., 1990) and late phases of suppressed mass loss (Currie and Aber, 1997; Harmon et al., 2009; Trofymow et al., 2002). We found that the single-pool decomposition model did not accurately estimate decomposition rates for the majority of our data based on resulting $R^2$ values that were less than 0.85 and intercept estimates outside the range of 95-105%. Although the dual exponential model appeared a better fit for data in which these two conditions were not met, our six collection points were insufficient to accurately characterize all parameters in this model (van Huysen et al., 2016).

Instead, we used a single-exponential equivalent integrated decomposition model following the methods of van Huysen et al. 2016. For litter decomposition experiments not carried out long enough for MR to equal essentially zero, we can estimate area, *A,* by linearly interpolating between successive collection points and calculating the area beneath each of these lines. To do this, we used Equation 1 in which *i* is each collection point from 1 to *I*, $t_i$ is the time (in years) at collection point *i* since bags were deployed at *t=0* and $M_i$ is the proportion of mass remaining at collection point *i*:

$$A = \sum_{i=1}^{I} (t_i - t_{i-1}) * M_i + (t_i - t_{i-1}) * \frac{(M_{i-1} - M_i)}{2} \quad \text{(Equation 1)}$$

We used *A* to determine the single exponential equivalent, $k_e$ (year$^{-1}$), the *k*-value that would result in the previously determined, *A,* if the data followed a single exponential model. We calculated $k_e$ using equation 2 in which *T* represents the total incubation time in years.

$$A = \frac{(1 - e^{-k_e T})}{k_e} \qquad \text{(Equation 2)}$$

Additionally, we estimated time to 50% MR (years) for each combination of watershed, stand mycorrhizal type, and litter species as an index of litter decomposition rates during the initial stages of litter decomposition. We calculated time to 50% MR using the following equation in which $M_0$ is the leaf litter mass at time zero, $k_e$ is the single exponential equivalent calculated using Equation 2, and T represents the total incubation time in years.

$$\frac{M_0}{2} = M_0 e^{-k_e T} \qquad \text{(Equation 3)}$$

**Litter chemistry analyses**

We measured a suite of initial leaf litter chemical properties for each of the six species in order to determine which litter chemical properties may have controlled decomposition rates. For all six litter species, a subsample of the initial leaf litter we collected for our decomposition experiment was oven-dried at 60° C and ground into a powder. We used three replicate subsamples of dried and ground litter from all six litter species in each of the following chemical analyses: total C and N concentrations using an elemental analyzer (Vario Micro Cube, Elementar, Hanau, Germany); P, potassium (K), calcium (Ca), magnesium (Mg), aluminum (Al), and manganese (Mn) concentrations of ashed and acid-digested samples (Jones et al., 2018) using an ICP-OES (Avio 200, Perkin Elmer, Waltham, Massachusetts, USA); acid-soluble carbohydrate concentration determined from analysis of two-step acid-hydrolysis filtrate using a UV-vis spectrophotometer (Genesys 20, Thermo Fisher, Waltham, Massachusetts, USA) (Sluiter et al., 2008); and acid-insoluble residue concentration determined from the ash-free mass of acid-hydrolysis retentate. We report lignin concentrations as the acid-insoluble residue concentrations.

**Statistical analyses**

We calculated integrated *k*-values and fit linear mixed models in SAS 3.8 (Proc Mixed, SAS Institute, Cary, NC, USA, 2018). All other statistical analyses were carried out in R 3.6.2 (R Core Team 2019). Statistical significance was determined based on $P < 0.05$.

To test for differences in initial litter chemistry among litter species, we conducted one-way ANOVAs with litter species as a fixed effect and each litter chemical property as the dependent variable. Post-hoc comparisons among species were performed using Tukey honestly significant difference (HSD) tests. We also averaged litter chemical properties across both ECM species and across all AM species to determine the effect of litter mycorrhizal type on litter chemistry. In this case, we conducted t-tests with litter mycorrhizal type as a fixed effect and each litter chemical property as the dependent variable. Manganese concentrations were ln-transformed to achieve normally distributed residuals as determined using the Shapiro-Wilk test. To determine the relationship among litter species in multivariate space defined by all measured litter chemical properties, we performed principal components analysis with centered and scaled data. The preceding analyses were conducted using the aov, tukeyHSD, and prcomp commands in the stats package in R (R Core Team 2019). We used the "adonis" function in the vegan package version 2.5-6 in R (Oksanen et al., 2019) to partition distance matrices among sources of variation and specifically, to determine how much of the variation between our six leaf litter species (as defined by the measured litter chemistry properties) could be explained by litter mycorrhizal type or litter decomposition speed (SAP and CIT defined as "fast", MIC, CEC, QUE and ORE defined as "slow").

To test for the effects of litter species and stand mycorrhizal type on integrated *k*-values, MR at each time point, and time to 50% MR, we used a mixed linear model with litter species,

stand mycorrhizal type, and the interaction between these terms as fixed variables, and watershed and the interaction between watershed and stand mycorrhizal type as random terms. These terms were modeled using a split-plot design in which the whole-plot factor, stand mycorrhizal type, was nested within the blocking factor, watershed, and the split-plot factor, litter species, was nested within the whole-plot factor. Watershed represented the random error term for the whole-plot and the interaction between site location and stand mycorrhizal type represented the random error term for the split-plot. Post-hoc comparisons among litter species and between stand mycorrhizal types were performed using Tukey HSD tests. Additionally, we partitioned the interaction between stand mycorrhizal type and litter species using the lsmeans and slice statements within Proc Mixed (SAS Institute, Cary, NC, USA), allowing us to test for the effect of stand mycorrhizal type on each litter species. To determine the effects of litter mycorrhizal type on integrated *k*-values, we also fit the linear mixed model with litter mycorrhizal type as the split-plot factor in place of litter species. We ln-transformed *k*-values and time to 50% MR to achieve normally distributed residuals as determined using the Shapiro-Wilk test and determined equality of variance based on the Levene statistic (Sokal and Rohlf, 1970).

To correlate decomposition rates with litter chemistry, we regressed integrated *k*-values with each litter chemical property measured (e.g., %C, %N, %P, %K, %Ca, %Mg, %Mn, %Al, %lignin, lignin:N, C:N, C:P, lignin:P and N:P). To determine multivariate models that best fit the observed integrated *k*-values, we used the "stepAIC" function in the MASS package in R (R Core Team 2019) to conduct backwards stepwise multiple linear regressions (Venables and Ripley, 2002). The analysis started with all litter chemical properties, sequentially removed insignificant terms, and left in the variables that parsimoniously best predicted decomposition as determined from the lowest AIC values.

## RESULTS

### Effect of litter mycorrhizal type on litter chemistry and decomposition rate

Species ranked differently across the litter chemical properties measured, and the two individual ECM litter species did not necessarily group separately from the four individual AM litter species (Figure 4.2). Calcium concentration, which was lower for both ECM species than all AM species, was the only litter chemical property for which the six individual litter species ranked according to mycorrhizal type (Figure 4.2a, $P < 0.0001$). Both ECM species, QUE and ORE, exhibited higher litter C:N ratios than two of the AM species (MIC and SAP, $P < 0.0001$) but lower litter C:N ratios than the other two AM species (CEC and CIT, $P < 0.0001$) (Figure 4.2b). Compared to all other species, QUE had the lowest chemical quality litter, with the highest lignin:N ratios and the lowest P and Mg concentrations (Figure 4.2c-e, $P < 0.0001$); QUE N concentrations were also lower than all species except CEC (Figure 4.2f, $P = 0.02$). In contrast, ORE had generally poorer chemical quality litter than only SAP, with higher lignin:N ratios and lower Mg, N and C concentrations (Figure 4.2c, e-g, $P < 0.0001$). For P concentrations, ORE was significantly higher than QUE, not significantly different from MIC, and lower than all other species (Figure 4.2d, $P < 0.01$). Both ECM species had higher C:P, lignin:P and N:P ratios than all AM species except MIC, which did not differ significantly from ORE for any of these variables (Figure C.1a-c, $P < 0.001$). Leaf litter nutrient concentrations were similar between ORE and MIC except for lower ORE Ca concentrations (Figure 4.2a, $P = 0.0003$) and higher ORE N and Mn concentrations (Figure 4.2f, k, $P = 0.003$ and $P < 0.0001$, respectively). When litter chemical properties were averaged across the two ECM species versus across the four AM species, AM leaf litter had higher Ca and P concentrations than ECM litter (Figure C.2a, d, $P < 0.05$). The AM leaf litter also had lower concentrations of lignin and Mn and lower ratios of

lignin:N, C:P, lignin:P, and N:P than ECM leaf litter (Figure C.2h, k, c, l-n $P < 0.01$). However, ECM and AM leaf litter did not differ significantly in N, C, K, Mg or Al concentrations, nor in C:N ratios (Figure C.2f, g, j, e, i, b, respectively).

In a PCA plot, litter species were not grouped by mycorrhizal association nor by decomposition rate when placed in multivariate space defined by all measured litter chemical properties (e.g., %C, %N, %P, %K, %Ca, %Mg, %Mn, %Al, %lignin, lignin:N, and C:N) (Figure C.3). Although litter mycorrhizal type explained 30% of the variation between litter species in multivariate space and decomposition speed (SAP and CIT defined as "fast", MIC, CEC, QUE and ORE defined as "slow") explained 39% of the variation among litter species in multivariate space, neither result was significant ($P = 0.23$, 0.19, respectively). The first principal component axis (PC1) explained 64% of variation between litter species, and separated SAP from all other litter species. The largest contributors to variance described by PC1 were lignin:N (14 %), Mg (13%), P (13%), N (12%) and lignin (12%) (Figure C.3). The second principal component axis (PC2) explained 14% of variation among species. The largest contributors to variance described by PC2 were Al (44%) and Mn (28%) (Figure C.3).

Leaf litter decomposition rates estimated from integrated *k*-values differed significantly among species (Figure 4.3; $F_{5,30} = 134$, $P < 0.001$). Leaf litter of the AM species, SAP, decomposed faster than that of all other species ($P < 0.0001$), and leaf litter of the AM species, CIT, decomposed faster than that of all species aside from SAP ($P < 0.0001$). Integrated *k*-values did not differ significantly among the other four species with the exception of ORE, an ECM species, having faster decomposition rates than two AM species, MIC and CEC ($P = 0.001$ and $P = 0.04$, respectively). When litter mycorrhizal type was used in place of litter species in the mixed linear model predicting integrated *k*-values, ECM leaf litter, which represented the

average of two ECM species, decomposed slower than AM leaf litter, which represented the average of four AM species ($F_{1,38} = 5.11$, $P = 0.03$). Initial stages of leaf litter mass loss, determined as the time to 50% MR, also differed significantly among species (Figure 4.4; $F_{5,30} = 134.5$, $P < 0.0001$). Comparisons of time to 50% MR among species displayed similar patterns as those for *k*-values: time to 50% MR was significantly faster for SAP than all other species ($P < 0.0001$), and time to 50% MR of CIT was significantly faster than all species aside from SAP ($P < 0.0001$). Time to 50% MR did not differ significantly among the four other species, with the exception of ORE which exhibited significantly faster initial decomposition than MIC and CEC ($P = 0.0014$, $P = 0.04$).

Across all litter species, integrated *k*-values were correlated to many of the litter chemical properties (Figure 3.5; Figure C.4; Figure C.5). Leaf litter P concentration was the strongest individual predictor of integrated *k*-values (Figure 4.5d, $R^2 = 0.82$). Leaf litter lignin:N ratios ($R^2 = 0.60$), N concentrations ($R^2 = 0.62$), lignin concentrations ($R^2 = 0.53$), K concentrations ($R^2 = 0.55$), and C:P ratios ($R^2 = 0.55$) were the next best individual predictors of integrated *k*-values (Figure 4.5c, f, h, j; Figure C.4a, respectively). The multiple regression model that best predicted decomposition rates included P, N, Mn and lignin:N concentrations as explanatory variables ($R^2 = 0.88$). The regression relationships were largely driven by SAP, which had the fastest decomposing leaf litter and highest leaf litter chemical quality as determined by the highest nutrient concentrations and lowest C:N and lignin:N ratios. When SAP was removed from the analyses, P concentrations (Figure C.5d, $R^2 = 0.58$) and Al concentrations (Figure C.5i, $R^2 = 0.56$) were the best individual predictors of decomposition rates.

**Effect of stand mycorrhizal type on decomposition rates**

Integrated *k*-values were marginally significantly lower in ECM- than AM-dominated stands when considering all species together (Fig C.6; $F_{1,3} = 7.74$, P = 0.07), with the effect of stand mycorrhizal type varying for individual species. Only CIT exhibited significantly slower decomposition in ECM-dominated stands relative to AM-dominated stands (Figure 4.3; P = 0.03); however, two other AM species, CEC and MIC, also trended towards slower decomposition in ECM-dominated relative to AM-dominated stands (Figure 4.3; P = 0.10 and 0.09, respectively). Time to 50% MR trended towards being longer in ECM-compared with AM-dominated stands when considering all species together ($F_{1,3} = 7.76$, P = 0.07). Only CIT exhibited significantly longer time to 50% MR in ECM- compared with AM-dominated stands (Fig 4.4; P = 0.03), and there was no significant interaction between litter species and stand mycorrhizal type for *k*-values nor time to 50%MR.

Although mass remaining (MR) did not differ significantly by stand mycorrhizal type for the first four time points (Figure 4.4), MR trended toward diverging between ECM- and AM-dominated stands at the 5$^{th}$ (12 months) and 6$^{th}$ collection points (15.5 or 24 months, depending on litter species) (Figure 4.4; $F_{1,3} = 5.86$, P = 0.09 and $F_{1,3} = 7.23$, P = 0.07, respectively). When the effect of stand mycorrhizal type on MR at the sixth time point was assessed for individual species, CEC and CIT had significantly more MR in ECM-dominated stands compared with AM-dominated stands (Figure 4.4b, e; P = 0.006 and P = 0.03, respectively); ORE leaf litter trended toward the same pattern (Figure 4.4d; P = 0.06).

## DISCUSSION

Slower leaf litter decomposition in ECM- relative to AM-dominated forests is thought to initiate distinct nutrient cycling patterns between these two forest types (e.g., Torti et al. 2001; McGuire et al. 2010; Schilling et al. 2016), but the mechanisms driving this difference in decomposition rates are uncertain. The roles of leaf litter quality and microbial competition for N are confounded by the correlation between leaf litter quality and mycorrhizal association of tree species in most studies on this topic (e.g., Cornelissen et al. 2001; Midgley et al. 2015). We utilized a wide range in leaf litter quality of the AM species found in a diverse tropical forest to separate the effects of these two mechanisms. We found that leaf litter decomposition rates did not differ among individual litter species based on their mycorrhizal association, but rather were directly controlled by leaf litter chemistry regardless of litter mycorrhizal type. We also found that only one litter species decomposed significantly slower in ECM-dominated stands relative to AM-dominated stands. While other litter species trended toward this pattern, the stand effect for these other species was not statistically detectable given the level of replication in our study (n = 4), which was consistent with other leaf litter decomposition studies (e.g., Trofymow et al. 1995; Gholz et al. 2000; Sun et al. 2018). For these other species, litter chemistry and environmental conditions likely dampened the effect of stand mycorrhizal type on leaf litter decomposition such that it may not meaningfully contribute to ECM versus AM stand differences in biogeochemical cycling. Here, we discuss the implications of our results for predicting mycorrhizal effects on leaf litter decomposition when ECM-associated trees are not assumed to produce poorer quality leaf litter than AM-associated trees.

**Effect of litter mycorrhizal type on leaf litter decomposition rates**

The role of litter mycorrhizal type in controlling leaf litter decomposition rates has been debated since a global analysis of foliar traits suggested that ECM association is not correlated with foliar chemistry (Koele et al., 2012). Although many studies report mycorrhizal differences in leaf litter quality in temperate and boreal ecosystems (e.g., Cornelissen et al. 2001; Midgley et al. 2015; Averill et al. 2019) others show that these differences do not necessarily occur in tropical ecosystems (Averill et al., 2019; McGuire et al., 2010). In our study, AM leaf litter had on average higher P and Ca concentrations and lower lignin concentrations, and lignin:N, lignin:P, C:P and N:P ratios than ECM leaf litter, suggesting overall higher chemical quality for the AM leaf litter. However, when individual species were compared, only one of the four AM species exhibited higher quality than the ECM species across all measures of litter chemical quality. The higher quality AM litter decomposed faster than lower quality ECM litter, consistent with results from temperate forests (Midgley et al., 2015; Phillips et al., 2013). ECM and AM litter similarly poor in chemical quality decomposed at similar rates, consistent with results from other tropical forests (McGuire et al., 2010; Torti et al., 2001). Surprisingly, leaf litter of CEC, a pioneer species, had low chemical quality and slow decomposition rates that were comparable to that of the slow-growing, shade-tolerant AM species, MIC, and the ECM species. Although we acknowledge that our small sample size of ECM and AM leaf litter species limits our ability to draw conclusions about potential differences in decomposition between ECM and AM leaf litter species, our results demonstrate that leaf litter decomposition rates do not vary predictably based on the mycorrhizal association of the tree species when litter chemistry is not confounded with mycorrhizal association. We suggest shifting focus away from defining a global relationship between ECM and AM litter quality because the relative decomposition of leaf litter from

contrasting mycorrhizal groups reflects the litter chemistry of the species being compared in a given study. Instead, litter chemistry of the dominant species present in studied ecosystems should be measured to determine the role of litter quality in driving mycorrhizal-associated differences in decomposition and nutrient cycling patterns.

Studies in N-limited temperate systems often utilize C:N and lignin:N ratios to define leaf litter quality and to explain mycorrhizal differences in decomposition rates (Cornelissen et al., 2001; Midgley et al., 2015; Schmidt et al., 2011; Sun et al., 2018). In our tropical study, the fastest decomposing species had the lowest C:N and lignin:N ratios, but these litter quality metrics did not correlate with decomposition rates across all species. Instead, litter P concentration was the best single predictor of decomposition rates, consistent with reports of P-limited microbial decomposition in tropical forest soils (Cleveland et al. 2002; Wieder et al. 2009; Waring 2012; Camenzind et al. 2018; Keller and Phillips 2019) where weathering losses and mineral sorption can lead to relatively low soil P (Sanchez et al., 1982; Walker and Syers, 1976). This suggests that single metrics of litter chemistry cannot be used to define litter chemical quality across biomes with different environmental contexts (Waring, 2012), such as differing nutrient limitation. Furthermore, the litter species included in our study ranked differently based on different chemical properties, highlighting that assessment of chemical quality depends on the properties considered. We therefore recommend that litter quality should be determined empirically for a given ecosystem using a broad set of litter chemical properties to allow discovery of which properties control decomposition rates.

**Effect of stand mycorrhizal type on leaf litter decomposition rates**

Competition for N between ECM and saprotrophic fungi has long been hypothesized to suppress leaf litter decomposition in ECM- relative to AM-dominated stands (Gadgil & Gadgil, 1971), yet this mechanism has been challenging to disentangle from the often confounded effect of litter quality (Averill, 2016; Fernandez et al., 2019; Smith and Wan, 2019). We selected tree species such that leaf litter quality was not correlated with mycorrhizal association and decomposed leaf litter in ECM- and AM-dominated stands that exhibit biogeochemical syndromes similar to those documented in temperate forests, with lower soil inorganic N concentrations and higher soil C:N ratios in ECM stands (Corrales et al., 2016b). The replicate forest stands differed somewhat in tree species diversity, AM species composition, and degree of ECM dominance, contributing to variability in observed litter decomposition rates. In addition, as is common in mycorrhizal association studies in natural settings, our study was limited to ECM stands dominated by a single tree species, *O. mexicana*; therefore, it is unknown if the stand mycorrhizal type effects we observed are applicable across a broad diversity of ECM species. Nevertheless, our data suggest a litter quality dependent effect of stand mycorrhizal type on decomposition, with slower decomposition rates in the *O. mexicana*-dominated stands compared to the AM-dominated stands detectable for only one of the higher quality AM species. Below we discuss how litter quality and environmental context may have led to an interaction between litter species and stand mycorrhizal type in which stand mycorrhizal type impacted decomposition of some species more strongly than others, as well as potential broader implications of our findings.

The species with the highest quality across many leaf litter chemical properties, SAP, exhibited similarly fast decomposition in both ECM- and AM-dominated stands. According to

the litter quality threshold hypothesis, we expected decomposition of this high-quality leaf litter would not be constrained by litter chemistry and would therefore decompose more slowly in ECM-dominated stands where ECM compete with saprotrophic fungi for N. However, this prediction is based on the assumption that microbial respiration is the dominant decomposition pathway driving litter mass loss. In our study site where MAP is high, ranging 5900-9000 mm, leaching can be a more important decomposition pathway than in temperate forests (Cleveland et al., 2006; Wieder et al., 2009). Compared to all other species in our study, SAP leaf litter had the lowest lignin concentration, which is inversely related to soluble fractions of leaf litter (Schreeg et al., 2013), and the fastest time to 50% mass remaining, an index for initial decomposition rates. Precipitation-related climate parameters strongly correlate with time to 50% mass remaining in tropical decomposition studies (Cusack et al., 2009), indicating the importance of leaching in initial decomposition phases. Mass loss by leaching may have dominated decomposition of SAP litter, dampening the effect of distinct decomposer communities in ECM and AM stands. This suggests that the interaction of MAP with leaf litter chemical quality can determine the potential for stand mycorrhizal type to influence decomposition.

Among the other five species with higher lignin concentrations, we found support for the litter quality threshold hypothesis which explains the interaction between litter chemistry and stand mycorrhizal type effects on leaf litter decomposition rates (Midgley et al., 2015; Taylor et al., 1991; Zhang et al., 2008). In temperate and boreal ecosystems, threshold values of lignin:N may dictate when litter chemistry rather than decomposer community limits microbial decomposition of leaf litter (Prescott, 2010; Taylor et al., 1991; Zhang et al., 2008). However, CIT was the only species in our study that exhibited detectably slower decomposition in ECM- compared to AM-dominated stands despite the fact that it had similar lignin:N as the other four

species. Litter P was the only chemical property for which CIT ranked higher in quality than the other species, suggesting that a litter P threshold could potentially limit decomposition. Decomposition of relatively P-rich CIT litter may therefore have been N-limited rather than P-limited. In ECM-dominated stands with low soil inorganic N (Brookshire and Thomas, 2013; Corrales et al., 2016b; Torti et al., 2001), competition for N between ECM fungi and saprotrophic decomposers could slow CIT litter decomposition compared to AM-dominated stands where relatively high soil inorganic N and CIT litter P enables faster decomposition. This litter P threshold effect is consistent with P-limited microbial decomposition in tropical forest soils (Cleveland et al. 2002; Waring 2012; Camenzind et al. 2018; Keller and Phillips 2019). This suggests that different litter chemical properties can constrain the strength of stand mycorrhizal type effects on leaf litter decomposition in temperate and tropical forests such that the effects of stand mycorrhizal type on low quality, slow decomposing litter species are not large enough to be ecologically meaningful.

Effects of stand mycorrhizal type can become more important in later stages of decomposition (McGuire et al., 2010). After soluble compounds have been leached from the decomposing substrate, local variation in microbial community composition likely exerts a stronger control over decomposition (Cusack et al., 2009; Waring, 2012). For all species in our study with the exception of the lowest quality species, QUE, litter mass remaining began to diverge between stand types after seven months to one year of incubation, with greater mass remaining in ECM stands compared with AM stands. Although our two-year study was longer than many of the litter decomposition experiments conducted in ECM versus AM stands (Cornelissen et al., 2001; Mayor and Henkel, 2006; Midgley et al., 2015), longer term

decomposition experiments may be necessary to fully capture the effect of stand mycorrhizal type on litter decomposition even in tropical forests where decomposition occurs rapidly.

## CONCLUSION

We found that both litter chemistry and stand mycorrhizal type regulated leaf litter decomposition rates, but these controls were context dependent. First, despite selecting AM species with both poor and high quality leaf litter to compare against ECM species in our study, we observed overall ECM- versus AM-associated species differences in leaf litter chemistry and decomposition rates. This pattern was driven by one high quality, fast-decomposing AM species which masked the effect of the two AM species with poor chemical quality and slow decomposition comparable to the ECM species. This demonstrates that we cannot predict litter decomposition rates based simply on litter mycorrhizal type but must measure the litter chemistry of the species in a study system to predict decomposition rates. Furthermore, the relative contribution of each species to stand litter inputs should be considered in predicting stand decomposition rates. Second, although C:N and lignin:N ratios are most often used to define litter quality (Cornwell et al., 2008; Midgley et al., 2015), in tropical forests where microbial decomposition can be P- rather than N-limited, litter quality metrics based on litter P may be better predictors of litter decomposition rates. Third, in ecosystems with high rainfall, mass loss of low lignin litter may occur predominantly via leaching rather than microbial respiration such that the effect of distinct microbial communities in ECM- and AM-dominated stands on respiratory decomposition is dampened. Our data suggest the need for direct investigation of the potential for this interaction between climate and litter quality to mediate stand mycorrhizal type effects on leaf litter decomposition rates. Fourth, stand mycorrhizal type

effects on litter decomposition may only be large enough to be ecologically meaningful when litter nutrient concentrations exceed a litter quality threshold. Overall, our findings do not support broad characterization of leaf litter decomposition patterns by litter mycorrhizal type or stand mycorrhizal type, but instead suggest that mycorrhizal effects depend on litter chemistry and environmental conditions.

## FIGURES

**Figure 4.1.** Experimental design at each of the four replicate watersheds used in the study. At two subreplicate locations within adjacent ectomycorrhizal and arbuscular mycorrhizal forest stands, a string of litter bags for each of six litter species was placed on the forest floor in parallel (litter species are denoted by different shades of grey in the figure). Each string included six litter bags to be collected at each of six time points over two years. Subreplicate sets of litter bags within each forest type were separated by at least twenty meters.

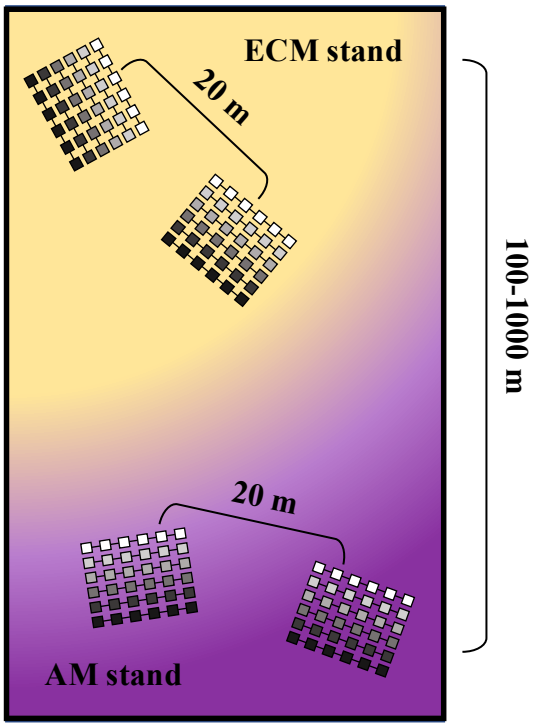

**Figure 4.2.** Comparison of initial leaf litter chemical properties among litter species. The two ectomycorrhizal-associated litter species (yellow) and four arbuscular mycorrhizal-associated litter species (purple) are ordered along the x-axis by increasing mean decomposition rate. All properties are concentrations reported as mass percent with the exception of ratios which are unitless. Bars and error bars represent means ± one standard error (n = 3); F-statistics and p-values are reported for the litter species effect in linear mixed models for each litter chemical property. Letters denote statistically significant differences based on Tukey post-hoc comparisons (P < 0.05).

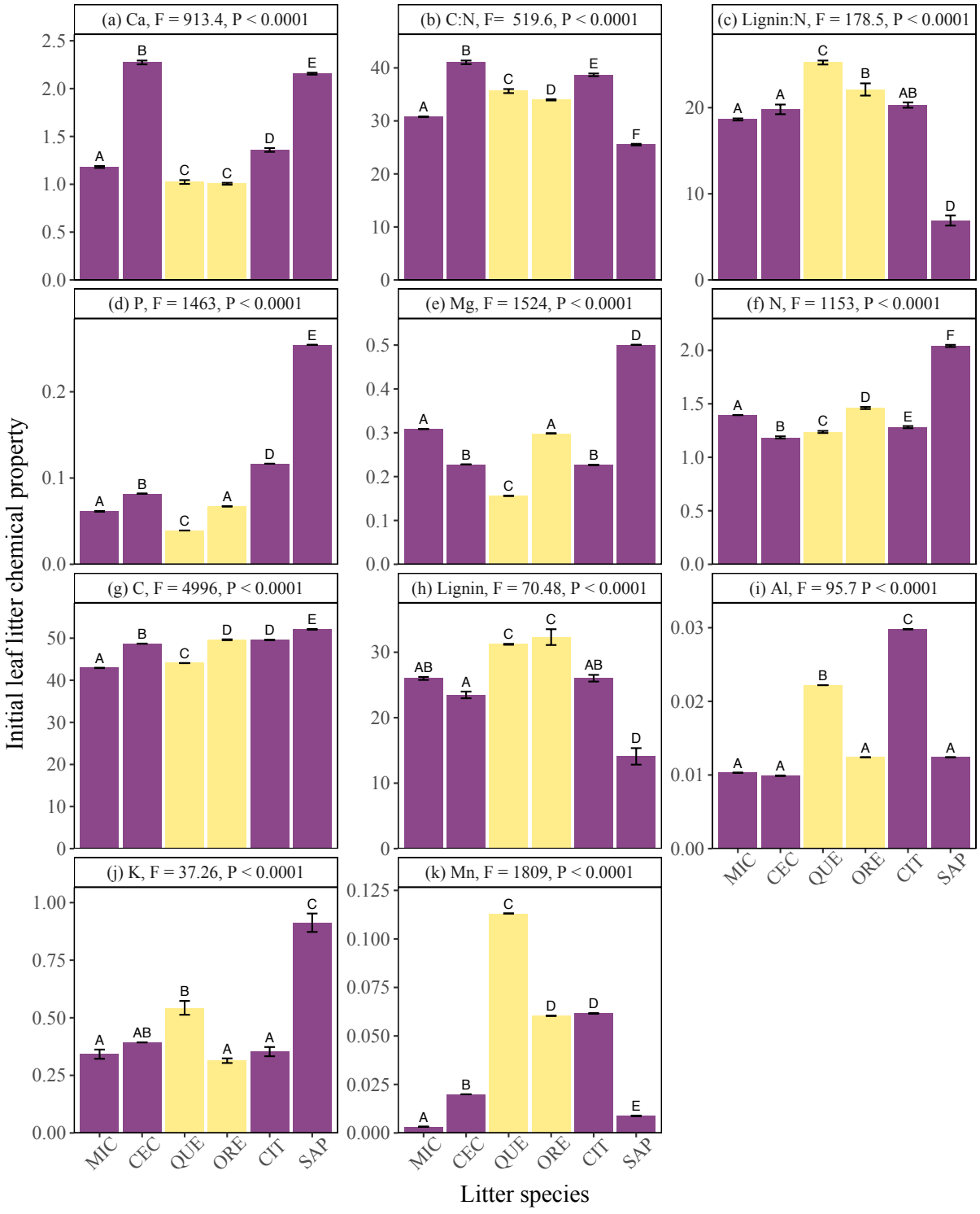

**Figure 4.3.** Boxplots of integrated *k*-values by litter species and stand mycorrhizal type. The two ectomycorrhizal-associated litter species (yellow) and four arbuscular mycorrhizal-associated litter species (purple) are ordered along the x-axis by increasing mean decomposition rate. The lighter shade indicates litter decomposed in ectomycorrhizal-dominated stands, and the darker shade indicates litter decomposed in arbuscular mycorrhizal-dominated stands. For a linear mixed model predicting integrated *k*-values, the litter species effect was significant ($F_{5,30}$= 134, P < 0.0001) while the stand effect ($F_{1,3}$ = 7.74, P = 0.07) and the litter species * stand interaction effect ($F_{5,30}$= 0.61, P = 0.69) were insignificant. Letters denote significant differences between litter species. Asterisks denote significant differences between stand types determined using lsmeans and slice statements within Proc Mixed (SAS Institute, Cary, NC, USA) to test for the effect of stand mycorrhizal type on each litter species.

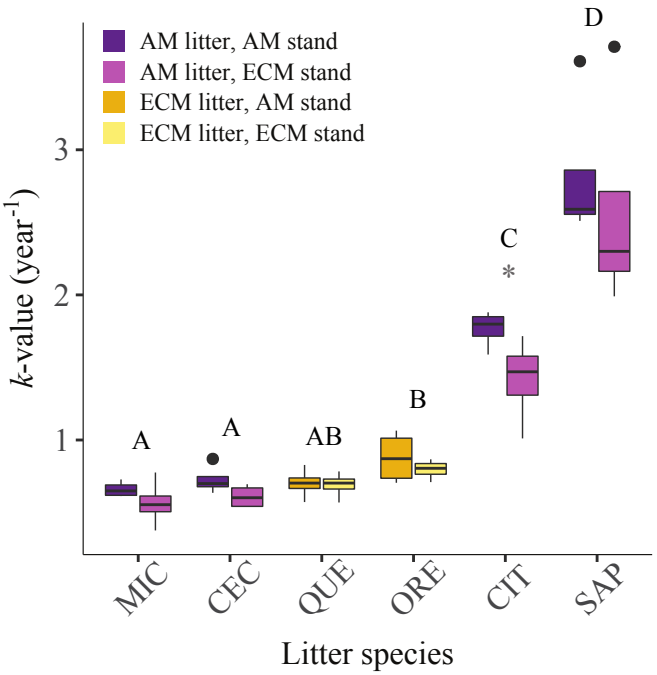

**Figure 4.4.** Percent mass remaining versus incubation time for six collection points over two years for (a) AM-associated *Micropholis melinoniana,* (b) AM-associated *Cecropia angustifolia*, (c) ECM-associated *Quercus insignis,* (d) ECM-associated *Oreomunnea mexicana*, (e) AM-associated *Citharexylum macradenium*, and (f) AM-associated *Sapium* sp., decomposed in ECM- (yellow) and AM-dominated (purple) stands. Asterisks denote significant differences between stand types determined using the lsmeans and slice statements within Proc Mixed (SAS Institute, Cary, NC, USA) to test for the effect of stand mycorrhizal type on percent mass remaining of each litter species at each collection point.

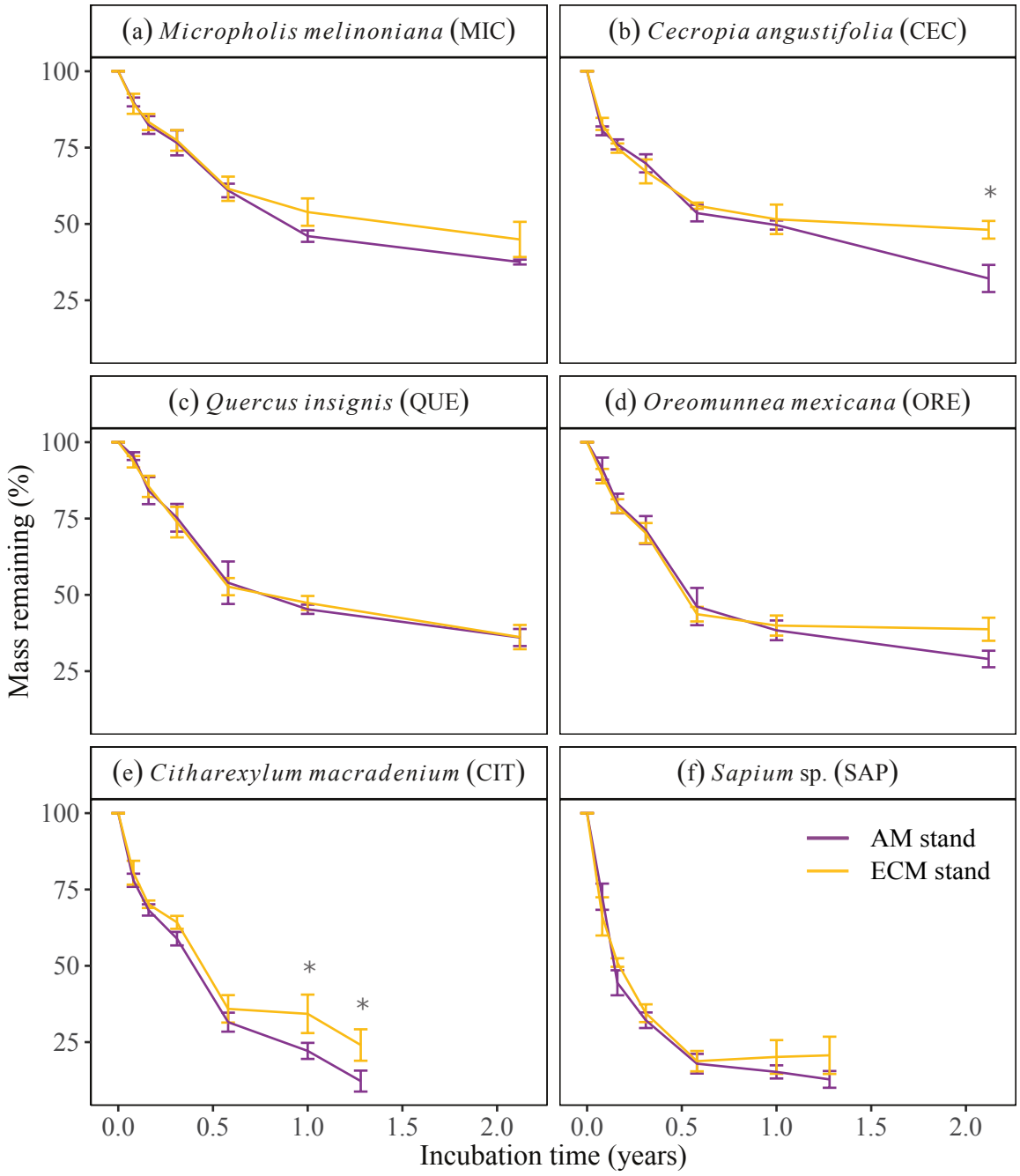

**Figure 4.5.** Integrated *k*-values versus initial leaf litter chemical properties for all litter species. The symbols represent the six litter species, with n=8 for each species: *Oreomunnea mexicana* (ORE; cross), *Quercus insignis* (QUE; diamond), *Cecropia angustifolia* (CEC; square), *Citharexylum macradenium* (CIT; circle), *Micropholis melinoniana* (MIC; triangle) and *Sapium* sp. (SAP; inverted triangle). The colors indicate the mycorrhizal association of the tree species from which the leaf litter was derived, with the two ectomycorrhizal-associated species in yellow and the four arbuscular mycorrhizal-associated species in purple. Solid lines indicate statistically significant relationships ($P < 0.05$), and dashed lines indicate non-significant relationships.

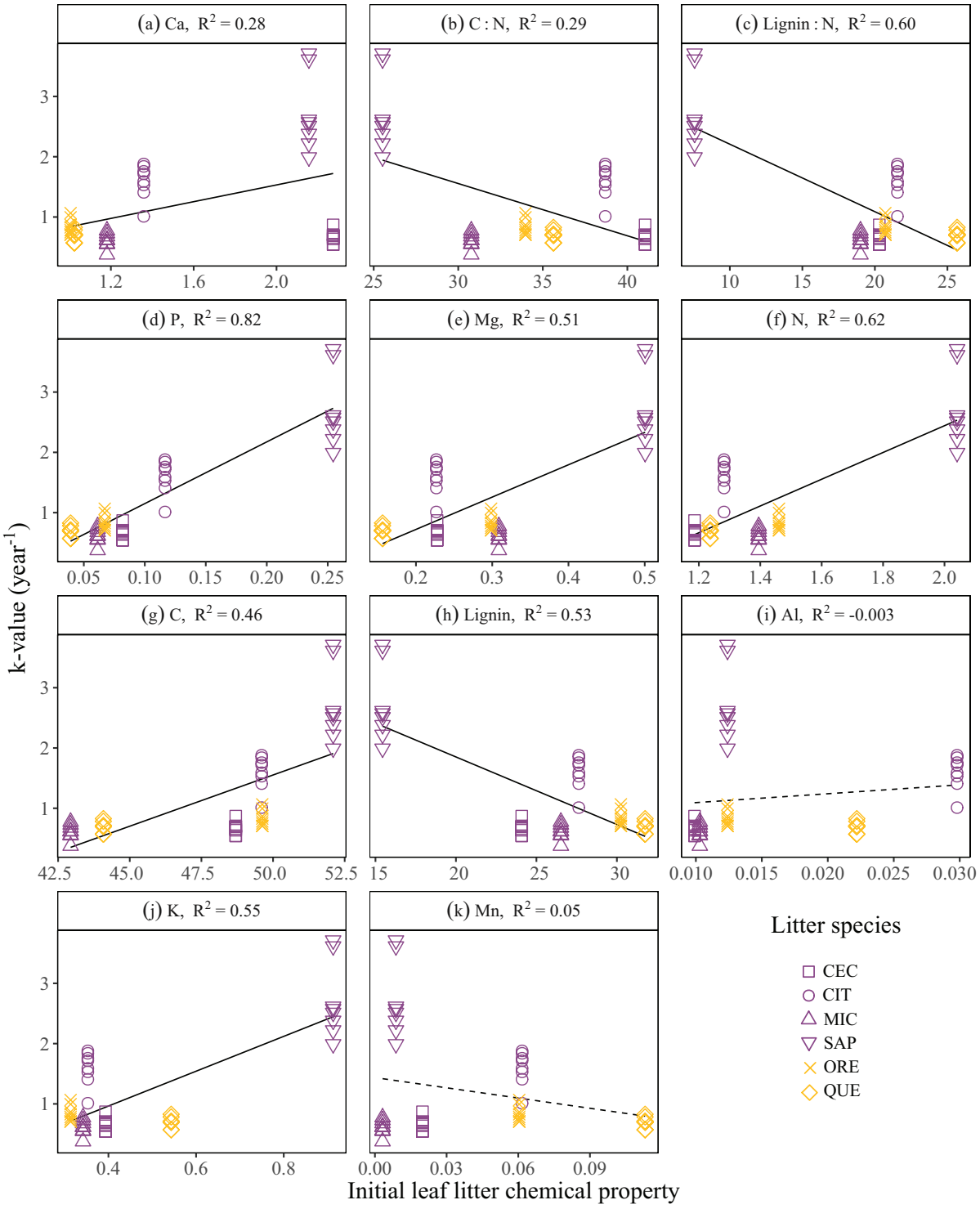

## REFERENCES

Andersen KM, Endara MJ, Turner BL, Dalling JW (2012) Trait-based community assembly of understory palms along a soil nutrient gradient in a lower montane tropical forest. Oecologia 168:519–531. https://doi.org/10.1007/s00442-011-2112-z

Averill C (2016) Slowed decomposition in ectomycorrhizal ecosystems is independent of plant chemistry. Soil Biol Biochem 102:52–54. https://doi.org/http://dx.doi.org/10.1016/j.soilbio.2016.08.003

Averill C, Bhatnagar JM, Dietze MC, et al (2019) Global imprint of mycorrhizal fungi on whole-plant nutrient economics. Proc Natl Acad Sci U S A. https://doi.org/10.1073/pnas.1906655116

Averill C, Turner BL, Finzi AC (2014) Mycorrhiza-mediated competition between plants and decomposers drives soil carbon storage. Nature 505:543–545. https://doi.org/10.1038/nature12901

Baldrian P, Kolaiřík M, Štursová M, et al (2012) Active and total microbial communities in forest soil are largely different and highly stratified during decomposition. ISME J. https://doi.org/10.1038/ismej.2011.95

Bending GD (2003) Litter decomposition, ectomycorrhizal roots and the "Gadgil" effect. New Phytol. 158:228–229

Blair JM (1988) Nitrogen, sulfur and phosphorus dynamics in decomposing deciduous leaf litter in the southern appalachians. Soil Biol Biochem 20:693–701. https://doi.org/10.1016/0038-0717(88)90154-X

Brookshire ENJ, Thomas SA (2013) Ecosystem consequences of tree monodominance for nitrogen cycling in lowland tropical forest. PLoS One 8:7.

https://doi.org/10.1371/journal.pone.0070491

Brzostek ER, Dragoni D, Brown ZA, Phillips RP (2015) Mycorrhizal type determines the magnitude and direction of root-induced changes in decomposition in a temperate forest. New Phytol 206:1274–1282. https://doi.org/10.1111/nph.13303

Camenzind T, Hättenschwiler S, Treseder KK, et al (2018) Nutrient limitation of soil microbial processes in tropical forests. Ecol Monogr 88:4–21. https://doi.org/10.1002/ecm.1279

Cavelier J, Solis D, Jaramillo MA (1996) Fog interception in montane forests across the Central Cordillera of Panama. J Trop Ecol 12:357–369. https://doi.org/10.1017/S026646740000955X

Chuyong GB, Newbery DM, Songwe NC (2002) Litter breakdown and mineralization in a central African rain forest dominated by ectomycorrhizal trees. Biogeochemistry. https://doi.org/10.1023/A:1020276430119

Clemmensen KE, Bahr A, Ovaskainen O, et al (2013) Roots and associated fungi drive long-term carbon sequestration in boreal forest. Science (80- ) 339:1615–1618. https://doi.org/10.1126/science.1231923

Clemmensen KE, Finlay RD, Dahlberg A, et al (2015) Carbon sequestration is related to mycorrhizal fungal community shifts during long-term succession in boreal forests. New Phytol. https://doi.org/10.1111/nph.13208

Cleveland, C C, Townsend AR, Schmidt SK (2002) Phosphorus limitation of microbial processes in moist tropical forests: Evidence from short-term laboratory incubations and field studies. Ecosystems 5:680–691. https://doi.org/10.1007/s10021-002-0202-9

Cleveland CC, Reed SC, Townsend AR (2006) Nutrient regulation of organic matter decomposition in a tropical rain forest. Ecology 87:492–503. https://doi.org/10.1890/05-

0525

Cornelissen JHC, Aerts R, Cerabolini B, et al (2001) Carbon cycling traits of plant species are linked with mycorrhizal strategy. Oecologia 129:611–619. https://doi.org/10.1007/s004420100752

Cornwell WK, Cornelissen JHC, Amatangelo K, et al (2008) Plant species traits are the predominant control on litter decomposition rates within biomes worldwide. Ecol Lett 11:1065–1071. https://doi.org/10.1111/j.1461-0248.2008.01219.x

Corrales A, Mangan SA, Turner BL, Dalling JW (2016) An ectomycorrhizal nitrogen economy facilitates monodominance in a neotropical forest. Ecol Lett 19:383–392. https://doi.org/10.1111/ele.12570

Craig ME, Turner BL, Liang C, et al (2018) Tree mycorrhizal type predicts within-site variability in the storage and distribution of soil organic matter. Glob Chang Biol 24:3317–3330. https://doi.org/10.1111/gcb.14132

Currie WS, Aber JD (1997) Modeling leaching as a decomposition process in humid montane forests. Ecology 78:1844–1860. https://doi.org/10.1890/0012-9658(1997)078[1844:MLAADP]2.0.CO;2

Cusack DF, Chou WW, Yang WH, et al (2009) Controls on long-term root and leaf litter decomposition in neotropical forests. Glob Chang Biol. https://doi.org/10.1111/j.1365-2486.2008.01781.x

Dalling JW, Turner BL (2021) Soils of the Fortuna Forest Reserve. Smithsonian Contributions to Botany, Volume 112, in press

Fernandez CW, Kennedy PG (2016) Revisiting the “Gadgil effect”: do interguild fungal interactions control carbon cycling in forest soils? New Phytol 209:1382–1394.

https://doi.org/10.1111/nph.13648

Fernandez CW, See CR, Kennedy PG (2019) Decelerated carbon cycling by ectomycorrhizal fungi is controlled by substrate quality and community composition. New Phytol 226:569–582. https://doi.org/10.1111/nph.16269

Gadgil RL, Gadgil PD (1971) Mycorrhiza and litter decomposition. Nature 233:133. https://doi.org/10.1038/233133a0

Gholz HL, Wedin DA, Smitherman SM, et al (2000) Long-term dynamics of pine and hardwood litter in contrasting environments: Toward a global model of decomposition. Glob Chang Biol. https://doi.org/10.1046/j.1365-2486.2000.00349.x

Harmon ME, Baker GA, Spycher G, Greene SE (1990) Leaf-litter decomposition in the Picea/tsuga forests of Olympic National Park, Washington, U.S.A. For Ecol Manage 31:55–66. https://doi.org/10.1016/0378-1127(90)90111-N

Harmon ME, Silver WL, Fasth B, et al (2009) Long-term patterns of mass loss during the decomposition of leaf and fine root litter: An intersite comparison. Glob Chang Biol 15:1320–1338. https://doi.org/10.1111/j.1365-2486.2008.01837.x

Jones JM, Heath KD, Ferrer A, et al (2018) Wood decomposition in aquatic and terrestrial ecosystems in the tropics: Contrasting biotic and abiotic processes. FEMS Microbiol Ecol 95:fiy223. https://doi.org/10.1093/femsec/fiy223

Keller AB, Phillips RP (2019) Leaf litter decay rates differ between mycorrhizal groups in temperate, but not tropical, forests. New Phytol 222:556–564. https://doi.org/10.1111/nph.15524

Koele N, Dickie IA, Oleksyn J, et al (2012) No globally consistent effect of ectomycorrhizal status on foliar traits. New Phytol 196:845–852. https://doi.org/10.1111/j.1469-

8137.2012.04297.x

Kohler A, Kuo A, Nagy LG, et al (2015) Convergent losses of decay mechanisms and rapid turnover of symbiosis genes in mycorrhizal mutualists. Nat Genet 47:410-U176. https://doi.org/10.1038/ng.3223

Koide RT, Fernandez C, Malcolm G (2014) Determining place and process: functional traits of ectomycorrhizal fungi that affect both community structure and ecosystem function. New Phytol 201:433–439. https://doi.org/10.1111/nph.12538

Lin G, Guo D, Li L, et al (2018) Contrasting effects of ectomycorrhizal and arbuscular mycorrhizal tropical tree species on soil nitrogen cycling: the potential mechanisms and corresponding adaptive strategies. Oikos 127:518–530. https://doi.org/10.1111/oik.04751

Lindahl BD, Ihrmark K, Boberg J, et al (2007) Spatial separation of litter decomposition and mycorrhizal nitrogen uptake in a boreal forest. New Phytol. https://doi.org/10.1111/j.1469-8137.2006.01936.x

Lindahl BD, Tunlid A (2015) Ectomycorrhizal fungi - potential organic matter decomposers, yet not saprotrophs. New Phytol 205:1443–1447. https://doi.org/10.1111/nph.13201

Mayor JR, Henkel TW (2006) Do ectomycorrhizas alter leaf-litter decomposition in monodominant tropical forests of Guyana? New Phytol 169:579–588. https://doi.org/10.1111/j.1469-8137.2005.01607.x

McGuire KL, Zak DR, Edwards IP, et al (2010) Slowed decomposition is biotically mediated in an ectomycorrhizal, tropical rain forest. Oecologia 164:785–795. https://doi.org/10.1007/s00442-010-1686-1

Meentemeyer V (1978) Macroclimate and lignin control of litter decomposition rates. Ecology 59:465–472. https://doi.org/10.2307/1936576

Melillo JM, Aber JD, Muratore JF (1982) Nitrogen and lignin control of hardwood leaf litter decomposition dynamics. Ecology 63:621–626. https://doi.org/10.2307/1936780

Midgley MG, Brzostek E, Phillips RP (2015) Decay rates of leaf litters from arbuscular mycorrhizal trees are more sensitive to soil effects than litters from ectomycorrhizal trees. J Ecol 103:1454–1463. https://doi.org/10.1111/1365-2745.12467

Oksanen J, Blanchet F, Friendly M, et al (2019) vegan: Community Ecology Package

Orwin KH, Kirschbaum MUF, St John MG, Dickie IA (2011) Organic nutrient uptake by mycorrhizal fungi enhances ecosystem carbon storage: a model-based assessment. Ecol Lett 14:493–502. https://doi.org/10.1111/j.1461-0248.2011.01611.x

Phillips RP, Brzostek E, Midgley MG (2013) The mycorrhizal-associated nutrient economy: A new framework for predicting carbon-nutrient couplings in temperate forests. New Phytol 199:41–51. https://doi.org/10.1111/nph.12221

Powers JS, Montgomery RA, Adair EC, et al (2009) Decomposition in tropical forests: A pan-tropical study of the effects of litter type, litter placement and mesofaunal exclusion across a precipitation gradient. J Ecol. https://doi.org/10.1111/j.1365-2745.2009.01515.x

Prada CM, Morris A, Andersen KM, et al (2017) Soils and rainfall drive landscape-scale changes in the diversity and functional composition of tree communities in premontane tropical forest. J Veg Sci 28:859–870. https://doi.org/10.1111/jvs.12540

Prescott CE (2010) Litter decomposition: What controls it and how can we alter it to sequester more carbon in forest soils? Biogeochemistry 101:133–149. https://doi.org/10.1007/s10533-010-9439-0

Read DJ, Perez-Moreno J (2003) Mycorrhizas and nutrient cycling in ecosystems - a journey towards relevance? New Phytol 157:475–492. https://doi.org/10.1046/j.1469-

8137.2003.00704.x

Sanchez PA, Bandy DE, Villachica JH, Nicholaides JJ (1982) Amazon Basin soils: Management for continuous crop production. Science (80- ) 216:821–827. https://doi.org/10.1126/science.216.4548.821

Schilling EM, Waring BG, Schilling JS, Powers JS (2016) Forest composition modifies litter dynamics and decomposition in regenerating tropical dry forest. Oecologia. https://doi.org/10.1007/s00442-016-3662-x

Schmidt MWI, Torn MS, Abiven S, et al (2011) Persistence of soil organic matter as an ecosystem property. Nature 478:49–56. https://doi.org/10.1038/nature10386

Schreeg LA, Mack MC, Turner BL (2013) Nutrient-specific solubility patterns of leaf litter across 41 lowland tropical woody species. Ecology 94:94–105

Sluiter A, Hames B, Ruiz RO, et al (2008) Determination of structural carbohydrates and lignin in biomass. Lab Anal Proced 1617:1–16

Smith GR, Wan J (2019) Resource-ratio theory predicts mycorrhizal control of litter decomposition. New Phytol 223:1595–1606. https://doi.org/10.1111/nph.15884

Sokal RR, Rohlf FJ (1970) Biometry. The principles and practice of statistics in biological research. Science (80- ). https://doi.org/10.1126/science.167.3915.165

Soudzilovskaia NA, van der Heijden MGA, Cornelissen JHC, et al (2015) Quantitative assessment of the differential impacts of arbuscular and ectomycorrhiza on soil carbon cycling. New Phytol 208:280–293. https://doi.org/10.1111/nph.13447

Sun T, Hobbie SE, Berg B, et al (2018) Contrasting dynamics and trait controls in first-order root compared with leaf litter decomposition. Proc Natl Acad Sci U S A. https://doi.org/10.1073/pnas.1716595115

Talbot JM, Allison SD, Treseder KK (2008) Decomposers in disguise: mycorrhizal fungi as regulators of soil C dynamics in ecosystems under global change. Funct Ecol 22:955–963. https://doi.org/10.1111/j.1365-2435.2008.01402.x

Taylor BR, Prescott CE, Parsons WJF, Parkinson D (1991) Substrate control of litter decomposition in four Rocky Mountain coniferous forests. Can J Bot 69:2422–2550. https://doi.org/10.1139/b91-281

Team RC (2019) R: A language and environment for statistical computing. R Fouondataion for Statistical Computing, Vienna, Austria

Torti SD, Coley PD, Kursar TA (2001) Causes and consequences of monodominance in tropical lowland forests. Am Nat 157:141–153. https://doi.org/10.1086/318629

Trofymow JA, Moore TR, Titus B, et al (2002) Rates of litter decomposition over 6 years in Canadian forests: Influence of litter quality and climate. Can J For Res 32:789–804. https://doi.org/10.1139/x01-117

Trofymow JA, Preston CM, Prescott CE (1995) Litter quality and its potential effect on decay rates of materials from Canadian forests. Water, Air, Soil Pollut. https://doi.org/10.1007/BF01182835

van Huysen TL, Perakis SS, Harmon ME (2016) Decomposition drives convergence of forest litter nutrient stoichiometry following phosphorus addition. Plant Soil 406:1–14. https://doi.org/10.1007/s11104-016-2857-6

Venables WN, Ripley BD (2002) Modern Applied Statistics with S. Fourth Edition

Walker TW, Syers JK (1976) Fate of phosphorus during pedogenesis. Geoderma 15:1–19. https://doi.org/10.1016/0016-7061(76)90066-5

Waring BG (2012) A Meta-analysis of climatic and chemical controls on leaf litter decay rates in

tropical forests. Ecosystems 15:999–1009. https://doi.org/10.1007/s10021-012-9561-z

Wieder WR, Cleveland CC, Townsend AR (2009) Controls over leaf litter decomposition in wet tropical forests. Ecology 12:3333–3341. https://doi.org/10.1890/08-2294.1

Zhang D, Hui D, Luo Y, Zhou G (2008) Rates of litter decomposition in terrestrial ecosystems: global patterns and controlling factors. J Plant Ecol 1:85–93. https://doi.org/10.1093/jpe/rtn002

# CHAPTER 5

# REVISING THE ROLE OF NITROGEN MINERALIZATION IN MYCORRHIZAL NUTRIENT SYNDROMES: A BACKSEAT DRIVER

## INTRODUCTION

The delineation between tree association with either ectomycorrhizal (ECM) or arbuscular mycorrhizal (AM) fungi has been used to integrate nutrient use traits of plants and associated microbial communities that form distinct nutrient syndromes observed in forests dominated by ECM- versus AM-associated trees (Averill et al., 2019; Lin et al., 2017; Phillips et al., 2013; Zak et al., 2019). Closed nitrogen (N) cycling with minimal ecosystem inorganic N loss is thought to result from the nutrient conservative traits of ECM fungi and associated trees that form an organic nutrient economy whereas open N cycling with higher nitrate ($NO_3^-$) leaching and gaseous N losses (Midgley and Phillips, 2016, 2014) results from the nutrient acquisitive traits of AM fungi and associated trees that form an inorganic nutrient economy (Phillips et al., 2013). In this originally proposed nutrient economy framework, differences in N mineralization rates initiate the distinct N cycling syndromes between mycorrhizal types. However, the importance of N mineralization to the formation of mycorrhizal nutrient syndromes has not yet been directly evaluated, contributing to uncertainty about the mechanisms driving mycorrhizal effects on soil organic matter and nutrient dynamics.

Observations of lower net N mineralization rates in ECM stands compared to AM stands (e.g. Lin et al., 2017; Midgley and Phillips, 2016; Mushinski et al., 2021) seemingly suggest that the contrasting N acquisition strategies of ECM and AM fungi and their associated trees directly mediate N mineralization (Averill et al., 2019; Wurzburger and Hendrick, 2009).

Ectomycorrhizal fungi possess the genetic potential to produce a suite of oxidative enzymes that mobilize N from SOM (Lindahl and Tunlid, 2015; Read and Perez-Moreno, 2003), allowing them to compete with free-living microbes for organic N (Averill, 2016; Fernandez and Kennedy, 2016; Gadgil and Gadgil, 1971). The production of low-N, high-lignin leaf litter by ECM trees suppresses decomposition rates to slow N mineralization, thereby complementing direct uptake of organic N by ECM fungi to form an organic nutrient economy with little ecosystem loss of inorganic N (Phillips et al., 2013). In contrast, arbuscular mycorrhizal fungi scavenge for inorganic N and therefore rely on and even stimulate the free-living decomposer community to mineralize N for their uptake (Herman et al., 2012; Paterson et al., 2016; Talbot et al., 2008). Higher-N, lower-lignin AM leaf litter rapidly decomposes to support inorganic N scavenging by AM fungi and an inorganic nutrient economy susceptible to ecosystem N loss (Phillips et al., 2013). Consistent with these mechanisms, AM fungi have been shown to prime the free-living decomposer community through exudation of labile photosynthates (Drigo et al., 2010; Frey, 2019; Kaiser et al., 2015; Wurzburger and Brookshire, 2017) while ECM fungi have been shown to suppress decomposition by outcompeting saprotrophic fungi for organic N (Bending, 2003; Fernandez and Kennedy, 2016; Gadgil and Gadgil, 1971). However, other studies show greater priming in ECM soils (Meier et al., 2015; Phillips and Fahey, 2006; Sulman et al., 2017) and provide evidence that priming interactions between mycorrhizae and free-living microbes are context dependent (Beidler et al., *in press*). Because net N mineralization rate measurements conflate production and consumption of inorganic N to potentially mask patterns in gross N mineralization, the effects of tree-mycorrhizal N acquisition strategies on N mineralization remain uncertain.

Alternatively, mycorrhizal type effects on soil acid-base chemistry are gaining recognition as a potentially important driver of mycorrhizal nutrient syndromes (Lin, *in press*; Seyfried et al., 2021a). Acidification of ECM soils may be partially driven by slow decay of low-N, high-lignin ECM leaf litter (Fernandez et al., 2019; Keller and Phillips, 2019), particularly in ECM soils where competitive interactions between ECM and saprotrophic fungal guilds can suppress saprotrophic activity (Fernandez and Kennedy, 2016; Gadgil and Gadgil, 1971). Suppressed leaf litter decay decreases the rate at which acid-buffering base cations are returned to the mineral soil and increases the production of organic acids as intermediate products during decomposition (de Schrijver et al., 2012; De Vries and Breeuwsma, 1987). Organic acids may also be excreted from ECM roots at a greater rate than from AM roots (Grayston et al., 1997). Under stressful abiotic conditions such as low pH, microbes must allocate more energy towards cellular maintenance as opposed to biomass synthesis, decreasing C use efficiency (CUE) (Li et al., 2021). This increase in C mineralization to carbon dioxide ($CO_2$) without N assimilation, therefore, leads to an increase in N mineralization. However, acidic ECM soils with low C:N ratios select for fungal-dominated microbial communities and specifically favor N-limited ECM fungi over typically C-limited saprotrophic fungi (Lindahl et al., 2007). Fueled by host-supplied C, ECM fungi may rapidly assimilate mineralized N (Langley and Hungate, 2003). Through these separate mechanisms, low soil pH in ECM stands can both stimulate N mineralization and N assimilation by microbes, leading to lower net N mineralization rates than in AM stands.

Mounting evidence of misalignment between mycorrhizal type effects on net mineralization and net nitrification patterns suggest that suppressed nitrification and downstream N losses in ECM stands are not necessarily driven by suppressed mineralization (Midgley and Phillips, 2016; Mushinski et al., 2021). Patterns in net mineralization vary, with studies reporting

lower (Lin et al., 2017; Midgley and Phillips, 2016), higher (Mushinski et al., 2021) and similar (Phillips et al., 2013) net mineralization rates in ECM compared to AM stands. Nevertheless, net nitrification and downstream N losses are consistently suppressed in ECM relative to AM stands (e.g. Lin et al., 2017; Midgley and Phillips, 2016; Phillips et al., 2013). Furthermore, net nitrification rates in ECM stands are not stimulated by addition of inorganic N (Midgley and Phillips, 2016). This suggests that substrate limitation due to slow mineralization in ECM stands may not drive low net nitrification rates as had been previously hypothesized (Brzostek et al., 2015; Lin et al., 2017; Phillips et al., 2013). In addition, ECM soils are characterized by lower abundances of ammonia-oxidizing bacteria compared to AM soils (Mushinski et al., 2021; Tatsumi et al., 2020), but saprotrophic fungi and prokaryotes that mineralize organic N to produce ammonium ($NH_4^+$) occur in similar abundance between stand mycorrhizal types (Tatsumi et al., 2020). Therefore the genetic potential for nitrification is lower in ECM soils despite similar genetic potential for N mineralization in ECM and AM soils. Altogether, this evidence suggest that mineralization and nitrification are mediated by distinct pathways such that mineralization rates may not necessarily determine nitrification rates.

Slower N mineralization may not be necessary to initiate closed N cycling in ECM stands because low soil pH can directly and indirectly inhibit chemoautotrophic growth of ammonia oxidizers, decreasing nitrification and downstream N loss pathways (Mushinski et al., 2021). Higher acidity in ECM soils can cause protonation of ammonia to ammonium which decreases substrate availability and may ultimately select for lower abundances of ammonia oxidizers (Mushinski et al., 2021). Ammonia oxidizer abundance may also be suppressed by aluminum (Al) toxicity that can result from greater solubility of $Al^{3+}$ in low pH soils (Prosser and Nicol, 2012). There may also be stronger competition from heterotrophs and plant roots for available N

in ECM soils where low soil pH is often correlated with high soil C:N ratios (Xiao et al., 2020). When C is in excess relative to N, ammonia uptake by heterotrophs and plant roots may constrain ammonia oxidizers (Chen et al., 2013; Horz et al., 2004; Veresoglou et al., 2012). Inhibition of $NO_3^-$ production by nitrification can have cascading effects on ecosystem N loss through leaching and denitrification by limiting $NO_3^-$ availability for N cycling processes downstream of nitrification. As such, soil acidification by ECM trees can lead to closed N cycling independently of ECM effects on N mineralization.

Here we investigated the role of N mineralization in driving mycorrhizal nutrient syndromes in ECM- versus AM-dominated temperate forest stands. We measured gross N cycling rates in addition to the more commonly measured net N cycling rates used to characterize the mycorrhizal nutrient syndromes (e.g. Lin et al., 2017; Midgley and Phillips, 2016; Phillips et al., 2013). First, we tested the hypothesis that ECM soils would be characterized by greater gross N mineralization rates relative to AM soils. In support of this hypothesis, we expected to observe greater gross mineralization rates in ECM stands despite greater net mineralization rates in AM stands. Second, we tested the hypothesis that nitrification is inhibited in ECM soils by mechanisms other than limited $NH_4^+$ supply. In support of this hypothesis we expected to observe lower gross and net nitrification rates in ECM soils relative to AM soils despite greater gross mineralization rates. We also expected that inorganic N addition would stimulate nitrification in AM-dominated stands but not ECM-dominated stands because the other factors would continue to suppress nitrification in ECM soils even with increased $NH_4^+$ supply.

## METHODS

### Site description

We conducted this study in Indiana University's Moores Creek Research and Teaching Preserve, an 80-year old mixed deciduous hardwood forest in South-Central Indiana. Moores Creek has a mean annual precipitation of 1200 mm and a mean annual temperature of 11.6 °C (Midgley and Phillips, 2016). Soils are thin, unglaciated Inceptisols, derived from sandstone (Midgley and Phillips, 2016). At Moores Creek, forest stands range from ECM- to AM-dominated, with >85% of the basal area represented by the dominant mycorrhizal type (Midgley and Phillips, 2016). Stands dominated by AM-associated trees are largely composed of *Acer saccharum* Marsh, *Liriodendron tulipifera* L, *Prunus serotina* Ehrh., and *Sassafras albidum* Nutt. whereas ECM-dominated stands are largely composed of *Quercus rubra* L., *Quercus velutina* Lam., *Quercus alba* L., *Carya glabra* P. Mill., and *Fagus grandifolia* Ehrh (Midgley and Phillips, 2016).

We utilized a long-term N fertilization experiment established in May 2011. Paired 20 m x 20 m N addition and control plots are located in each of seven ECM-dominated stands and each of seven AM-dominated stands at Moores Creek. Beginning in 2011, equal parts $NH_4SO_4$ and $NaNO_3$ was applied monthly from May to October in the N addition plots at a total rate of 50 kg N $ha^{-1}$ $yr^{-1}$ (Midgley and Phillips, 2016).

### Soil Sampling

Soil was collected from each plot at four dates throughout the 2018 growing season (May, July, September, and October) to account for temporal variability in N cycling process rates. To avoid transient stimulatory effects of fertilizer addition on N cycling processes,

sampling was conducted two weeks after fertilizer was applied to the N addition plots. Within each plot we randomly sampled five cores, one from each quadrant of the plot and one from near the center of the plot. We used a 10 cm diameter quantitative corer to collect soil from 0-5 cm depth beneath the litter layer. The five cores from each plot were combined such that a single composite soil sample was analyzed from each replicate plot. Soils were stored in plastic bags at ambient temperature overnight before the soil assays were conducted.

**Potential nitrification and denitrification rates**

We assayed the soil samples for potential nitrification rates as an index of the maximum capacity of the extant soil microbial community to nitrify $NH_4^+$. We used the Berg and Rosswall, (1985) methodology as described by Kandeler et al. (1999). Briefly, we added 20 mL of 10 mM $NH_4^+$ solution as excess substrate and 0.1 mL of 1.5 M $NaClO_3$ as a biotic $NO_2^-$ reduction inhibitor to a 5 g sample of soil. We aerated the soil slurry during a 5 h incubation at room temperature (23 °C) by vigorously shaking it on a rotary shaker. During this time, another subsample of each soil sample was mixed with the $NH_4^+$ solution and placed in a -20 °C freezer to act as an abiotic control accounting for changes background soil $NO_2^-$ concentrations caused by abiotic $NO_2^-$ reactions. After the incubation, all samples were extracted in 2 M KCl, and extracts were analyzed for $NO_2^-$ concentrations colorimetrically (Genesys 20 Visible Spectrophometer, Thermo-Scientific, Waltham, MA, USA). To determine the potential nitrification rate for each sample, the $NO_2^-$ concentration in the frozen soil subsample was subtracted from the unfrozen shaken subsample to calculate the rate of $NO_2^-$ production through biotic nitrification over the 5 h incubation period.

We also assayed the soil samples for potential rates of complete and incomplete denitrification as indices of the maximum capacity of the extant soil microbial community to denitrify $NO_3^-$ to the gaseous end products of $N_2O$ and $N_2$. We used the Environmental Protection Agency protocol # RSKSOP-310. Briefly, 25 mL of 0.015 M $NO_3^-$ solution was added to two 25 g soil subsamples in sealed 150 mL Wheaton vials which had been flushed with helium (He) to create anaerobic conditions. To measure total denitrification, one 25 g subsample was injected with 15 mL ~10% acetylene ($C_2H_2$), inhibiting $N_2O$ reduction to $N_2$. To measure total incomplete denitrification, a second 25 g subsample was injected with 20 mL He, resulting in similar headspace pressure as the $C_2H_2$ treatment. Beginning directly after gas was added to the headspace, we shook soil slurries vigorously and sampled 10 mL of headspace gas at four time points over 45 minutes. Gas samples were stored in sealed pre-evacuated Wheaton vials and analyzed using a gas chromatograph equipped with an electron capture detector (ECD) and a thermal conductivity detector (TCD) for $N_2O$ and $CO_2$ analysis, respectively (Shimadzu GC-2014, Colombia, MD). We calculated potential total denitrification rates from the linear change in headspace $N_2O$ concentrations from the $C_2H_2$ treatment, and potential incomplete denitrification rates from the linear change in headspace $N_2O$ concentrations from the He only treatment. To calculate potential complete denitrification rates, we subtracted potential incomplete denitrification rates from potential total denitrification rates. We omitted data from 8 out of 82 samples with non-linear changes in headspace $N_2O$ concentrations and $CO_2$ concentrations (i.e., $R2 < 0.80$) precluded determination of potential denitrification rates.

**Gross mineralization and nitrification rates**

We measured gross rates of N mineralization and nitrification using the $^{15}N$ pool dilution technique (Kirkham and Bartholomew, 1954) as described by (Hart et al., 1994). Briefly, two 150 g subsamples of root- and rock-free soil samples were placed in separate plastic bags, with one bag receiving $^{15}NH_4Cl$ to quantify gross N mineralization, $NH_4^+$ assimilation rates, and nitrification-derived net $N_2O$ fluxes and the other bag receiving $K^{15}NO_3$ to quantify gross nitrification rates, $NO_3^-$ assimilation rates, and denitrification-derived net $N_2O$ fluxes. Two mL of 99 atom% $^{15}N$ (Cambridge Isotopes, Tewksbury, MA) label solution in DI water was pipetted onto each subsample and mixed by hand to homogenously distribute the $^{15}N$ label. Label solution concentrations ranged 0.58- 5.85 $\mu gN\ mL^{-1}$ among treatments (unfertilized ECM, fertilized ECM, unfertilized AM, and fertilized AM) in order to target 10 atom% $^{15}N$ enrichment across the range of background $NH_4^+$ and $NO_3^-$ concentrations across treatments; actual $^{15}N$ enrichment ranged 0.27-5.90 atom% due to variability in background $NH_4^+$ and $NO_3^-$ concentrations within treatments. We extracted 50 g of soil in 150 ml 2M KCl at 15 minutes and 4 hours after the addition of $^{15}N$ label solution to represent the initial and final time points. The KCl extracts were analyzed colorimetrically for $NH_4^+$ and $NO_3^-$ concentrations on a SmartChem 200 discrete analyzer (KPM analytics, Westborough, MA). The $^{15}N$ isotopic composition of the KCl-extractable $NO_3^-$ and $NH_4^+$ pools were determined using the acid trap diffusion method (Herman et al., 1995) followed by analysis on a Vario Micro Cube elemental analyzer (Hanau, Germany) interfaced with an IsoPrime 100 isotope ratio mass spectrometer (Cheadle Hulme, UK).

**Microbial biomass and N assimilation rates**

We measured rates of microbial N assimilation as soil $NH_4^+$ and $NO_3^-$ consumption pathways and concentrations of microbial biomass N as indices of the microbial biomass pool size. For these measurements, we used direct chloroform extraction (Setia et al., 2012). At 15 minutes and 4 h of the soil incubation with the $^{15}N$ label, two 15 g soil subsamples were extracted in 30 mL of 0.5M $K_2SO_4$, with one subsample incubated with 0.5 mL of chloroform for 1 h before filtration. All extracts were digested with potassium persulfate (Brookes et al., 1985; Cabrera and Beare, 1993) before colorimetric analysis of $NO_3^-$ on a SpectraMax M2 plate reader (Molecular Devices, San Jose, CA). The $^{15}N$ isotopic composition of the $NO_3^-$ in digested control and chloroform-treated extracts was determined using the acid trap diffusion method and EA-IRMS analysis as described earlier. Assimilation rates of $NH_4^+$ and $NO_3^-$ were calculated from the $^{15}NH_4^+$ and $^{15}NO_3^-$ labeled soils, respectively, according to Templer et al. (2008). Microbial biomass N was calculated assuming a chloroform extraction efficiency of 0.54 (Brookes et al., 1985).

**Gas fluxes**

We measured nitrification-derived net $N_2O$ fluxes, denitrification-derived net $N_2O$ fluxes from the $^{15}NH_4^+$ and $^{15}NO_3^-$ label additions, respectively, as gaseous N loss pathways. We also measured $CO_2$ fluxes as representative of C mineralization rates from the free-living microbial community in the 4 hr $^{15}N$ pool dilution laboratory incubations. At 15 minutes of the soil incubation with the $^{15}N$ label, we weighed 100 g subsamples of the $^{15}N$-labeled soil into 490 mL mason jars that were sealed with lids fitted with septum ports. Several room air samples were collected and stored in pre-evacuated Wheaton vials as the soil samples were sealed in the jars to

represent the initial time point for gas flux calculations. At 4 hr of the soil incubation, we sampled 90 mL of headspace gas and stored the gas sample in a 60 mL pre-evacuated Wheaton vial. We analyzed a 5 mL subsample of the stored gas samples for $CO_2$ and $N_2O$ concentrations on the GC as described above. The remainder of each gas sample was analyzed for N isotopic composition of $N_2O$ on an IsoPrime 100 isotope ration mass spectrometer interfaced with an IsoPrime trace gas analyzer (Cheadle Hulme, UK) and Gilson GX-271 autosampler (Middleton, WI). Total net $N_2O$ fluxes and $CO_2$ fluxes were calculated from the linear change in $N_2O$ and $CO_2$ concentrations over time. Net $^{15}N_2O$ fluxes were calculated from the linear change over time in $^{15}N_2O$ abundance, which was determined from $N_2O$ concentrations and the $^{15}N$ atom% enrichment of $N_2O$. Nitrification-derived net $N_2O$ fluxes were estimate by dividing the $^{15}N_2O$ flux from the $^{15}NH4^+$ label treatment by the average $^{15}N$ atom% enrichment of the $NH_4^+$ pool over the 4 hr incubation; denitrification-derived net $N_2O$ fluxes were similarly estimated from the $^{15}NO_3^-$ label treatment.

**Net N mineralization and nitrification rates**

We measured net N mineralization and nitrification rates to be able to relate our measurements of gross N process rates with the more commonly measured indices of N process rates. After the soil samples had been subsampled for all other assays, including analysis of initial soil $NH_4^+$ and $NO_3^-$ concentrations, we incubated the remaining soil in their plastic bags for three weeks. At the end of the incubation, we extracted a 30 g subsample of soil in 100 mL KCl to determine the final soil $NH_4^+$ and $NO_3^-$ concentrations as described earlier. We calculated net mineralization and nitrification rates from the change in $NH_4^+$ plus $NO_3^-$ concentrations for

net mineralization or the change in $NO_3^-$ concentrations only for net nitrification over the three week incubation.

### Statistical methods

All statistics were carried out in R 3.6.2 (R Core Team 2019). Statistical significance was determined based on $P<0.05$. To test for differences in soil chemical properties and N process rates, we fit linear mixed models with stand mycorrhizal type (ECM or AM), N addition (control or N addition), and the interaction between stand mycorrhizal type and N addition as the fixed effects and with plot pair and sample dates as random effects. We performed pairwise comparisons between each level of stand mycorrhizal and N addition using the "emmeans" function in the emmeans package (Russell, 2021), with Tukey's adjustment method for multiple comparisons. The following soil chemical properties served as dependent variables: pH, $NH_4^+$ concentration, $NO_3^-$ concentration, potential nitrification rates, potential denitrification rates, net N mineralization rates, net nitrification rates, gross N mineralization rates, gross nitrification rates, net $N_2O$ fluxes (total, nitrification-derived, and denitrification-derived), microbial biomass N, and N assimilation rates (of $NH_4^+$ and $NO_3^-$). Dependent variables were ln-transformed when necessary to meet assumptions of normality.

## RESULTS

### Stand mycorrhizal type effects

We found a strong effect of stand mycorrhizal type across all dependent variables measured in this study with the exception of $NH_4^+$ concentrations which were similar across ECM and AM forest types (Figure 5.1a). We found that net and gross N mineralization rates differed significantly between ECM and AM forest stands, but the effects of stand mycorrhizal

type was opposite for the two metrics of mineralization (Figure 5.1c, 5.2a). Net mineralization rates were significantly greater in AM stands compared to ECM stands ($F_{1, 12} = 49.41$, $P < 0.0001$; Figure 5.1c) while gross mineralization rates were greater in ECM stands compared to AM stands ($F_{1,11.86} = 11.32$, $P = 0.006$; Figure 5.2a). Consistent with the gross N mineralization patterns, $CO_2$ fluxes, a measure of C mineralization rates, were significantly greater in ECM compared to AM stands ($F_{1,12.03} = 48.96$, $P<0.0001$; Figure 5.2b). Soil pH was significantly greater in AM compared to ECM stands ($F_{1, 13.77} = 31.18$, $P < 0.01$; Figure 5.3).

We found a consistent effect of stand mycorrhizal type on all metrics of N cycling processes downstream of N mineralization. Potential and net nitrification rates as well as soil $NO_3^-$ concentrations were significantly greater in AM compared to ECM stands (potential rates, $F_{1, 12} = 5.47$, $P=0.04$; net rates, $F_{1,12} = 266.91$, $P < 0.0001$; concentrations, $F_{1, 12} = 39.98$, $P < 0.0001$; Figure 5.1bd, D.1). Similarly, potential total denitrification and potential incomplete denitrification were significantly greater in AM compared to ECM stands ($F_{1,12.10} = 27.35$, $P<0.0002$; $F_{1,12.05} = 41.63$, $P<0.0001$, respectively; Figure D.2ab). Finally, total, nitrification-derived and denitrification-derived net $N_2O$ fluxes all exhibited a similar pattern with greater fluxes in AM compared to ECM stands (total, $F_{1,203.15} = 19.29$, $P<0.0001$; nitrification-derived, $F_{1,11.93} = 7.46$, $P = 0.018$; denitrification-derived, $F_{1,79} = 10.34$, $P<0.0001$; Figure 5.4a-c) although for nitrification derived $N_2O$ fluxes, this effect was only significant in N addition plots.

We found that microbial biomass N and inorganic N assimilation rates exhibited different patterns. Microbial biomass N was significantly greater in ECM stands compared with AM stands ($F_{1, 11.93} = 70.66$, $P < 0.0001$; Figure 5.5). In contrast, the effect of stand mycorrhizal type on microbial $NH_4^+$ assimilation rates depended on the N addition treatment: microbial $NH_4^+$ assimilation was significantly greater in ECM stands relative to AM stands in N addition plots

(P=0.0001), but this effect was only marginally significant in control plots (P=0.07; Figure 5.6a). There was no effect of stand mycorrhizal type on $NO_3^-$ assimilation rates in either N addition or control treatments (Figure 5.6b).

**Nitrogen addition effects**

The effects of N addition on dependent variables measured in this study were not always consistent between stand mycorrhizal types. Nitrogen addition resulted in greater soil $NH_4^+$ and $NO_3^-$ concentrations ($F_{1,93} = 17.45$, $P < 0.0001$; $F_{1,93} = 54.85$, $P < 0.0001$; Figure 5.1ab), and decreased soil pH ($F_{1,94.90} = 7.05$, $P = 0.01$; Figure 5.3) with average pH values of 4.57 and 4.71 for N addition and control plots respectively. Similarly, net N mineralization rates were significantly higher in N addition relative to control treatments, though this effect was only significant in AM stands ($P < 0.0001$ and $P = 0.79$ for AM and ECM stands, respectively; Figure 5.1c). For $NH_4^+$ and $NO_3^-$ assimilation rates, the effect of N addition varied between stand types with significantly greater assimilation rates in N addition compared to control plots in ECM stands (P=0.03; P=0.02, respectively), but no effect of N addition in AM stands (Figure 5.6ab). Total net $N_2O$ fluxes were significantly greater in N addition compared to control plots ($F_{1,203.14} = 3.07$, $P < 0.0001$; Figure 5.4c). However, this effect was only marginally significant in AM stands ($P < 0.0001$, $P = 0.06$, for ECM and AM stands, respectively; Figure 5.4c).

## DISCUSSION

Tree association with ECM versus AM fungi clearly mediates distinct nutrient syndromes (e.g. Averill et al., 2014; Corrales et al., 2016; Lin et al., 2017; Phillips et al., 2013; Zhu et al., 2018), yet the mechanisms driving these mycorrhizal type patterns have remained unclear

(Averill et al., 2019; Keller and Phillips, 2019; Lin et al., 2017). Suppressed N mineralization due to slow decomposition of low quality ECM litter and organic N uptake by ECM fungi has been proposed to initiate cascading effects that result in an organic nutrient economy with closed N cycling in ECM stands (Brzostek et al., 2015; Phillips et al., 2013). However, lower net rates of N mineralization quantified in past studies conflate gross production and consumption of inorganic N (e.g. Lin et al., 2017; Midgley and Phillips, 2016; Mushinski et al., 2021). In this study we demonstrated that lower net N mineralization rates can occur in ECM stands compared to AM stands due to both higher gross N mineralization rates and microbial inorganic N assimilation rates. Strikingly, despite higher gross N mineralization rates in ECM stands and similar soil $NH_4^+$ concentrations between stand mycorrhizal types, we observed lower nitrification and denitrification rates in ECM stands. This suggests that suppressed N mineralization is not a prerequisite for closed ecosystem N cycling. Here we discuss how our results improve understanding of the potential mechanisms driving mycorrhizal nutrient syndromes, suggest revisions to the originally proposed mycorrhizal-associated nutrient economy (MANE) framework that centers on lower N mineralization in ECM stands (Phillips et al., 2013), and outline future studies to evaluate the proposed revised framework.

**Challenge to the original framework**

Controls on N mineralization in ECM versus AM soils has previously been considered in the context of litter chemical quality and microbial competition for limited N, but other factors can also affect N mineralization. Slower leaf litter decomposition and greater microbial N limitation in ECM stands have previously been documented at our study site in Moores Creek, Indiana (Midgley et al., 2015; Midgley and Phillips, 2016; Phillips et al., 2013). However, we

observed higher gross N mineralization rates in ECM stands, opposite of the pattern predicted by the original MANE framework. We hypothesize that this may result from lower CUE that can occur under stressful low pH conditions (Li et al., 2021), which are consistently observed in ECM soils (Lin, *in press*). Microbes in acidic ECM soils consume energy to maintain the necessary pH gradient between their cytoplasm and the environment (Booth, 1985). Microbial survival in acidic conditions requires significant investment in cellular maintenance, which occurs at the expense of biomass synthesis, to overcome disruption of diffusion and solute transport by high extracellular proton concentrations (Krulwich et al., 1998; Malik et al., 2018; Matin, 1990) and diffusion of conjugate acids through the cellular membrane (Russell, 1992). Higher maintenance respiration relative to growth respiration results in low carbon use efficiency and increased rates of both C and N mineralization. In support of this hypothesized mechanism, we observed greater $CO_2$ fluxes and gross N mineralization rates in more acidic ECM soils relative to AM soils. Therefore, mycorrhizal effects on soil pH may indirectly drive mycorrhizal type differences in gross N mineralization rates, outweighing effects from differences in leaf litter decomposition and microbial competition for N.

Alternatively, despite the putative capacity of ECM fungi to directly uptake organic molecules and bypass inorganic N cycling (Lindahl and Tunlid, 2015; Read and Perez-Moreno, 2003), greater gross mineralization rates in ECM stands may indicate that ECM fungi stimulate N mineralization by free-living decomposers (Meier et al., 2015; Phillips and Fahey, 2006; Sulman et al., 2017). Positive priming effects on gross N mineralization have been shown to correlate with N-acquiring hydrolytic enzyme activities in ECM soils (Yin et al., 2021) such that exclusion of ECM hyphae decreases enzyme activities (Brzostek et al., 2015; Yin et al., 2021). Exudation of labile C compounds in can stimulate N transformations (Dijkstra et al., 2013; Meier

et al., 2017) and increase N availability, such that C exudation rates are often greater in low-N soils (Pausch and Kuzyakov, 2018). In our temperate study site, lower N ECM leaf litter decomposes slower than higher N AM leaf litter (Midgley et al., 2015; Phillips et al., 2013), resulting in N limited free-living microbes in ECM soils where N return from decomposition of ECM leaf litter is lower. Nitrogen limitation may explain significantly greater C exudation rates in ECM compared to AM soils (Phillips and Fahey, 2005; Yin et al., 2014). Furthermore, physically accessible particulate organic matter that accumulates in ECM surface soils (Averill et al., 2019; Craig et al., 2018) may be vulnerable to priming effects (Kuzyakov, 2010). Specifically, standing fungal biomass, which can be up to 2.5 times greater in ECM stands relative to AM stands (Cheeke et al., 2017), represents a relatively high turnover SOM pool that has been shown to undergo accelerated decay in the presence of primed microbial communities (Meier et al., 2017). In contrast, mineral-associated organic matter that dominates SOM pools in AM soils (Cotrufo et al., 2019; Craig et al., 2018) is spatially diffuse and physically protected such that priming SOM decomposition may not be worth the C cost (Brzostek et al., 2015; Sulman et al., 2017). Therefore, rather than suppressing mineralization, slow leaf litter decomposition rates in ECM stands may indirectly stimulate mineralization by driving ECM trees to allocate more C belowground to prime SOM decomposition by rhizosphere microbial communities.

**A proposed revised framework**

Here we show that gross N mineralization rates can be higher in ECM soils, contrasting with the original MANE framework in which slower leaf litter decomposition rates and smaller inorganic $NH_4^+$ concentrations were assumed to reflect lower gross mineralization rates in ECM

soils (Phillips et al., 2013) (Figure 5.7bc). Furthermore, we found that higher gross N mineralization and N assimilation by free-living microbes result in lower net mineralization rates in ECM compared to AM soils. Net rates are traditionally thought to reflect inorganic N supply to plants and mycorrhizal fungi, such that greater net mineralization and $NH_4^+$ concentrations in AM stands have been incorrectly interpreted to reflect larger gross mineralization rates and greater $NH_4^+$ available for uptake in AM soils. Instead, we show that ECM soils exhibit faster cycling of $NH_4^+$ with rapid N assimilation by free-living microbes masking rapid N mineralization.

Inorganic N assimilation by the free-living decomposer community was not explicitly considered in the original MANE framework such that $NH_4^+$ pools were assumed to fuel nitrification. However, we provide evidence that microbial assimilation can be an important sink for $NH_4^+$ in ECM stands (Figure 5.7bc). We found that addition of inorganic N increased microbial assimilation of $NH_4^+$ and $NO_3^-$ in ECM, but not AM soils, demonstrating the stronger demand by free-living microbes for inorganic N in ECM soils. Inorganic N sink strength may be driven by differences in microbial biomass between stand mycorrhizal types. Despite the fact that fungal-dominated microbial communities in ECM soils have higher C:N ratios than bacterial-dominated microbial communities in AM soils (Cheeke et al., 2017), microbial biomass N was higher in ECM soils. This may be driven by the nearly 2.5 times greater standing fungal biomass in ECM compared to AM soils at our study site (Cheeke et al., 2017). Due to relatively slow N recycling from slow decomposition of low quality ECM leaf litter, and high C:N ratios of particulate organic matter in ECM surface soils, microbial communities may be N-limited (John M Blair, 1988; Olson, 1963) and therefore rapidly assimilate $NH_4^+$. In contrast, bacterial-dominated microbial communities in AM soils may satisfy greater stoichiometric N demand

through decomposition of higher-N leaf litter and therefore experience greater C relative to N limitation such that they mineralize N (Midgley and Phillips, 2016). Overall, we provide evidence that N assimilation by free-living microbes is an important component of mycorrhizal N cycling syndromes.

Suppressed mineralization in ECM stands has been assumed to initiate cascading effects on nitrification and downstream N loss pathways due to limitation of inorganic N as a substrate for those processes (Brzostek et al., 2015; Phillips et al., 2013), but we found that mineralization patterns did not dictate nitrification patterns (Figure 5.7bc). Specifically, gross mineralization rates were higher, but net nitrification rates and $NO_3^-$ concentrations were lower in ECM relative to AM soils at our study site, showing that nitrification is inhibited by mechanisms other than limited production of soil $NH_4^+$. We suggest three non-mutually exclusive mechanisms by which nitrification can be suppressed despite significant $NH_4^+$ production in ECM stands. First, acidic conditions in ECM stands may protonate ammonia to ammonium, decreasing the substrate available for chemoautotrophic growth of ammonia oxidizing bacteria (Mushinski et al., 2019; Xiao et al., 2020). Second, heterotrophs may outcompete nitrifiers for $NH_4^+$ when substrate C:N ratios are high and heterotrophs are relatively more N limited than C limited. This mechanism may be particularly relevant in ECM surface soils that are characterized by accumulation of high C:N particulate organic matter (Averill et al., 2019; Craig et al., 2018). Third, protonation of ammonia to ammonium and heterotrophic N demand may decrease the availability of $NH_4^+$ to ammonia oxidizers in ECM soils. Therefore, low pH and high C:N ratios in ECM soils may result in decreased nitrifier abundance and suppressed nitrification (Mushinski et al., 2019; Scharko et al., 2015). Leaf litter decomposition dynamics may play a role in formation low pH, high C:N ECM substrate that can indirectly suppress nitrification. However, we provide evidence

that slower decomposition of lower quality leaf litter inputs in ECM compared to AM stands does not drive nitrification via suppressed mineralization. Instead, separate mechanistic pathways may govern mineralization and nitrification in ECM soils.

**Opportunities for future studies**

Here we proposed a revised framework for understanding mechanisms that could create the open versus closed ecosystem N cycles characteristic of AM versus ECM forest stands. In particular, future studies should directly evaluate priming and soil acidification as mechanisms leading to stimulation of N mineralization in ECM stands. Priming of free-living decomposers by ECM fungi may be context dependent (Beidler et al., *in press*), while acidification of ECM soils compared to AM soils has consistently been demonstrated from forest to continental scales (Lin, *in press*). Therefore, clarifying mechanistic drivers of ECM effects on N mineralization may allow us to better understand the applicability of our revised framework across systems.

Interactions between roots, mycorrhizal fungi and free-living microbial communities are often acknowledged to drive distinct mycorrhizal syndromes, but these interactions are seldomly included in experiments testing for mycorrhizal effects. Most studies compare N cycling dynamics between ECM and AM soils under lab conditions such that measured process rates only represent contributions from the free-living microbial community. We showed that $NH_4^+$ is a rapidly cycling pool in ECM surface soils with greater gross N mineralization and $NH_4^+$ assimilation relative to AM surface soils. However, to fully understand the balance between gross N mineralization and $NH_4^+$ consumption, future work should focus on conducting N cycling experiments *in situ* such that interactions between mycorrhizal fungi, roots and free-living microbes are accounted for.

Spatial heterogeneity in microbial activity may explain the apparent contradiction between slow leaf litter decomposition and fast gross mineralization in ECM soils. Low-N, high lignin ECM leaf litter may decompose slowly and result in N-limited bulk soil microbes. However, greater belowground C allocation by ECM trees may prime rhizosphere microbial communities and increase N transformation rates in rhizosphere soils (Meier et al., 2015; Phillips and Fahey, 2006; Sulman et al., 2017). Despite evidence that rhizosphere microbes may drive gross mineralization in ECM stands, this has not been explicitly tested because most studies do not consider bulk and rhizosphere soils separately. Therefore, future studies should quantify gross N cycling rates in rhizosphere and bulk soil of ECM- and AM-dominated stands.

## CONCLUSION

The effects of tree mycorrhizal type on soil pH and N limitation have been consistently demonstrated across systems (e.g. Averill et al., 2014; Corrales et al., 2016; Lin, *in press*; Lin et al., 2017; Phillips et al., 2013; Zhu et al., 2018), but the mechanisms driving these effects remain unclear (Averill et al., 2019; Keller and Phillips, 2019; Lin et al., 2017). The original MANE framework proposed that low quality ECM leaf litter and organic N uptake by ECM fungi suppressed decomposition rates and initiated a cascading effect that resulted in an organic nutrient economy in ECM stands (Phillips et al., 2013). However, N mineralization and consumption pathways can be greater in ECM compared to AM soils, resulting in similar $NH_4^+$ concentrations across forest types. Instead, strong inorganic N demand by free-living microbes and soil acidity effects on nitrification may lead to the closed ecosystem N cycle characteristic of ECM forest stands compared to the open ecosystem N cycle of AM-dominated forest stands. Overall, we conclude that N mineralization does not play a central role in forming mycorrhizal

nutrient syndromes as previously thought but rather has the role of a backseat driver, indirectly affecting nitrification and downstream N cycling processes.

## FIGURES

**Figure 5.1.** Boxplots showing the effect of stand mycorrhizal type and nitrogen (N) addition on (a) soil ammonium concentrations, (b) soil nitrate concentrations, (c) net N mineralization rates, and (d) net nitrification rates. Data from arbuscular mycorrhizal (AM)- dominated stands and ectomycorrhizal (ECM)-dominated stands are represented by purple and yellow, respectively. Ammonium concentrations were significantly greater in N addition compared to control plots ($F_{1,93} = 17.45$, $P < 0.0001$) but did not differ between AM- and ECM-dominated stands. The effects of nitrogen addition and stand mycorrhizal type were significant for net N mineralization rates ($F_{1,93} = 16.60$, $P < 0.0001$; $F_{1,12} = 49.41$, $P < 0.0001$, respectively), $NO_3^-$ concentrations ($F_{1,93} = 54.84$, $P < 0.0001$; $F_{1,12} = 39.99$, $P < 0.0001$, respectively) and net nitrification rates ($F_{1,93} = 32.06$, $P < 0.0001$; $F_{1,12} = 266.91$, $P < 0.0001$, respectively), with greater concentrations and net rates in AM- compared to ECM-dominated stands and in N addition compared to control plots. Asterisks denote significant differences between stand types.

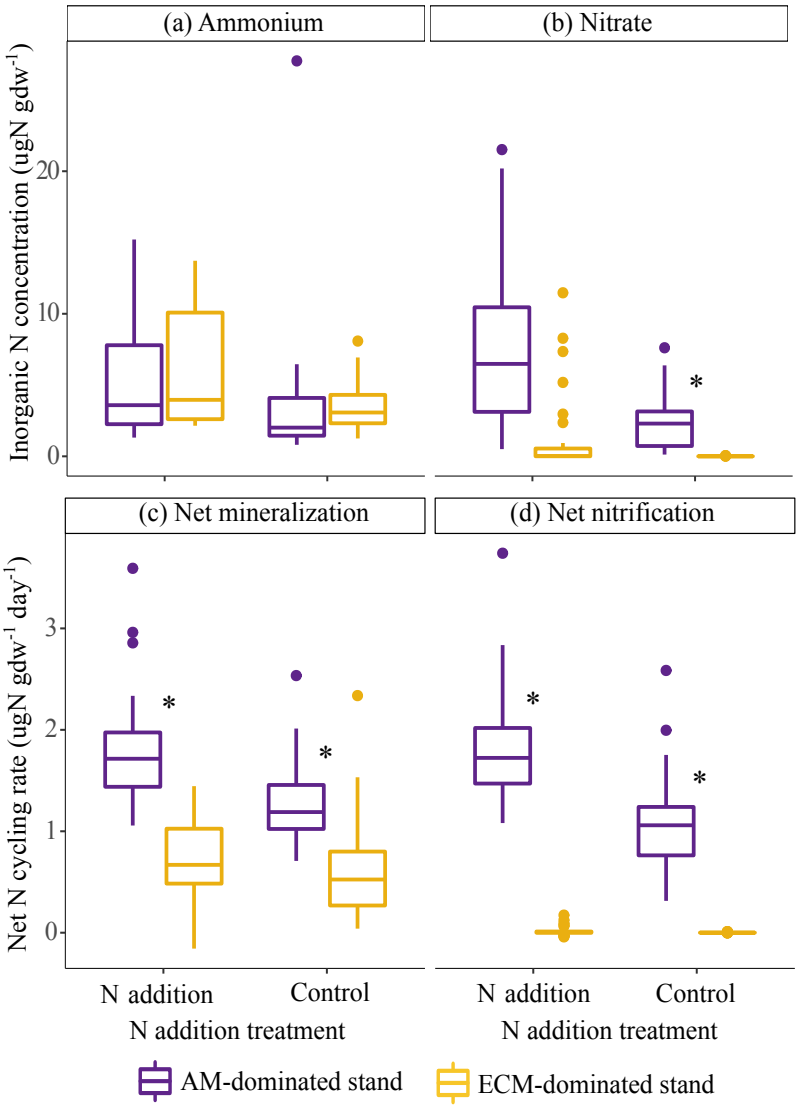

**Figure 5.2.** Boxplots showing the effects of stand mycorrhizal type and nitrogen (N) addition treatment on (a) gross N mineralization rates and (b) carbon (C) mineralization rates. Asterisks indicate significant effects of stand mycorrhizal type: gross N mineralization rates and C mineralization rates were significantly greater in ECM (yellow) compared to AM (purple) stands ($F_{1,11.86} = 11.32$, $P = 0.006$; $F_{1,12.03} = 48.96$, $P < 0.0001$). There was no statistically significant effect of N addition treatment on either N or C mineralization.

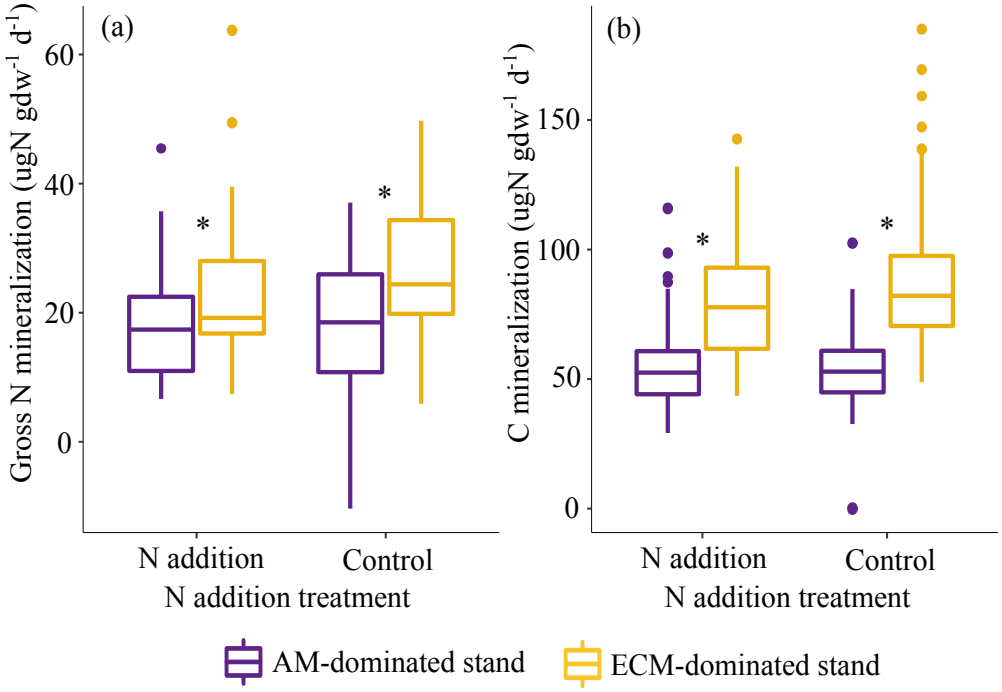

**Figure 5.3.** Boxplot showing the effects of stand mycorrhizal type and nitrogen (N) addition treatment on soil pH. Asterisks indicate significant effects of stand mycorrhizal type: pH was significantly greater in ECM (yellow) compared to AM (purple) stands ($F_{1, 11.93} = 70.66$, $P < 0.0001$). Soil pH decreased significantly with N addition in AM stands (P=0.0009), but not in ECM stands.

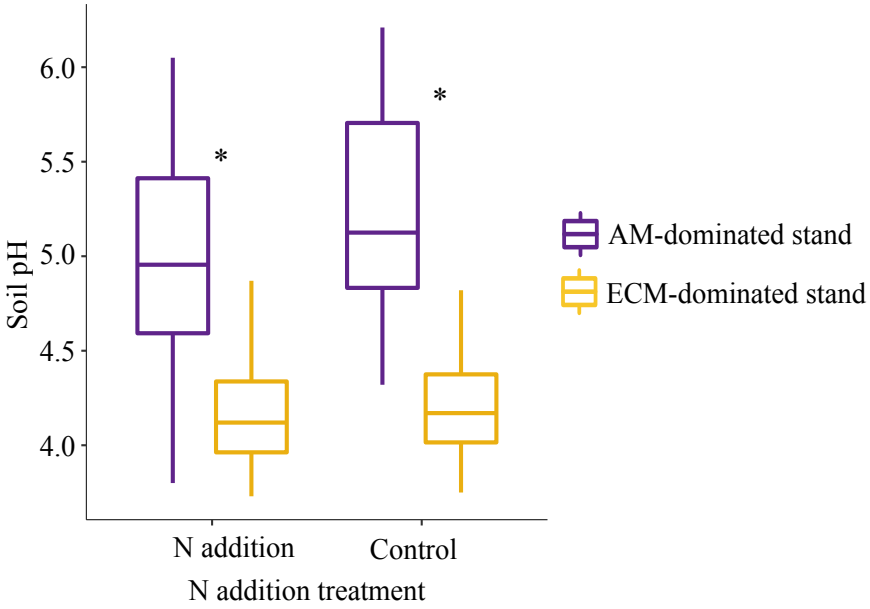

**Figure 5.4.** Boxplots showing the effects of stand mycorrhizal type and nitrogen (N) addition treatment on (a) total net nitrous oxide ($N_2O$) fluxes, (b) nitrification-derived net $N_2O$ fluxes and (c) denitrification-derived net $N_2O$ fluxes. Asterisks indicate significant effects of stand mycorrhizal type with significantly greater total net $N_2O$ fluxes, nitrification -derived net $N_2O$ fluxes, and denitrification-derived net $N_2O$ fluxes in AM (purple) relative to ECM (yellow) stands (total, $F_{1,11.86} = 11.32$, P=0.006; nitrification-derived, $F_{1,12} = 27.89$, P=0.0002; denitrification-derived, $F_{1,12.11} = 34.57$, P<0.0001). Total and source-partitioned net $N_2O$ fluxes were significantly greater in N addition compared to control plots (total, $F_{1,204.07} = 1.87$, P<0.0001; nitrification-derived, $F_{1,93} = 9.07$, P=0.003; denitrification-derived, $F_{1,92.25} = 13.56$, P<0.0004); however, this effect was only significant in AM stands for denitrification-derived $N_2O$ fluxes (P=0.0002, 0.22 for ECM and AM stands, respectively).

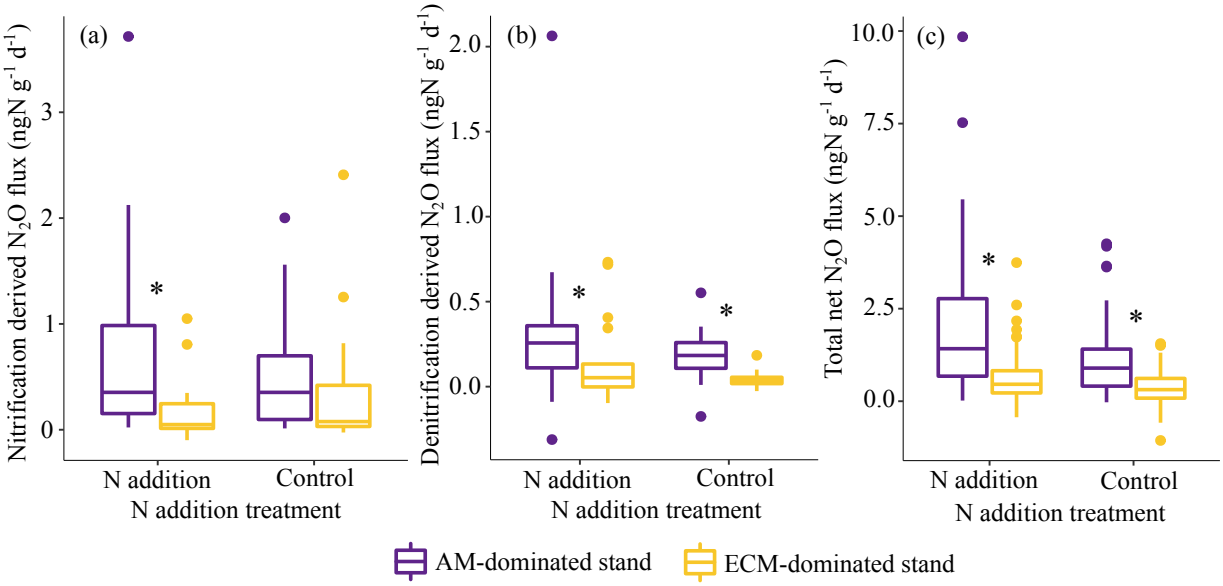

**Figure 5.5.** Boxplot showing the effects of stand mycorrhizal type and nitrogen (N) addition treatment on microbial biomass N. Asterisks indicate significant effects of stand mycorrhizal type: microbial biomass N was significantly greater in ECM (yellow) compared to AM (purple) stands ($F_{1, 11.93} = 70.66$, $P < 0.0001$). There was no statistically significant effect of N addition on microbial biomass N.

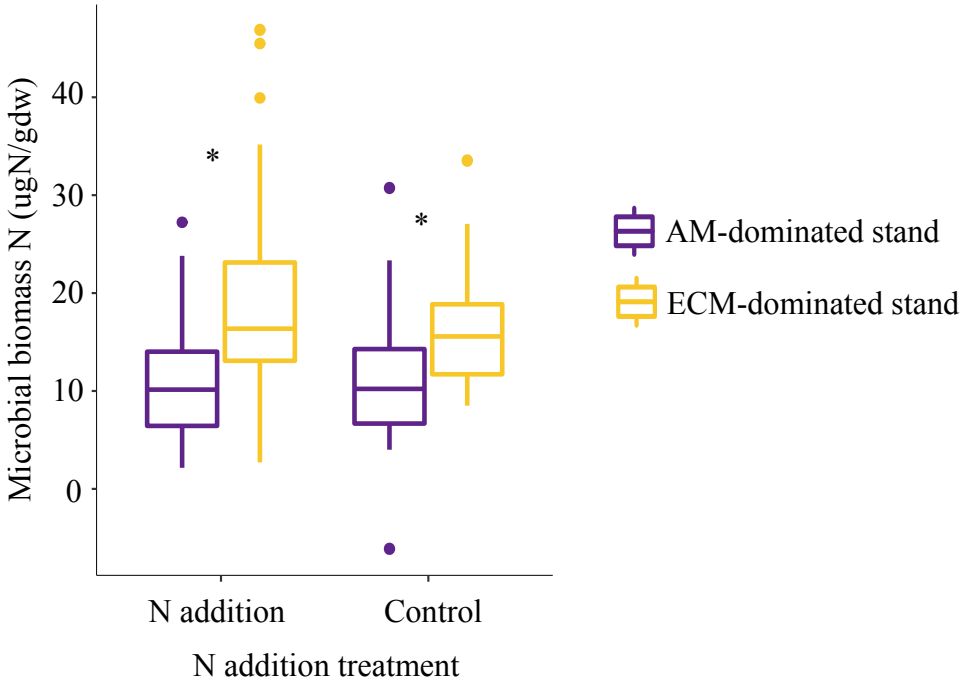

**Figure 5.6.** Boxplot showing the effects of stand mycorrhizal type and nitrogen (N) addition treatment on (a) microbial ammonium ($NH_4^+$) assimilation rates and (b) microbial nitrate ($NO_3^-$) assimilation rates. Asterisks indicate significant effects of stand mycorrhizal type. Ammonium assimilation rates were significantly greater in ECM (yellow) compared to AM (purple) stands in N addition plots (P=0.0001), but not in control plots. Nitrate assimilation rates were greater in N addition compared to control plots in ECM stands only (P=0.03). There was no statistically significant effect of stand mycorrhizal type on $NO_3^-$ assimilation rates or of N addition on $NH_4^+$ assimilation rates.

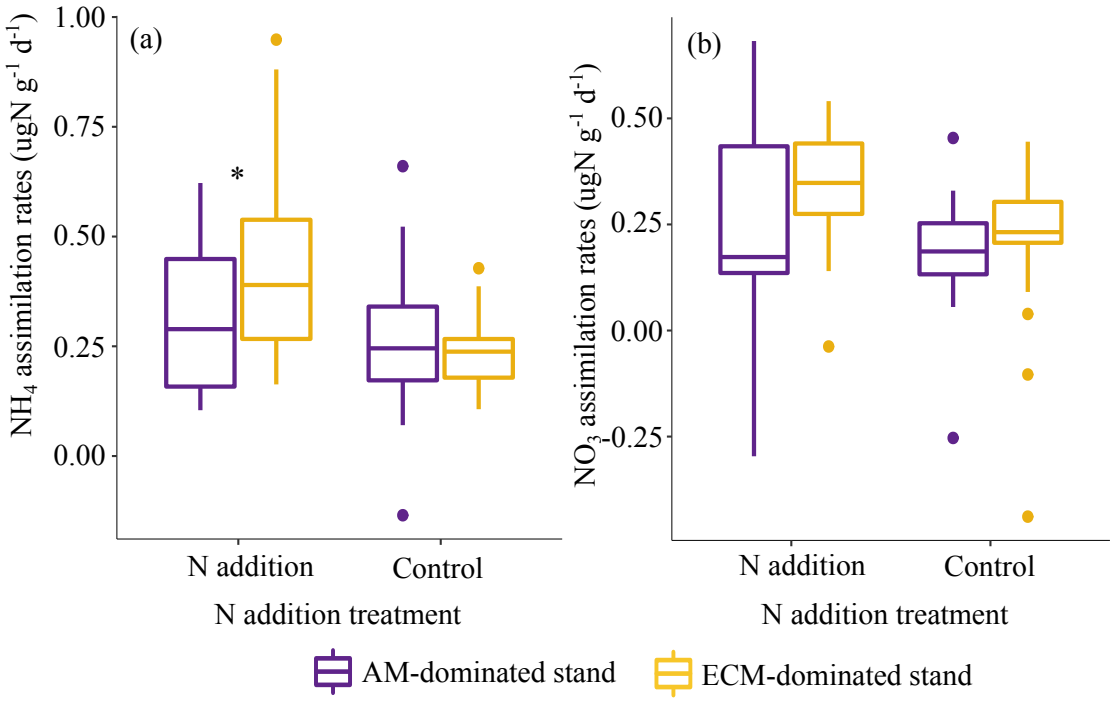

**Figure 5.7.** Conceptual diagram illustrating N cycling in (a) the originally proposed mycorrhizal-associated nutrient economy framework (Phillips et al., 2013) and (b) the proposed revised framework based on our study findings. Our proposed revisions to the original framework are notated by arrows outlined in red in panels (b) and (c). In the original framework, faster decomposition of high N, low lignin AM leaf litter results in higher N mineralization rates initiates rapid cycling of inorganic N and ultimately leads to an open N cycle characterized by ecosystem N losses through leaching and denitrification. In contrast, slower decomposition of lower N, higher lignin ECM leaf litter results in lower N mineralization rates that results in cycling of organic N and ultimately leads to a closed N cycle characterized by limited N losses. In the revised framework, lower soil pH in ECM stands results in higher gross N mineralization rates than in AM stands due to lower microbial carbon use efficiency. However, high rates of free-living microbial $NH_4^+$ assimilation and also high demand for inorganic N by ECM fungi and trees limits N availability for nitrification and denitrification, creating a closed N cycle in the ECM stands despite the higher gross N mineralization rates.

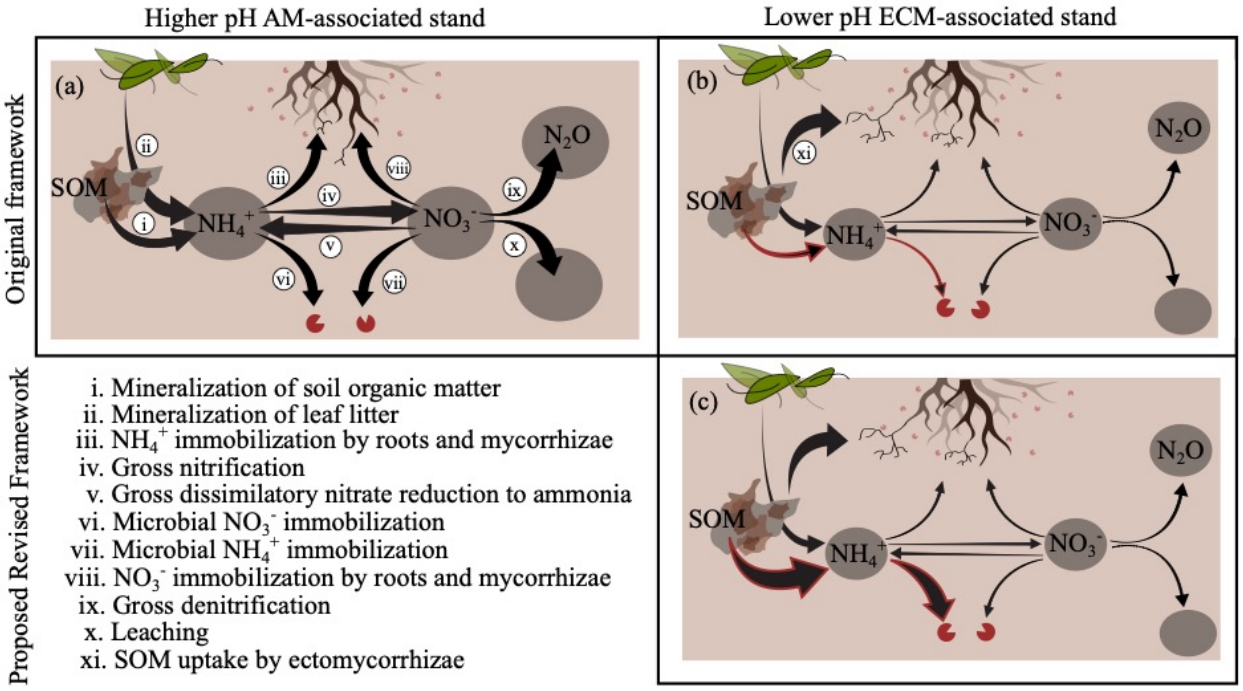

## REFERENCES

Averill, C., 2016. Slowed decomposition in ectomycorrhizal ecosystems is independent of plant chemistry. Soil Biology and Biochemistry 102, 52–54. doi:http://dx.doi.org/10.1016/j.soilbio.2016.08.003

Averill, C., Bhatnagar, J.M., Dietze, M.C., Pearse, W.D., Kivlin, S.N., 2019. Global imprint of mycorrhizal fungi on whole-plant nutrient economics. Proceedings of the National Academy of Sciences of the United States of America 46, 23163–23168. doi:10.1073/pnas.1906655116

Averill, C., Turner, B.L., Finzi, A.C., 2014. Mycorrhiza-mediated competition between plants and decomposers drives soil carbon storage. Nature 505, 543–545. doi:10.1038/nature12901

Beidler, K. V., Young, O.E., Pritchard, S.G., Phillips, R.P., n.d. Mycorrhizal roots slow the decay of belowground litters in a temperate hardwood forest.

Bending, G.D., 2003. Litter decomposition, ectomycorrhizal roots and the "Gadgil" effect. New Phytologist. doi:10.1046/j.1469-8137.2003.00752.x

Berg, P., Rosswall, T., 1985. Ammonium oxidizer numbers, potential and actual oxidation rates in two swedish arable soils. Biology and Fertility of Soils 1, 131–140. doi:10.1007/BF00301780

Blair, J.M., 1988. Nutrient release from decomposing foliar litter of three tree species with spicial reference to calcium, magnesium and potassium dynamics. Plant and Soil 110, 49–55.

Booth, I.R., 1985. Regulation of cytoplasmic pH in bacteria. Microbiological Reviews 49, 359–378. doi:10.1128/mr.49.4.359-378.1985

Brookes, P.C., Landman, A., Pruden, G., Jenkinson, D.S., 1985. Chloroform fumigation and the

release of soil nitrogen: A rapid direct extraction method to measure microbial biomass nitrogen in soil. Soil Biology and Biochemistry 17, 837–842. doi:https://doi.org/10.1016/0038-0717(85)90144-0

Brzostek, E.R., Dragoni, D., Brown, Z.A., Phillips, R.P., 2015. Mycorrhizal type determines the magnitude and direction of root-induced changes in decomposition in a temperate forest. New Phytologist 206, 1274–1282. doi:10.1111/nph.13303

Cabrera, M.L., Beare, M.H., 1993. Alkaline persulfate oxidation for determining total nitrogen in microbial biomass extracts. Soil Science Society of America Journal 57, 1007–1012.

Cheeke, T.E., Phillips, R.P., Brzostek, E.R., Rosling, A., Bever, J.D., Fransson, P., 2017. Dominant mycorrhizal association of trees alters carbon and nutrient cycling by selecting for microbial groups with distinct enzyme function. New Phytologist 214, 432–442. doi:10.1111/nph.14343

Chen, Y.-L., Chen, B.-D., Hu, Y.-J., Li, T., Zhang, X., Hao, Z.-P., Wang, Y.-S., 2013. Direct and indirect influence of arbuscular mycorrhizal fungi on abundance and community structure of ammonia oxidizing bacteria and archaea in soil microcosms. Pedobiologia 56, 205–212. doi:https://doi.org/10.1016/j.pedobi.2013.07.003

Corrales, A., Mangan, S.A., Turner, B.L., Dalling, J.W., 2016. An ectomycorrhizal nitrogen economy facilitates monodominance in a neotropical forest. Ecology Letters 19, 383–392. doi:10.1111/ele.12570

Cotrufo, M.F., Ranalli, M.G., Haddix, M.L., Six, J., Lugato, E., 2019. Soil carbon storage informed by particulate and mineral-associated organic matter. Nature Geoscience 12, 989–994. doi:10.1038/s41561-019-0484-6

Craig, M.E., Turner, B.L., Liang, C., Clay, K., Johnson, D.J., Phillips, R.P., 2018. Tree

mycorrhizal type predicts within-site variability in the storage and distribution of soil organic matter. Global Change Biology 24, 3317–3330. doi:10.1111/gcb.14132

de Schrijver, A., de Frenne, P., Staelens, J., Verstraeten, G., Muys, B., Vesterdal, L., Wuyts, K., van Nevel, L., Schelfhout, S., de Neve, S., Verheyen, K., 2012. Tree species traits cause divergence in soil acidification during four decades of postagricultural forest development. Global Change Biology 18, 1127–1140. doi:https://doi.org/10.1111/j.1365-2486.2011.02572.x

De Vries, W., Breeuwsma, A., 1987. The relation between soil acidification and element cycling. Water, Air, and Soil Pollution 35, 293–310.

Dijkstra, F., Carrillo, Y., Pendall, E., Morgan, J., 2013. Rhizosphere priming: a nutrient perspective. Frontiers in Microbiology 4. doi:10.3389/fmicb.2013.00216

Drigo, B., Pijl, A.S., Duyts, H., Kielak, A.M., Gamper, H.A., Houtekamer, M.J., Boschker, H.T.S., Bodelier, P.L.E., Whiteley, A.S., van Veen, J.A., Kowalchuk, G.A., 2010. Shifting carbon flow from roots into associated microbial communities in response to elevated atmospheric CO2. Proceedings of the National Academy of Sciences of the United States of America 107, 10938–10942. doi:10.1073/pnas.0912421107

Fernandez, C.W., Kennedy, P.G., 2016. Revisiting the "Gadgil effect": do interguild fungal interactions control carbon cycling in forest soils? New Phytologist 209, 1382–1394. doi:10.1111/nph.13648

Fernandez, C.W., See, C.R., Kennedy, P.G., 2019. Decelerated carbon cycling by ectomycorrhizal fungi is controlled by substrate quality and community composition. New Phytologist 226, 569–582. doi:10.1111/nph.16269

Frey, S.D., 2019. Mycorrhizal Fungi as Mediators of Soil Organic Matter Dynamics. Annual

Review of Ecology, Evolution, and Systematics. doi:10.1146/annurev-ecolsys-110617-062331

Gadgil, R.L., Gadgil, P.D., 1971. Mycorrhiza and litter decomposition. Nature 233, 133. doi:10.1038/233133a0

Grayston, S.J., Vaughan, D., Jones, D., 1997. Rhizosphere carbon flow in trees, in comparison with annual plants: The importance of root exudation and its impact on microbial activity and nutrient availability. Applied Soil Ecology 5, 29–56.

Hart, S., Nason, G., Myrold, D., Perry, D., 1994. Dynamics of Gross Nitrogen Transformations in an Old-Growth Forest: The Carbon Connection. Ecology 75, 880. doi:10.2307/1939413

Herman, D.J., Brooks, P.D., Ashraf, M., Azam, F., Mulvaney, R.L., 1995. Evaluation of methods for nitrogen-15 analysis of inorganic nitrogen in soil extracts. II. Diffusion methods. Communications in Soil Science and Plant Analysis 26, 1675–1685. doi:10.1080/00103629509369400

Herman, D.J., Firestone, M.K., Nuccio, E., Hodge, A., 2012. Interactions between an arbuscular mycorrhizal fungus and a soil microbial community mediating litter decomposition. Fems Microbiology Ecology 80, 236–247. doi:10.1111/j.1574-6941.2011.01292.x

Horz, H.-P., Barbrook, A., Field, C.B., Bohannan, B.J.M., 2004. Ammonia-oxidizing bacteria respond to multifactorial global change. Proceedings of the National Academy of Sciences of the United States of America 101, 15136 LP – 15141. doi:10.1073/pnas.0406616101

Kaiser, C., Kilburn, M.R., Clode, P.L., Fuchslueger, L., Koranda, M., Cliff, J.B., Solaiman, Z.M., Murphy, D. V, 2015. Exploring the transfer of recent plant photosynthates to soil microbes: mycorrhizal pathway vs direct root exudation. New Phytologist 205, 1537–1551. doi:https://doi.org/10.1111/nph.13138

Kandeler, E., Tscherko, D., Spiegel, H., 1999. Long-term monitoring of microbial biomass, N mineralisation and enzyme activities of a Chernozem under different tillage management. Biology and Fertility of Soils 28, 343–351. doi:10.1007/s003740050502

Keller, A.B., Phillips, R.P., 2019. Leaf litter decay rates differ between mycorrhizal groups in temperate, but not tropical, forests. New Phytologist 222, 556–564. doi:10.1111/nph.15524

Kirkham, D., Bartholomew, W. V, 1954. Equations for Following Nutrient Transformations in Soil, Utilizing Tracer Data. Soil Science Society of America Journal 18, 33–34. doi:https://doi.org/10.2136/sssaj1954.03615995001800010009x

Krulwich, T.A., Ito, M., Hicks, D.B., Gilmour, R., Guffanti, A.A., 1998. pH homeostasis and ATP synthesis: studies of two processes that necessitate inward proton translocation in extremely alkaliphilic Bacillus species. Extremophiles 2, 217–222. doi:10.1007/s007920050063

Kuzyakov, Y., 2010. Priming effects: Interactions between living and dead organic matter. Soil Biology and Biochemistry 42, 1363–1371. doi:https://doi.org/10.1016/j.soilbio.2010.04.003

Langley, J.A., Hungate, B.A., 2003. Mycorrhizal controls on belowground litter quality. Ecology 84, 2302–2312. doi:10.1890/02-0282

Li, T., Wang, R., Cai, J., Meng, Y., Wang, Z., Feng, X., Liu, H., Turco, R.F., Jiang, Y., 2021. Enhanced carbon acquisition and use efficiency alleviate microbial carbon relative to nitrogen limitation under soil acidification. Ecological Processes 10, 32. doi:10.1186/s13717-021-00309-1

Lin, n.d. Mycorrhizal associations of tree species influence soil nitrogen dynamics via effects on soil acid-base chemistry.

Lin, G., McCormack, M.L., Ma, C., Guo, D., 2017. Similar below-ground carbon cycling

dynamics but contrasting modes of nitrogen cycling between arbuscular mycorrhizal and ectomycorrhizal forests. New Phytologist 213, 1440–1451. doi:10.1111/nph.14206

Lindahl, B.D., Ihrmark, K., Boberg, J., Trumbore, S.E., Högberg, P., Stenlid, J., Finlay, R.D., 2007. Spatial separation of litter decomposition and mycorrhizal nitrogen uptake in a boreal forest. New Phytologist 173, 611–620. doi:10.1111/j.1469-8137.2006.01936.x

Lindahl, B.D., Tunlid, A., 2015. Ectomycorrhizal fungi - potential organic matter decomposers, yet not saprotrophs. New Phytologist 205, 1443–1447. doi:10.1111/nph.13201

Malik, A.A., Puissant, J., Buckeridge, K.M., Goodall, T., Jehmlich, N., Chowdhury, S., Gweon, H.S., Peyton, J.M., Mason, K.E., van Agtmaal, M., Blaud, A., Clark, I.M., Whitaker, J., Pywell, R.F., Ostle, N., Gleixner, G., Griffiths, R.I., 2018. Land use driven change in soil pH affects microbial carbon cycling processes. Nature Communications 9, 3591. doi:10.1038/s41467-018-05980-1

Matin, A., 1990. Bioenergetics parameters and transport in obligate acidophiles. Biochimica et Biophysica Acta (BBA) - Bioenergetics 1018, 267–270. doi:https://doi.org/10.1016/0005-2728(90)90264-5

Meier, I.C., Finzi, A.C., Phillips, R.P., 2017. Root exudates increase N availability by stimulating microbial turnover of fast-cycling N pools. Soil Biology and Biochemistry 106, 119–128. doi:https://doi.org/10.1016/j.soilbio.2016.12.004

Meier, I.C., Pritchard, S.G., Brzostek, E.R., McCormack, M.L., Phillips, R.P., 2015. The rhizosphere and hyphosphere differ in their impacts on carbon and nitrogen cycling in forests exposed to elevated CO2. New Phytologist 205, 1164–1174. doi:https://doi.org/10.1111/nph.13122

Midgley, M.G., Brzostek, E., Phillips, R.P., 2015. Decay rates of leaf litters from arbuscular

mycorrhizal trees are more sensitive to soil effects than litters from ectomycorrhizal trees. Journal of Ecology 103, 1454–1463. doi:10.1111/1365-2745.12467

Midgley, M.G., Phillips, R.P., 2016. Resource stoichiometry and the biogeochemical consequences of nitrogen deposition in a mixed deciduous forest. Ecology 97, 3369–3378. doi:https://doi.org/10.1002/ecy.1595

Midgley, M.G., Phillips, R.P., 2014. Mycorrhizal associations of dominant trees influence nitrate leaching responses to N deposition. Biogeochemistry 117, 241–253. doi:10.1007/s10533-013-9931-4

Mushinski, R.M., Payne, Z.C., Raff, J.D., Craig, M.E., Pusede, S.E., Rusch, D.B., White, J.R., Phillips, R.P., 2021. Nitrogen cycling microbiomes are structured by plant mycorrhizal associations with consequences for nitrogen oxide fluxes in forests. Global Change Biology 27, 1068–1082. doi:10.1111/gcb.15439

Mushinski, R.M., Phillips, R.P., Payne, Z.C., Abney, R.B., Jo, I., Fei, S., Pusede, S.E., White, J.R., Rusch, D.B., Raff, J.D., 2019. Microbial mechanisms and ecosystem flux estimation for aerobic $NO_y$ emissions from deciduous forest soils. Proceedings of the National Academy of Sciences 116, 2138 LP – 2145. doi:10.1073/pnas.1814632116

Olson, J.S., 1963. Energy Storage and the Balance of Producers and Decomposers in Ecological Systems. Ecology. doi:10.2307/1932179

Paterson, E., Sim, A., Davidson, J., Daniell, T.J., 2016. Arbuscular mycorrhizal hyphae promote priming of native soil organic matter mineralisation. Plant and Soil 408, 243–254. doi:10.1007/s11104-016-2928-8

Pausch, J., Kuzyakov, Y., 2018. Carbon input by roots into the soil: Quantification of rhizodeposition from root to ecosystem scale. Global Change Biology 24, 1–12.

doi:https://doi.org/10.1111/gcb.13850

Phillips, R.P., Brzostek, E., Midgley, M.G., 2013. The mycorrhizal-associated nutrient economy: A new framework for predicting carbon-nutrient couplings in temperate forests. New Phytologist 199, 41–51. doi:10.1111/nph.12221

Phillips, R.P., Fahey, T.J., 2006. Tree species and mycorrhizal associations influence the magnitude of rhizosphere effects. Ecology 87, 1302–1313. doi:10.1890/0012-9658(2006)87[1302:TSAMAI]2.0.CO;2

Phillips, R.P., Fahey, T.J., 2005. Patterns of rhizosphere carbon flux in sugar maple (Acer saccharum) and yellow birch (Betula allegheniensis) saplings. Global Change Biology 11, 983–995. doi:https://doi.org/10.1111/j.1365-2486.2005.00959.x

Prosser, J.I., Nicol, G.W., 2012. Archaeal and bacterial ammonia-oxidisers in soil: the quest for niche specialisation and differentiation. Trends in Microbiology 20, 523–531. doi:https://doi.org/10.1016/j.tim.2012.08.001

R Development Core Team, 2019. R: A language and environment for statistical computing. R Fouondataion for Statistical Computing, Vienna, Austria.

Read, D.J., Perez-Moreno, J., 2003. Mycorrhizas and nutrient cycling in ecosystems - a journey towards relevance? New Phytologist 157, 475–492. doi:10.1046/j.1469-8137.2003.00704.x

Russell, J.B., 1992. Another explanation for the toxicity of fermentation acids at low pH: anion accumulation versus uncoupling. Journal of Applied Bacteriology 73, 363–370. doi:https://doi.org/10.1111/j.1365-2672.1992.tb04990.x

Russell, V.L., 2021. emmeans: Estimated Marginal Means, aka Least-Squares Means.

Scharko, N.K., Schütte, U.M.E., Berke, A.E., Banina, L., Peel, H.R., Donaldson, M.A., Hemmerich, C., White, J.R., Raff, J.D., 2015. Combined Flux Chamber and Genomics

Approach Links Nitrous Acid Emissions to Ammonia Oxidizing Bacteria and Archaea in Urban and Agricultural Soil. Environmental Science & Technology 49, 13825–13834. doi:10.1021/acs.est.5b00838

Setia, R., Verma, S.L., Marschner, P., 2012. Measuring microbial biomass carbon by direct extraction – Comparison with chloroform fumigation-extraction. European Journal of Soil Biology 53, 103–106. doi:https://doi.org/10.1016/j.ejsobi.2012.09.005

Seyfried, G.S., Canham, C.D., Dalling, J.W., Yang, W.H., 2021. The effects of tree-mycorrhizal type on soil organic matter properties from neighborhood to watershed scales. Soil Biology and Biochemistry 108385. doi:https://doi.org/10.1016/j.soilbio.2021.108385

Sulman, B.N., Brzostek, E.R., Medici, C., Shevliakova, E., Menge, D.N.L., Phillips, R.P., 2017. Feedbacks between plant N demand and rhizosphere priming depend on type of mycorrhizal association. Ecology Letters 20, 1043–1053. doi:https://doi.org/10.1111/ele.12802

Talbot, J.M., Allison, S.D., Treseder, K.K., 2008. Decomposers in disguise: mycorrhizal fungi as regulators of soil C dynamics in ecosystems under global change. Functional Ecology 22, 955–963. doi:10.1111/j.1365-2435.2008.01402.x

Tatsumi, C., Taniguchi, T., Du, S., Yamanaka, N., Tateno, R., 2020. Soil nitrogen cycling is determined by the competition between mycorrhiza and ammonia-oxidizing prokaryotes. Ecology 101, e02963. doi:https://doi.org/10.1002/ecy.2963

Templer, P.H., Silver, W.L., Pett-Ridge, J., DeAngelis, K.M., Firestone, M.K., 2008. Plant and microbial controls on nitrogen retention and loss in a humid tropical forest. Ecology 89, 3030–3040. doi:10.1890/07-1631.1

Veresoglou, S.D., Chen, B.D., Rillig, M.C., 2012. Arbuscular mycorrhiza and soil nitrogen cycling. Soil Biology & Biochemistry 46, 53–62. doi:10.1016/j.soilbio.2011.11.018

Wurzburger, N., Brookshire, E.N.J., 2017. Experimental evidence that mycorrhizal nitrogen strategies affect soil carbon. Ecology 98, 1491–1497. doi:https://doi.org/10.1002/ecy.1827

Wurzburger, N., Hendrick, R.L., 2009. Plant litter chemistry and mycorrhizal roots promote a nitrogen feedback in a temperate forest. Journal of Ecology 97, 528–536. doi:10.1111/j.1365-2745.2009.01487.x

Xiao, R., Qiu, Y., Tao, J., Zhang, X., Chen, H., Reberg-Horton, S.C., Shi, W., Shew, H.D., Zhang, Y., Hu, S., 2020. Biological controls over the abundances of terrestrial ammonia oxidizers. Global Ecology and Biogeography 29, 384–399. doi:https://doi.org/10.1111/geb.13030

Yin, H., Wheeler, E., Phillips, R.P., 2014. Root-induced changes in nutrient cycling in forests depend on exudation rates. Soil Biology and Biochemistry 78, 213–221. doi:https://doi.org/10.1016/j.soilbio.2014.07.022

Yin, L., Dijkstra, F.A., Phillips, R.P., Zhu, B., Wang, P., Cheng, W., 2021. Arbuscular mycorrhizal trees cause a higher carbon to nitrogen ratio of soil organic matter decomposition via rhizosphere priming than ectomycorrhizal trees. Soil Biology and Biochemistry 157, 108246. doi:https://doi.org/10.1016/j.soilbio.2021.108246

Zak, D.R., Pellitier, P.T., Argiroff, W.A., Castillo, B., James, T.Y., Nave, L.E., Averill, C., Beidler, K. V., Bhatnagar, J., Blesh, J., Classen, A.T., Craig, M., Fernandez, C.W., Gundersen, P., Johansen, R., Koide, R.T., Lilleskov, E.A., Lindahl, B.D., Nadelhoffer, K.J., Phillips, R.P., Tunlid, A., 2019. Exploring the role of ectomycorrhizal fungi in soil carbon dynamics. New Phytologist 223, 33–39. doi:10.1111/nph.15679

Zhu, K., McCormack, M.L., Lankau, R.A., Egan, J.F., Wurzburger, N., 2018. Association of ectomycorrhizal trees with high carbon-to-nitrogen ratio soils across temperate forests is

driven by smaller nitrogen not larger carbon stocks. Journal of Ecology 106, 524–535. doi:10.1111/1365-2745.12918

# CHAPTER 6

# CONCLUSION

For my doctoral dissertation, I explored the mechanisms driving formation of distinct biogeochemical syndromes mediated by tree-mycorrhizal associations. My research revealed the central role of environmental and geologic context in determining the mechanisms driving ectomycorrhizal (ECM) effects at spatial scales from individual trees to forest stands to watersheds.

For my second chapter, I used spatially explicit and non-spatially explicit modelling techniques to determine the effects of ECM-associated *Oreomunnea mexicana* on soil organic matter (SOM) dynamics within tree neighborhoods in mixed ECM-arbuscular mycorrhizal (AM) forest stands, along mycorrhizal gradients, and among watersheds varying in soil parent material. I found that ECM effects mostly manifested at the stand scale rather than at the scale of an individual tree neighborhood. The magnitude and direction of ECM effects along mycorrhizal gradients varied among watersheds that differed in underlying soil pH and fertility. Therefore, while ECM effects on SOM properties scale with ECM dominance within a forest stand, the strength and direction of these effects depend on soil pH and fertility.

For my third chapter, I measured fungal communities beneath *O. mexicana* focal trees to investigate fungal community composition as a potential driver of variation in ECM effects on SOM accumulation and N cycling. I sampled in mixed ECM-AM forest and in ECM-dominated stands across four watersheds previously shown to exhibit distinct ECM effects on soil organic matter properties. In the lowest soil pH and fertility watershed, overall fungal communities and ECM:saprotrophic (SAP) ratios differed significantly between mixed ECM-AM stands and ECM-dominated stands. However, in the highest pH and fertility watershed, overall fungal

communities and ECM:SAP ratios were similar between stand types despite apparent ECM effects on soil properties. This suggests that fungal community composition and function may partially drive ECM effects in lower pH and fertility watersheds, whereas in higher pH and fertility watersheds ECM effects on soil chemical properties may be driven by other aspects of the tree-mycorrhizal symbiosis such as conservative nutrient use traits that are characteristic of ECM trees. Overall, my results suggest that the mechanisms driving ECM effects on SOM accumulation and N cycling can vary based on geological context.

For my fourth chapter, I aimed to disentangle the often-confounded effects of leaf litter quality and stand mycorrhizal type on leaf litter decomposition rates. In a high rainfall tropical montane forest, I found that only one litter species with intermediate chemical quality decomposed significantly faster in AM- compared to ECM-dominated stands. High rainfall at my study site may increase the importance of leaching as a mass loss pathway, driving similar decomposition rates between stand types because leaching is not affected by distinct decomposer communities that establish in ECM- vs AM-dominated stands. Therefore, I conclude that litter chemical quality and environmental conditions mediate the manifestation of slower decomposition in ECM stands such that leaf litter decomposition rates cannot be predicted directly from litter mycorrhizal type or stand mycorrhizal type.

For my fifth chapter, I aimed to clarify the role of mineralization in driving closed nitrogen (N) cycling in ECM-dominated stands. I quantified gross rates of the individual N cycling processes contributing to slower net N cycling rates and smaller inorganic N pools that commonly characterize ECM stands in temperate forests. I showed that gross mineralization rates were greater in ECM stands despite net mineralization rates and downstream N transformations being greater in AM stands. This demonstrates that suppressed N mineralization

in ECM stands may not be necessary to form the closed N cycle of ECM stands, challenging the current paradigm of an organic nutrient economy occurring in ECM stands versus an inorganic nutrient economy in AM stands.

Overall, my work emphasizes the importance of integrating environmental and geological context into our understanding of mycorrhizal mediated C and N cycling. I conclude that the mechanisms driving mycorrhizal effects can vary across ecosystems, informing efforts to predict mycorrhizal effects at the global scale.

# APPENDIX A

# SUPPLEMENTARY MATERIAL FOR CHAPTER 2

**Section A.1.** To account for the contribution of roots <1.5 cm diameter to the measured bulk density, we quantified bulk density with and without roots <1.5 cm diameter in a subset of 16 O horizon samples. We regressed bulk density with roots removed against bulk density with roots included ($R^2 = 0.98$) and used the resulting linear regression equation to estimate root-free bulk density in the remaining O horizon samples. To account for heterogeneity in O horizon depth, we took depth measurements on the four sides of the 0.25 m × 0.25 m O horizon sample and averaged the four values to calculate O horizon volume. Soil bulk density was not estimated for the deep mineral soil samples because sample volume could not be quantified with the soil probe used for sampling. Instead, for the mineral soils to 20 cm depth, we assumed bulk density based on the shallow mineral soil sampling effort along mycorrhizal gradients in which a quantitative soil corer was used. For soils below 20 cm depth, bulk density was estimated using the compliant cavity method (Grossman and Reinsch, 2002) in a single 2 m deep soil pit in each watershed (Turner and Dalling 2021).

## Tables and Figures

**Table A.1.** Mean annual precipitation and mean monthly dry season rainfall for four watersheds in Fortuna (Prada et al., 2017)**.**

| Watershed | Honda | Zorro | Hornito | Alto Frio |
|---|---|---|---|---|
| Mean annual precipitation (mm) | 6159 ± 617 | 4964 ± 863 | 5164 ± 232 | 4641 ± 623 |
| Mean monthly dry season rainfall (mm) | 332 ± 34 | 159 ± 27 | 203 ± 28 | 94 ± 27 |

(Mean ± SE, n=7 for Honda and Hornito, n=2 for Alto Frio and Zorro)

**Table A.2.** Base cation concentrations for ECM- and AM-dominated stands within four watersheds in Fortuna (Mean ± SE, n =3).

| | | Honda: lower fertility | | Zorro: lower fertility | | Hornito: higher fertility | | Alto Frio: higher fertility | |
|---|---|---|---|---|---|---|---|---|---|
| | Depth (cm) | ECM-dominated stand | AM-dominated stand | ECM-dominated stand | AM-dominated stand | ECM-dominated stand | AM-dominated stand | ECM-dominated stand | AM-dominated stand |
| Al (cmol (+) $kg^{-1}$) | 0-20 | 5.44 ± 1.39 | 6.57± 1.18 | 2.84 ±0.04 | 3.36 ± 0.73 | 5.66 ± 0.73 | 0.62 ± 0.50 | 2.16 ± 0.33 | 0.05 ± 0.04 |
| | 20-40 | 1.65 ± 0.14 | 3.72 ± 0.42 | 0.99 ± 0.41 | 1.49 ± 0.33 | 4.52 ± 0.31 | | 2.59 ± 0.53 | 0.01 ± 0.06 |
| Fe (cmol (+) $kg^{-1}$) | 0-20 | 0.13 ± 0.05 | 0.31 ± 0.07 | 0.10 ± 0.02 | 0.18 ± 0.05 | 0.24 ± 0.20 | 0.03 ± 0.05 | 0.08 ± 0.02 | 0.03 ± 0.03 |
| | 20-40 | 0.05 ± 0.03 | 006 ± 0.02 | 0.04 ± 0.01 | 0.11 ± 0.04 | 0.05 ± 0.01 | | 0.04 ± 0.04 | n.d. |
| Ca (cmol (+) $kg^{-1}$) | 0-20 | 0.68 ± 0.02 | 1.39 ± 0.22 | 0.083 ± 0.03 | 0.95 ± 0.20 | 0.88 ± 0.13 | 8.09 ± 1.92 | 2.19 ± 0.80 | 8.83 ± 1.41 |
| | 20-40 | 0.68 ±0.07 | 0.65 ± 0.05 | 0.77 ± 0.08 | 0.73 ± 0.04 | 0.63 ± 0.04 | | 0.98 ± 0.33 | 3.87 ± 0.69 |
| K (cmol (+) $kg^{-1}$) | 0-20 | 0.15 ± 0.05 | 0.34 ± 0.05 | 0.19 ± 0.002 | 0.21 ± 0.02 | 0.20 ± 0.02 | 0.37 ± 0.16 | 0.10 ± 0.04 | 0.16 ± 0.01 |
| | 20-40 | 0.28 ± 0.11 | 0.19 ± 0.05 | 0.12 ± 0.03 | 0.10 ± 0.01 | 0.09 ± 0.01 | | 0.05 ± 0.02 | 0.11 ± 0.02 |
| Mg (cmol (+) $kg^{-1}$) | 0-20 | 0.16 ± 0.02 | 0.52 ± 0.06 | 0.24 ± 0.02 | 0.40 ± 0.07 | 0.32 ± 0.05 | 2.43 ± 0.78 | 0.92 ± 0.33 | 2.63 ± 0.37 |
| | 20-40 | 0.22 ± 0.05 | 0.23 ± 0.03 | 0.19 ± 0.01 | 0.24 ± 0.04 | 0.21 ± 0.03 | | 0.32 ± 0.04 | 1.62 ± 0.40 |
| Mn (cmol (+) $kg^{-1}$) | 0-20 | 0.00 ± 0.00 | 0.02 ±0.01 | 0.00 ± 0.00 | 0.01 ± 0.001 | 0.02 ± 0.00 | 0.85 ± 0.24 | 0.06 ± 0.02 | 0.45 ± 0.04 |
| | 20-40 | 0.00 ± 0.01 | 0.00 ± 0.01 | 0.00 ± 0.001 | 0.00 ± 0.00 | 0.01 ± 0.00 | | 0.03 ± 0.01 | 0.38 ± 0.06 |
| Na (cmol (+) $kg^{-1}$) | 0-20 | 0.63 ± 0.23 | 0.70 ± 0.10 | 0.44 ± 0.15 | 0.27 ± 0.09 | 0.29 ± 0.10 | 0.08 ± 0.05 | 0.19 ± 0.06 | 0.13 ± 0.01 |
| | 20-40 | 0.88 ± 0.32 | 0.33 ± 0.08 | 0.64 ± 0.13 | 0.19 ± 0.02 | 0.17 ± 0.02 | | 0.47 ± 0.19 | 0.24 ± 0.16 |

n.d. = not detectable

**Table A.3.** Alternative models used to describe spatial variability in forest floor leaf litter and soil properties along mycorrhizal gradients in four watersheds within Fortuna.

| Function | Equation | Site-specific parameters |
|---|---|---|
| Mean model | $Y = a$ | |
| Site-means model | $Y = a_s$ | Site-specific mean |
| Linear | $Y = a_s + b * X$ | |
| | $Y = a_s + b * X$ | Site-specific intercept |
| | $Y = a + b_s * X$ | Site-specific slope |
| | $Y = a_s + b_s * X$ | Site-specific intercept and slope |
| Logistic | $Y = a + \frac{d}{1 + {X}/{c}^{b}}$ | |
| | $Y = a_s + \frac{d}{1 + {X}/{c}^{b}}$ | Site-specific intercept |
| | $Y = a + \frac{d}{1 + {X}/{c}^{b_s}}$ | Site-specific b parameter |
| Michaelis-Menton | $Y = a + \frac{b * X}{X + \frac{b}{c}}$ | |
| | $Y = a_s + \frac{b * X}{X + \frac{b}{c}}$ | Site-specific slope |
| | $Y = a_s + \frac{b_s * X}{X + \frac{b_s}{c}}$ | Site-specific slope b parameter |
| | $Y = a + \frac{b * X}{X + \frac{b}{c_s}}$ | Site-specific slope c parameter |
| Inverted Weibull | $Y = a + b * (1 - e^{-c * X^d})$ | |
| | $Y = a_s + b * (1 - e^{-c * X^d})$ | Site-specific intercept |
| | $Y = a + b_s * (1 - e^{-c * X^d})$ | Site-specific b parameter |

**Table A.4.** Model output for the models the lowest $AIC_c$ scores for each of the dependent variables we measured and for models within 2 $AIC_c$ units of the best model.

| Layer | Dependent variable | Independent variable | Model | Site-specific parameters | Maximum likelihood | Number of parameters | $AIC_c$ | Slope | $R^2$ |
|---|---|---|---|---|---|---|---|---|---|
| Litter | C concentration | ECM dominance | Linear | Intercept | -172.32 | 6 | 358.11 | 1.00 | 0.40 |
| | TN concentration | ECM dominance | Mean | None | -136.08 | 2 | 276.36 | 63.94 | NA |
| | | ECM dominance | Linear | None | -135.62 | 3 | 277.65 | 1.00 | 0.01 |
| | | Neighborhood | Linear | None | -134.49 | 3 | 277.66 | 1.00 | 0.05 |
| | C:N | ECM dominance | Linear | None | -161.87 | 3 | 330.15 | 1.00 | 0.26 |
| | | Neighborhood | Linear | None | -161.00 | 3 | 330.67 | 1.00 | 0.28 |
| | | ECM dominance | Linear | Intercept | -158.66 | 6 | 330.79 | 1.00 | 0.33 |
| | $\delta^{13}C_{litter}$ | ECM dominance | Logistic | Intercept | -32.65 | 8 | 83.91 | 1.00 | 0.20 |
| | | ECM dominance | Logistic | None | -36.90 | 5 | 84.83 | 1.00 | 0.09 |
| | $\delta^{15}N_{litter}$ | ECM dominance | Linear | Slope | -187.17 | 6 | 387.82 | 1.01 | 0.74 |
| | | ECM dominance | Inverted Weibull | Slope | -184.65 | 8 | 387.93 | 1.00 | 0.76 |
| | | ECM dominance | Michaelis-Menton | Slope | -186.15 | 7 | 388.30 | 1.03 | 0.75 |
| O horizon | pH | ECM dominance | Michaelis-Menton | Intercept, slope | -11.54 | 10 | 47.32 | 1.00 | 0.85 |
| | O horizon depth | Neighborhood | Linear | Slope | -147.68 | 7 | 311.39 | 0.99 | 0.65 |
| | SOC stock | ECM dominance | Logistic | Slope | -101.68 | 8 | 222.03 | 1.01 | 0.60 |
| | TN stock | ECM dominance | Logistic | Slope | -60.11 | 8 | 138.89 | 1.00 | 0.62 |
| | C:N | ECM dominance | Linear | Slope | -148.33 | 6 | 310.15 | 0.99 | 0.17 |
| | | ECM dominance | Logistic | Slope | -145.77 | 8 | 310.20 | 1.00 | 0.23 |
| | | ECM dominance | Site-means | Intercept | -149.65 | 5 | 310.35 | 1.00 | 0.13 |
| | C concentration | Neighborhood | Linear | Intercept | -199.05 | 7 | 414.13 | 1.00 | 0.69 |

**Table A.4. (cont.)**

| | | | | | | | | | |
|---|---|---|---|---|---|---|---|---|---|
| | TN concentration | ECM dominance | Linear | Intercept | -27.28 | 6 | 68.06 | 1.00 | 0.61 |
| | | ECM dominance | Linear | Intercept, slope | -23.37 | 9 | 68.13 | 1.02 | 0.66 |
| | | ECM dominance | Linear | Slope | -27.98 | 6 | 69.47 | 0.99 | 0.60 |
| Cumulative mineral soil | SOC stock | ECM dominance | Linear | Intercept, slope | -144.21 | 6 | 301.95 | 1.00 | 0.23 |
| | TN stock | ECM dominance | Linear | Intercept | -109.41 | 6 | 232.35 | 0.99 | 0.34 |
| | C:N | ECM dominance | Linear | Intercept, slope | -101.23 | 9 | 223.93 | 1.01 | 0.52 |
| Mineral (0-10 cm) | pH | ECM dominance | Linear | Intercept, slope | -0.76 | 9 | 22.85 | 1.00 | 0.80 |
| | | ECM dominance | Inverted Weibull | Intercept, slope | 1.57 | 11 | 23.95 | 1.00 | 0.81 |
| | C concentration | ECM dominance | Linear | Intercept | -140.03 | 6 | 293.58 | 1.01 | 0.28 |
| | | ECM dominance | Linear | Intercept, slope | -136.82 | 9 | 295.09 | 1.01 | 0.36 |
| | | ECM dominance | Inverted Weibull | Intercept | -137.67 | 8 | 294.07 | 1.00 | 0.33 |
| | TN concentration | ECM dominance | Inverted Weibull | Intercept | -104.06 | 8 | 226.84 | 1.01 | 0.45 |
| | C:N | ECM dominance | Linear | Intercept, slope | -104.40 | 9 | 230.25 | 1.00 | 0.45 |
| | | ECM dominance | Michaelis-Menton | None | -111.20 | 4 | 231.11 | 1.00 | 0.31 |
| | | ECM dominance | Linear | Intercept | -108.91 | 6 | 231.34 | 1.00 | 0.36 |
| | | ECM dominance | Inverted Weibull | Intercept | -106.70 | 8 | 232.13 | 1.00 | 0.40 |
| | SOC stock | ECM dominance | Linear | Intercept | -101.08 | 6 | 215.69 | 1.00 | 0.27 |
| | | ECM dominance | Inverted weibull | Intercept | -98.67 | 8 | 216.06 | 1.01 | 0.33 |
| | | ECM dominance | Linear | Intercept, slope | -97.83 | 9 | 217.13 | 0.99 | 0.35 |
| | TN stock | ECM dominance | Linear | Intercept | -69.16 | 6 | 151.84 | 1.01 | 0.36 |
| | | ECM dominance | Inverted Weibull | Intercept | -65.61 | 8 | 149.93 | 1.00 | 0.43 |
| | | ECM dominance | Linear | Intercept, slope | -65.72 | 9 | 152.90 | 0.99 | 0.44 |

**Table A.4. (cont.)**

| | | | | | | | | | |
|---|---|---|---|---|---|---|---|---|---|
| Mineral | | | | | | | | | |
| (10-20 cm) | pH | ECM dominance | Linear | Intercept, slope | 8.53 | 9 | 4.28 | 1.00 | 0.74 |
| | SOC stock | ECM dominance | Mean | None | -122.87 | 2 | 249.95 | 61.87 | 0.00 |
| | | ECM dominance | Site-means | Intercept | -119.38 | 5 | 249.83 | 1.00 | 0.11 |
| | | ECM dominance | Linear | Intercept | -118.49 | 6 | 250.50 | 0.99 | 0.13 |
| | TN stock | ECM dominance | Linear | Intercept | -82.10 | 6 | 177.73 | 1.00 | 0.22 |
| | | ECM dominance | Linear | None | -86.49 | 3 | 179.40 | 1.00 | 0.10 |
| | C:N | ECM dominance | Michaelis-Menton | None | -108.84 | 7 | 233.76 | 1.00 | 0.46 |
| | C concentration | ECM dominance | Site-means | Intercept | -127.22 | 5 | 265.51 | 1.00 | 0.11 |
| | | ECM dominance | Mean | None | -130.86 | 2 | 265.93 | 62.04 | 0.00 |
| | | ECM dominance | Linear | None | -126.34 | 6 | 266.21 | 0.99 | 0.14 |
| | TN concentration | ECM dominance | Linear | Intercept | -89.59 | 6 | 192.71 | 1.00 | 0.25 |
| Cumulative | | | | | | | | | |
| MOAM | SOC stock | ECM dominance | Linear | Intercept | -157.18 | 6 | 327.87 | 1.01 | 0.46 |
| | TN stock | ECM dominance | Linear | Intercept | -132.18 | 6 | 277.85 | 0.99 | 0.52 |
| | C:N | ECM dominance | Linear | Intercept, slope | -86.27 | 9 | 193.94 | 1.00 | 0.65 |
| MAOM | | | | | | | | | |
| (0-10 cm) | SOC stock | ECM dominance | Linear | Intercept | -106.15 | 6 | 225.81 | 1.00 | 0.51 |
| | | ECM dominance | Linear | Intercept, slope | -102.35 | 9 | 226.10 | 0.99 | 0.57 |
| | | Neighborhood | Linear | Intercept | -105.54 | 6 | 227.11 | 1.00 | 0.52 |
| | TN stock | ECM dominance | Linear | Intercept | -84.82 | 6 | 183.14 | 1.01 | 0.55 |
| | | ECM dominance | Linear | Intercept, slope | -81.10 | 9 | 183.60 | 1.01 | 0.60 |
| | C:N | ECM dominance | Linear | Intercept, slope | -83.55 | 9 | 188.50 | 1.00 | 0.63 |

**Table A.4. (cont.)**

| | | | | | | | | | |
|---|---|---|---|---|---|---|---|---|---|
| | C concentration | ECM dominance | Linear | Intercept, slope | -142.73 | 9 | 306.86 | 1.00 | 0.61 |
| | | ECM dominance | Linear | Intercept | -146.80 | 6 | 307.10 | 1.00 | 0.55 |
| | | Neighborhood | Linear | Intercept | -146.04 | 6 | 308.11 | 0.99 | 0.57 |
| | TN concentration | ECM dominance | Linear | Intercept | -125.19 | 6 | 263.89 | 1.00 | 0.60 |
| | | ECM dominance | Linear | Intercept, slope | -121.82 | 9 | 265.04 | 1.02 | 0.64 |
| | $\delta^{13}C_{MAOM\text{-}litter}$ | ECM dominance | Site-means | Intercept | -59.71 | 5 | 130.45 | 1.00 | 0.19 |
| | | ECM dominance | Linear | Intercept | -58.66 | 6 | 130.79 | 1.01 | 0.21 |
| | | ECM dominance | Linear | Slope | -59.19 | 6 | 131.86 | 0.99 | 0.20 |
| | | ECM dominance | Inverted Weibull | Intercept | -56.69 | 8 | 132.01 | 1.00 | 0.26 |
| | | Neighborhood | Linear | Intercept | -58.11 | 6 | 132.21 | 1.00 | 0.23 |
| | | ECM dominance | Inverted Weibull | Slope | -57.03 | 8 | 132.69 | 1.02 | 0.27 |
| | $\delta^{15}N_{MAOM\text{-}litter}$ | ECM dominance | Inverted Weibull | Slope | -64.69 | 8 | 148.00 | 0.99 | 0.75 |
| MAOM | | | | | | | | | |
| (10-20 cm) | SOC stock | ECM dominance | Linear | Intercept | -129.90 | 6 | 273.30 | 1.00 | 0.36 |
| | | ECM dominance | Site-means | Intercept | -131.63 | 5 | 274.32 | 1.01 | 0.33 |
| | TN stock | ECM dominance | Linear | Intercept | -103.95 | 6 | 221.40 | 1.01 | 0.42 |
| | | ECM dominance | Michaelis-Menton | Intercept | -103.36 | 7 | 222.76 | 1.00 | 0.43 |
| | C:N | ECM dominance | Michaelis-Menton | Intercept | -106.22 | 7 | 228.49 | 1.00 | 0.50 |
| | | ECM dominance | Inverted Weibull | Intercept | -105.48 | 8 | 229.62 | 1.00 | 0.51 |
| | C concentration | ECM dominance | Linear | Intercept | -139.23 | 6 | 291.95 | 1.00 | 0.40 |
| | | ECM dominance | Site-means | Intercept | -141.26 | 5 | 293.57 | 0.99 | 0.36 |
| | TN concentration | ECM dominance | Linear | Intercept | -113.92 | 6 | 241.33 | 1.01 | 0.46 |
| | $\delta^{13}C_{MAOM\text{-}litter}$ | ECM dominance | Site-means | Intercept | -54.92 | 5 | 120.88 | 0.99 | 0.18 |

**Table A.4. (cont.)**

| | | | | | | | | | |
|---|---|---|---|---|---|---|---|---|---|
| | $\delta^{15}N_{MAOM\text{-}litter}$ | ECM dominance | Linear | Intercept, slope | -59.41 | 9 | 140.16 | 0.99 | 0.66 |
| | | ECM dominance | Linear | Slope | -63.52 | 6 | 140.51 | 1.00 | 0.61 |
| Cumulative | | | | | | | | | |
| POM | SOC stock | ECM dominance | Linear | Slope | -165.00 | 6 | 343.50 | 1.00 | 0.49 |
| | TN stock | ECM dominance | Linear | Intercept, slope | -105.54 | 9 | 232.48 | 0.99 | 0.44 |
| | C:N | ECM dominance | Linear | Intercept, slope | -149.79 | 9 | 320.97 | 1.01 | 0.61 |
| | | ECM dominance | Linear | Slope | -154.20 | 6 | 321.90 | 1.01 | 0.55 |
| | | ECM dominance | Inverted Weibull | Intercept | -151.92 | 8 | 322.51 | 1.00 | 0.58 |
| POM | | | | | | | | | |
| (0-10 cm) | SOC stock | ECM dominance | Linear | Slope | -124.64 | 6 | 262.78 | 1.03 | 0.40 |
| | | ECM dominance | Inverted Weibull | Slope | -122.49 | 8 | 263.64 | 1.00 | 0.44 |
| | TN stock | ECM dominance | Linear | Intercept, slope | -64.00 | 9 | 149.40 | 1.02 | 0.39 |
| | | ECM dominance | Inverted Weibull | Intercept, slope | -62.06 | 11 | 151.30 | 0.98 | 0.43 |
| | C:N | ECM dominance | Site-means | Intercept | -158.27 | 5 | 327.60 | 1.00 | 0.48 |
| | | ECM dominance | Site-means | site-means | -158.27 | 5 | 327.60 | 1.00 | 0.48 |
| | | ECM dominance | Michaelis-Menton | Intercept | -155.68 | 7 | 327.39 | 1.01 | 0.52 |
| | C concentration | ECM dominance | Linear | Slope | -169.92 | 6 | 353.34 | 1.00 | 0.47 |
| | TN concentration | ECM dominance | Linear | Intercept, slope | -110.00 | 9 | 241.40 | 0.99 | 0.44 |
| | $\delta^{13}C_{POM\text{-}litter}$ | ECM dominance | Site-means | Intercept | -70.07 | 5 | 151.18 | 1.01 | 0.38 |
| | | ECM dominance | Linear | Intercept | -69.73 | 6 | 152.96 | 1.00 | 0.39 |
| | $\delta^{15}N_{POM\text{-}litter}$ | ECM dominance | Inverted Weibull | Slope | -64.69 | 8 | 148.00 | 0.99 | 0.75 |
| POM | | | | | | | | | |
| (10-20 cm) | SOC stock | ECM dominance | Linear | Slope | -130.12 | 6 | 273.75 | 0.99 | 0.48 |
| | TN stock | ECM dominance | Site-means | Intercept | -88.65 | 5 | 188.35 | 1.02 | 0.19 |

**Table A.4. (cont.)**

| | | | | | | | | | |
|---|---|---|---|---|---|---|---|---|---|
| | | ECM dominance | Linear | Slope | -87.50 | 6 | 188.51 | 1.00 | 0.22 |
| | C:N | ECM dominance | Michaelis-Menton | Intercept | -176.78 | 7 | 369.59 | 1.00 | 0.42 |
| | | ECM dominance | Linear | Slope | -178.12 | 6 | 369.74 | 1.00 | 0.40 |
| | | ECM dominance | Linear | Intercept | -178.29 | 6 | 370.08 | 1.00 | 0.39 |
| | | ECM dominance | Inverted Weibull | Intercept | -176.05 | 8 | 370.77 | 1.00 | 0.43 |
| | | ECM dominance | Linear | Intercept, slope | -174.79 | 9 | 370.97 | 1.01 | 0.45 |
| | C concentration | ECM dominance | Linear | Slope | -144.46 | 6 | 302.42 | 1.00 | 0.51 |
| | TN concentration | ECM dominance | Linear | Slope | -99.49 | 6 | 212.48 | 1.01 | 0.26 |
| | | ECM dominance | Site-means | Intercept | -101.37 | 5 | 213.80 | 1.03 | 0.21 |
| | $\delta^{13}C_{POM\text{-}litter}$ | ECM dominance | Site-means | Intercept | -82.47 | 5 | 176.00 | 0.98 | 0.35 |
| | | ECM dominance | Linear | Intercept | -81.85 | 6 | 177.21 | 1.00 | 0.36 |
| | $\delta^{15}N_{POM\text{-}litter}$ | ECM dominance | Linear | Intercept | -79.58 | 6 | 172.63 | 1.00 | 0.70 |
| | | ECM dominance | Linear | Intercept, slope | -76.11 | 9 | 173.56 | 1.00 | 0.73 |
| Mineral (0-10 cm) | $MAOM_{SOC}$:$POM_{SOC}$ | ECM dominance | Linear | Intercept, slope | -228.03 | 9 | 477.46 | 1.00 | 0.72 |
| | $MAOM_{TN}$:$POM_{TN}$ | ECM dominance | Linear | Intercept, slope | -218.65 | 9 | 458.70 | 1.00 | 0.65 |
| Mineral (10-20 cm) | $MAOM_{SOC}$:$POM_{SOC}$ | ECM dominance | Linear | Intercept, slope | -222.38 | 9 | 466.16 | 1.01 | 0.74 |
| | $MAOM_{TN}$:$POM_{TN}$ | ECM dominance | Linear | Intercept, slope | -212.13 | 9 | 445.66 | 0.99 | 0.65 |

**Figure A.1.** The relationship between ectomycorrhizal-associated *Oreomunnea mexicana* dominance and organic horizon properties as described by a spatially explicit neighborhood models for (a) soil organic carbon concentrations (N=63, $R^2$ = 0.69) and by non-spatial likelihood models for (b) total nitrogen concentrations (N=63, $R^2$ = 0.61), (c) soil organic carbon stocks (N=63, $R^2$ = 0.60), and (d) total nitrogen stocks (N=63, $R^2$ = 0.62). Colored lines indicate relationships for each of the following four watersheds when watershed-specific slope and/or intercept parameter estimates were significant in the model: Alto Frio (green), Honda (orange), Hornito (purple) and Zorro (pink). Shaded regions indicate 2-unit support intervals.

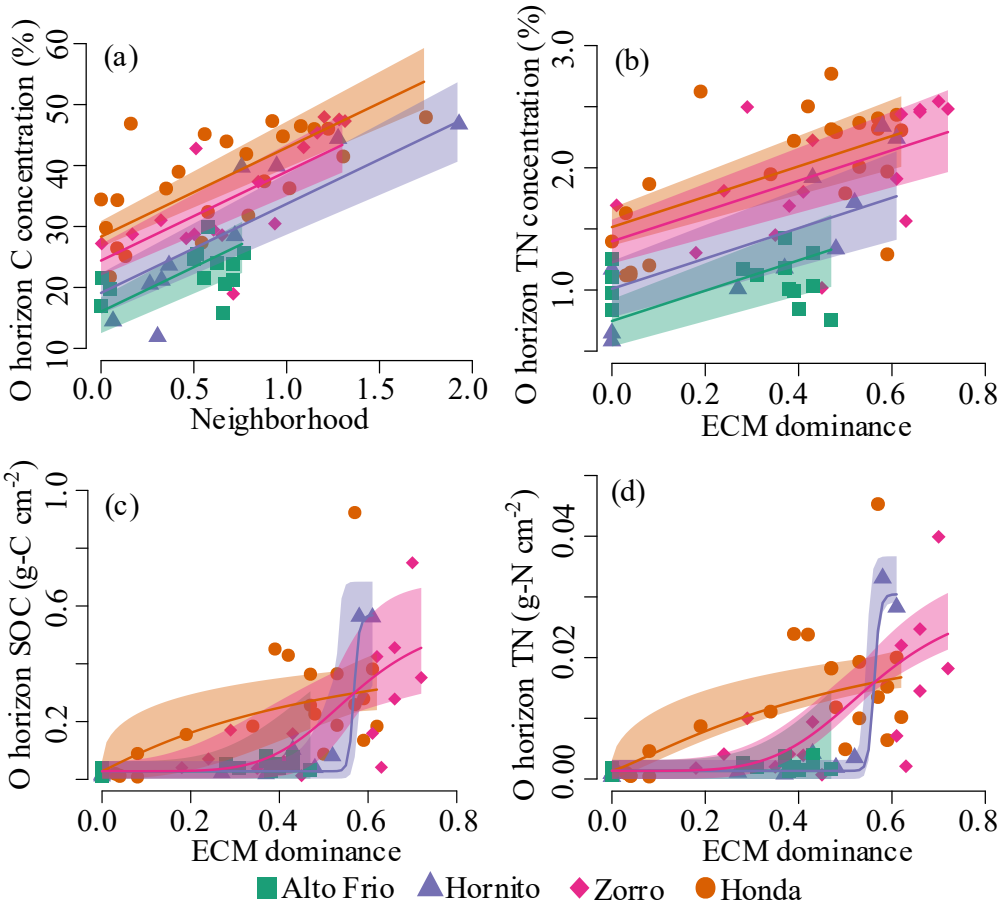

**Figure A.2.** Predicted decrease of the influence of an ECM-associated *Oreomunnea mexicana* individual with a DBH of 30 cm on organic horizon (a) depth and (b) carbon concentration as a function of the distance the *Oreomunnea mexicana* individual.

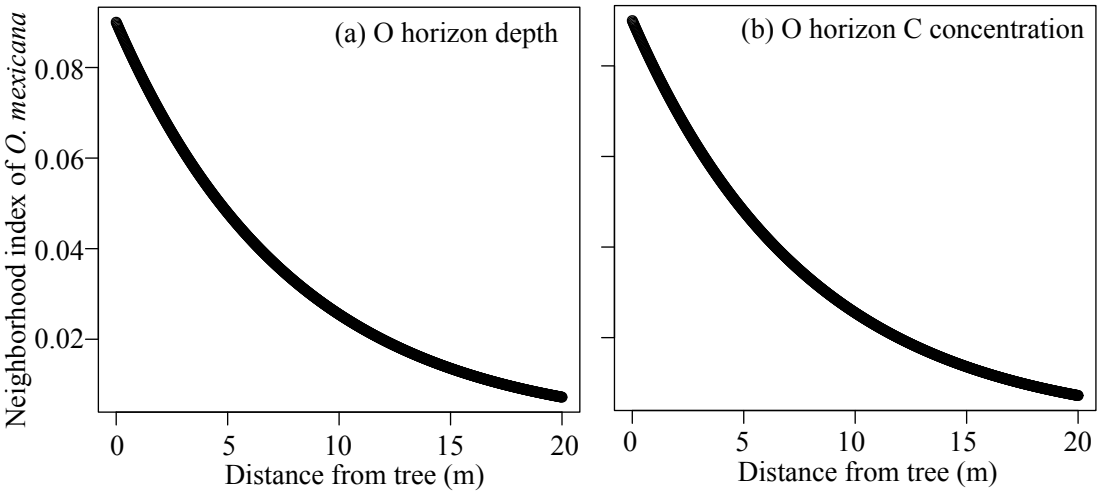

**Figure A.3.** The relationship between ectomycorrhizal-associated *Oreomunnea mexicana* dominance (percent basal area *O. mexicana*) and pH in the (a) O horizon (N=63, $R^2$ = 0.85) and (b) 10-20 cm depth mineral soil (N=64, $R^2$ = 0.74) as described by non-spatial likelihood models. Colored lines indicate relationships for each of the following four watersheds when watershed-specific slope and/or intercept parameter estimates were significant in the model: Alto Frio (green), Honda (orange), Hornito (purple) and Zorro (pink). Shaded regions indicate 2-unit support intervals.

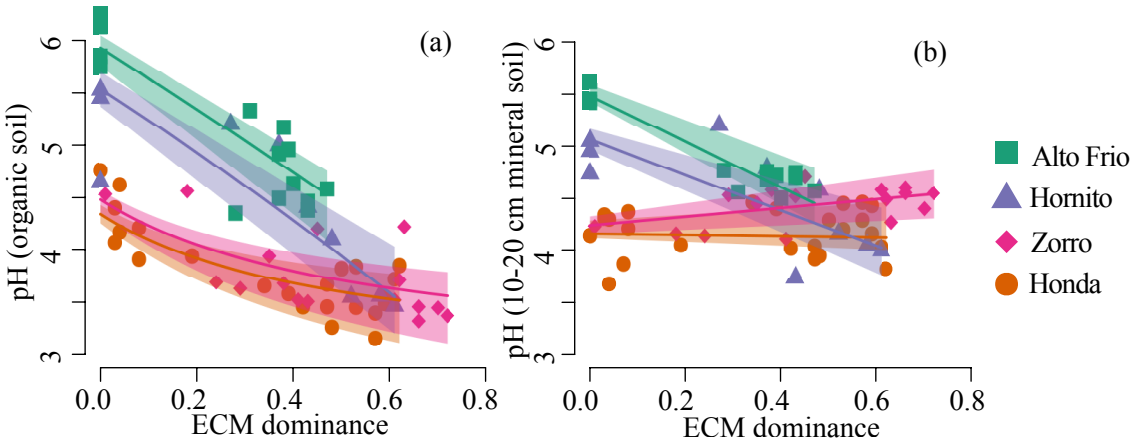

**Figure A.4.** The relationship between ectomycorrhizal-associated *Oreomunnea mexicana* dominance and 0-20 cm depth bulk mineral soil (a) organic carbon stocks (N=62, $R^2$ = 0.23) and (b) total nitrogen stocks (N=62, $R^2$ = 0.34), 0-20 cm depth mineral soil MAOM fraction (c) soil organic carbon stocks (N=63, $R^2$ = 0.23) and (d) total nitrogen stocks (N=63, $R^2$ = 0.34) and 0-20 cm depth mineral soil POM fraction (e) organic carbon stocks (N=63, $R^2$ = 0.49) and (f) total nitrogen stocks (N=63, $R^2$ = 0.44) as described by non-spatial likelihood models. Colored lines indicate relationships for each of the following four watersheds when watershed-specific slope and/or intercept parameter estimates were significant in the model: Alto Frio (green), Honda (orange), Hornito (purple) and Zorro (pink). Shaded regions indicate 2-unit support intervals.

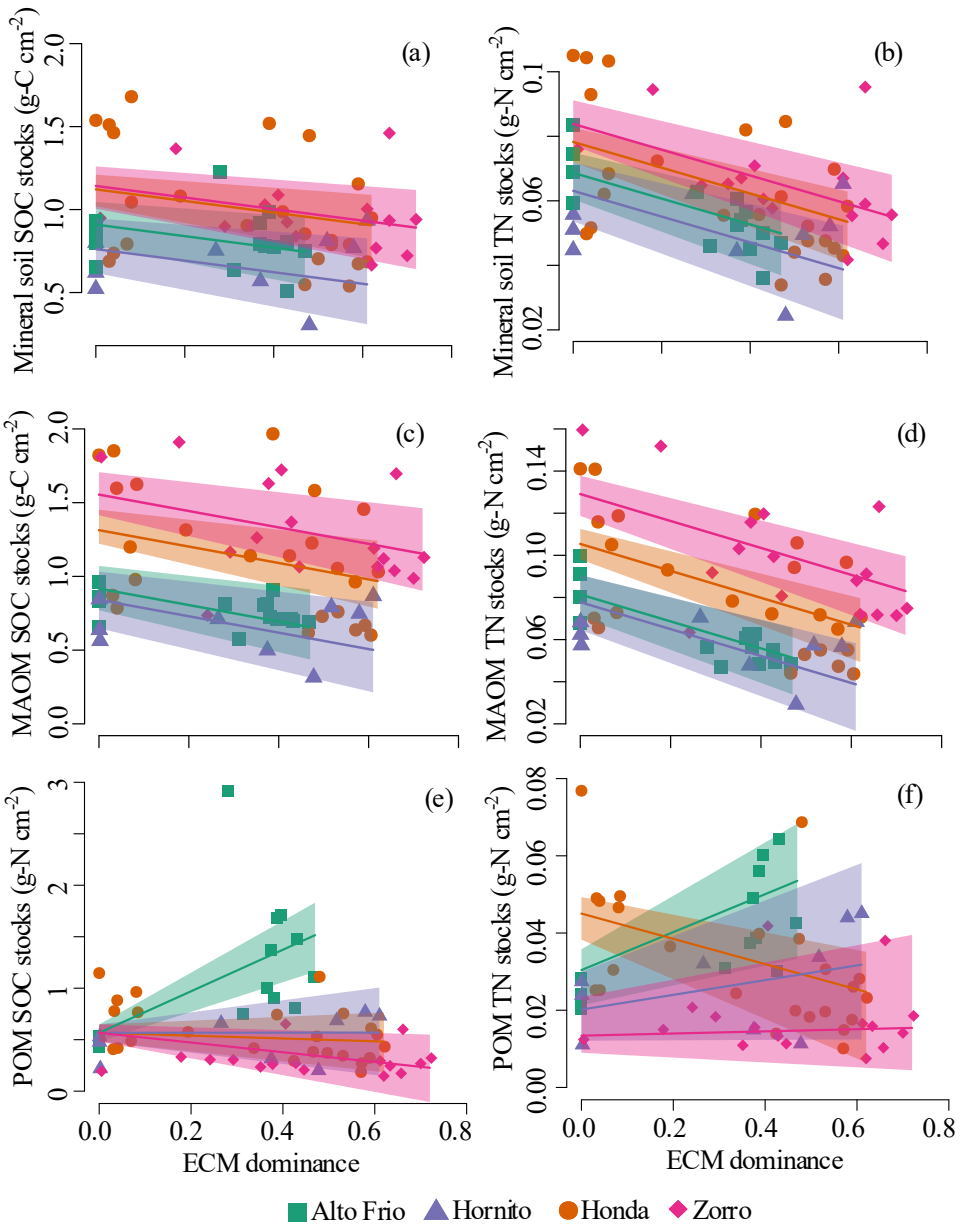

**Figure A.5.** The relationship between ectomycorrhizal-associated Oreomunnea mexicana dominance (percent basal area) and forest floor leaf litter properties as described by non-spatial likelihood models: (a) carbon concentration (%) (N=64, $R^2$= 0.40), (b) total nitrogen concentration (%) (N=64) and (c) $\delta^{13}C$ (N=64, $R^2$=0.20). Colored lines indicate relationships for each of the following four watersheds when watershed-specific slope and/or intercept parameter estimates were significant in the model: Alto Frio (green), Honda (orange), Hornito (purple) and Zorro (pink). A single black line represents the relationship for all watersheds together when the relationship did not vary among the four watersheds. Shaded regions indicate 2-unit support intervals.

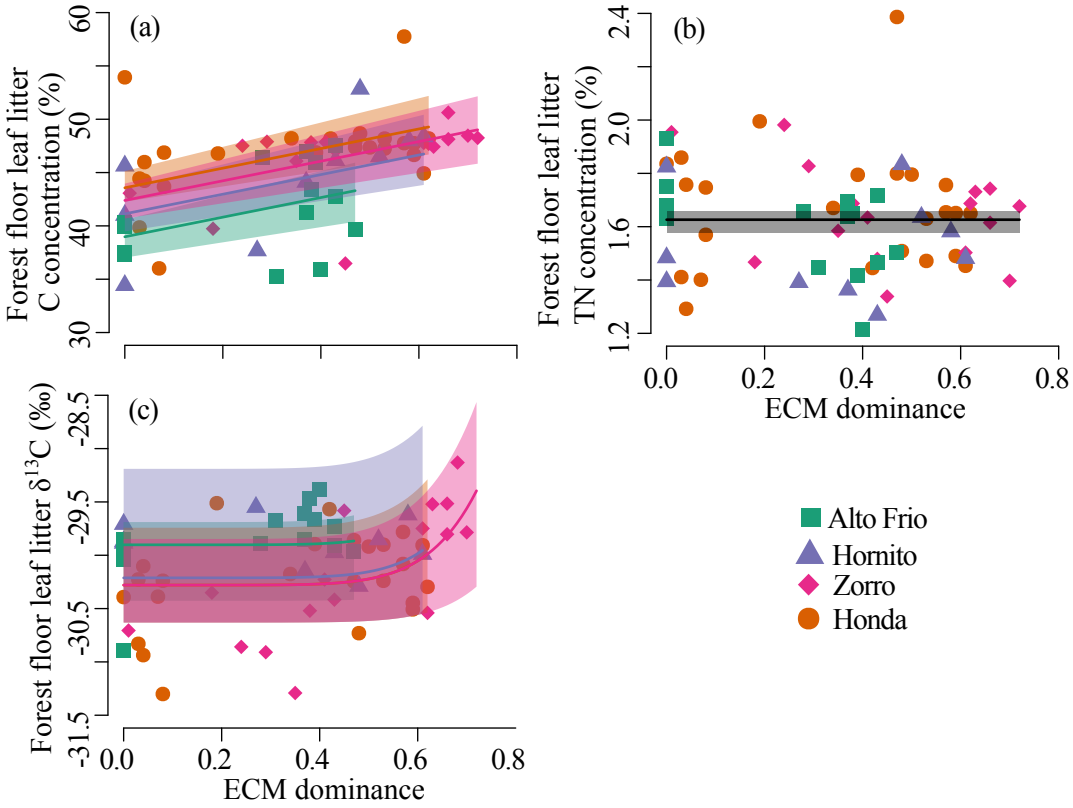

**Figure A.6.** Mineral soil properties versus reference soil mineral masses for soil samples taken in 20 cm increments to 1 m depth (N=3). The colors represent the four study watersheds: Alto Frio (green), Hornito (purple), Honda (orange), and Zorro (orange). Line type represents stand mycorrhizal association, with ectomycorrhizal-dominated stands as dotted lines and arbuscular mycorrhizal stands as solid lines. Stars indicate a statistically significant difference among the four watersheds, and triangles indicate a statistically significant difference between ectomycorrhizal and arbuscular mycorrhizal forest stands ($p < 0.05$).

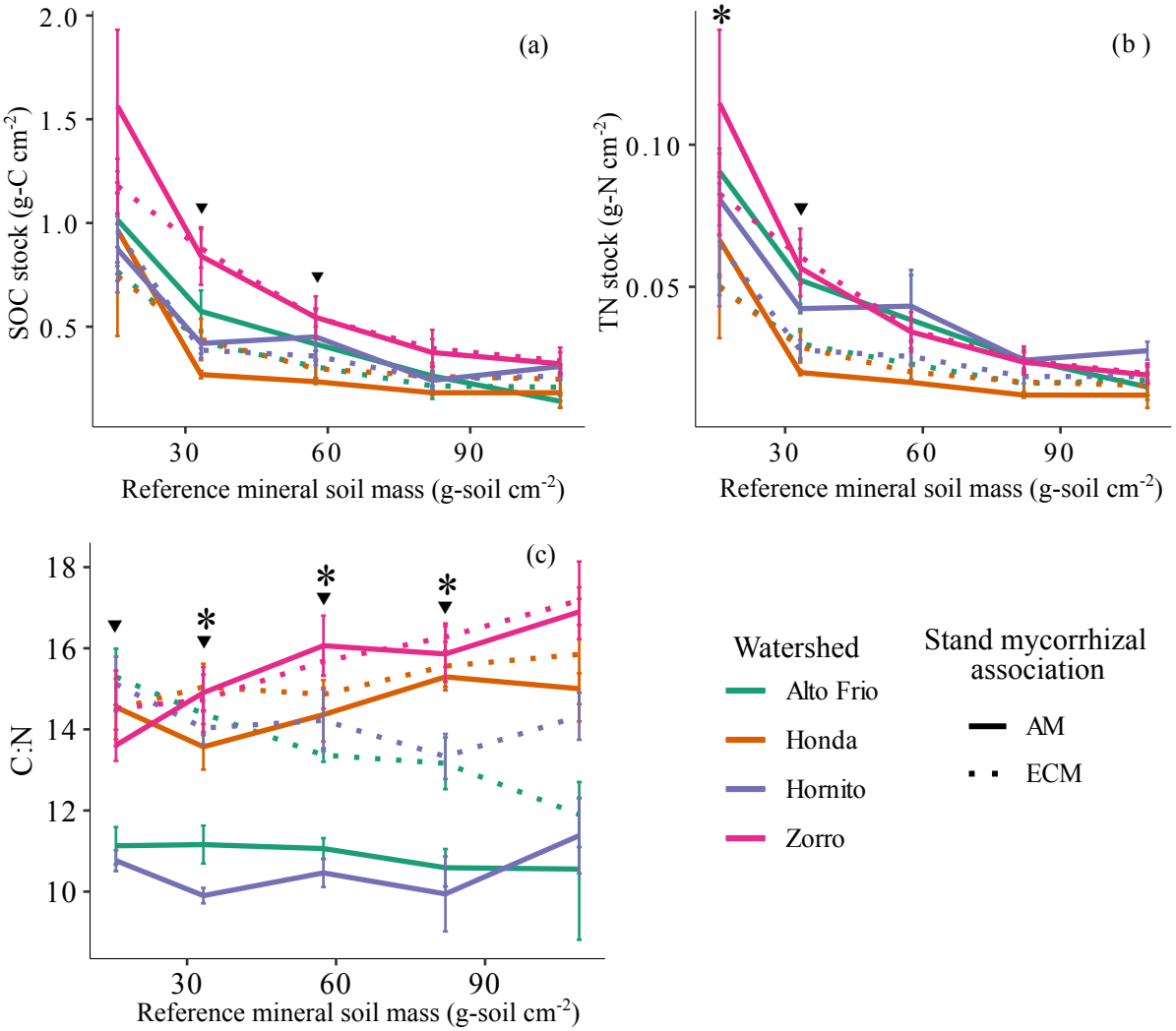

# APPENDIX B

# SUPPLEMENTARY MATERIAL FOR CHAPTER 3

## Tables

**Table B.1**. Chemical properties of forest floor leaf litter, organic horizon, 0-5 cm depth mineral soil, and 15-20 cm depth mineral soil beneath *O. mexicana* focal trees in mixed ECM-AM and ECM-dominated stands in four watersheds in the Fortuna Forest Reserve, Panama (Mean ± SE, n =3).

| | Alto Frio | | | | | |
|---|---|---|---|---|---|---|
| | Mixed ECM-AM | | | ECM-dominated | | |
| Chemical property | Forest floor leaf litter | Mineral (0-5 cm) | Mineral (15-20 cm) | Forest floor leaf litter | Mineral (0-5 cm) | Mineral (15-20 cm) |
| pH | NA | 4.73 ± 0.26 | 4.74 ± 0.08 | NA | 4.70 ± 0.13 | 4.50 ± 0.19 |
| Soil moisture (g $H_2O$ $g^{-1}$ soil) | 0.84 ± 0.01 | 0.39 ± 0.01 | 0.38 ± 0.02 | 0.82 ± 0.03 | 0.42 ± 0.01 | 0.30 ± 0.09 |
| C concentration (%) | 46.15 ± 2.78 | 8.66 ± 1.61 | 3.87 ± 0.97 | 46.52 ± 1.71 | 8.23 ± 0.44 | 4.29 ± 0.38 |
| N concentration (%) | 1.52 ± 0.09 | 0.58 ± 0.05 | 0.30 ± 0.04 | 1.59 ± 0.13 | 0.53 ± 0.02 | 0.30 ± 0.03 |
| C:N | 30.60 ± 2.93 | 14.63 ± 1.28 | 12.72 ± 1.32 | 29.56 ± 2.03 | 15.59 ±0.39 | 14.24 ± 0.18 |
| $\delta^{13}C$ (‰) | -29.85 ± 0.16 | -27.76 ± 0.11 | -26.61 ± 0.24 | -29.56 ± 0.03 | -27.61 ± 0.10 | -26.68 ± 0.17 |
| $\delta^{13}C_{\text{mineral soil-litter}}$ (‰) | NA | 2.09 ± 0.10 | 3.23 ± 0.38 | NA | 1.95 ± 0.10 | 2.87 ± 0.20 |
| $\delta^{15}N$ (‰) | 0.57 ± 0.07 | 3.21 ± 0.32 | 4.70 ± 0.49 | 0.62 ± 0.20 | 2.70 ± 0.09 | 4.14 ± 0.24 |
| $\delta^{15}N_{\text{mineral soil-litter}}$ (‰) | NA | 2.64 ± 0.27 | 4.13 ± 0.42 | NA | 2.08 ± 0.11 | 3.51 ± 0.36 |

**Table B.1. (cont.)**

| | Hornito | | | | | | |
|---|---|---|---|---|---|---|---|
| | Mixed ECM-AM | | | ECM-dominated | | | |
| Chemical property | Forest floor leaf litter | Mineral (0-5 cm) | Mineral (15-20 cm) | Forest floor leaf litter | O | Mineral (0-5 cm) | Mineral (15-20 cm) |
| pH | NA | 4.32 ± 0.10 | 4.17 ± 0.01 | NA | 3.78 ± 0.05 | 3.68 ± 0.07 | 4.02 ± 0.04 |
| Soil moisture (g $H_2O$ $g^{-1}$ soil) | 0.88 ± 0.01 | 0.56 ± 0.01 | 0.49 ± 0.01 | 0.84 ± 0.01 | 0.81 ± 0.02 | 0.49 ± 0.01 | 0.43 ± 0.01 |
| C concentration (%) | 48.32 ± 0.85 | 11.12 ± 0.47 | 3.96 ± 1.33 | 49.78 ± 0.52 | 48.59 ± 2.23 | 8.44 ± 0.69 | 3.50 ± 0.46 |
| N concentration (%) | 1.67 ± 0.07 | 0.67 ± 0.01 | 0.30 ± 0.10 | 1.44 ± 0.06 | 2.20 ± 0.08 | 0.52 ± 0.05 | 0.24 ± 0.03 |
| C:N | 28.88 ± 0.69 | 16.50 ± 0.47 | 13.22 ± 0.14 | 34.78 ± 1.73 | 22.08 ± 0.88 | 16.15 ± 0.43 | 14.62 ± 0.34 |
| $\delta^{13}C$ (‰) | -29.80 ± 0.01 | -27.73 ± 0.14 | -26.38 ± 0.34 | -29.54 ± 0.15 | -28.44 ± 0.03 | -26.88 ± 0.07 | -25.88 ± 0.18 |
| $\delta^{13}C_{mineral\ soil\text{-}litter}$ (‰) | NA | 2.07 ± 0.15 | 3.42 ± 0.35 | NA | 1.10 ± 0.15 | 2.66 ± 0.20 | 3.66 ± 0.31 |
| $\delta^{15}N$ (‰) | 1.15 ± 0.18 | 2.46 ± 0.00 | 4.55 ± 0.47 | -0.33 ± 0.02 | 0.56 ± 0.16 | 2.77 ± 0.17 | 4.83 ± 0.15 |
| $\delta^{15}N_{mineral\ soil\text{-}litter}$ (‰) | NA | 1.31 ± 0.18 | 3.40 ± 0.65 | NA | 0.89 ± 0.17 | 3.10 ± 0.16 | 5.16 ± 0.15 |

**Table B.1. (cont.)**

| | Honda | | | | | | | |
|---|---|---|---|---|---|---|---|---|
| | Mixed ECM-AM | | | | ECM-dominated | | | |
| | Forest floor leaf litter | Organic | Mineral (0-5 cm) | Mineral (15-20 cm) | Forest floor leaf litter | Organic | Mineral (0-5 cm) | Mineral (15-20 cm) |
| pH | NA | 3.39 ± 0.22 | 4.08 ± 0.10 | 4.32 ± 0.12 | NA | 3.06 ± 0.12 | 3.87 ± 0.09 | 4.23 ± 0.01 |
| Soil moisture | 0.86 ± 0.01 | 0.77 ± 0.02 | 0.66 ± 0.02 | 0.62 ± 0.03 | 0.88 ± 0.02 | 0.82 ± 0.01 | 0.58 ± 0.02 | 0.53 ± 0.04 |
| C concentration (%) | 49.49 ± 0.18 | 43.89 ± 0.60 | 17.63 ± 3.07 | 8.79 ± 0.95 | 50.81 ± 0.15 | 51.04 ± 0.30 | 5.85 ± 0.07 | 2.58 ± 0.29 |
| N concentration (N) | 1.52 ± 0.04 | 1.88 ± 0.10 | 1.00 ± 0.17 | 0.53 ± 0.06 | 1.52 ± 0.07 | 2.43 ± 0.16 | 0.37 ± 0.01 | 0.17 ± 0.02 |
| C:N | 32.50 ± 0.83 | 23.46 ± 0.94 | 17.56 ± 0.20 | 16.75 ± 0.47 | 33.54 ± 1.48 | 21.18 ± 1.34 | 15.79 ± 0.15 | 14.76 ± 0.42 |
| $\delta^{13}C$ | -30.38 ± 0.23 | -28.73 ± 0.23 | -28.26 ± 0.07 | -27.56 ± 0.13 | -29.82 ± 0.02 | -28.68 ± 0.10 | -27.15 ± 0.08 | -26.72 ± 0.11 |
| $\delta^{13}C_{mineral\ soil\text{-}litter}$ | NA | 1.65 ± 0.23 | 2.12 ± 0.23 | 2.82 ± 0.27 | NA | 1.14 ± 0.11 | 2.67 ± 0.10 | 3.10 ± 0.10 |
| $\delta^{15}N$ | 0.17 ± 0.15 | 0.92 ± 0.15 | 2.02 ± 0.16 | 3.18 ± 0.23 | -1.84 ± 0.22 | 0.59 ± 0.23 | 4.59 ± 0.08 | 5.59 ± 0.12 |
| $\delta^{15}N_{mineral\ soil\text{-}litter}$ | NA | 0.76 ± 0.01 | 1.85 ± 0.28 | 3.02 ± 0.32 | NA | 2.44 ± 0.35 | 6.43 ± 0.14 | 7.43 ± 0.30 |

**Table B.1. (cont.)**

| | Zorro | | | | | | | |
|---|---|---|---|---|---|---|---|---|
| | Mixed ECM-AM | | | | ECM-dominated | | | |
| | Forest floor leaf litter | Organic | Mineral (0-5 cm) | Mineral (15-20 cm) | Forest floor leaf litter | Organic | Mineral (0-5 cm) | Mineral (15-20 cm) |
| pH | NA | 3.96 ± 0.06 | 4.25 ± 0.03 | 4.53 ± 0.11 | NA | 3.80 ± 0.06 | 4.34 ± 0.12 | 4.56 ± 0.11 |
| Soil moisture | 0.83 ± 0.01 | 0.80 ± 0.03 | 0.58 ± 0.03 | 0.53 ± 0.04 | 0.83 ± 0.01 | 0.79 ± 0.01 | 0.55 ± 0.01 | 0.45 ± 0.01 |
| C concentration (%) | 48.15 ± 0.86 | 41.82 ± 4.51 | 13.84 ± 2.04 | 7.23 ± 1.26 | 50.69 ± 0.08 | 43.6 ± 2.37 | 8.17 ± 0.48 | 4.72 ± 0.35 |
| N concentration (N) | 1.51 ± 0.05 | 1.66 ± 0.06 | 0.81 ± 0.09 | 0.43 ± 0.06 | 1.57 ± 0.02 | 2.23 ± 0.07 | 0.54 ± 0.03 | 0.29 ± 0.02 |
| C:N | 31.97 ± 1.67 | 25.35 ± 3.38 | 16.90 ± 0.66 | 16.71 ± 0.49 | 32.26 ± 0.44 | 19.53 ± 0.58 | 15.11 ± 0.12 | 16.06 ± 0.81 |
| $\delta^{13}C$ | -29.83 ± 0.13 | -29.23 ± 0.35 | -27.81 ± 0.07 | -26.67 ± 0.16 | -29.65 ± 0.10 | -28.53 ± 0.06 | -26.92 ± 0.07 | -26.29 ± 0.17 |
| $\delta^{13}C_{mineral\ soil\text{-}litter}$ | NA | 0.93 ± 0.42 | 2.02 ± 0.07 | 3.17 ± 0.03 | NA | 1.12 ± 0.13 | 2.73 ± 0.04 | 3.36 ± 0.11 |
| $\delta^{15}N$ | 0.11 ± 0.09 | 0.58 ± 0.69 | 2.63 ± 0.18 | 4.34 ± 0.19 | -0.74 ± 0.03 | 1.00 ± 0.20 | 3.63 ± 0.00 | 4.87 ± 0.24 |
| $\delta^{15}N_{mineral\ soil\text{-}litter}$ | NA | 1.11 ± 0.07 | 2.52 ± 0.09 | 4.23 ± 0.15 | NA | 1.73 ± 0.22 | 4.37 ± 0.04 | 5.61 ± 0.22 |

**Table B.2.** Guild classifications assigned to OTUs by FungalTraits (Põlme et al., 2020) and the broad guild classifications combining FungalTraits (Põlme et al., 2020) classifications that were used in this study.

| FUNguild classifications | Broad guild classification |
|---|---|
| Animal endosymbiont | Animal endosymbiont |
| Arbuscular mycorrhizal | Arbuscular mycorrhizal |
| Ectomycorrhizal | Ectomycorrhizal |
| Foliar endophyte | Endophyte |
| Root endophyte | Endophyte |
| Epiphyte | Epiphyte |
| Lichenized | Lichenized |
| Algal parasite | Parasite |
| Animal parasite | Parasite |
| Lichen parasite | Parasite |
| Mycoparasite | Parasite |
| Plant pathogen | Plant pathogen |
| Dung saprotroph | Saprotroph |
| Litter saprotroph | Saprotroph |
| Nectar/tap saprotroph | Saprotroph |
| Pollen saprotroph | Saprotroph |
| Soil saprotroph | Saprotroph |
| Unspecified saprotroph | Saprotroph |
| Wood saprotroph | Saprotroph |
| Sooty mold | Sooty mold |
| Unassigned | Unassigned |
| Unspecified symbiotroph | Unspecified symbiotroph |

**Table B.3.** Results from permutational analysis of variance on samples collected from beneath *O. mexicana* focal trees. We tested for the effects of watershed, stand mycorrhizal type, and the interaction between watershed and stand type on overall fungal and ectomycorrhizal (ECM) community composition in the forest floor leaf litter, organic horizon, and mineral soil.

| Overall fungal community | | | |
|---|---|---|---|
| Layer | Term | $R^2$ value | P-value |
| Forest floor leaf litter | Watershed | 0.21 | 0.002 |
| | Stand type | 0.06 | 0.001 |
| | Watershed*stand type | 0.17 | 0.001 |
| Organic horizon | Watershed | 0.21 | 0.002 |
| | Stand type | 0.11 | 0.001 |
| | Watershed*stand type | 0.08 | 0.10 |
| Mineral soil (0-5 cm) | Watershed | 0.24 | 0.001 |
| | Stand type | 0.06 | 0.01 |
| | Watershed*stand type | 0.16 | 0.001 |
| Mineral soil (15-20 cm) | Watershed | 0.29 | 0.001 |
| | Stand type | 0.06 | 0.005 |
| | Watershed*stand type | 0.16 | 0.001 |
| Ectomycorrhizal community | | | |
| Layer | Term | $R^2$ value | P-value |
| Organic horizon | Watershed | 0.25 | 0.001 |
| | Stand type | 0.09 | 0.10 |
| | Watershed*stand type | 0.08 | 0.20 |
| Mineral soil (0-5 cm) | Watershed | 0.24 | 0.001 |
| | Stand type | 0.05 | 0.05 |
| | Watershed*stand type | 0.18 | 0.001 |
| Mineral soil (15-20 cm) | Watershed | 0.26 | 0.001 |
| | Stand type | 0.05 | 0.10 |
| | Watershed*stand type | 0.17 | 0.001 |

**Table B.4**. Fungal genera beneath *O. mexicana* focal trees that differ significantly in relative abundance among the four watersheds ($p<0.05$). Using a multivariate generalized linear model analysis with the 100 most abundant fungal genera, we tested for the effects of watershed, stand mycorrhizal type, and the interaction between watershed and stand type. Wald test statistics and p-values were determined using an analysis of variance. Simplified guild assignments and exploration types are provided for each fungal genus.

| Layer | Genus | P-value (effect of stand type | Test statistic (effect of stand type | P-value (effect of watershed) | Test statistic (effect of watershed) | P-value (effect of interaction between stand type and watershed) | Test statistic (effect of interaction between stand type and watershed) | Guild | Exploration type |
|---|---|---|---|---|---|---|---|---|---|
| Forest floor leaf litter | Angustimassarina | 0.73 | 0.16 | 0.02 | 10.35 | 0.53 | 0.00 | Mycoparasite | |
| | Candida | 0.13 | 4.06 | 0.02 | 9.63 | 0.53 | 0.00 | Nectar/tap saprotroph | |
| | Euteratosphaeria | 0.41 | 0.79 | 0.01 | 12.68 | 0.11 | 4.64 | Plant pathogen | |
| | Lophodermium | 0.23 | 1.75 | 0.05 | 8.99 | 0.52 | 3.68 | Plant pathogen | |
| | Aspergillus | 0.14 | 2.62 | 0.04 | 11.44 | 0.36 | 4.27 | Unspecified saprotroph | |
| Organic horizon | Sugiyamaella | 0.08 | 6.05 | 0.01 | 12.69 | 0.85 | 0.06 | Animal endosymbiont | |
| | Phialemonium | 0.25 | 1.82 | 0.00 | 15.28 | 0.99 | 0.00 | Animal parasite | |
| | Beauveria | 0.39 | 0.00 | 0.02 | 7.44 | 0.41 | 0.00 | Animal parasite | |
| | Hydnum | 0.20 | 0.00 | 0.03 | 8.34 | 0.78 | 0.00 | Ectomycorrhizal | |
| | Craterellus | 0.33 | 1.87 | 0.05 | 6.29 | 0.42 | 0.00 | Ectomycorrhizal | |
| | Nectriopsis | 0.25 | 3.20 | 0.04 | 7.43 | 0.57 | 0.00 | Lichen parasite | |
| | Pyxine | 0.57 | 0.38 | 0.01 | 12.34 | 0.09 | 2.45 | Lichenized | |
| Mineral soil (0-5 cm) | Clavulina | 0.84 | 0.06 | 0.05 | 5.78 | 0.46 | 0.95 | Ectomycorrhizal | |
| | Tolypocladium | 0.12 | 2.32 | 0.03 | 10.56 | 0.49 | 2.46 | Animal parasite | |
| | Tuber | 0.66 | 0.31 | 0.01 | 13.54 | 0.01 | 10.70 | Ectomycorrhizal | |
| | Austroboletus | 0.56 | 0.63 | 0.01 | 10.38 | 0.44 | 0.00 | Ectomycorrhizal | medium distance fringe |
| | Leotia | 0.16 | 2.61 | 0.02 | 11.74 | 0.33 | 3.11 | Ectomycorrhizal | |
| | Tomentella | 0.43 | 0.87 | 0.03 | 13.82 | 0.25 | 6.82 | Ectomycorrhizal | |
| | Neoboletus | 0.39 | 1.37 | 0.03 | 9.84 | 0.32 | 1.74 | Ectomycorrhizal | Long distance |
| | Inocybe | 0.03 | 6.56 | 0.04 | 9.67 | 0.68 | 0.83 | Ectomycorrhizal | |
| | Elaphomyces | 0.62 | 0.29 | 0.04 | 12.69 | 0.14 | 6.30 | Ectomycorrhizal | |
| | Sebacina | 0.53 | 0.42 | 0.04 | 6.92 | 0.36 | 6.00 | Ectomycorrhizal | |
| | Campylospora | 0.62 | 0.33 | 0.01 | 14.11 | 0.03 | 9.59 | Litter saprotroph | |
| | Chloridium | 0.35 | 1.11 | 0.03 | 9.82 | 0.09 | 5.02 | Litter saprotroph | |
| | Hypomyces | 0.52 | 0.44 | 0.02 | 11.16 | 0.88 | 0.00 | Mycoparasite | |
| | Lipomyces | 0.01 | 12.46 | 0.04 | 9.96 | 0.47 | 0.00 | Nectar/tap saprotroph | |
| | Polyscytalum | 0.34 | 1.92 | 0.00 | 14.21 | 0.53 | 0.00 | Plant pathogen | |
| | Aquamyces | 0.02 | 8.59 | 0.00 | 22.25 | 0.42 | 0.00 | Pollen saprotroph | |
| | Leohumicola | 0.74 | 0.15 | 0.00 | 16.16 | 0.87 | 0.40 | Soil saprotroph | |
| | Archaeorhizomyces | 0.98 | 0.00 | 0.00 | 22.72 | 0.47 | 3.38 | Soil saprotroph | |

**Table B.4. (cont.)**

| | | | | | | | | | |
|---|---|---|---|---|---|---|---|---|---|
| | Mucor | 0.10 | 3.98 | 0.00 | 17.94 | 0.04 | 6.26 | Soil saprotroph | |
| | Absidia | 0.42 | 1.07 | 0.00 | 20.08 | 0.53 | 0.00 | Soil saprotroph | |
| | Staphylotrichum | 0.97 | 0.00 | 0.00 | 20.16 | 0.28 | 3.61 | Soil saprotroph | |
| | Saitozyma | 0.31 | 1.07 | 0.00 | 11.82 | 0.68 | 1.94 | Soil saprotroph | |
| | Geminibasidium | 0.80 | 0.09 | 0.02 | 11.37 | 0.15 | 6.77 | Soil saprotroph | |
| | Phialocephala | 0.14 | 2.58 | 0.03 | 10.45 | 0.07 | 5.31 | Soil saprotroph | |
| | Penicillium | 0.59 | 0.32 | 0.00 | 16.39 | 0.36 | 4.60 | Unspecified saprotroph | |
| Mineral soil (15-20 cm) | Sugiyamaella | 0.83 | 0.06 | 0.04 | 8.37 | 0.34 | 1.12 | Animal endosymbiont | |
| | Tolypocladium | 0.44 | 0.74 | 0.04 | 10.56 | 0.15 | 8.78 | Animal parasite | |
| | Cortinarius | 0.07 | 5.02 | 0.00 | 20.75 | 0.53 | 0.00 | Ectomycorrhizal | medium distance fringe |
| | Austroboletus | 0.25 | 1.75 | 0.01 | 14.90 | 0.26 | 2.07 | Ectomycorrhizal | medium distance fringe |
| | Inocybe | 0.89 | 0.02 | 0.03 | 10.08 | 0.11 | 8.85 | Ectomycorrhizal | |
| | Cenococcum | 0.95 | 0.00 | 0.03 | 9.54 | 0.67 | 0.73 | Ectomycorrhizal | medium distance fringe |
| | Leotia | 0.11 | 4.33 | 0.03 | 10.04 | 0.21 | 2.15 | Ectomycorrhizal | |
| | Thozetella | 0.97 | 0.00 | 0.00 | 17.89 | 0.03 | 6.69 | Litter saprotroph | |
| | Tremella | 0.77 | 0.13 | 0.02 | 11.11 | 0.14 | 2.98 | Mycoparasite | |
| | Cordana | 0.73 | 0.23 | 0.01 | 16.22 | 0.13 | 3.96 | Plant pathogen | |
| | Polyscytalum | 0.03 | 7.71 | 0.02 | 9.49 | 0.40 | 0.00 | Plant pathogen | |
| | Nalanthamala | 0.31 | 1.44 | 0.02 | 9.67 | 0.49 | 0.00 | Plant pathogen | |
| | Aquamyces | 0.67 | 0.40 | 0.03 | 9.62 | 0.45 | 0.00 | Pollen saprotroph | |
| | Archaeorhizomyces | 0.90 | 0.03 | 0.00 | 19.62 | 0.09 | 5.92 | Soil saprotroph | |
| | Saitozyma | 0.06 | 3.73 | 0.00 | 16.61 | 0.00 | 21.27 | Soil saprotroph | |
| | Leohumicola | 0.90 | 0.01 | 0.00 | 16.85 | 0.06 | 9.44 | Soil saprotroph | |
| | Cladophialophora | 0.38 | 0.96 | 0.00 | 16.64 | 0.95 | 0.15 | Soil saprotroph | |
| | Bifiguratus | 0.15 | 2.22 | 0.00 | 13.36 | 0.42 | 2.97 | Soil saprotroph | |
| | Absidia | 0.84 | 0.03 | 0.01 | 12.96 | 0.40 | 1.16 | Soil saprotroph | |
| | Geminibasidium | 0.84 | 0.05 | 0.01 | 12.49 | 0.12 | 7.20 | Soil saprotroph | |
| | Gongronella | 0.23 | 1.76 | 0.02 | 10.03 | 0.56 | 0.00 | Soil saprotroph | |
| | Oidiodendron | 0.66 | 0.19 | 0.02 | 11.58 | 0.50 | 3.01 | Soil saprotroph | |
| | Umbelopsis | 0.02 | 6.12 | 0.02 | 10.90 | 0.70 | 0.59 | Soil saprotroph | |
| | Staphylotrichum | 0.17 | 2.77 | 0.03 | 11.24 | 0.04 | 9.58 | Soil saprotroph | |
| | Penicillium | 0.52 | 0.53 | 0.00 | 26.41 | 0.36 | 4.97 | Unspecified saprotroph | |
| | Sagenomella | 0.46 | 0.56 | 0.00 | 15.28 | 0.07 | 2.33 | Unspecified saprotroph | |
| | Acremonium | 0.48 | 0.88 | 0.03 | 10.89 | 0.58 | 0.61 | Unspecified saprotroph | |
| | Scytalidium | 0.39 | 0.94 | 0.01 | 15.43 | 0.32 | 2.97 | Wood saprotroph | |
| | Trechispora | 0.45 | 1.01 | 0.03 | 9.24 | 0.49 | 0.00 | Wood saprotroph | |
| Mineral soil (0-5 and 15-20 cm) | Sugiyamaella | 0.67 | 0.14 | 0.03 | 9.38 | 0.39 | 2.76 | Animal endosymbiont | |
| | Tolypocladium | 0.24 | 1.14 | 0.00 | 17.69 | 0.74 | 0.97 | Animal parasite | |

**Table B.4. (cont.)**

| | | | | | | | | |
|---|---|---|---|---|---|---|---|---|
| | Brachyphoris | 0.98 | 0.00 | 0.01 | 12.51 | 0.00 | 18.56 | Animal parasite | |
| | Leotia | 0.03 | 4.88 | 0.00 | 19.26 | 0.09 | 5.55 | Ectomycorrhizal | |
| | Austroboletus | 0.20 | 2.40 | 0.00 | 22.01 | 0.21 | 2.00 | Ectomycorrhizal | Long-distance |
| | Tylopilus | 0.78 | 0.12 | 0.00 | 18.51 | 0.53 | 0.00 | Ectomycorrhizal | Long distance |
| | Cortinarius | 0.01 | 8.82 | 0.00 | 15.27 | 0.24 | 2.38 | Ectomycorrhizal | Medium-distance fringe |
| | Elaphomyces | 0.72 | 0.12 | 0.00 | 19.23 | 0.20 | 5.81 | Ectomycorrhizal | Short-distance |
| | Octaviania | 0.73 | 0.11 | 0.01 | 14.33 | 0.85 | 0.03 | Ectomycorrhizal | Long-distance |
| | Hydnum | 0.07 | 4.61 | 0.01 | 10.82 | 0.59 | 0.00 | Ectomycorrhizal | |
| | Lactifluus | 0.02 | 4.65 | 0.01 | 9.41 | 0.00 | 23.35 | Ectomycorrhizal | |
| | Tuber | 0.91 | 0.01 | 0.02 | 10.33 | 0.01 | 12.79 | Ectomycorrhizal | Short-distance |
| | Amanita | 0.80 | 0.08 | 0.02 | 16.66 | 0.01 | 14.79 | Ectomycorrhizal | |
| | Cenococcum | 0.70 | 0.08 | 0.03 | 6.01 | 0.59 | 1.65 | Ectomycorrhizal | Short-distance |
| | Sebacina | 0.58 | 0.27 | 0.05 | 6.39 | 0.23 | 5.37 | Ectomycorrhizal | |
| | Laccaria | 0.54 | 0.48 | 0.05 | 7.45 | 0.05 | 11.21 | Ectomycorrhizal | Medium-distance fringe |
| | Inocybe | 0.36 | 0.89 | 0.05 | 6.82 | 0.06 | 8.86 | Ectomycorrhizal | Short-distance |
| | Rinodina | 1.00 | 0.00 | 0.03 | 8.89 | 0.01 | 11.20 | Lichenized | |
| | Thozetella | 0.75 | 0.12 | 0.00 | 15.65 | 0.02 | 9.09 | Litter saprotroph | |
| | Campylospora | 0.43 | 0.72 | 0.01 | 12.65 | 0.10 | 6.98 | Litter saprotroph | |
| | Hypomyces | 0.34 | 1.30 | 0.01 | 11.56 | 0.52 | 2.08 | Mycoparasite | |
| | Trichoderma | 0.41 | 0.44 | 0.05 | 5.36 | 0.28 | 2.60 | Mycoparasite | |
| | Lipomyces | 0.95 | 0.00 | 0.03 | 11.67 | 0.01 | 10.84 | Nectar/tap saprotroph | |
| | Cordana | 0.34 | 1.21 | 0.00 | 20.88 | 0.37 | 4.64 | Plant pathogen | |
| | Polyscytalum | 0.67 | 0.17 | 0.00 | 23.34 | 0.51 | 0.00 | Plant pathogen | |
| | Ganoderma | 0.23 | 1.81 | 0.01 | 13.93 | 0.99 | 0.01 | Plant pathogen | |
| | Entorrhiza | 0.32 | 1.25 | 0.02 | 12.43 | 0.31 | 5.76 | Plant pathogen | |
| | Aquamyces | 0.57 | 0.42 | 0.00 | 29.55 | 0.57 | 0.00 | Pollen saprotroph | |
| | Sagenomella | 0.19 | 2.03 | 0.00 | 22.54 | 0.28 | 2.59 | Saprotroph | |
| | Penicillium | 0.93 | 0.01 | 0.00 | 33.05 | 0.33 | 4.05 | Saprotroph | |
| | Geminibasidium | 0.68 | 0.21 | 0.00 | 22.30 | 0.01 | 13.91 | Soil saprotroph | |
| | Bifiguratus | 0.00 | 10.99 | 0.00 | 12.69 | 0.07 | 7.95 | Soil saprotroph | |
| | Absidia | 0.60 | 0.38 | 0.00 | 26.31 | 0.21 | 2.14 | Soil saprotroph | |
| | Saitozyma | 0.03 | 4.77 | 0.00 | 22.86 | 0.24 | 3.87 | Soil saprotroph | |
| | Archaeorhizomyces | 0.97 | 0.00 | 0.00 | 40.45 | 0.40 | 3.37 | Soil saprotroph | |
| | Staphylotrichum | 0.10 | 3.11 | 0.00 | 19.08 | 0.06 | 9.87 | Soil saprotroph | |
| | Phialocephala | 0.50 | 0.50 | 0.03 | 10.70 | 0.17 | 4.58 | Soil saprotroph | |
| | Entoloma | 0.74 | 0.09 | 0.04 | 8.98 | 0.83 | 0.92 | Soil saprotroph | |
| | Dactylella | 0.54 | 0.43 | 0.01 | 9.83 | 0.53 | 0.82 | Wood saprotroph | |
| | Porotheleum | 0.04 | 5.59 | 0.02 | 8.78 | 0.38 | 0.00 | Wood saprotroph | |

**Table B.5.** Fungal genera beneath *O. mexicana* focal trees that differ significantly in relative abundance between mixed ECM-AM and ECM-dominant stands (<0.05). Using a multivariate generalized linear model analysis with the 100 most abundant fungal genera, we tested for the effects of watershed, stand mycorrhizal type, and the interaction between watershed and stand type. Wald test statistics and p-values were determined using an analysis of variance. Simplified guild assignments and exploration types are provided for each fungal genus.

| Layer | Genus | P-value (effect of stand type | Test statistic (effect of stand type | P-value (effect of watershed) | Test statistic (effect of watershed) | P-value (effect of interaction between stand type and watershed) | Test statistic (effect of interaction between stand type and watershed) | Guild | Exploration type |
|---|---|---|---|---|---|---|---|---|---|
| Forest floor leaf litter | *Scolecobasidium* | 0.02 | 9.07 | 0.33 | 4.57 | 0.73 | 0.00 | Animal parasite | |
| | *Diaporthe* | 0.01 | 9.81 | 0.33 | 4.65 | 0.68 | 0.00 | Plant pathogen | |
| | *Sporisorium* | 0.02 | 5.96 | 0.52 | 0.93 | 0.03 | 13.66 | Plant pathogen | |
| | *Mortierella* | 0.03 | 8.54 | 0.16 | 8.88 | 0.65 | 0.38 | Soil saprotroph | |
| | *Umbelopsis* | 0.05 | 5.72 | 0.58 | 3.19 | 0.75 | 0.00 | Soil saprotroph | |
| | *Saitozyma* | 0.05 | 5.94 | 0.69 | 1.15 | 0.37 | 2.54 | Soil saprotroph | |
| | *Oidiodendron* | 0.05 | 4.03 | 0.26 | 5.20 | 0.21 | 4.60 | Soil saprotroph | |
| Organic horizon | *Cortinarius* | 0.04 | 4.49 | 0.07 | 4.52 | 0.10 | 3.81 | Ectomycorrhizal | medium distance fringe |
| | *Cryptodiscus* | 0.02 | 9.22 | 0.06 | 6.69 | 0.26 | 0.00 | Lichen parasite | |
| | *Rhexodenticula* | 0.03 | 9.09 | 0.06 | 6.67 | 0.52 | 0.00 | Litter saprotroph | |
| | *Odontia* | 0.04 | 6.53 | 0.69 | 1.71 | 0.81 | 0.00 | Litter saprotroph | |
| | *Cylindrocladiella* | 0.02 | 8.52 | 0.79 | 0.38 | 0.55 | 0.00 | Plant pathogen | |
| | *Glutinomyces* | 0.01 | 10.23 | 0.67 | 0.83 | 0.72 | 0.18 | Root endophyte | |
| | *Apiotrichum* | 0.01 | 11.13 | 0.65 | 0.99 | 0.42 | 0.00 | Soil saprotroph | |
| | *Oidiodendron* | 0.03 | 7.91 | 0.90 | 0.22 | 0.29 | 1.23 | Soil saprotroph | |
| | *Mariannaea* | 0.02 | 10.20 | 0.76 | 0.81 | 0.36 | 0.00 | Wood saprotroph | |
| Mineral soil (0-5 cm) | *Rhizophydium* | 0.05 | 6.01 | 0.80 | 1.15 | 0.08 | 8.19 | Algal parasite | |
| | *Lactifluus* | 0.01 | 8.48 | 0.20 | 4.74 | 0.00 | 17.23 | Ectomycorrhizal | |
| | *Inocybe* | 0.03 | 6.56 | 0.04 | 9.67 | 0.68 | 0.83 | Ectomycorrhizal | |
| | *Cortinarius* | 0.03 | 6.77 | 0.14 | 7.45 | 0.30 | 1.68 | Ectomycorrhizal | |
| | | 0.00 | 11.91 | 0.20 | 3.94 | 0.04 | 12.84 | Litter saprotroph | |
| | *Chaetosphaeria* | 0.05 | 5.41 | 0.13 | 5.52 | 0.19 | 6.51 | Litter saprotroph | |

**Table B.5. (cont.)**

| | | | | | | | | |
|---|---|---|---|---|---|---|---|---|
| | *Lipomyces* | 0.01 | 12.46 | 0.04 | 9.96 | 0.47 | 0.00 | Nectar/tap saprotroph | |
| | *Mycoleptodiscus* | 0.04 | 5.36 | 0.32 | 4.45 | 0.46 | 0.00 | Plant pathogen | |
| | *Protrudomyces* | 0.01 | 9.35 | 0.80 | 2.38 | 0.19 | 1.48 | Pollen saprotroph | |
| | *Aquamyces* | 0.02 | 8.59 | 0.00 | 22.25 | 0.42 | 0.00 | Pollen saprotroph | |
| | *Bifiguratus* | 0.00 | 9.81 | 0.08 | 5.76 | 0.28 | 5.09 | Soil saprotroph | |
| | *Crepidotus* | 0.04 | 5.33 | 0.27 | 5.46 | 0.68 | 0.00 | Wood saprotroph | |
| Mineral soil (15-20) | *Chaetomium* | 0.00 | 8.39 | 0.46 | 2.24 | 0.01 | 19.54 | Litter saprotroph | |
| | *Hymenoscyphus* | 0.01 | 8.12 | 0.28 | 5.13 | 0.25 | 3.07 | Litter saprotroph | |
| | *Polyscytalum* | 0.03 | 7.71 | 0.02 | 9.49 | 0.40 | 0.00 | Plant pathogen | |
| | *Umbelopsis* | 0.02 | 6.12 | 0.02 | 10.90 | 0.70 | 0.59 | Soil saprotroph | |
| | *Mortierella* | 0.04 | 3.77 | 0.67 | 1.30 | 0.35 | 4.25 | Soil saprotroph | |
| | *Gymnascella* | 0.05 | 8.20 | 0.22 | 4.35 | 0.53 | 0.00 | Soil saprotroph | |
| Mineral soil (0-5 and 15-20) | *Rhizophydium* | 0.01 | 8.13 | 0.61 | 1.28 | 0.09 | 8.16 | Algal parasite | |
| | *Cortinarius* | 0.01 | 8.82 | 0.00 | 15.27 | 0.24 | 2.38 | Ectomycorrhizal | Medium-distance fringe |
| | *Lactifluus* | 0.02 | 4.65 | 0.01 | 9.41 | 0.00 | 23.35 | Ectomycorrhizal | |
| | *Leotia* | 0.03 | 4.88 | 0.00 | 19.26 | 0.09 | 5.55 | Ectomycorrhizal | |
| | *Lactarius* | 0.03 | 4.88 | 0.87 | 0.47 | 0.19 | 6.23 | Ectomycorrhizal | |
| | *Chaetomium* | 0.00 | 20.20 | 0.11 | 5.44 | 0.00 | 24.34 | Litter saprotroph | |
| | *Hymenoscyphus* | 0.01 | 7.13 | 0.26 | 5.08 | 0.16 | 2.39 | Litter saprotroph | |
| | *Wickerhamiella* | 0.01 | 8.84 | 0.43 | 7.82 | 0.57 | 2.65 | Nectar/tap saprotroph | |
| | *Sporisorium* | 0.04 | 4.50 | 0.30 | 3.15 | 0.05 | 8.80 | Plant pathogen | |
| | *Protrudomyces* | 0.01 | 10.81 | 0.94 | 0.37 | 0.18 | 5.98 | Pollen saprotroph | |
| | *Paranamyces* | 0.02 | 5.61 | 0.09 | 5.55 | 0.16 | 6.71 | Pollen saprotroph | |
| | *Bifiguratus* | 0.00 | 10.99 | 0.00 | 12.69 | 0.07 | 7.95 | Soil saprotroph | |
| | *Mortierella* | 0.02 | 3.89 | 0.96 | 0.21 | 0.20 | 3.10 | Soil saprotroph | |
| | *Saitozyma* | 0.03 | 4.77 | 0.00 | 22.86 | 0.24 | 3.87 | Soil saprotroph | |
| | *Crepidotus* | 0.03 | 6.39 | 0.19 | 6.45 | 0.75 | 0.00 | Wood saprotroph | |
| | *Porotheleum* | 0.04 | 5.59 | 0.02 | 8.78 | 0.38 | 0.00 | Wood saprotroph | |

# APPENDIX C

# SUPPLEMENTARY MATERIAL FOR CHAPTER 4

## Table and Figures

**Table C.1.** Location, environmental variables, percent ectomycorrhizal (ECM) basal area, and abundant arbuscular mycorrhizal (AM) tree species (DBH > 10 cm) of ECM and AM stands in the four study watersheds.

| Watershed | Stand mycorrhizal type | Latitude (ºN) | Longitude (ºE) | Elevation (m) | Mean annual precipitation (mm) | Mean annual temperature (ºC) | ECM basal area (%) | Most abundant AM species |
|---|---|---|---|---|---|---|---|---|
| Honda | AM | 8.751 | -82.239 | 1155 | 6255 | 17.7 | 0% | *Guarea glabra, Alsophila cuspidate, Bilia rosea, Dendropanax arboreus, Inga exalata, Hedyosmum, costaricense* |
| Honda | ECM | 8.756 | -82.243 | 1240 | 6159 | 17.9 | 49% | *Guarea glabra, Viburnum costaricanum, Cassipourea elliptica, Eschweilera panamensis, Dendropanax arboreus, Ardisia* sp.*, Pouteria cuspidata* |
| Zorro | AM | 8.754 | -82.259 | 1135 | 5184 | 18.5 | 0% | *Aiouea* sp.*, Citharexylum macradenium, Mollinedia viridiflora , Dendropanax arboreus , Micropholis melinoniana, Romanophile hylonomum, Inga oerstediana* |
| Zorro | ECM | 8.754 | -82.259 | 1135 | 5184 | 18.5 | 63% | *Guatteria costaricensis, Dendropanax arboreus, Pouteria reticulata, Aiouea* sp.*, Bilia rosea, Inga acuminata* |

**Table C.1. (cont.)**

| | | | | | | | | |
|---|---|---|---|---|---|---|---|---|
| Hornito | AM | 8.674 | -82.214 | 1330 | 5164 | 17.2 | 0% | *Pouteria juruana, Myrtaceae* sp.*, Brosimum guainense , Dendropanax arboreus, Desmopsis maxonii, Peltostigma guatemalensis, Myrtaceae* sp.*, Hyperbaena* sp.*, Sloanea deflexiflora* |
| Hornito | ECM | 8.677 | -82.212 | 1315 | 5164 | 17.2 | * | *Pouteria reticulata, Inga sierrae, Guatteria costaricensis* |
| Alto Frio | AM | 8.654 | -82.215 | 1100 | 4641 | 21.4 | 0% | *Lauraceae* sp.*, Garcinia madruno, Prunus fortunensis, Symplocos limoncello, Zinowiewia costaricensis, Inga longispica, Lacistema aggregatum* |
| Alto Frio | ECM | 8.654 | -82.215 | 1100 | 4641 | 21.4 | * | *Ouratea lucens* |

* Denotes decomposition experiments outside censused forest for which we chose based on visual consistency with censused ECM-dominated forest in Honda and Zorro watersheds (i.e., litter layer dominated by *Oreomunnea mexicana* leaf litter and canopy dominated by *Oreomunnea mexicana* trees). In these stands, we estimated the most abundant AM species from censused forest adjacent to the litter decomposition bags (<50m).

**Figure C.1.** Comparison of initial leaf litter nutrient ratios (unitless) among litter species. The two ectomycorrhizal-associated litter species (yellow) and four arbuscular mycorrhizal-associated litter species (purple) are ordered along the x-axis by increasing mean decomposition rate. Bars and error bars represent means ± one standard error (n = 3). Letters denote statistically significant differences based on Tukey post-hoc comparisons ($p < 0.05$).

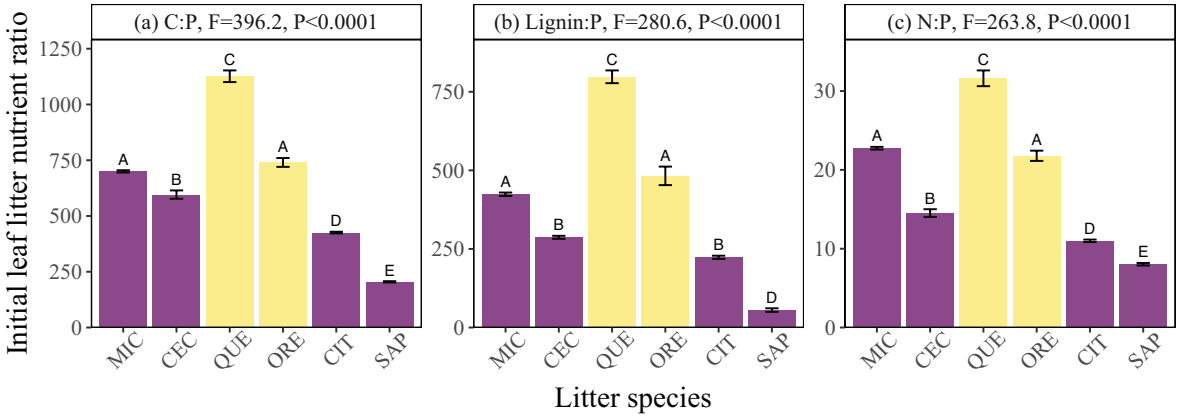

**Figure C.2.** Comparison of initial leaf litter chemical properties by litter mycorrhizal type. All properties are concentrations reported as mass percent with the exception of ratios which are unitless. The bars represent averages across the two ectomycorrhizal-associated litter species (yellow; n = 16) and the four arbuscular mycorrhizal-associated litter species (purple; n = 32); error bars represent one standard error.

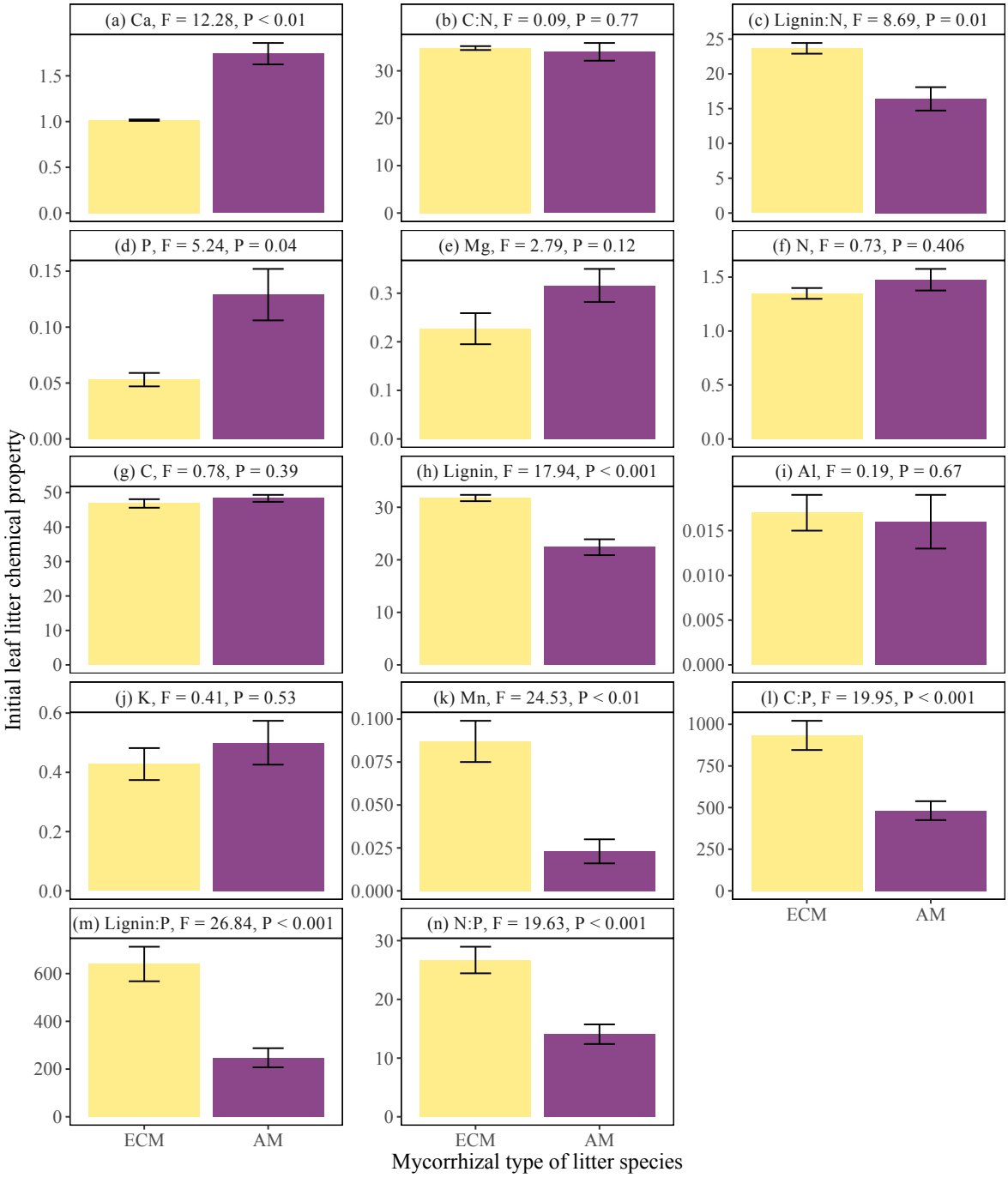

**Figure C.3.** Principal component analysis (PCA) of initial leaf litter chemical properties. Ectomycorrhizal-associated species are shown in yellow and arbuscular mycorrhizal-associated species are shown in purple. The largest contributors to variance described by PC1 are lignin:nitrogen (14 %), magnesium (13%), phosphorus (12%), nitrogen (12%) and lignin (12%). The largest contributor to variance described by PC2 are aluminum (41%) and manganese (29%). Leaf litter species do not group by mycorrhizal association.

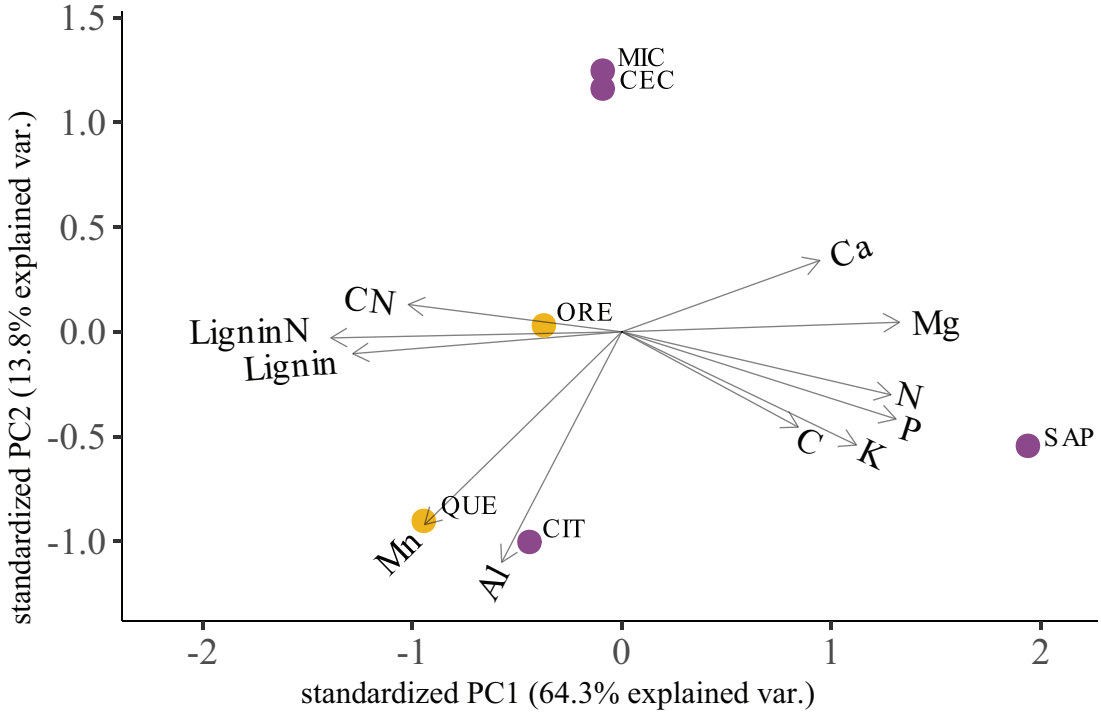

**Figure C.4.** Integrated *k*-values versus initial leaf litter nutrient ratios (unitless) for all six litter species. The symbols represent the six litter species, with n=8 for each species: *Cecropia angustifolia*. (CEC; square), *Citharexylum macradenium* (CIT; circle), *Micropholis melinoniana* (MIC; triangle), *Sapium* sp. (SAP; inverted triangle), *Oreomunnea mexicana* (ORE; cross), *Quercus insignis* (QUE; diamond). The colors indicate litter mycorrhizal type, with the two ectomycorrhizal-associated litter species in yellow and the four arbuscular mycorrhizal-associated litter species in purple. Solid lines indicate statistically significant relationships ($p < 0.05$).

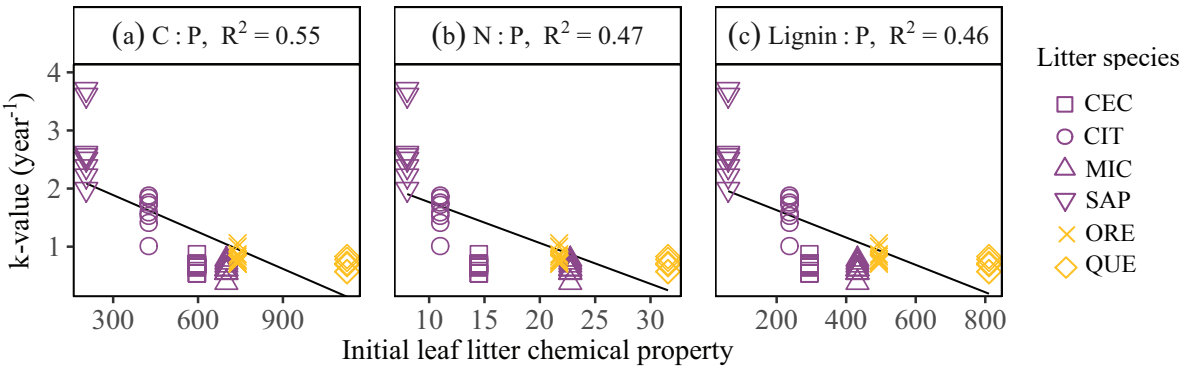

**Figure C.5.** Integrated *k*-values versus initial leaf litter chemical properties for all litter species except *Sapium* sp. All properties are concentrations reported as mass percent with the exception of ratios which are unitless. The symbols represent the six litter species, with n=8 for each species: *Cecropia angustifolia* (CEC; square), *Citharexylum macradenium* (CIT; circle), *Micropholis melinoniana* (MIC; triangle), *Oreomunnea mexicana* (ORE; cross), *Quercus insignis* (QUE; diamond). The colors indicate litter mycorrhizal type, with the two ectomycorrhizal-associated litter species in yellow and the four arbuscular mycorrhizal-associated litter species in purple. Solid lines indicate statistically significant relationships ($P < 0.05$), and dashed lines indicate non-significant relationships.

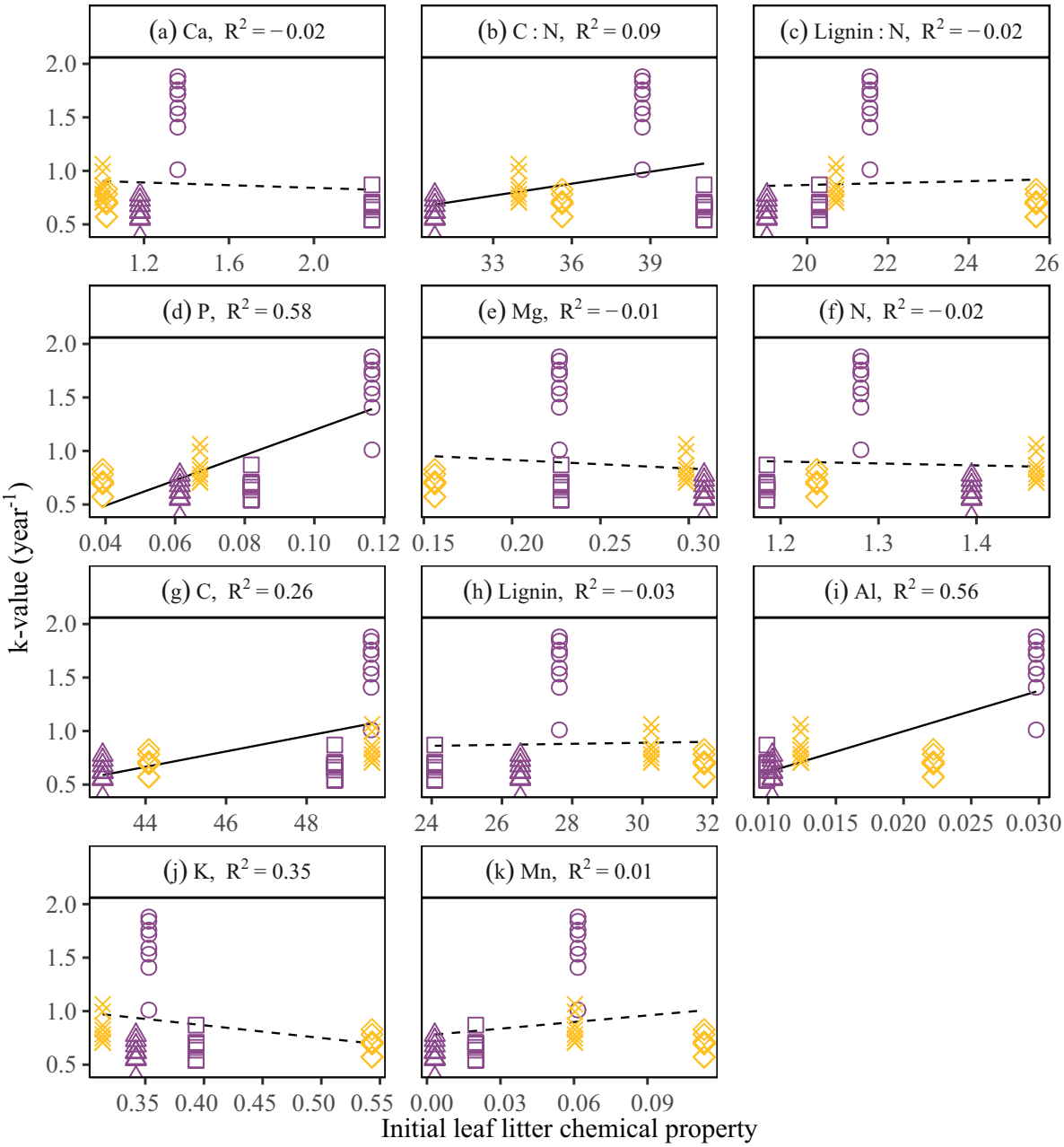

**Figure C.6.** Boxplots of integrated *k*-values across all litter species by stand mycorrhizal type. Leaf litter decomposition in ectomycorrhizal-dominated stands is shown in yellow and in arbuscular mycorrhizal-dominated stands is shown in purple (n = 24 per stand type). For a linear mixed model predicting *k*-values, there was no statistically significant difference between stand types ($F_{1,3} = 7.74$, P = 0.07).

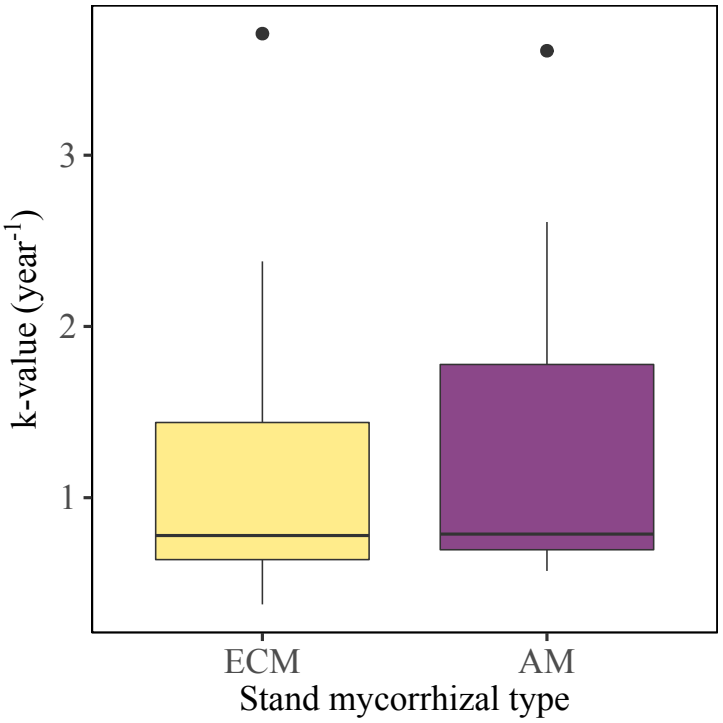

# APPENDIX D

# SUPPLEMENTARY MATERIAL FOR CHAPTER 5

## Figures

**Figure D.1.** Boxplots showing the effects of stand mycorrhizal type and nitrogen (N) addition treatment on potential nitrification rates. Data from arbuscular mycorrhizal (AM)- dominated stands and ectomycorrhizal (ECM)-dominated stands are represented by purple and yellow, respectively. Potential nitrification rates were significantly greater in AM- compared to ECM-dominated stands ($F_{1, 12} = 5.47$, P=0.04), but did not differ between control and N addition plots. Asterisks denote significant differences between stand types.

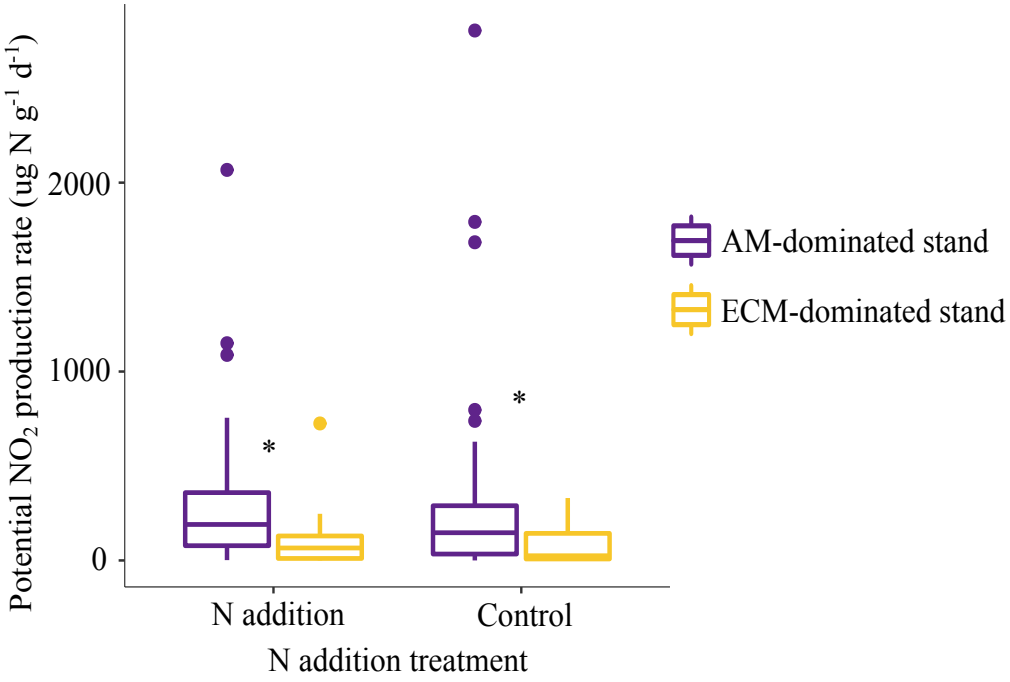

**Figure D.2.** Boxplots showing the effects of stand mycorrhizal type and nitrogen (N) addition treatment on (a) potential total denitrification and (b) potential incomplete denitrification. Data from arbuscular mycorrhizal (AM)-dominated stands and ectomycorrhizal (ECM)-dominated stands are represented by purple and yellow, respectively. Potential total denitrification rates and potential incomplete denitrification rates were significantly greater in AM- compared to ECM-dominated stands ($F_{1,12.12} = 27.35$, $P<0.0002$; $F_{1,12.05} = 41.63$, $P<0.0001$, respectively), but did not differ between control and N addition plots. Asterisks denote significant differences between stand types.